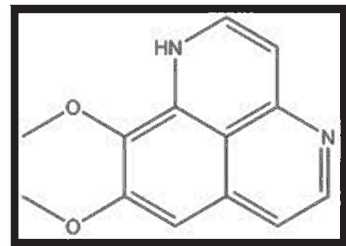
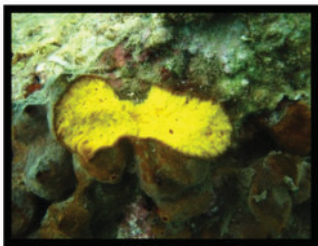


# New cytotoxic natural products from marine invertebrates

(Neue zytotoxische Naturstoffe aus marinen  
Invertebraten)



## Inaugural-Dissertation

zur Erlangung des Doktorgrades  
der Mathematisch-Naturwissenschaftlichen Fakultät  
der Heinrich-Heine-Universität Düsseldorf  
vorgelegt von

**Cong-Dat Pham**

Aus Tönisvorst, Bundesrepublik Deutschland

Düsseldorf, 03.02.2014

**Aus dem Institut für Pharmazeutische Biologie und Biotechnologie  
der Heinrich-Heine Universität Düsseldorf**

**Gedruckt mit der Genehmigung der  
Mathematisch-Naturwissenschaftlichen Fakultät der  
Heinrich-Heine-Universität Düsseldorf**

**Gedruckt mit der Unterstützung des  
BMBF**

**Referent: Prof. Dr. Peter Proksch  
Koreferent: Prof. Dr. Matthias U. Kassack  
Tag der mündlichen Prüfung: \_\_\_\_\_**

*„Ich habe keine besondere Begabung, sondern bin nur  
leidenschaftlich neugierig.“*

**Albert Einstein**

## CONTENTS

<b>1. ABSTRACT</b>	6
<b>2. ZUSAMMENFASSUNG</b>	9
<b>3. INTRODUCTION</b>	12
<b>3.1 Significance of the study</b>	12
<b>3.2 Marine invertebrates</b>	12
3.2.1 Sponges	13
3.2.2 Ascidians	15
3.2.3 Microbial communities in marine invertebrates	17
<b>3.3 Marine natural products and their biological activities</b>	18
3.3.1 Angiogenesis	20
3.3.2 Apoptosis	20
3.3.3 Mitosis	21
3.3.4 Topoisomerases and DNA polymerases	23
<b>3.4 Current marine derived drugs in pre-clinical and clinical trials</b>	23
<b>3.5 Aim of the study</b>	25
<b>4. PUBLICATION 1: <i>AAPTOS SUBERITOIDES</i></b>	26
<b>5. PUBLICATION 2: <i>POLYCARPA AURATA</i></b>	55
<b>6. PUBLICATION 3: <i>CALLYSPONGIA SP.</i></b>	77
<b>7. DISCUSSION</b>	118
<b>7.1. Isolated natural products from <i>Aaptos suberitoides</i></b>	118
7.1.1 Benzo[de][1,6]-naphthyridine alkaloids	118
<b>7.2. Isolated natural products from <i>Polycarpa aurata</i></b>	121
7.2.1 Sulfur containing guanidine alkaloids	121
7.2.2 $\alpha$ -carboline alkaloids	124
<b>7.3. Isolated natural products from <i>Callyspongia sp.</i></b>	125
7.3.1 Polyketide macrolides	125
<b>8. BIBLIOGRAPHY</b>	129
<b>9. ABBREVIATIONS</b>	133
<b>10. RESEARCH CONTRIBUTIONS</b>	135
<b>11. DECLARATION OF ACADEMIC HONESTY/ERKLÄRUNG</b>	136
<b>12. ACKNOWLEDGEMENTS</b>	138



### 1. Abstract

More than 50% of all pharmaceuticals on the market are based on natural products. Traditionally, terrestrial plants were the major source for natural products. With the discovery of antibiotics in the early 20<sup>th</sup> century began a thorough search for pharmaceuticals from bacterial and fungal sources. Whereas the terrestrial environment has been screened for sources of new drugs for more than 4,000 years, until recently, the marine environment was to a large extent inaccessible for such investigations. Only the advent of SCUBA diving techniques about 60 years granted access to this thitherto almost completely untapped source of natural products. Since then more than 10,000 new metabolites have been isolated and described from marine organisms, many of them possess highly interesting pharmaceutical properties. In the everlasting combat against diseases and drug resistances thousands of anti-infective and anticancer drugs have been identified and are being tested in pre-clinical and clinical trials. In 2010 Halaven® (eribulin mesylate) was introduced to the - yet short - list of FDA/EMEA approved marine derived therapeutic drugs consisting of Prialt® (also known as ziconotide), Yondelis® (known also as trabectedin or ET-743), Cytosar-U® (cytarabine), Vira-A® (vidarabine) and Adcetris® (brentuximab). Much focus is laid on sessile organisms such as sponges and ascidians, as they are bound to produce highly bioactive chemical defensives for their own survival from which potent therapeutic drug may be developed. Common biological activities include cytotoxicity, antimicrobial, antifungal and antifouling activities. The compounds isolated from these organisms possess chemical structures which are so unique and complex that structure elucidation is rendered more difficult and modern state-of-the-art techniques and devices have to be employed, e.g. advanced 1D&2D NMR spectroscopy (<sup>1</sup>H, <sup>13</sup>C, <sup>15</sup>N, DEPT, COSY, HMQC, HMBC) including the usage of highly sensitive probes and J coupled experiments and high resolution mass spectrometry. Sometimes chemical approaches have to be made such as proof synthesis or derivatisation reactions for configurational studies, in order to achieve a complete structure elucidation.

Overall, in this work 15 secondary metabolites were isolated from two sponges and one ascidian, of which 7 are identified as new natural products. Additionally, one compound was obtained through total synthesis. The isolated compounds were examined for their cytotoxicity using different assays and cancer cell lines. In the present dissertation, results already published in scientific journals or submitted for publication are presented in the form of the respective manuscripts:

*Polycarpa aurata*

From the crude extract of the ascidian *Polycarpa aurata* six compounds were isolated, two of which were identified as new. Five of them are metabolites of the dimeric sulfur containing alkaloid polycarpine which features a 4-methoxyphenyl substructure and a five membered heterocyclic system. The other is N,N-didesmethylgrossularine-1, a  $\alpha$ -carboline alkaloid. The new compounds, polycarpathiamine A and B, contain a 3-amino-1,2,4-thiadiazole ring and their structures were unambiguously determined by 1D, 2D NMR, and HRESIMS measurements and further confirmed by comparison with a closely related analogue, 3-dimethylamino-5-benzoyl-1,2,4-thiadiazole, that was prepared by chemical synthesis. Polycarpathiamine A and the known compounds polycarpaurine C and N,N-didesmethylgrossularine-1 showed significant cytotoxic activity against L5178Y murine lymphoma cells.

*Aaptos suberitoides*

Chromatographic separation of the crude extract of the sponge *Aaptos suberitoides* yielded eight benzo[de][1,6]naphthyridine alkaloids (aaptamine derivatives) of which four were identified as new. The structures of the isolated compounds were unambiguously determined by 1D, 2D NMR, and HRESIMS measurements. All compounds were tested for cytotoxic activity, among which only one new compound and two known compounds, aaptamine and demethylaaptamine, were found to be active against L5178Y murine lymphoma cells. Furthermore, considerations on the structure activity relationship of the isolated aaptamine congeners were made in this study.

*Callyspongia* sp.

Sponges belonging to the genus *Callyspongia* have proven to be rich sources of various cytotoxic substances, such as polyketides, polyacetylenes, alkaloids, and cyclic peptides. Macrolides, however, have not been reported from this genus prior to this study. In the search for bioactive metabolites from marine organisms, the methanolic extract of the sponge *Callyspongia* sp., collected in Indonesia, was found to completely inhibit the growth of the murine lymphoma cell line L5178Y at a concentration of 10  $\mu\text{g/mL}$ . Chromatographic separation of the extract afforded a new bioactive macrolide, named callyspongiolide. The planar structure was unambiguously elucidated by means of 1D, 2D NMR, and HRESIMS measurements. The relative configuration of the macrocyclic core was established by analysing and interpreting the short and long range  $^1\text{H}$  to  $^{13}\text{C}$  coupling constants obtained from HSQC-HECADE. The absolute configuration at C-21 could not be

## 8 Abstract

---

assigned using the Mosher's method because the formation of the corresponding esters failed due to steric hindrance of C-21. Callyspongiolide exhibited strong activity against L51578 murine lymphoma cells, Jurkat T-lymphocytes and Ramos B-lymphocytes. Furthermore, it was subjected to an apoptosis induction assay (Nicoletti assay). However, the effect of callyspongiolide on viability could not be blocked by the parallel treatment with QVD-OPh, a caspase-inhibitor, thus suggesting a caspase independent induction of cell death.

In the final chapter possible biosynthetic pathways, mechanisms of action and the biogenetic origin of the isolated compounds are discussed.

### 2. Zusammenfassung

Mehr als 50% aller heutigen Medikamente auf dem Markt stammen von Naturstoffen ab. Traditionell wurden terrestrische Pflanzen als die Hauptproduzenten von Naturstoffen angesehen. Mit der Entdeckung der Antibiotika Anfang des 20. Jahrhunderts begann eine umfassende Suche nach Wirkstoffen aus Bakterien und Schimmelpilzen. Im Gegensatz zu ihren terrestrischen Vertretern, die seit als 4000 Jahren als Wirkstoffe Anwendung finden, waren marine Naturstoffe noch kaum erforscht. Erst mit der Entwicklung von Drucklufttauchgeräten (engl. SCUBA für self contained underwater breathing apparatus) vor etwa 60 Jahren konnte mit den Ozeanen eine neue Quelle für zukünftige Pharmazeutika erschlossen werden. Seitdem wurden mehr als 10000 neue marine Wirkstoffe mit interessanten pharmazeutische Eigenschaften entdeckt. Im ewigen Kampf gegen Krankheiten und Arzneimittelresistenzen wurden Tausende von möglichen Antiinfektiva und antitumoralen Wirkstoffen gefunden. Einige davon sind derzeit in präklinischen und klinischen Studien. Im Jahr 2010 wurde Halaven® (Eribulinmesylat) in die – bis jetzt noch kurze – Liste der von der FDA/EMA zugelassenen marinen Medikamente aufgenommen. Auf der Liste befinden sich momentan Prialt® (Ziconotid), Yondelis® (Trabectedin oder ET-743), Cytosar-U® (Cytarabin), Vira-A® (Vidarabin) and Adcetris® (Brentuximab). Heute sind marine Organismen wie Schwämme und Seescheiden mehr und mehr in den Fokus der Naturstoffforschung gerückt, da sie aufgrund ihrer Ortsgebundenheit hochwirksame Metaboliten produzieren müssen, um sich vor Fressfeinden und Lebensraumkonkurrenten zu schützen. Zytotoxische, antimikrobielle, antimykotische and antifouling Aktivitäten zählen zu den geläufigsten Wirkungen aus diesen Organismen. Die aus solchen Organismen isolierten Stoffe sind strukturell so einzigartig und komplex, dass der Gebrauch von hochmodernen Techniken und Geräten auf dem neuesten Stand der Dinge für die Strukturaufklärung unverzichtbar ist, wie beispielsweise 1D&2D NMR Spektroskopie ( $^1\text{H}$ ,  $^{13}\text{C}$ ,  $^{15}\text{N}$ , DEPT, COSY, HMQC, HMBC) einschließlich dem Einsatz von hochempfindlichen Probenköpfen und J-gekoppelte Experimente und hochauflösende Massenspektrometrie. Manchmal ist auch der Einsatz von chemischen Methoden wie organische Synthese oder Derivatisierungsreaktion für Konfigurationsbestimmung von Nöten, um eine komplette Strukturaufklärung zu erreichen. In dieser Arbeit wurden insgesamt 15 sekundäre Metaboliten aus zwei Schwämmen und einer Seescheide isoliert, von denen sieben als neu identifiziert wurden. Zusätzlich wurde eine Substanz vollsynthetisch präpariert. Die isolierten Stoffe wurden auf ihre zytotoxischen Eigenschaften untersucht. Dabei wurden verschiedene Bioassays und

Tumorzelllinien verwendet. In der vorliegenden Dissertation wurden die schon in wissenschaftlichen Journals veröffentlichten oder zur Veröffentlichung eingereichten Ergebnisse in Form von ihren entsprechenden Manuskripten dargestellt:

### *Polycarpa aurata*

Der Rohextrakt der Seescheide *Polycarpa aurata* lieferte sechs Substanzen, von denen zwei neu sind. Fünf von ihnen sind Abbauprodukte von Polycarpin, einem schwefelhaltigen Alkaloid mit einem 5 gliedrigen Heterozyklus und einer 4-Methoxyphenyl-Teilstruktur. Bei der anderen Substanz handelt es sich um N,N-didesmethylgrossularin-1, ein  $\alpha$ -Carbolinalkaloid. Die neuen Substanzen, Polycarpathiamin A und B, besitzen einen 3-amino-1,2,4-thiadiazol Ring. Die Strukturen wurden mithilfe von 1D, 2D NMR, and HRESIMS Messungen zweifelsfrei aufgeklärt. Weiterhin wurde die gesuchte heterozyklische Teilstruktur durch Vergleichen mit einem vollsynthetisierten Analogon, dem 3-Dimethylamino-5-benzoyl-1,2,4-thiadiazol, bestätigt. Polycarpathiamin A und die bekannten Substanzen Polycarpaurine C and N,N-Didesmethylgrossularin-1 zeigten eine signifikante zytotoxische Aktivität gegenüber murinen L5178Y Lymphomen.

### *Aaptos suberitoides*

Durch chromatographische Auftrennung des Rohextrakts von *Aaptos suberitoides* wurden acht Benzo[de][1,6]naphthyridinalkaloide (Aaptaminderivate) isoliert, von denen vier neue Naturstoffe sind. Die Strukturen der isolierten Substanzen wurden mithilfe von 1D, 2D NMR, and HRESIMS Messungen eindeutig bestimmt. Alle Substanzen wurden auf Zytotoxizität getestet, unter denen nur eine neue und zwei bekannte Metaboliten, Aaptamin and Demethylaaptamin, gegen murine L5178Y Lymphome eine nennenswerte Aktivität aufweisen. Desweiteren wurden Strukturaktivitätsbeziehungen von Aaptaminderivaten in dieser Studie diskutiert.

### *Callyspongia* sp.

In dieser Studie wird die Isolierung eines neuen Makrolids, Callyspogiolid, beschrieben, das einen 14 gliedrigen Ring besitzt. Ferner ist es das erste Makrolid überhaupt, das in einem *Callyspongia* Schwamm gefunden wurde. Seine planare Struktur wurde eindeutig per 1D, 2D NMR, und HRESIMS Messungen aufgeklärt. Die relative Konfiguration des Makrozyklus erhielt man nach Analyse und Interpretation von Kopplungskonstanten von  $^1\text{H}$  zu  $^{13}\text{C}$  über einfache und mehrere Atombindungen, erhalten durch HSQC-HECADE. Eine Bestimmung der absoluten Konfiguration eines Stereozentrums bei C-12 nach der

Mosher Methode war nicht möglich, da die Bildung der entsprechenden Mosher-Ester durch sterische Hinderung bei C-21 verhindert wurde. Callyspongiolid war hoch aktiv gegen murine L5178Y Lymphome, Jurkat T-Lymphozyten und Ramos B-Lymphozyten. Außerdem wurde mit der Substanz ein Apoptose-Induktions-Assay nach Nicoletti durchgeführt. Jedoch konnte die zytotoxische Wirkung von Callyspongiolide bei Zugabe von QVD-OPh, einem Caspase-Inhibitor, nicht blockiert werden. Aufgrund dieser Tatsache wird ein Caspase-unabhängiger Zelltod postuliert.

Im letzten Kapitel werden mögliche Biosynthesewege, Wirkmechanismen und der biogenetische Ursprung der isolierten Substanzen diskutiert.

### **3. Introduction**

More than 70% of our planet's surface is covered by the oceans, and life on Earth has its origin in the sea. This outstanding ecosystem called sea treasures a huge biodiversity – 34 of 36 extant phyla are solely found in the sea (Penn 2008; Arrieta, Arnaud-Haond et al. 2009) - and thus imparts an extraordinary chemical library of marine natural products with a diverse array of biological activities. Eventually, the marine environment opens up new frontiers to scientists from all kinds of disciplines such as pharmacology, biology, ecology, organic and bioorganic chemistry. With the advent of SCUBA diving in 1960s and modern high tech spectroscopic and mass spectrometric instruments since the 1980s, discovery of new natural products has skyrocketed: Until now over 17,000 different marine molecules have been discovered, 10,000 in the last two decades alone (Singh, Kumar et al. 2008).

#### **3.1 Significance of the study**

Chemistry and biological activities of marine natural products are an attractive investment for massive research efforts. The fact that an efficient anti-infective and cancer therapy is hindered by multi drug resistances and the very narrow therapeutic margins of most chemotherapeutic drugs necessitates the discovery and thorough study of novel potential drug candidates with prospectively novel mechanisms of action. Recent drug development has brought forth quite a number of drug leads such as Prilact® (ziconotide) or Yondelis® (trabectedin) which are successfully used in medical treatment, to mention only a few. With the rate of success and growth in natural product sciences, it is expected that the market for marine-derived pharmaceutical products will double by 2018 according to a report of Transparency Market Research. In order to meet these expectations and demands, further investigation in this research field must be done, as myriads of future potential remedies are still waiting to be discovered.

#### **3.2 Marine invertebrates**

Marine invertebrates are denoted as animals which lack a vertebral column and inhabit the sea. Common marine invertebrates comprise sponges, cnidarians, sea squirts, marine worms, lophophorates, mollusks, arthropods, echinoderms and the hemichordates. Approximately 60% of all marine animals are invertebrates (Ausubel, Crist et al. 2010). Many of these marine organisms especially sponges and ascidians are immobile and prone to feeding by predators and biofouling by other organisms, once they reach adulthood. In order to overcome this weakness they have developed different strategies to deter predators,

to prevent biofoulers to grow over them and to compete with rivals. This can be achieved by physical means such as continuous renewal of epithelial layers, change of wettability, production of mucus and spicules and more desirably by the production of highly potent secondary metabolites. The latter is the main reason why these animals have become the subject of immense interest.

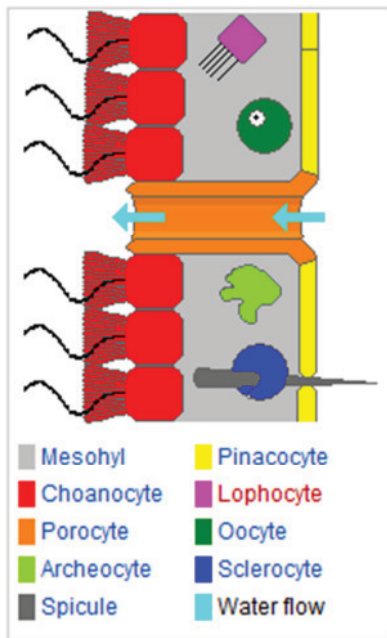
### 3.2.1 Sponges

Sponges or porifera constitute a phylum within the kingdom animalia. They are among the oldest living multicellular organisms with a fossil record dating back to about 600 million years. Their typical morphological characteristics are pores as indicated in “porifera” (from Latin porus (“pore”) + ferre (“to bear, to carry”)) (Brusca and Brusca 1990). They are often considered to be the most primitive animal group, largely due to their simple body structure that lacks actual tissues or organs, yet they represent a highly specialized and successful group of benthic suspension-feeders in marine and fresh waters. Sponges are widely distributed around the globe: besides tropical or subtropical zones which are the most common habitats for sponges, some species e.g. *Cinachyra antarctica* can also be found in inhospitable regions such as the Antarctic zone. The phylum porifera can be divided into three distinct classes: the Calcarea (calcareous sponges), the Hexactinellida (glass sponges) and the Demospongiae (demosponges). The latter forms the largest and most diverse class comprising 95% of all sponge species. Currently, about 8,000 extant species have been described, but the true number is estimated to be over 15,000 (van Soest et al. 2008: [www.marinespecies.org/porifera](http://www.marinespecies.org/porifera)). Typical habitats are tropical and subtropical coral reefs in temperate waters, but some species can also be found in the polar region, in the deep sea and fresh waters (Hooper, Van Soest et al. 2002). Unlike cnidarians, arthropoda and chordata including vertebrates sponges possess no real tissue and thus no organs and a nervous system, though their cells are differentiated and able to perform different body functions. The sponges’ hollow body is held in shape by the mesohyl, a jelly-like substance consisting mainly of collagen and reinforced by a dense network of fibers also consisting of collagen. Within this layer one can find different cell types moving and living in it (s. fig.1.1) such as lophocytes, collencytes, rhabdiferous cells, sclerocytes, which are responsible for maintaining the sponge’s structural stability by producing collagen and spicules, oocytes for the reproduction, myocytes (“muscle cells”) which conduct signals and cause parts of the animal to contract, “grey cells” as the sponge’s equivalent to the immune system and archaeocytes or amoebocytes which are totipotent cells capable of transforming into any other cell type.



The sponge's surface is covered by pinacocytes and the sponge's interior by choanocytes which are responsible for the uptake of nutrition via pino- and phagocytosis into vesicles by flagella and microvilli (Ruppert, Fox et al. 2004). Furthermore, the sponge's mesohyl can also contain endosymbionts, including bacteria, archaea, microalgae, and fungi. In some cases, these microbial associates comprise as much as 40% of the sponge volume. As sponges are filter feeders, they have to completely rely on the water flow carrying the nutrients. The water enters the central cavity within the sponge's body through the ostia (intake pores) where the choanocytes can take up the nutrients. The filtered water is ejected through the osculum at the top ("little mouth"). Since ambient currents are faster at the top, the suction effect that they produce does some of the work for free. Sponges can control the water flow by various combinations of wholly or partially closing the osculum and ostia and varying the beat of the flagella, and may shut it down if there is a lot of sand or silt in the water.

The body shapes of sponges vary immensely ranging from thin encrusting to massive hemispherical forms, from branching and tree-like forms, to plate or vase shapes, to spherical-, barrel- or volcano-shaped forms with a variety of colours (s. fig. 1.2-5).



Main cell types of Porifera<sup>[7]</sup>

**Figure 1.1** Ruppert et. al, 2004, Invertebrate Zoology (7<sup>th</sup> ed), Brooks/Cole, pp (. 78-82)



**Figure 1.2** *Callyspongia* sp.<sup>[1]</sup>



**Figure 1.3** *Xestospongia muta*<sup>[2]</sup>



**Figure 1.4** *Aaptos suberitoides*<sup>[3]</sup>

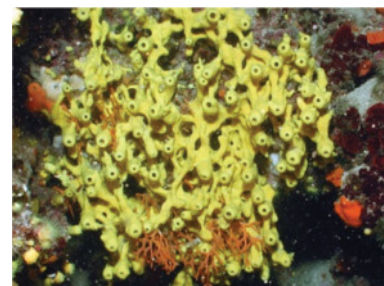


**Figure 1.5** *Aplysina cavernicola*<sup>[4]</sup>

[1] <http://tidechaser.blogspot.de/2013/03/sponges-porifera-singapore.html>  
 [2] [http://coralpedia.bio.warwick.ac.uk/en/sponges/xestospongia\\_muta.html](http://coralpedia.bio.warwick.ac.uk/en/sponges/xestospongia_muta.html)  
 [3] [http://www.fobi.web.id/fbi/d/46684-2/Aaptos-suberitoides\\_Pasir-Putih\\_FM\\_002.jpg](http://www.fobi.web.id/fbi/d/46684-2/Aaptos-suberitoides_Pasir-Putih_FM_002.jpg)  
 [4] [http://www.natuurlijkmooi.net/adriatische\\_zee/sponzen/aplysina\\_cavernicola.htm](http://www.natuurlijkmooi.net/adriatische_zee/sponzen/aplysina_cavernicola.htm)

### 3.2.2 Ascidians

Ascidians which are also known as sea squirts are animals whose typical anatomic feature is the tough outer “tunicate” made of tunicin (cellulose). Despite their sponge-like appearance ascidians constitute a class within the chordate phylum, thus making them closer related to vertebrates than any other animals from this phylum. There are about 3,000 known species of ascidians. These range from tiny ones 1 mm long, to those more than 10 cm. Like sponges ascidians exist in a variety of shapes, consistency (soft, rough, tough) and colours (s. fig. 1.6-1.9). Most are found in shallow waters but some species are found in very deep waters. In their larval stage ascidians possess a notochord which is a rigid cartilaginous rod-like structure - a feature which is shared by all chordates – which can function as “backbone”, though in adulthood this structure will eventually form back. Like sponges ascidians are widely distributed around the globe, even in the Antarctic waters (Núñez-Pons, Carbone et al. 2012). Ascidians can be solitary or colony forming like corals. Colonial species, e.g. *Didemnum molle*, consist of small zooids embedded in a common, usually gelatinous, test with varying degrees of complexity of colonial systems.



Figure 1.6 *Polycarpa aurata* <sup>[5]</sup>



Figure 1.7 *Megalodicopia hians* <sup>[6]</sup>



Figure 1.8 *Didemnum molle*.<sup>[7]</sup>

Although primitive compared to vertebrates, ascidians possess a much more complex body plan (s. fig. 4) than animals from many other phyla, especially *Porifera*. A heart, a circulatory system, nervous system, digestive system, gonads etc. are typical organs of higher developed animals. As filter feeders ascidians utilize two siphons to draw water through their bodies. The buccal siphon draws water and tiny food particles into the body where food is filtered against the pharyngeal basket and passed to the esophagus for digestion. Filtered water, body wastes, eggs and sperm, and in some species larvae, all exit the body by way of the atrial siphon.

[5] <http://www.ryanphotographic.com/images/JPEGS/Polycarpa%20aurata.jpg>

[6] <http://www.ryanphotographic.com/images/JPEGS/Megalodicopia%20hians%20predatory%20tunicate.jpg>

[7] <http://www.ryanphotographic.com/images/JPEGS/Didemnum%20molle.jpg>

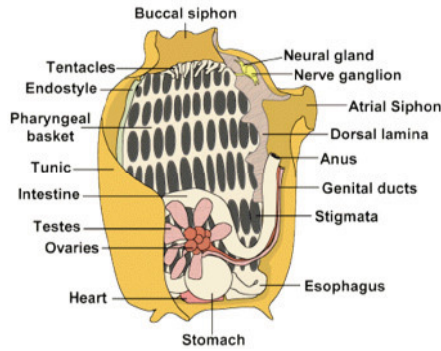


**Figure 1.9** Anatomy of a generalized, solitary ascidian. Redrawn from Barnes 1980

The heart is a curved muscular tube lying in the postabdomen, or close to the stomach. Each end opens into a single vessel, one running to the endostyle - longitudinal ciliated groove on the ventral wall of the pharynx which produces mucus to gather food particles - , and the other to the dorsal surface of the pharynx. The vessels are connected by a series of sinuses, through which the blood flows. Additional sinuses run from that on the dorsal surface, supplying blood to the visceral organs, and smaller vessels commonly run from both sides into the tunic. Nitrogenous waste, in the form of ammonia, is excreted directly from the blood through the walls of the pharynx, and expelled through the atrial siphon (Barnes 1982). There are four different types of blood cells: lymphocytes, phagocytic amoebocytes, nephrocytes and morula cells. The nephrocytes collect waste material such as uric acid and accumulate it in renal vesicles close to the digestive tract. The morula cells help to form the tunic, and can often be found within the tunic substance itself. They also possess immunomodulatory functions (Ballarin, Franchini et al. 2001). In some species, the morula cells possess pigmented reducing agents containing iron (hemoglobin), giving the blood a red colour, or vanadium giving it a green colour (Barnes 1982). In that case the cells are also referred to as *vanadocytes* (Michibata, Uyama et al. 2002). The ascidian central nervous system is formed from a plate that rolls up to form a neural tube. The number of cells within the central nervous system is very small. The neural tube is composed of the sensory vesicle, the neck, the visceral or tail ganglion, and the caudal nerve cord. Although there is no true brain, the largest ganglion is located in the connective tissue between the two siphons, and sends nerves throughout the body. Beneath this ganglion lies an exocrine gland that empties into the pharynx. The gland is formed from the nerve tube, and is therefore homologous to the spinal cord of vertebrates (Barnes 1982). Although the body wall has numerous individual receptors for touch, chemoreception, and the detection of light (Barnes 1982), ascidians have no real sense organs.

### 3.2.3 Microbial communities in marine invertebrates

Microbial symbioses have been described from most phyla of marine invertebrates: Porifera, Cnidaria, Bryozoa, Mollusca, Pogonophora, Echinodermata, Urochordata and Crustacea. Symbionts include bacteria, archaea and unicellular eukaryotes such as dinoflagellates. Interesting natural products have been found particularly in sponges, ascidians, cnidarians, bryozoans, and nudibranchs (Anthoni et al., 1990). The most prominent natural products of microbial (bacterial) origin are polyketide macrolides as it is known in the terrestrial environment from e.g. erythromycin produced by the actinobacteria *Streptomyces erythreus*. Although complex polyketides are generally regarded as microbial secondary metabolites, some have been isolated from metazoans. For example, bryostatin, halichondrin and leiodermatolide are complex polyketides isolated from bryozoans and sponges respectively (Pettit, Herald et al. 1982; Hirata 1986; Paterson, Dalby et al. 2011). However, since no metazoan polyketide synthases – the enzyme which is responsible for the polyketide synthesis – are known so far, one can assume that these compounds hail from the bacterial symbionts. Although this symbiont hypothesis remained unproven because of a general inability to cultivate the suspected producers, an investigation in 2001 showed a piece of evidence. Haygood et al. were able to provide evidence that the bryostatins are of bacterial origin, more precisely *Candidatus Endobugula sertula*, through gene cloning, cultivation with antibiotics and subsequent measurement of the bryostatin concentration (Davidson, Allen et al. 2001). In another investigation Piel et al. were able to identify an uncultured *Pseudomonas* sp. symbiont as the most likely producer of the defensive antitumor polyketide pederin in *Paederus fuscipes* beetles by cloning the putative biosynthesis genes. Therein, they report closely related genes isolated from the highly complex metagenome of the marine sponge *Theonella swinhoei*, which is the source of the onnamides and theopederins, a group of polyketides that structurally resemble pederin. They found that sequence features of the isolated genes clearly indicate that it belongs to a prokaryotic genome and should be responsible for the biosynthesis of almost the entire portion of the polyketide structure that is correlated with antitumor activity (Piel, Hui et al. 2004).

### 3.3 Marine natural products and their biological activities

Whereas the terrestrial environment has been screened for sources of new drugs for more than 4,000 years, until recently, the marine environment was to a large extent inaccessible for such investigations. Marine natural products exhibit a huge variety of biological activities. Undoubtedly cytotoxic, antimicrobial and antifouling make up the biggest portion of bioactivities, since those are the most relevant ones for survival. In addition to these, other marine natural products have been described in a recent review: Mayer et al. compiled a list of marine compounds with antidiabetic, antifungal, anti-inflammatory, antiprotozoal, antituberculosis and antiviral activities and activities affecting the immune and nervous systems (Mayer, Rodriguez et al. 2013). This thesis solely focuses on cytotoxic marine natural products due to their immense importance in the anticancer drug development.

The discovery of antitumor drugs aims at identifying chemical entities for use in the treatment of cancer. Unique metabolites produced by marine organisms have increasingly become major players in antitumor drug discovery. At the same time rapid advances have occurred in the understanding of tumor biology and molecular medicine giving new insights into mechanisms responsible for neoplastic disease. Recently identified molecular targets have created exciting new means for disrupting tumor-specific cell signaling, cell division, energy metabolism, gene expression, drug resistance, and blood supply. Such tumor-specific treatments could someday decrease the reliance on traditional cytotoxicity-based chemotherapy (chlorambucil, cyclophosphamide, platinum complexes, nucleobase analogues, epirubicine (s.fig. 1.10)) with severe side effects such as anemia, neutropenia, thrombocytopenia, nausea, vomiting, diarrhea, oral ulcerations, fatigue, nephrotoxicity, hepatotoxicity, cardiotoxicity, secondary infections etc.. They will also provide new less toxic treatment options with significantly fewer side effects. In addition to recent anticancer drug developments which have brought forth several “newer” agents with more specific targets such as imatinib (tyrosine kinase inhibitor), trastuzumab (Her2 receptor antagonist), bortezomib (proteasome inhibitor) cytotoxic marine natural products (s.fig. 1.11) can contribute a great portion to current anticancer treatment.

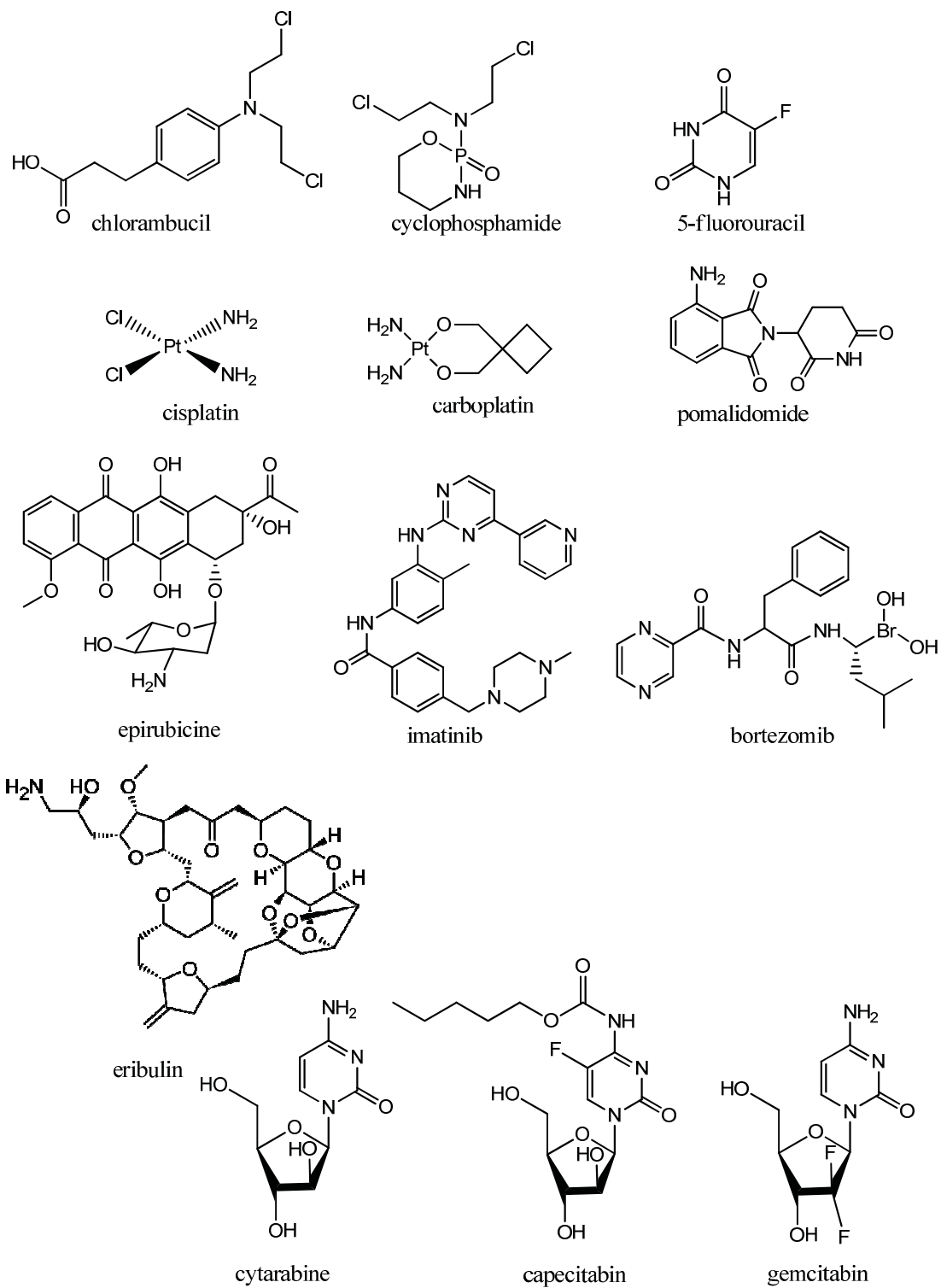


Figure 1.10 some of current anticancer therapeutic drugs



### 3.3.1 Angiogenesis

Angiogenesis is the physiological process through which new blood vessels form from pre-existing vessels. It is a normal and vital process in growth and development, as well as in wound healing and in the formation of granulation tissue. However, in the case of cancer it is also a fundamental step in the transition of tumors from a benign state to a malignant one. As the tumor grows, it requires more nutrients from the blood. Its increased demand can only be met by forming new blood vessels through overexpression and release of growth factors such as the vascular endothelial growth factor. Furthermore, this enables the tumor to spread throughout the body forming metastases. Current angiogenesis inhibitors include pomalidomide (thalidomide analogue), aflibercept and bevacizumab (monoclonal antibodies) targeting the VEGF.

From marine sources several antiangiogenic agents have been discovered. Among them are fascaplysin, indole alkaloids from the marine sponge *Fascaplysinopsis* sp., which were found to specifically inhibit the Cyclin dependent kinase 4. CDK4 is a key player in the regulation of the G0–G1 phase of the cell and is required for the G1/S phase transition. Furthermore, it also blocks the VEGF which would explain its antiangiogenic activity (Zheng, Lu et al. 2010).

Cortistatins are a family of eleven steroidal alkaloids isolated from the marine sponge *Corticium simplex*. Out of them, cortistatin A shows the most potent antiangiogenic activity. It was able to selectively inhibit the proliferation, migration and tube formation of human umbilical vein endothelial cells (HUVECs) (Aoki, Watanabe et al. 2006), which might be associated with its suppression of the phosphorylation of the unidentified 110 kDa protein in HUVECs (Aoki, Watanabe et al. 2007) and some kinases such as ROCK, CDK8 and CDK11 (Cee, Chen et al. 2009). The dimethylamino group and isoquinoline unit in the side chain of cortistatin A seemed to be crucial for its antiangiogenic and kinase inhibitory activities (Aoki, Watanabe et al. 2006).

### 3.3.2 Apoptosis

Apoptosis is the process of programmed cell death. As a cell undergoes this process, it shrinks, apoptotic bodies (vesicles containing cell organelles) are formed, chromatin condensation and DNA fragmentation occur as hallmarks of apoptosis. Inflammation does not occur, as opposed to necrosis in which the cell membrane ruptures and releases its contents initiating an inflammatory response. Apoptosis is important to a variety of normal processes such as fetal development, tissue homeostasis, immune response, aging, etc.. The

process of apoptosis is controlled by a diverse range of cell signals, which may originate either extracellularly (extrinsic inducers) or intracellularly (intrinsic inducers). The extrinsic pathway is a receptor mediated process meaning activation through ligand-receptor binding (“death receptor”) whereas the intrinsic pathway does not involve such. Extracellular signals may include toxins, hormones, growth factors or cytokines which induce the caspase dependent pathway. The stimuli for the intrinsic pathway are generally cell and DNA damage caused by radiation, toxins and viral infections. In the case of cancer apoptosis is only insufficient due to mutations in proto-oncogenes such as RAS and MYC (overexpression) and tumor suppressor genes such as p53 (underexpression).

Aurilide is a potent cytotoxic marine natural product that induces apoptosis in cultured human cells at the picomolar to nanomolar range. Results of a recent investigation by Sato et al. showed that aurilide selectively binds to prohibitin 1 (PHB1) in the mitochondria, activating the proteolytic processing of optic atrophy 1 (OPA1) and resulting in mitochondria-induced apoptosis (Sato, Murata et al. 2011). The mechanism of aurilide cytotoxicity suggests that PHB1 is an apoptosis-regulating protein amenable to modulation by small molecules. Aurilide may serve as a small-molecule tool for studies of mitochondria-induced apoptosis (Sato, Murata et al. 2011).

Some marine derived compounds that regulate protein kinases and phosphatases can indirectly affect the apoptotic process by modulating signal input/transmission to cell-death pathways: For example, bryostatins are macrocyclic lactones isolated from the marine bryozoan *Bugula neritica*. Bryostatin 1 - the most abundant of this group - was first known to inhibit the growth of murine P388 leukemia cells at subnanomolar concentrations (Pettit, Herald et al. 1982) through overactivation of protein kinase C. As a result, the PKC gene expression is significantly down-regulated, leading to inhibition of growth and apoptosis. Bryostatin is currently under phase I clinical trials (Mayer 2013).

### 3.3.3 Mitosis

Marine natural products that interrupt mitotic processes constitute perhaps the most important class of anticancer drug leads, as more have been characterized than perhaps any other class of antitumor/anticancer marine natural product (Hamel and Covell 2002). Tubulin is the major component of cellular microtubules, which maintain cell shape in interphase and form the mitotic spindle. Current drugs in medical treatment which target this structure are Vinca alkaloids and taxol which inhibit microtubule polymerisation and depolymerisation respectively.



One prominent example of important antimetabolic marine natural products is halichondrin B from the marine sponge *Halichondria okadai* (Hirata 1986) whose synthetic analogue eribulin mesylate is now marketed as Halaven™ since 2010 (Mayer 2013). It was shown to bind onto the vinca domain of tubulin (Bai, Paull et al. 1991).

More recently, leiodermatolide, a polyketide macrolide, was isolated from the marine sponge *Leiodermatium* sp.. It exhibited potent antimetabolic activity, and strongly inhibited cell proliferation in several cancer cell lines, including the human A549 lung adenocarcinoma, PANC pancreatic carcinoma, DLD-1 colorectal carcinoma, NCI/ADR-Res ovarian adenocarcinoma, P388 murine leukaemia, with IC<sub>50</sub> values of 3.3 nM, 5.0 nM, 8.3 nM, 233 nM, and 3.3 nM, respectively. However, the exact mechanism of action has not been identified yet (Paterson, Dalby et al. 2011).

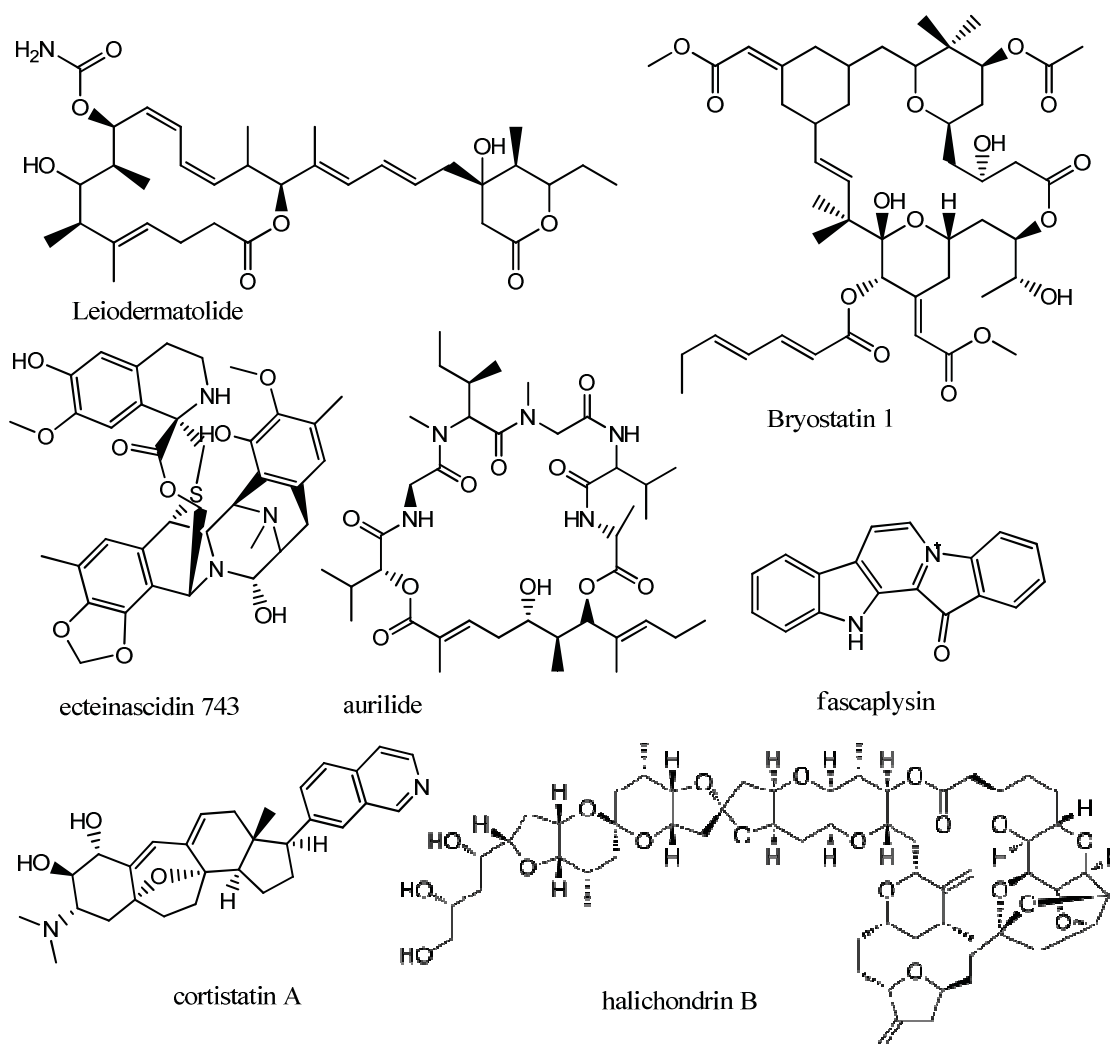


Figure 1.11 cytotoxic/anticancer marine natural products

### 3.3.4 Topoisomerases and DNA polymerases

The enzymes that control the number and topological conformations of supercoils in DNA are topoisomerases. Two types of topoisomerases have been isolated from both prokaryotes and eukaryotes - Type I (topo I) and Type II topoisomerase (topo II). Because of their role in regulating DNA tertiary structures, topoisomerases are essential to cellular processes such as DNA replication or recombination. Following the uncoiling the DNA replication is carried out by a DNA polymerase (pol) complex consisting of pol  $\alpha$ , pol  $\delta$ , and pol  $\epsilon$ .

Ecteinascidin 743 or trabectedin – marketed under the name of Yondelis® - from the sea squirt *Ecteinascidia turbinata* is an alkaloid featuring three fused tetrahydroisoquinoline rings. Two ring systems (subunits A+B) covalently bind the DNA and cause cross links, thus inhibiting any proteins essential for DNA replication such as topoisomerases and DNA polymerase. Additionally, the third ring (subunit C) protrudes from the DNA duplex, apparently allowing interactions with adjacent nuclear proteins, for example those which are involved in DNA repair (Dubois and Cohen 2009). Trabectedin also causes modulation of the production of cytokines and chemokines by tumor and normal cells, suggesting that the antitumor activity could also be ascribed to changes in the tumor microenvironment (D'Incalci and Galmarini 2010).

In 1951 Bergmann and Feeny reported the presence of the unusual arabinosyl nucleosides, spongothymidine, spongosine and spongouridine from the sponge *Cryptotethia crypta* (Bergmann and Feeney 1951). This work provided the lead compounds for the development of dozens of nucleoside analogues which are therapeutically used nowadays in anticancer treatment: Ara-C (cytarabine), gemcitabin, capecitabin, 5-fluorouracil etc.. As antimetabolites the nucleobase analogues are converted into nucleoside diphosphates and triphosphates which are then able to inhibit both the DNA and RNA polymerase and also cause DNA chain termination after being integrated as “false” nucleobases.

## 3.4 Current marine derived drugs in pre-clinical and clinical trials

Marine natural products proved appealing for scientific interests. Consequently, this led to the discovery of potentially active metabolites considered valuable for further preclinical or clinical trials. The FDA (Food and Drug Administration) approved Prialt® (also known as ziconotide) as a potent analgesic for severe chronic pain and Yondelis® (known also as trabectedin or ET-743) as an antitumor agent for the treatment of advanced soft tissue

sarcoma are the among well-known examples of marine derived drugs which have successfully been used in medical treatment. In 2010 Halaven™ (eribulin mesylate) entered the US drug market. In addition Aplidin® (plitidepsin), kahalalide F, and Zalypsis® (jorumycin derivative) are in clinical trials for treatment of solid tumors and haematological malignancies. Other drugs such as cytarabine and vidarabine are long known in the standard anticancer and antiviral treatment. Currently, there are still 11 other candidates to be tested in clinical trials, chiefly in cancer therapy (s. fig. 1.16 and 1.17). Furthermore about 1,000 other drug candidates with a huge array of biocativities are undergoing pre-clinical trials (Mayer, Rodriguez et al. 2013).

Clinical Status	Compound Name	Trademark	Marine Organism <sup>a</sup>	Chemical Class	Molecular Target	Clinical Trials <sup>b</sup>	Disease Area	Company/Institution <sup>c</sup>
FDA-Approved	Cytarabine (Ara-C)	Cytosar-U®	Sponge	Nucleoside	DNA polymerase	814	Cancer	1
	Vidarabine (Ara-A)	Vira-A®	Sponge	Nucleoside	Viral DNA polymerase	0	Antiviral	NA
	Ziconotide	Prialt®	Cone snail	Peptide	N-Type Ca channel	5	Pain	3
	Eribulin Mesylate (E7389)	Halaven®	Sponge	Macrolide	Microtubules	62	Cancer	4
	Omega-3-acid ethyl esters	Lovaza®	Fish	Omega-3 fatty acids	Trygliceride-synthesizing enzymes	124	Hypertriglyceridemia	5
	Trabectedin (ET-743) (EU Registered only)	Yondelis®	Tunicate	Alkaloid	Minor groove of DNA	42	Cancer	6
	Brentuximab vedotin (SGN-35)	Adcetris®	Mollusk/cyanobacterium	Antibody drug conjugate (MM auristatin E)	CD30 & microtubules	35	Cancer	7

**Figure 1.16** current pipeline of FDA approved marine derived pharmaceuticals as of Feb. 2013 (Mayer, A.M.S. Marine pharmaceuticals: the clinical pipeline. Midwestern University, Feb. 2013. Web.10.08.2013)

Phase III	Plitidepsin	Aplidin®	Tunicate	Depsipeptide	Rac1 & JNK activation	7	Cancer	6
Phase II	DMXBA (GTS-21)	NA	Worm	Alkaloid	α7 nicotinic acetylcholine receptor	4	Schizophrenia	UCHSC
	Plinabulin (NPI 2358)	NA	Fungus	Diketopiperazine	Microtubules & JNK stress protein	2	Cancer	8
	PM00104	Zalypsis®	Mollusk	Alkaloid	DNA-binding	3	Cancer	6
	PM01183	NA	Tunicate	Alkaloid	Minor groove of DNA	4	Cancer	6
	CDX-011	NA	Mollusk/cyanobacterium	Antibody drug conjugate (MM auristatin E)	Glycoprotein NMB & microtubules	3	Cancer	9
Phase I	Marizomib (Satinosporamide A; NPI-0052)	NA	Bacterium	Beta-lactone-gamma lactam	20S proteasome	4	Cancer	8
	PM060184	NA	Sponge	Polyketide	Minor groove of DNA	1	Cancer	6
	Bryostatins	NA	Bryozoan	Macrolide lactone	Protein kinase C	38	Cancer	10
	SGN-75	NA	Mollusk/cyanobacterium	Antibody drug conjugate (MM auristatin F)	CD70 & microtubules	2	Cancer	7
	ASG-5ME	NA	Mollusk/cyanobacterium	Antibody drug conjugate (MM auristatin E)	ASG-5 & microtubules	2	Cancer	7

**Figure 1.17** current clinical pipeline of marine derived pharmaceuticals as of Feb. 2013 (Mayer, A.M.S. Marine pharmaceuticals: the clinical pipeline. Midwestern University, Feb. 2013. Web. 10.08.2013)

### **3.5 Aim of the study**

Bioprospecting of marine natural products has yielded over 17,000 different unique compounds, most of them with potent biological activities against various microbes and cancer cells. Yet only a tiny fraction of the marine flora and fauna have been explored. Thus, this study will make its contribution to the quest in finding new leads from the sea. Based on the previous findings, this study focuses on the isolation and structure elucidation of secondary metabolites of the cytotoxic extracts from two sponges and one ascidian collected from Indonesia. The isolation work includes the use of separating columns, TLC and HPLC. Complete structure elucidation of the isolated compounds involves mass spectrometry, UV-, IR- and NMR-spectroscopy (routine experiments and more advanced coupled 2D NMR experiments such as HECAD-<sup>1</sup>HMQC), as well as a total synthesis of an analogous molecule as described in the second publication. Subsequently, bioassays such as the cytotoxicity assay against lymphoma L5178Y cell line, the viability assay and apoptosis induction assay against Jurkat J16 T lymphocytes and Ramos B lymphocytes round up this study on marine natural products.

#### **4. Publication 1: *Aaptos suberitoides***

Published in: “Journal of Natural Products”

Impact factor: 3.258

Contribution: 80%, first author, conducting most of the experiments (except those mentioned in “Declaration of academic honesty/Erklärung”), manuscript writing

Reprinted with permission from “Pham CD, Hartmann R, Müller W.E.G., de Voogd Nicole, Lai DW, Proksch P. (2013) Aaptamine Derivatives from the Indonesian Sponge *Aaptos suberitoides*”. J. Nat. Prod., 76: 103–106. Copyright 2013 American Chemical Society

## Aptamine Derivatives from the Indonesian Sponge *Aptos suberitoides*

Cong-Dat Pham, Rudolf Hartmann, Werner E. G. Müller, Nicole de Voogd, Daowan Lai, and Peter Proksch\*<sup>†</sup>

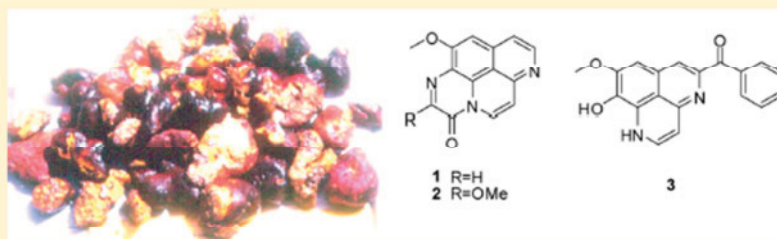
<sup>†</sup>Institute of Pharmaceutical Biology and Biotechnology, Heinrich-Heine University, Universitaetsstrasse 1, 40225 Duesseldorf, Germany

<sup>‡</sup>Institute of Complex Systems (ICS-6), Forschungszentrum Jülich GmbH, 52425 Jülich, Germany

<sup>§</sup>Institute of Physiological Chemistry and Pathobiochemistry, Johannes-Gutenberg-University, Duesbergweg 6, 55128 Mainz, Germany

<sup>⊥</sup>Naturalis Biodiversity Center, Darwinweg 2, 2300 RA Leiden, The Netherlands

### Supporting Information



**ABSTRACT:** Four new aptamine derivatives (1–4) along with aptamine (5) and three related compounds (6–8) were isolated from the ethanol extract of the sponge *Aptos suberitoides* collected in Indonesia. The structures of the new compounds were unambiguously determined by one- and two-dimensional NMR and by HRESIMS measurements. Compounds 3, 5, and 6 showed cytotoxic activity against the murine lymphoma L5178Y cell line, with  $IC_{50}$  values ranging from 0.9 to 8.3  $\mu$ M.

Marine invertebrates such as sponges are well-known sources of a wide variety of natural products, many of them containing nitrogen atoms.<sup>1</sup> One of the most prominent is aptamine, a benzo[de][1,6]naphthyridine alkaloid. It was first isolated from the Japanese sponge *Aptos aptos* and characterized by Nakamura et al. in 1982.<sup>2</sup> After that, numerous congeners were reported, which showed various biological activities, including cytotoxic, antiviral, antimicrobial, antifungal, antiparasitic,  $\alpha$ -adrenergic antagonistic, radical scavenging, and antifouling activity, as described by Larghi et al. in a recent review.<sup>3</sup> Furthermore, aptamine exhibits proteasomal inhibitory activity.<sup>4</sup> Aptamine-like compounds have also been found in sponges of other genera such as *Xestospongia*, *Suberites*, *Hymeniacion*, and *Luffariella*.<sup>3</sup> In particular, the genus *Aptos* continues to be an abundant source of novel aptamine alkaloids,<sup>3,5</sup> which still spurs interest in finding new bioactive metabolites.

In our search for bioactive metabolites<sup>6–8</sup> from marine organisms, we observed that the EtOH extract of the sponge *Aptos suberitoides*, collected in Ambon, Indonesia, inhibited the growth of the murine lymphoma L5178Y cell line at a concentration of 10  $\mu$ g/mL. Bioassay-guided separation afforded four new compounds (1–4), together with four known compounds, which were identified as aptamine (5)<sup>2</sup> demethyloptamine (6),<sup>9</sup> 8,9,9-trimethoxy-

9H-benzo[de][1,6]naphthyridine (7), and 8-methoxybenzimidazo[6,7,1-def][1,6]naphthyridine (8)<sup>10</sup> based on their spectroscopic data and by comparison with data in the literature. In this paper we describe the isolation, structure elucidation, and cytotoxicity of the four new compounds (1–4) as well as the bioactivity of the known compounds.

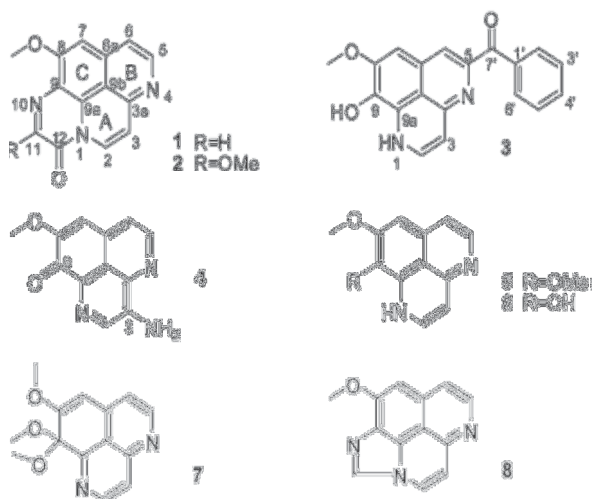
### RESULTS AND DISCUSSION

Compound 1 was obtained as a yellow solid, having greenishyellow fluorescence in MeOH solution. The HRESIMS spectrum of 1 showed a pseudomolecular ion peak at  $m/z$  252.07656  $[M + H]^+$ , indicating the molecular formula  $C_{14}H_9N_3O_2$ . The occurrence of two sets of coupled protons at  $\delta_H$  8.86 (d,  $J = 8.0$  Hz) and 7.55 (d,  $J = 8.0$  Hz), 8.69 (d,  $J = 5.8$  Hz) and 7.81 (d,  $J = 5.8$  Hz), one isolated singlet at  $\delta_H$  7.38, and one aromatic methoxy proton signal at  $\delta_H$  4.20 in the  $^1H$  NMR spectrum indicated that compound 1 was an aptamine congener, with an 8-methoxybenzo[de][1,6]naphthyridine skeleton.<sup>2</sup> Key HMBC correlations from H-2 ( $\delta_H$  8.86, d) to the aromatic carbons C-3 ( $\delta_C$  119.1), C-3a ( $\delta_C$  149.8), and C-9a ( $\delta_C$  128.9), from H-3 ( $\delta_H$  7.55, d) to C-2 ( $\delta_C$  127.5) and C

Received: November 13, 2012

Published: January 2, 2013





9b ( $\delta_C$  114.3), from H-5 ( $\delta_H$  8.69, d) to C-3a, C-6 ( $\delta_C$  118.6) and C-6a ( $\delta_C$  140.4), from H-6 ( $\delta_H$  7.81, d) to C-7 ( $\delta_C$  100.5) and C-9b, from H-7 ( $\delta_H$  7.38, s) to C-6, C-8 ( $\delta_C$  159.3), C-9 ( $\delta_C$  122.2), and C-9b, and from 8-OMe ( $\delta_H$  4.20) to C-8 confirmed this hypothesis (Figure 1). Apart from these signals,

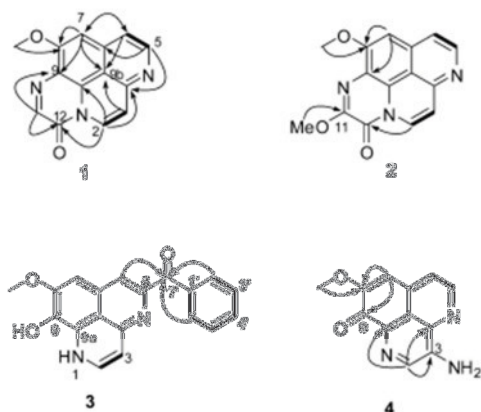


**Figure 1.** Selected HMBC (H→C) and COSY (bold line) correlations of 1–4 (only key correlations are shown; for full sets of HMBC correlations see Tables S1–S3 in the Supporting Information).

one olefinic methine ( $\delta_H$  8.50 s,  $\delta_C$  144.0 CH) and one quaternary sp<sup>2</sup> carbon ( $\delta_C$  152.7) remained unassigned. The latter was revealed to be attached to N-1 on the basis of the HMBC correlation from H-2 to this carbon (C-12), whereas the former was located at C-11 as suggested by the weak HMBC correlation from the olefinic methine proton (H-11,  $\delta_H$  8.50) to C-2 of the aaptamine nucleus. Additional correlation from H-11 to C-12 also supported the direct linkage between C-11 and C-12. This methine carbon (C-11) was further linked to C-9 via a heteroatom on the basis of the HMBC correlation from H-11 to C-9 as well as on consideration of its chemical shifts. The molecular formula indicated that this heteroatom could be either nitrogen or oxygen. An ether linkage between C-11 and C-9 was not supported by the chemical shifts of C-8 ( $\delta_C$  159.3) and C-9 ( $\delta_C$  122.2) when compared to demethylaaptamine (6)<sup>9</sup>; hence this possibility was ruled out. On the other hand, a nitrogen bridge between C-11 and C-9 could rationalize all the previously mentioned data. These data were also in good agreement with those of the reported aaptamine derivatives with 9-nitrogen substitution.<sup>10</sup> Finally, the quaternary carbon at C 12 ( $\delta_C$  152.7) has to be an amide carbonyl according to the molecular formula. Therefore, the structure of compound 1, which features a novel triazapyrene lactam skeleton, was unambiguously assigned. A substituted triazapyrene without a lactam has previously been reported.<sup>10</sup> Compound 2 was also obtained as a yellow solid and showed greenish yellow fluorescence in MeOH solution. HRESIMS of 2 showed its pseudomolecular ion peak at  $m/z$  282.08736 [ $M + H$ ]<sup>+</sup>, indicating the molecular formula C<sub>15</sub>H<sub>11</sub>N<sub>3</sub>O<sub>3</sub>, which differed from that of 1 by an additional methoxy group. The NMR spectroscopic data of 2 (Table 1) closely resembled those of 1, except for the presence of an additional aromatic methoxy signal at  $\delta_H$  4.23,  $\delta_C$  55.3. This methoxy group (11-OMe) was positioned at C-11, as confirmed by the HMBC correlation from 11-OMe to C-11 ( $\delta_C$  153.6). Thus, compound 2 was identified as the 11-methoxy derivative of 1. Compound 3 was obtained as a dark orange solid. HRESIMS analysis revealed a pseudomolecular ion at  $m/z$  319.1079 [ $M + H$ ]<sup>+</sup>, indicating the molecular formula C<sub>19</sub>H<sub>14</sub>N<sub>2</sub>O<sub>3</sub>. The NMR data of 3 (Table 2) were closely related to those of demethylaaptamine (6)<sup>9</sup> suggesting that they shared a

**Table 1.** <sup>1</sup>H (600 MHz) and <sup>13</sup>C NMR (150 MHz) Data of Compounds 1, 2, and 4 (CD<sub>3</sub>OD)

position	1		2		4	
	$\delta_C$ , type <sup>a</sup>	$\delta_H$ , mult. (J)	$\delta_C$ , type <sup>a</sup>	$\delta_H$ , mult. (J)	$\delta_C$ , type	$\delta_H$ , mult. (J)
2	127.5, CH	8.86, d (8.0)	129.7, CH	8.85, d (7.8)	134.8, CH	8.34, brs
3	119.1, CH	7.55, d (8.0)	114.8, CH	7.37, d (7.8)	149.7, C	
3a	149.8, C		147.7, C		136.4, C	
5	148.2, CH	8.69, d (5.8)	141.3, CH	8.42, d (6.0)	152.6, CH	8.83, d (7.8)
6	118.6, CH	7.81, d (5.8)	118.5, CH	7.79, d (6.0)	124.5, CH	7.67, d (7.8)
6a	140.4, C		137.8, C		136.9, C	
7	100.5, CH	7.38, s	101.6, CH	7.48, s	108.6, CH	6.95, s
8	159.3, C		159.9, C		158.6, C	
9	122.2, C		119.7, C		177.1, C	
9a	128.9, C		126.1, C		133.8, C	
9b	114.3, C		114.5, C		119.9, C	
11	144.0, CH	8.50, s	153.6, C			
12	152.7, C		148.2, C			
8-OMe	56.9, CH <sub>3</sub>	4.20, s	57.0, CH <sub>3</sub>	4.20, s	56.7, CH <sub>3</sub>	3.97 s
11-OMe			55.3, CH <sub>3</sub>	4.23, s		

<sup>a</sup>Data extracted from HSQC and HMBC spectra.

Table 2.  $^1\text{H}$  (600 MHz), and  $^{13}\text{C}$  (150 MHz) NMR Data of Compound 3 ( $\text{CD}_3\text{OD}$ ) and HMBC Correlations

no.	$\delta_{\text{C}}$ , type	$\delta_{\text{H}}$ , mult. (J)	HMBC (H $\rightarrow$ C)
2	143.65, CH	7.85, d <sup>a</sup>	3, 3a, 9a (weak)
3	99.1, CH	6.58, d (6.1)	2, 9b
3a	153.2, C		
5	143.67, C		
6	124.1, CH	7.42, s	6a, 7, 9b, 7'
6a	135.3, C		
7	106.1, CH	7.34, s	6, 8 (weak), 9, 9b
8	153.2, C		
9	135.0, C		
9a	127.1, C		
9b	119.0, C		
1'	137.2, C		
2'(6')	130.5, CH	7.86, d <sup>a</sup>	7', 4', 6'(2')
3'(5')	129.9, CH	7.60, t (7.6)	1', 5'(3')
4'	134.3, CH	7.72, t (7.4)	2'(6')
7'	190.0, C		
8-OMe	57.3, CH <sub>3</sub>	4.04, s	8

<sup>a</sup>Signal partially overlapped.

common aaptamine skeleton. This was confirmed by similar HMBC correlations within the skeleton, as described for compounds 1 and 2 (Figure 1). However, an additional benzoyl group was found in 3, as evidenced by the occurrence of one triplet at  $\delta_{\text{H}}$  7.72 (H-4'), one triplet integrated as 2H at  $\delta_{\text{H}}$  7.60 (H-3' and -5'), and one doublet integrated as 2H at  $\delta_{\text{H}}$  7.86 (H-2' and -6') in the  $^1\text{H}$  NMR spectrum and their corresponding carbon signals at  $\delta_{\text{C}}$  134.3 (CH, C-4'), 129.9 (2CH, C-3' and -5'), 130.5 (2CH, C-2' and -6'), 137.2 (C, C-1'), and 190.0 (keto group, C-7') in the  $^{13}\text{C}$  NMR spectrum. Moreover, the HMBC experiment not only confirmed the presence of the benzoyl group but also established its linkage to the aaptamine nucleus. The correlations from H-2'(6') to C-1', C-4', C-6'(2'), and C-7', from H-3'(5') to C-1' and C-5'(3'), and from H-4' to C-2'(6') revealed a benzoyl substructure, which was connected to the skeleton at C-5 because H-6 ( $\delta_{\text{H}}$  7.42, s) correlated with C-7' as well. Therefore, compound 3 was identified as the 5-benzoyl derivative of 6 and given the name 5-benzoyldemethylaaptamine. This structure represents a hitherto unprecedented benzoyl-aaptamine skeleton.

Compound 4 was obtained as a dark red-violet solid. HRESIMS analysis revealed pseudomolecular ions at  $m/z$  228.0766  $[\text{M} + \text{H}]^+$ , 250.0587  $[\text{M} + \text{Na}]^+$ , and 477.1280  $[2\text{M} + \text{Na}]^+$ , indicating the molecular formula  $\text{C}_{12}\text{H}_9\text{N}_3\text{O}_2$ . The NMR data (Table 1) indicated that compound 4 was an aaptamine derivative. However, in this molecule H-2 ( $\delta_{\text{H}}$  8.34, brs) occurs as a singlet and the chemical shift of C-3 is at 149.7 ppm, thus leading to the conclusion that C-3 is a quaternary carbon connected to a heteroatom. Moreover, a carbonyl group ( $\delta_{\text{C}}$  177.1) located at C-9 was detected in the  $^{13}\text{C}$  NMR spectrum, which can be rationalized by the HMBC correlation from H-7 ( $\delta_{\text{H}}$  6.95, s) to C-9. Finally, the molecular formula indicated that a  $\text{NH}_2$  has to be connected to C-3. Both proton and carbon-13 chemical shifts of compound 4 are comparable with those of demethyl(oxy)aaptamine described by Calcut et al.<sup>10</sup> Thus, compound 4 is established as the 3-amino derivative of demethyl(oxy)aaptamine and named 3-amino demethyl(oxy)-aaptamine.

Compounds 1–8 were examined for their effects on the growth of the L5178Y mouse lymphoma cell line using the

MTT assay. Compound 6 showed pronounced cytotoxicity against the L5178Y cell line ( $\text{IC}_{50}$  0.9  $\mu\text{M}$ ) compared to the positive control kahalalide F ( $\text{IC}_{50}$  4.3  $\mu\text{M}$ ), while compounds 3 and 5 inhibited the growth of L5178Y cells, with  $\text{IC}_{50}$  values of 5.5 and 8.3  $\mu\text{M}$ , respectively, as shown in Table 3. The remaining compounds exhibited no activity ( $\text{IC}_{50} > 10 \mu\text{M}$ ).

Table 3. Cytotoxic Activities of Compounds 1–8

compound	L5178Y growth inhibition in % (at 10 $\mu\text{g}/\text{mL}$ )	$\text{IC}_{50}$ ( $\mu\text{M}$ )
1	0.0	n.d. <sup>a</sup>
2	38.6	n.d.
3	93.7	5.5
4	64.4	n.d.
5	100.0	8.3
6	100.0	0.9
7	51.2	n.d.
8	98.7	13.5
kahalalide F <sup>b</sup>		4.3

<sup>a</sup> n.d. = not determined. <sup>b</sup>Positive control.

A tentative suggestion on the structure–activity relationships of the aaptamine derivatives is proposed on the basis of these results. Demethylaaptamine (6) showed the strongest activity among all of the isolated compounds, whereas methylation of the hydroxy group at C-9 as in compound 5 ( $\text{IC}_{50}$  8.3  $\mu\text{M}$ ) caused a significant decrease of the activity. Loss of aromaticity in ring C, more specifically modification at C-9 as in compound 7, resulted in a further decrease of bioactivity (51.2% inhibition at 10  $\mu\text{g}/\text{mL}$ ). Similarly, hydrogenation of ring B at C-5 and C-6 also negatively affected the activity as described by Shen et al.<sup>11</sup> Substitution at both C-9 and N-1 decreased the inhibitory activity, as in the case of compound 8 ( $\text{IC}_{50}$  13.5  $\mu\text{M}$ ) compared to 5 ( $\text{IC}_{50}$  8.3  $\mu\text{M}$ ) and 6 ( $\text{IC}_{50}$  0.9  $\mu\text{M}$ ), whereas the presence of an additional carbonyl group at C-12 rendered compounds 1 and 2 inactive even at a concentration of 10  $\mu\text{g}/\text{mL}$  (growth inhibition: 0% and 38.6%). In addition, substitution at C-5 as in compound 3 also led to a decrease of bioactivity. However, substitution at C-3 does not result in a loss of general cytotoxicity, as similar compounds with or without this substitution showed significant activity against CEM-SS (T-lymphoblastic leukemia).<sup>12</sup> Oxidation of C-9 into C=O as for compound 4 also correlated with a significant decrease of activity.

## EXPERIMENTAL SECTION

**General Experimental Procedures.** UV spectra were measured in a Perkin-Elmer Lambda 25 UV/vis spectrometer.  $^1\text{H}$ ,  $^{13}\text{C}$ , and 2D NMR spectra were recorded at 25  $^{\circ}\text{C}$  in  $\text{CD}_3\text{OD}$  on a Bruker ARX 600 NMR spectrometer (for 3 and 4) or on a Varian Inova 600 MHz spectrometer (for 1 and 2) equipped with a Z-axis pulse-field-gradient triple resonance cryoprobe. Standard pulse sequences were used for HSQC and HMBC experiments. Chemical shifts were referenced to the solvent residual peaks,  $\delta_{\text{H}}$  3.31 for  $^1\text{H}$  and  $\delta_{\text{C}}$  49.0 for  $^{13}\text{C}$ . Mass spectra (ESI) were recorded with a Finnigan LCQ Deca mass spectrometer, and HRMS (ESI) spectra were obtained with an FTHRMS-Orbitrap (Thermo-Finnigan) mass spectrometer. Solvents were distilled prior to use, and spectral grade solvents were used for spectroscopic measurements. HPLC analysis was performed with a Dionex UltiMate3400 SD with an LPG-3400SD pump coupled to a photodiode array detector (DAD3000RS); routine detection was at 235, 254, 280, and 340 nm. The separation column (125  $\times$  4 mm) was pre-filled with Eurosphere-10 C18 (Knauer), and the



following gradient was used (MeOH, 0.02% H<sub>3</sub>PO<sub>4</sub> in H<sub>2</sub>O): 0 min (10% MeOH); 5 min (10% MeOH); 35 min (100% MeOH); 45 min (100% MeOH). Semipreparative HPLC was performed using a Merck Hitachi HPLC System (UV detector L-7400; pump L-7100; Eurosphere-100 C18, 300 × 8 mm, Knauer). Column chromatography included Diaion HP-20, LH-20 Sephadex, and Merck MN silica gel 60 M (0.04–0.063 mm). TLC plates with silica gel F254 (Merck) were used to monitor fractions (CH<sub>2</sub>Cl<sub>2</sub>/MeOH mixtures as mobile phase); detection was under UV at 254 and 366 nm or by spraying the plates with anisaldehyde reagent.

**Animal Material.** The sponge was collected by scuba in Ambon, Indonesia, on October 1996 at the depth of 3 m and identified as *Aaptos suberitoides* by one of the authors (N.d.V.). The color of its exterior was dark brown, and the interior is yellow; the specimen turns dark brown upon collection. The sponge was preserved in a mixture of EtOH and H<sub>2</sub>O (70:30) and stored in a –20 °C freezer. A voucher specimen (number RMNH POR.7268) is stored in the sponge collection at the Naturalis Biodiversity Center.

**Extraction and Isolation.** The frozen material was thawed and cut into small pieces (wet weight: 500 g) and then extracted with MeOH. The subsequent liquid–liquid phase separation gave a 1-butanol (8 g) and an EtOAc (1.0 g) fraction. At first the 1-butanol fraction was subjected to chromatographic separation using Diaion HP-20 employing a step gradient of H<sub>2</sub>O/MeOH to yield five fractions, H1–H5. H5 (880 mg) was submitted to consecutive LH-20 Sephadex size exclusion chromatography. From these fractions compounds 1, 2, 4, 5, and 8 were obtained by semipreparative HPLC and preparative TLC. In the same manner compounds 3, 6, and 7 were isolated from the EtOAc fraction. The yields were as follows: 1 (0.93 mg), 2 (0.92 mg), 3 (3.32 mg), 4 (5.45 mg), 5 (2.1 mg), 6 (0.6 mg), 7 (0.43 mg), and 8 (2.8 mg).

#### **11-Methoxy-3H-[1,6]naphthyridino[6,5,4-def]**

**quinoxalin-3-one (1):** yellow solid (greenish-yellow fluorescence in MeOH); UV ( $\lambda_{\max}$ , MeOH) (log  $\epsilon$ ) 203.3 (3.83), 222.9 (3.74), 270.9 (3.40), 280.6 (3.40), 414.9 (3.30), 436.9 (3.26) nm; <sup>1</sup>H and <sup>13</sup>C NMR data, see Table 1; ESIMS m/z 252.1 [M + H]<sup>+</sup>; HRESIMS m/z 252.07656 [M + H]<sup>+</sup> (calcd for C<sub>14</sub>H<sub>10</sub>N<sub>3</sub>O<sub>2</sub>, 252.07675).

#### **2,11-Dimethoxy-3H-[1,6]naphthyridino[6,5,4-def]**

**quinoxalin-3-one (2):** yellow solid (greenish-yellow fluorescence in MeOH); UV ( $\lambda_{\max}$ , MeOH) (log  $\epsilon$ ) 204.1 (3.29), 221.3 (3.27), 259.8 (3.20), 278.7 (3.17), 359.2 (2.74), 380.0 (2.86), 399.6 (2.98), 422.2 (2.93) nm; <sup>1</sup>H and <sup>13</sup>C NMR data, see Table 1; ESIMS m/z 282.1 [M + H]<sup>+</sup>; HRESIMS m/z 282.08736 [M + H]<sup>+</sup> (calcd for C<sub>15</sub>H<sub>12</sub>N<sub>3</sub>O<sub>3</sub>, 282.08732).

**5-Benzoyldemethylaaptamine (3):** dark orange solid; UV ( $\lambda_{\max}$ , MeOH) (log  $\epsilon$ ) 233.3 (4.19), 266.1 (sh) (3.96), 407.3 (3.73) nm; <sup>1</sup>H and <sup>13</sup>C NMR data, see Table 2; ESIMS m/z 319.3 [M + H]<sup>+</sup>; HRESIMS m/z 319.1079 [M + H]<sup>+</sup> (calcd for C<sub>19</sub>H<sub>15</sub>N<sub>2</sub>O<sub>3</sub>, 319.1077).

**3-Aminodemethyl(oxy)aaptamine (4):** dark red-violet solid; UV ( $\lambda_{\max}$ , MeOH) (log  $\epsilon$ ) 245.4 (3.69), 275.7 (3.60), 478.1 (3.43) nm; <sup>1</sup>H and <sup>13</sup>C NMR data, see Table 1; ESIMS m/z 228.2 [M + H]<sup>+</sup>, 250.1 [M + Na]<sup>+</sup>, 476.9 [2M + Na]<sup>+</sup>; HRESIMS m/z 228.0766 [M + H]<sup>+</sup> (calcd for C<sub>12</sub>H<sub>10</sub>N<sub>3</sub>O<sub>2</sub>, 228.0768), 250.0587 [M + Na]<sup>+</sup> (calcd for C<sub>12</sub>H<sub>9</sub>N<sub>3</sub>O<sub>2</sub>Na, 250.0587), 477.1280 [2M + Na]<sup>+</sup> (calcd for C<sub>24</sub>H<sub>18</sub>N<sub>6</sub>O<sub>4</sub>Na, 477.1282).

**Bioassay.** Cytotoxicity was tested against L5178Y mouse lymphoma cells using the microculture tetrazolium (MTT) assay and compared to that of untreated controls, as described previously.<sup>13,14</sup> Experiments were repeated three times and carried out in triplicate. As negative controls, media with 0.1% EGMME/ DMSO were included in the experiments. The

depsipeptide kahalalide F, isolated from *Elysia grandifolia*<sup>13</sup>, was used as a positive control.

## ■ ASSOCIATED CONTENT

### Supporting Information

<sup>1</sup>H, <sup>13</sup>C, <sup>2</sup>D NMR, and MS spectra for compounds 1–4 and full sets of HMBC correlations for compounds 1, 2 and 4 (see Tables S1–S3) are available free of charge via the Internet at <http://pubs.acs.org>.

## ■ AUTHOR INFORMATION

### Corresponding Author

\*Tel: +49 211 81 14187 (D.L.), +49 211 81 14163 (P.P.). Fax: +49 211 81 11923. E-mail: [laidaowan123@gmail.com](mailto:laidaowan123@gmail.com) (D.L.), [proksch@uni-duesseldorf.de](mailto:proksch@uni-duesseldorf.de) (P.P.).

### Notes

The authors declare no competing financial interest.

## ■ ACKNOWLEDGMENTS

P.P. thanks BMBF for support. We thank E. Ferdinandus and L.A. Pattisina (Marine Science Center, Fisheries Faculty, Pattimura University, Ambon, Indonesia) and Sudarsono (Faculty of Pharmacy, Gadjah Mada University, Yogyakarta, Indonesia) for help while collecting the sponges.

## ■ REFERENCES

- Blunt, J. W.; Copp, B. R.; Munro, M. H. G.; Northcote, P. T.; Prinsep, M. R. *Nat. Prod. Rep.* 2011, 28, 196–268.
- Nakamura, H.; Kobayashi, J.; Ohizumi, Y.; Hirata, Y. *Tetrahedron Lett.* 1982, 23, 5555–5558.
- Larghi, E. L.; Bohn, M. L.; Kaufman, T. S. *Tetrahedron* 2009, 65, 4257–4282.
- Tsukamoto, S.; Yamanokuchi, R.; Yoshitomi, M.; Sato, K.; Ikeda, T.; Rotinsulu, H.; Mangindaan, R. E. P.; de Voogd, N. J.; van Soest, R. W. M.; Yokosawa, H. *Bioorg. Med. Chem. Lett.* 2010, 20, 3341–3343.
- Liu, C.; Tang, X.; Li, P.; Li, G. *Org. Lett.* 2012, 14, 1994–1997.
- Liu, D.; Xu, J.; Jiang, W.; Deng, Z.; de Voogd, N. J.; Proksch, P.; Lin, W. *Helv. Chim. Acta* 2011, 94, 1600–1607.
- Lai, D.; Li, Y.; Xu, M.; Deng, Z.; van Ofwegen, L.; Qian, P.; Proksch, P.; Lin, W. *Tetrahedron* 2011, 67, 6018–6029.
- Yan, P.; Deng, Z.; van Ofwegen, L.; Proksch, P.; Lin, W. *Chem. Biodiversity* 2011, 8, 1724–1734.
- Nakamura, H.; Kobayashi, J.; Ohizumi, Y.; Hirata, Y. *J. Chem. Soc., Perkin Trans. 1* 1987, 173–176.
- Calcul, L.; Longeon, A.; Mourabit, A. A.; Guyot, M.; Bourguet-Kondracki, M.-L. *Tetrahedron* 2003, 59, 6539–6544.
- Shen, Y.-C.; Lin, T.-T.; Sheu, J.-H.; Duh, C.-Y. *J. Nat. Prod.* 1999, 62, 1264–1267.
- Shaari, K.; Ling, K. C.; Mat Rashid, Z.; Jean, T. P.; Abas, F.; Raof, S. M.; Zainal, Z.; Lajis, N. H.; Mohamad, H.; Ali, A. M. *Mar. Drugs* 2009, 7, 1–8.
- Ashour, M.; Edrada, R.; Ebel, R.; Wray, V.; Wätjen, W.; Padmakumar, K.; Müller, W. E. G.; Lin, W. H.; Proksch, P. *J. Nat. Prod.* 2006, 69, 1547–1553.
- Carmichael, J.; DeGraff, W. G.; Gazdar, A. F.; Minna, J. D.; Mitchell, J. B. *Cancer Res.* 1987, 47, 943–946.

## Supporting information

### **Aptamine derivatives from the Indonesian sponge *Aaptos suberitoides***

Cong-Dat Pham,<sup>†</sup> Rudolf Hartmann,<sup>‡</sup> Werner E. G. Müller,<sup>§</sup> Nicole de Voogd,<sup>⊥</sup>

Daowan Lai,<sup>†,\*</sup> Peter Proksch<sup>†,\*</sup>

<sup>†</sup> Institute of Pharmaceutical Biology and Biotechnology, Heinrich-Heine University, Universitätsstrasse 1, 40225 Duesseldorf, Germany;

<sup>‡</sup> Institute of Complex Systems (ICS-6), Forschungszentrum Jülich GmbH, 52425 Jülich, Germany;

<sup>§</sup> Institute of Physiological Chemistry and Pathobiochemistry, Johannes-Gutenberg-University, Duesbergweg 6, 55128 Mainz, Germany;

<sup>⊥</sup> Naturalis Biodiversity Center, Darwinweg 2, 2300 RA Leiden, The Netherlands.

\* Corresponding authors.

Tel.: +49 211 81 14187 (D.L.), +49 211 81 14163 (P.P.); Fax: +49 211 81 11923.

E-mail addresses: laidaowan123@gmail.com (D.L.), proksch@uni-duesseldorf.de (P.P.).

## Contents

Table S1 $^1\text{H}$ and $^{13}\text{C}$ NMR data and HMBC correlations of compound 1 ( $\text{CD}_3\text{OD}$ ).....	33
Table S2 $^1\text{H}$ and $^{13}\text{C}$ NMR data and HMBC correlations of compound 2 ( $\text{CD}_3\text{OD}$ ).....	34
Table S3 $^1\text{H}$ and $^{13}\text{C}$ NMR data and HMBC correlations of compound 4 ( $\text{CD}_3\text{OD}$ ).....	35
Fig 1-1 $^1\text{H}$ NMR spectrum of 1 in $\text{CD}_3\text{OD}$ .....	36
Fig 1-2 HSQC spectrum of 1 in $\text{CD}_3\text{OD}$ .....	37
Fig 1-3 HMBC spectrum of 1 in $\text{CD}_3\text{OD}$ .....	38
Fig 1-4 HRESIMS spectrum of 1 .....	39
Fig 2-1 $^1\text{H}$ NMR spectrum of 2 in $\text{CD}_3\text{OD}$ .....	40
Fig 2-2 HSQC spectrum of 2 in $\text{CD}_3\text{OD}$ .....	41
Fig 2-3 HMBC spectrum of 2 in $\text{CD}_3\text{OD}$ .....	42
Fig 2-4 HRESIMS spectrum of 2 .....	42
Fig 3-1-1 $^1\text{H}$ NMR spectrum of 3 in $\text{CD}_3\text{OD}$ .....	43
Fig 3-1-2 $^1\text{H}$ NMR spectrum of 3 in $\text{CD}_3\text{OD}$ (Enlargement of aromatic region).....	43
Fig 3-2 $^{13}\text{C}$ NMR spectrum of 3 in $\text{CD}_3\text{OD}$ .....	44
Fig 3-3 $^1\text{H}$ , $^1\text{H}$ COSY spectrum of 3 in $\text{CD}_3\text{OD}$ .....	45
Fig 3-4 HSQC spectrum of 3 in $\text{CD}_3\text{OD}$ .....	46
Fig 3-5 HMBC spectrum of 3 in $\text{CD}_3\text{OD}$ .....	47
Fig 3-6 HRESIMS spectrum of 3 .....	48
Fig 4-1 $^1\text{H}$ NMR spectrum of 4 in $\text{CD}_3\text{OD}$ .....	49
Fig 4-2 $^{13}\text{C}$ NMR spectrum of 4 in $\text{CD}_3\text{OD}$ .....	50
Fig 4-3 DEPT 135 spectrum of 4 in $\text{CD}_3\text{OD}$ .....	51
Fig 4-4 HSQC spectrum of 4 in $\text{CD}_3\text{OD}$ .....	52
Fig 4-5 HMBC spectrum of 4 in $\text{CD}_3\text{OD}$ .....	53
Fig 4-6 HRESIMS spectrum of 4 .....	54

Table S1 <sup>1</sup>H and <sup>13</sup>C NMR data and HMBC correlations of compound 1 (CD<sub>3</sub>OD)

Position	δ <sub>H</sub>	δ <sub>C</sub> *	HMBC (H→C)
2	8.86 d (8.0)	127.5 CH	3, 3a, 9a, 12
3	7.55 d (8.0)	119.1 CH	2, 3a (w), 6a (w), 9b
3a	-	149.8 C	-
5	8.69 d (5.8)	148.2 CH	3a, 6, 6a, 9b (w)
6	7.81 d (5.8)	118.6 CH	5, 6a (w), 7, 9a (w), 9b
6a	-	140.4 C	-
7	7.38 s	100.5 CH	6, 8, 9, 9a (w), 9b
8	-	159.3 C	-
9	-	122.2 C	-
9a	-	128.9 C	-
9b	-	114.3 C	-
11	8.50 s	144.0 CH	2 (w), 9, 9a (w), 12 (w)
12	-	152.7 C	-
8-OMe	4.20 s	56.9 CH <sub>3</sub>	7 (w), 8

\* Data extracted from HSQC, and HMBC spectra.

w: indicates “weak” correlation

Table S2 <sup>1</sup>H and <sup>13</sup>C NMR data and HMBC correlations of compound 2 (CD<sub>3</sub>OD)

Position	$\delta_{\text{H}}$	$\delta_{\text{C}}^*$	HMBC (H→C)
2	8.85 d (7.8)	129.7 CH	3 (w), 3a, 9a, 12
3	7.37 d (7.8)	114.8 CH	2, 9b
3a	-	147.7 C	-
5	8.42 d (6.0)	141.3 CH	3a, 6, 6a, 9b (w)
6	7.79 d (6.0)	118.5 CH	5, 6a (w), 7, 9a (w), 9b
6a	-	137.8 C	-
7	7.48 s	101.6 CH	6, 8, 9, 9a (w), 9b
8	-	159.9 C	-
9	-	119.7 C	-
9a	-	126.1 C	-
9b	-	114.5 C	-
11	-	153.6 C	-
12	-	148.2 C	-
8-OMe	4.20 s	57.0 CH <sub>3</sub>	8
11-OMe	4.23 s	55.3 CH <sub>3</sub>	11

\* Data extracted from HSQC, and HMBC spectra.

w: indicates "weak" correlation

Table S3  $^1\text{H}$  and  $^{13}\text{C}$  NMR data and HMBC correlations of compound 4 ( $\text{CD}_3\text{OD}$ )

Position	$\delta_{\text{H}}$	$\delta_{\text{C}}$	HMBC (H $\rightarrow$ C)
2	8.34 br.s	134.8 CH	3, 3a, 9a
3	-	149.7 C	-
3a	-	136.4 C	-
5	8.83 d (7.8)	152.6 CH	3a, 6, 6a, 9b (w)
6	7.67 d (7.8)	124.5 CH	5, 7, 9b
6a	-	136.9 C	-
7	6.95 s	108.6 CH	6a (w), 6, 8, 9, 9b
8	-	158.6 C	-
9	-	177.1 C	-
9a	-	133.8 C	-
9b	-	119.9 C	-
8-OMe	3.97 s	56.7 $\text{CH}_3$	7 (w), 8

w: indicates "weak" correlation

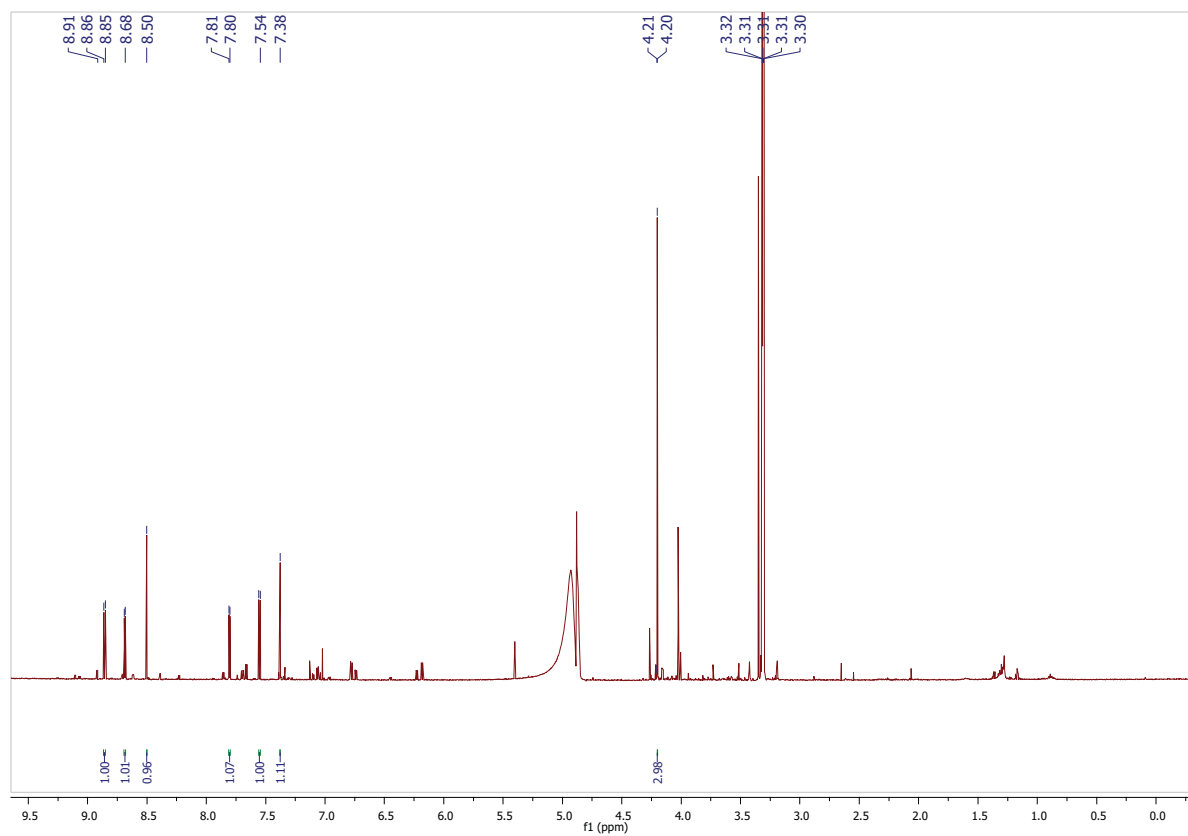


**Fig 1-1**  $^1\text{H}$  NMR spectrum of **1** in  $\text{CD}_3\text{OD}$

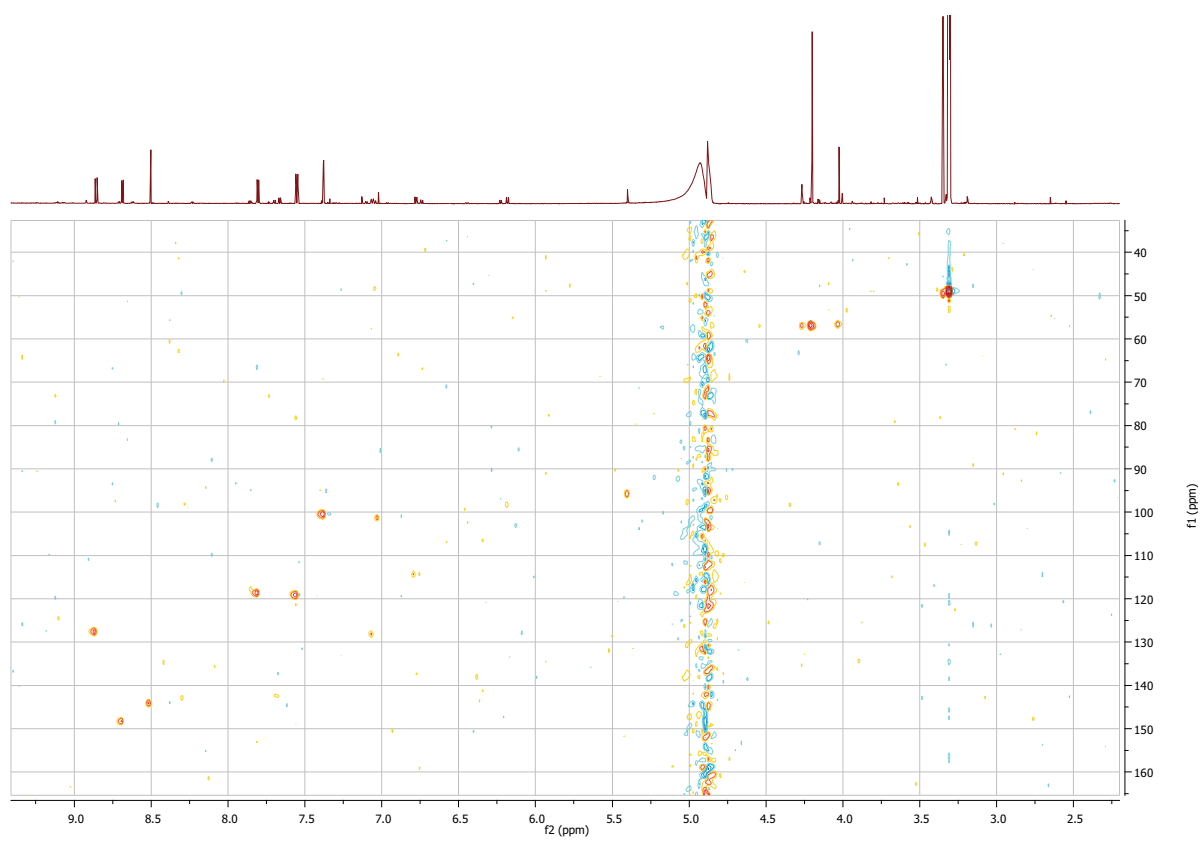


**Fig 1-2** HSQC spectrum of **1** in CD<sub>3</sub>OD



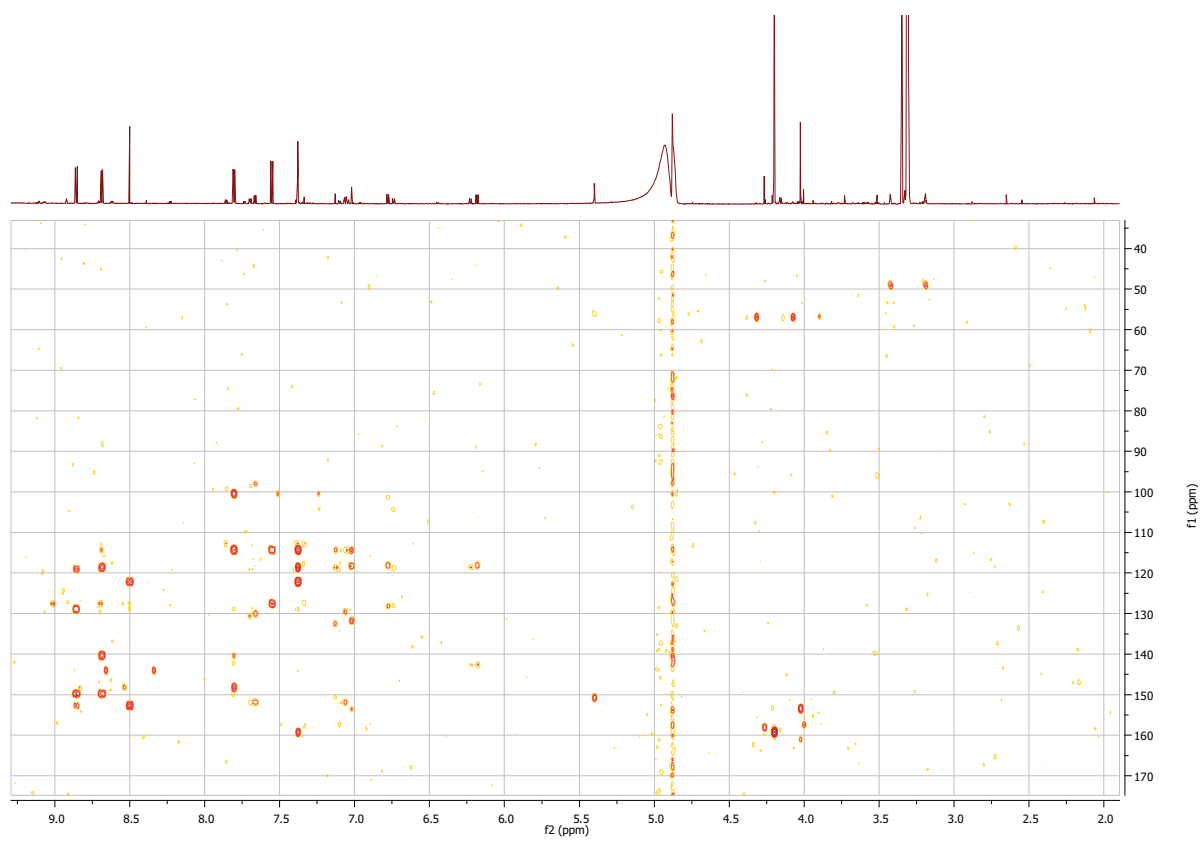
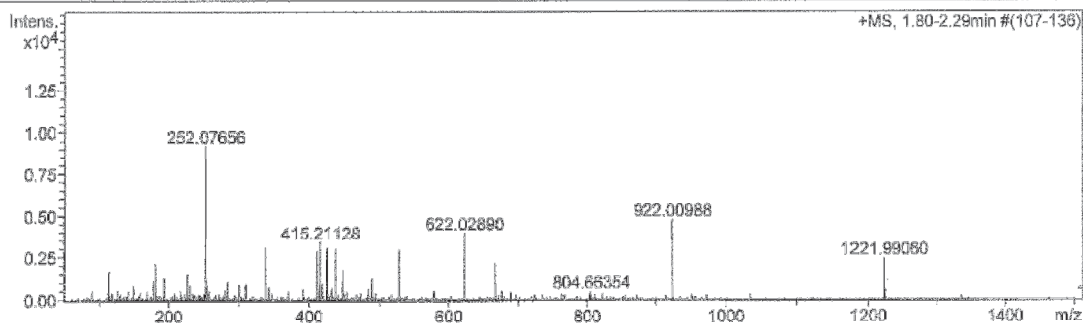


**Fig 1-3** HMBC spectrum of **1** in CD<sub>3</sub>OD

## Mass Spectrum SmartFormula Report

Analysis Info Acquisition Date 8/9/2012 10:19:44 AM  
Analysis Name D:\Data\HHU Services\Proksch000012.d  
Method tune\_low.m Operator Peter Tommes  
Sample Name Cong-Dat Pham TF33BH5.3 TLC MeOH (CH3CN/H2O) Instrument / Ser# maXis 4G 20213  
Comment

Acquisition Parameter  
Source Type ESI Ion Polarity Positive Set Nebulizer 0.3 Bar  
Focus Not active Set Capillary 4000 V Set Dry Heater 180 °C  
Scan Begin 50 m/z Set End Plate Offset -500 V Set Dry Gas 4.0 l/min  
Scan End 1500 m/z Set Collision Cell RF 600.0 Vpp Set Divert Valve Source



Meas. m/z	#	Formula	Score	m/z	err [mDa]	err [ppm]	mSigma	rdc	e <sup>-</sup> Conf	N-Rule
252.07656	1	C 14 H 10 N 3 O 2	100.00	252.07675	0.19	0.76	9.7	11.5	even	ok

Fig 1-4 HRESIMS spectrum of 1

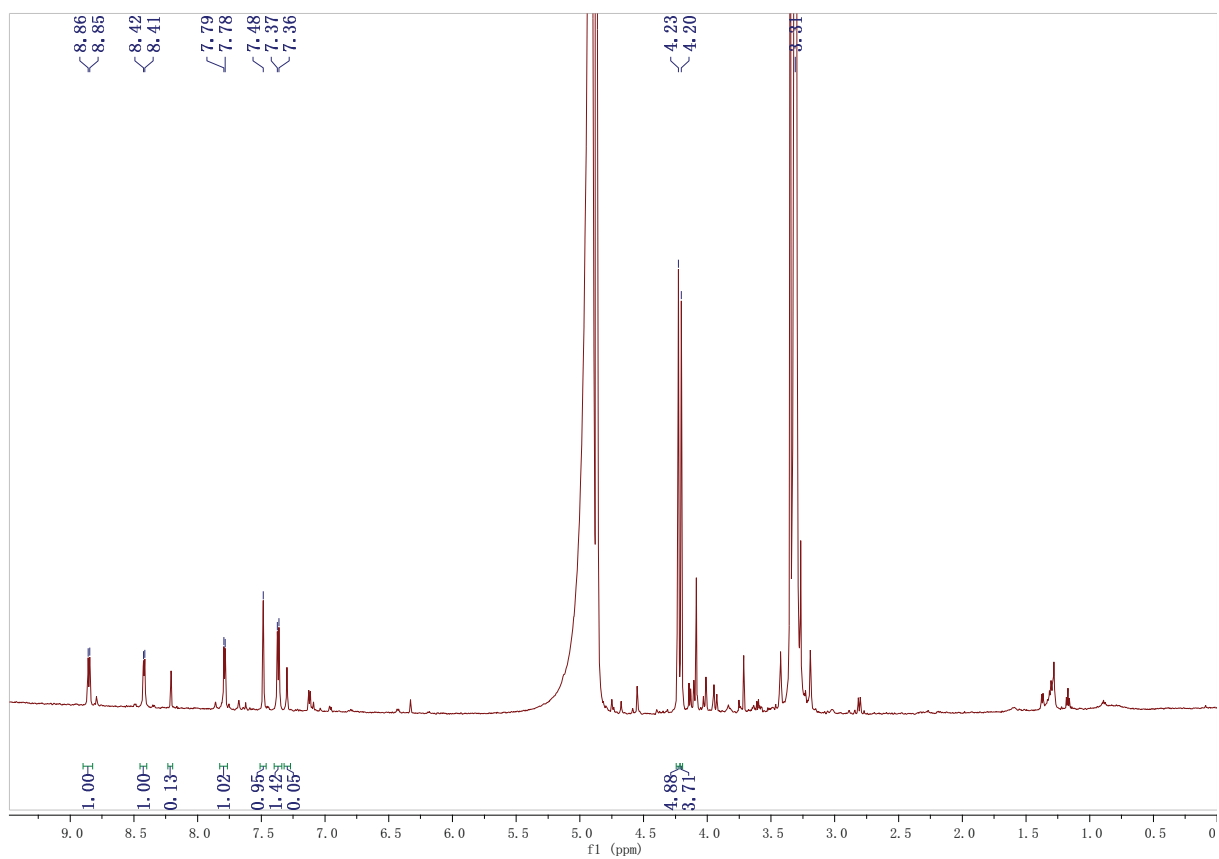
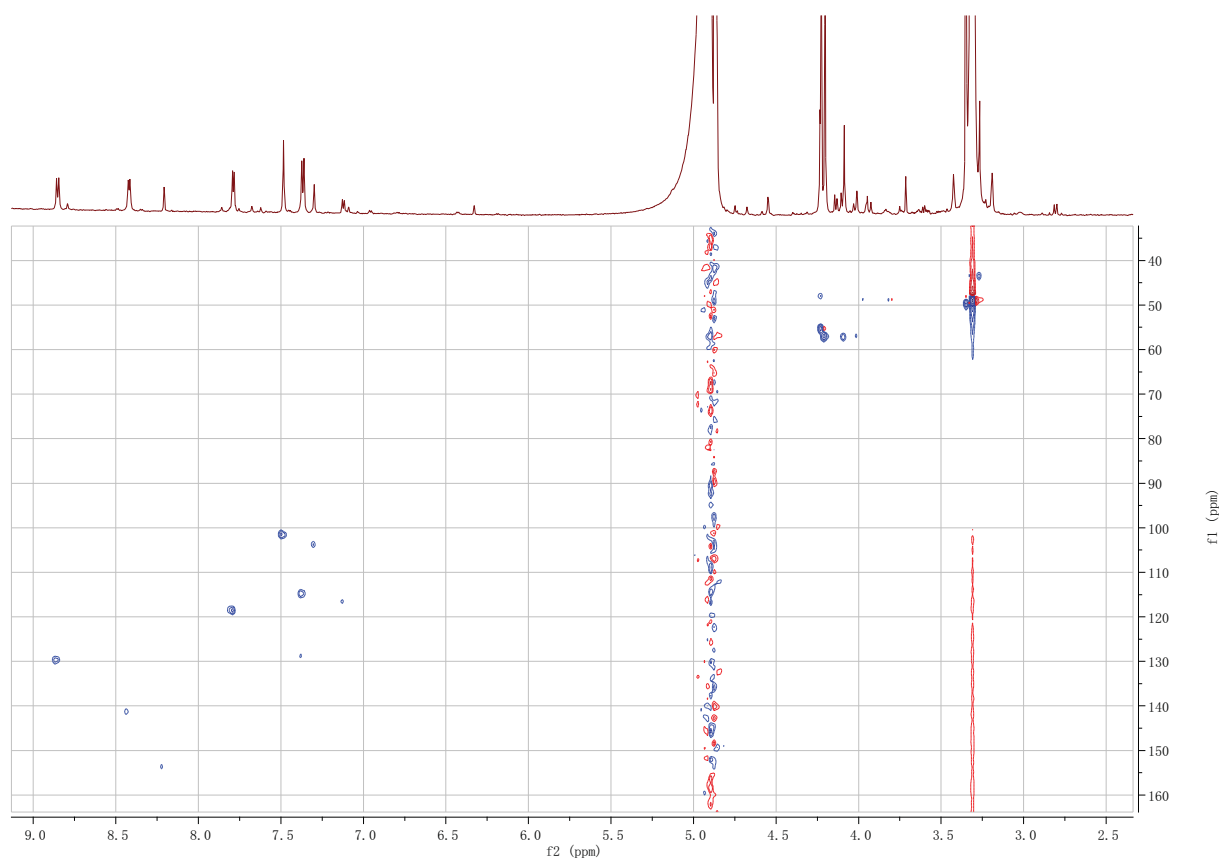
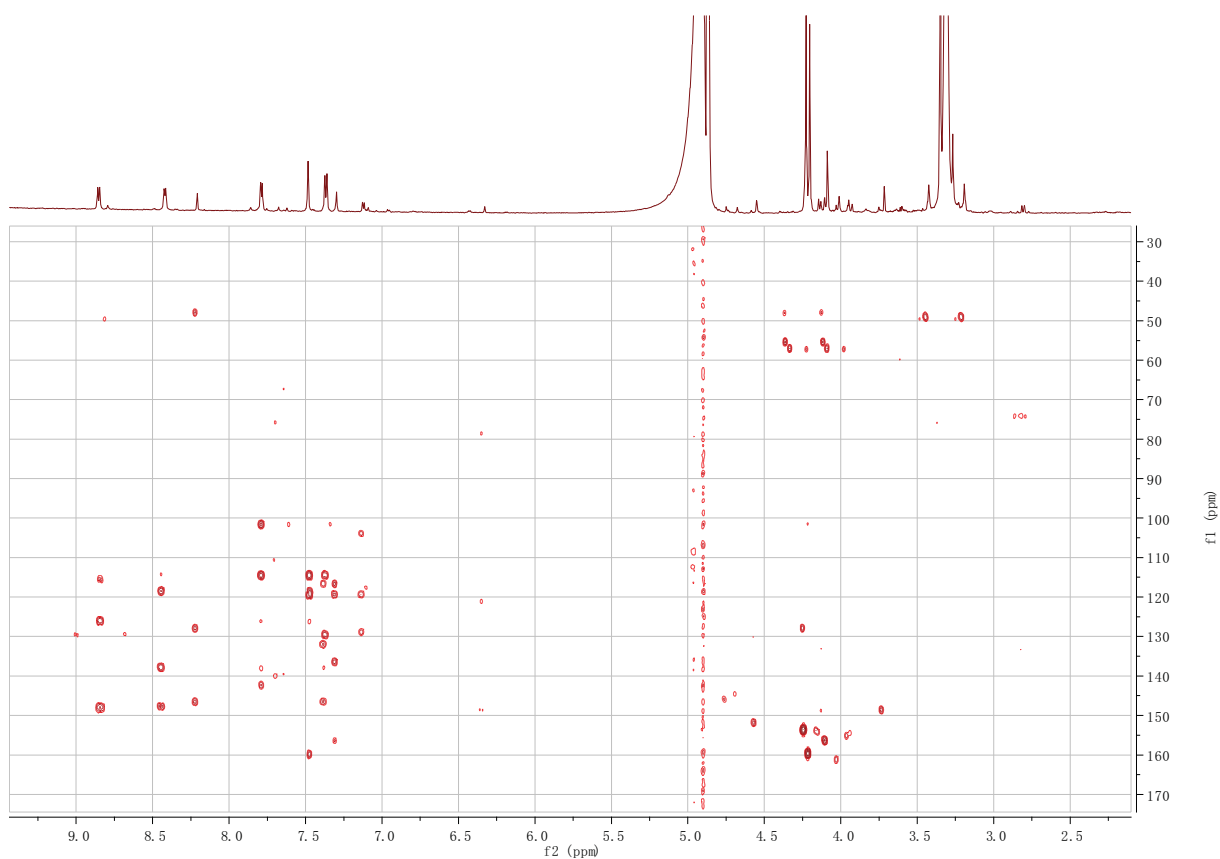


Fig 2-1  $^1\text{H}$  NMR spectrum of **2** in  $\text{CD}_3\text{OD}$



**Fig 2-2** HSQC spectrum of **2** in CD<sub>3</sub>OD

Fig 2-3 HMBC spectrum of 2 in CD<sub>3</sub>OD

### Mass Spectrum SmartFormula Report

Analysis Info		Acquisition Date	
Analysis Name	D:\Data\HHU Service\Proksch000007.d	7/30/2012 3:20:21 PM	
Method	tune_low.m	Operator	Peter Tommes
Sample Name	Cong-Dat Pham TF33BH5S8.3 SP3 (CH <sub>3</sub> CN/H <sub>2</sub> O)	Instrument / Ser#	maXis 4G 20213
Comment			

Acquisition Parameter			
Source Type	ESI	Ion Polarity	Positive
Focus	Not active	Set Capillary	4000 V
Scan Begin	50 m/z	Set End Plate Offset	-600 V
Scan End	1500 m/z	Set Collision Cell RF	600.0 Vpp
		Set Nebulizer	0.3 Bar
		Set Dry Heater	180 °C
		Set Dry Gas	4.0 l/min
		Set Divert Valve	Source

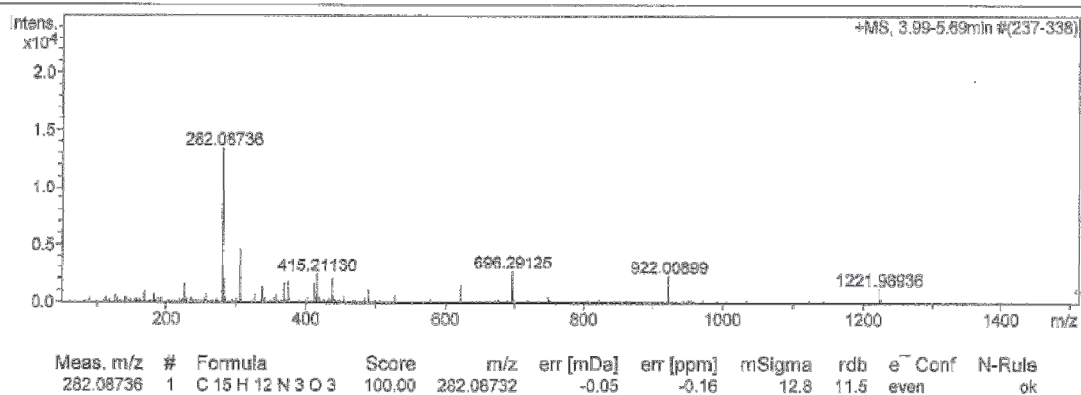
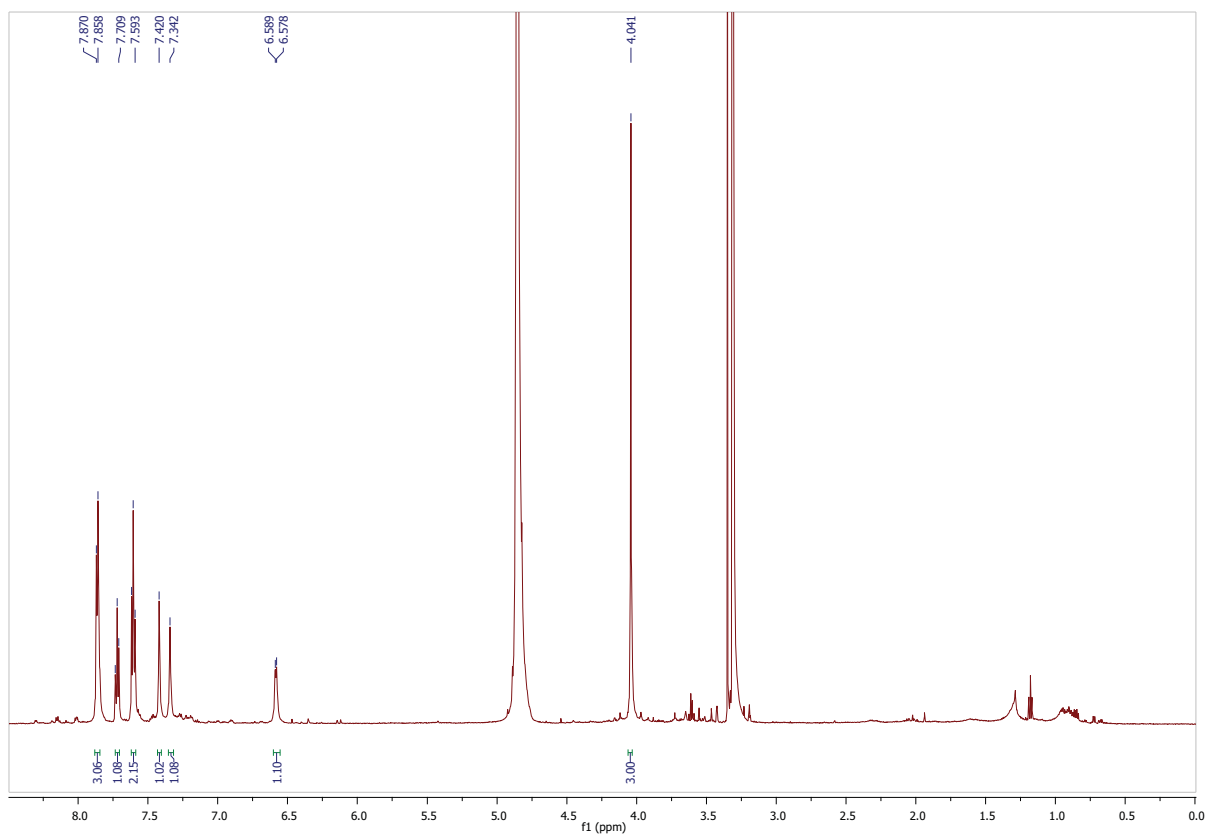
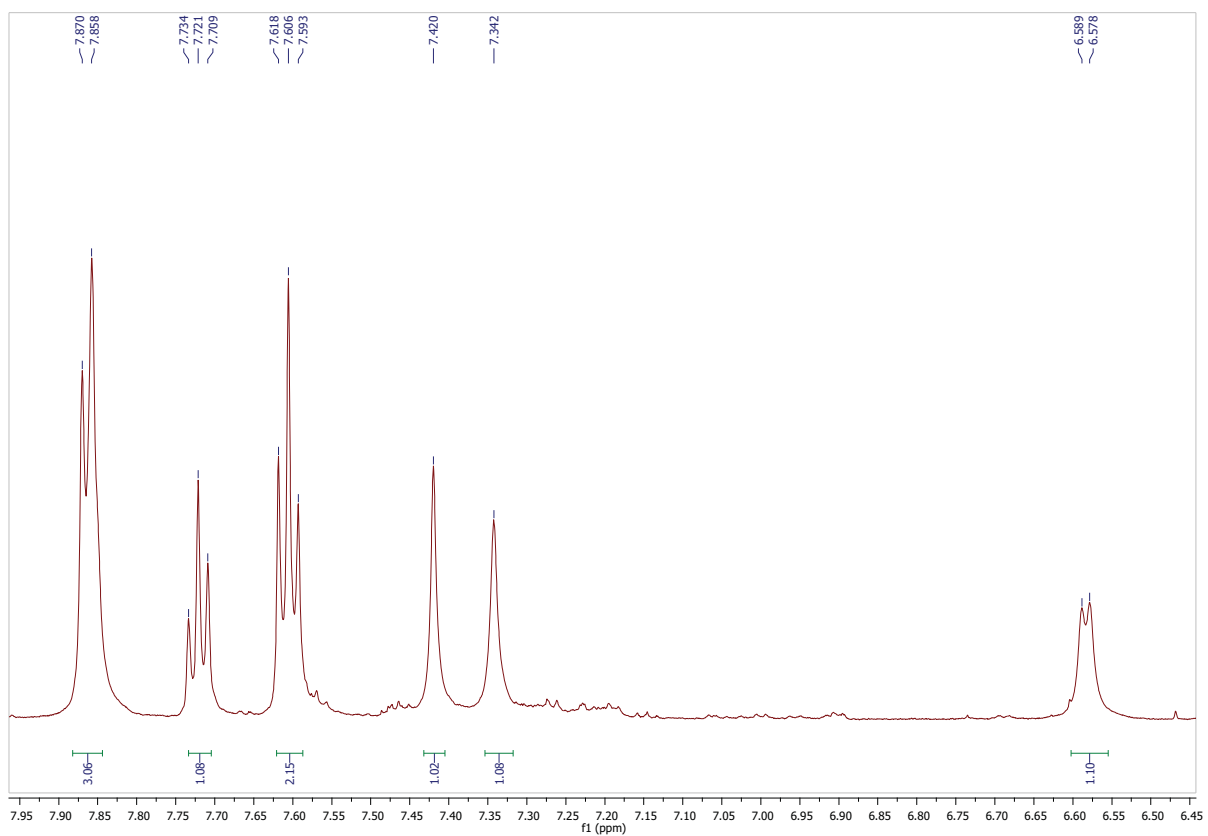
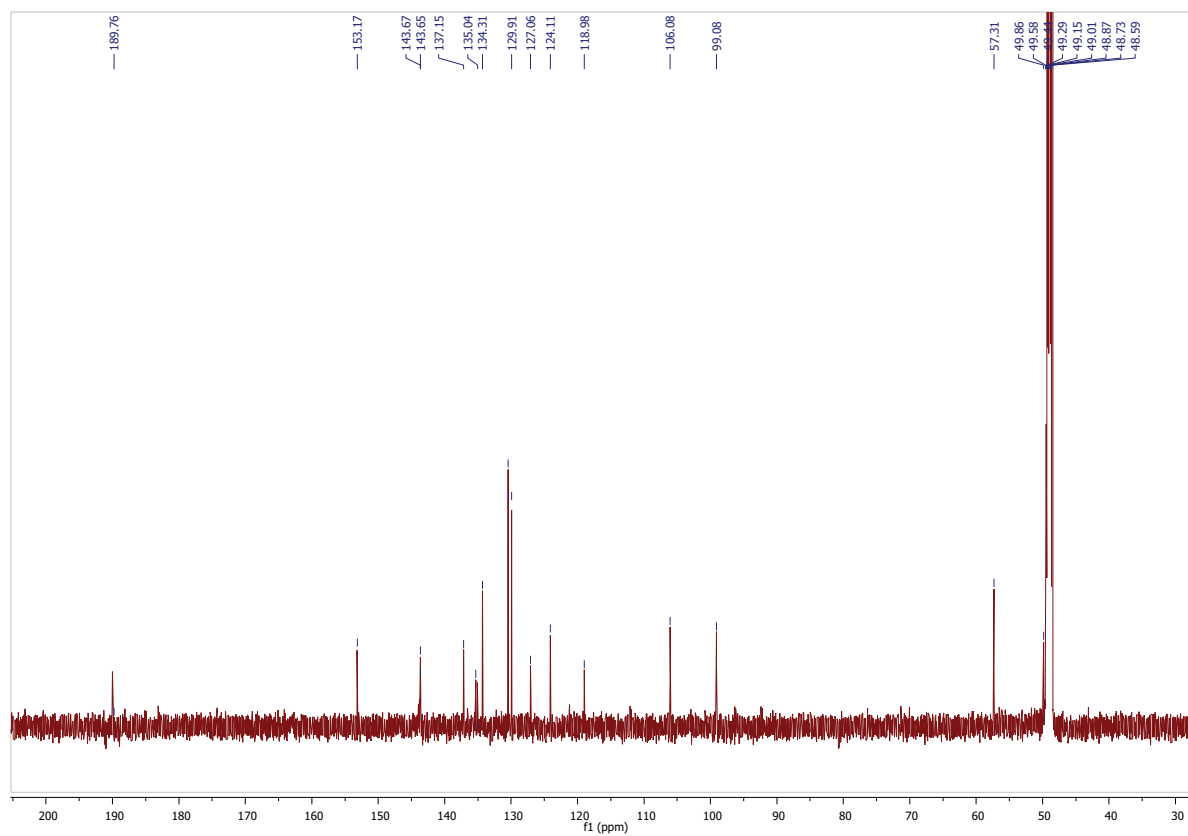
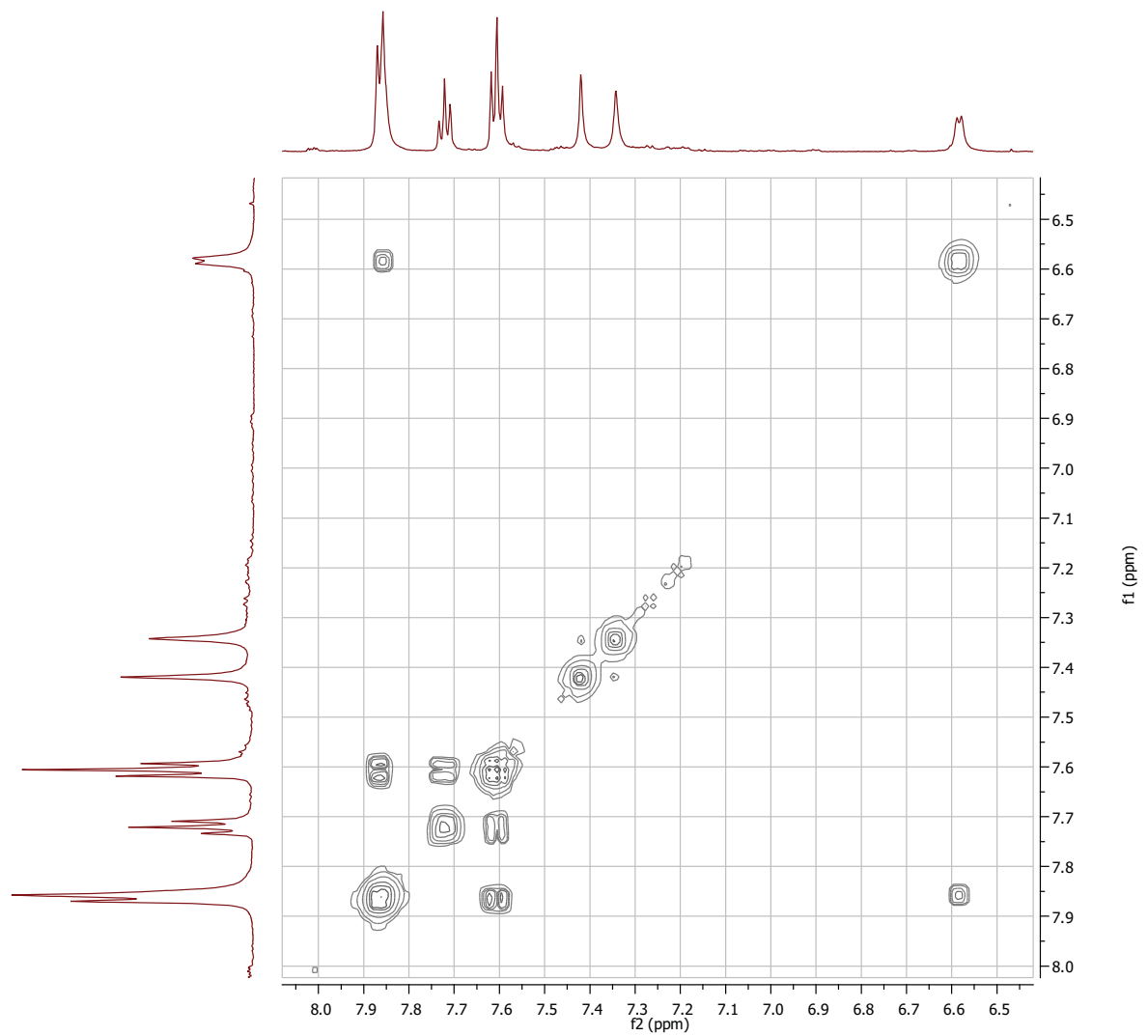


Fig 2-4 HRESIMS spectrum of 2

**Fig 3-1-1**  $^1\text{H}$  NMR spectrum of **3** in  $\text{CD}_3\text{OD}$ **Fig 3-1-2**  $^1\text{H}$  NMR spectrum of **3** in  $\text{CD}_3\text{OD}$  (Enlargement of aromatic region)



**Fig 3-2**  $^{13}\text{C}$  NMR spectrum of **3** in  $\text{CD}_3\text{OD}$



**Fig 3-3**  $^1\text{H}$ ,  $^1\text{H}$  COSY spectrum of **3** in  $\text{CD}_3\text{OD}$



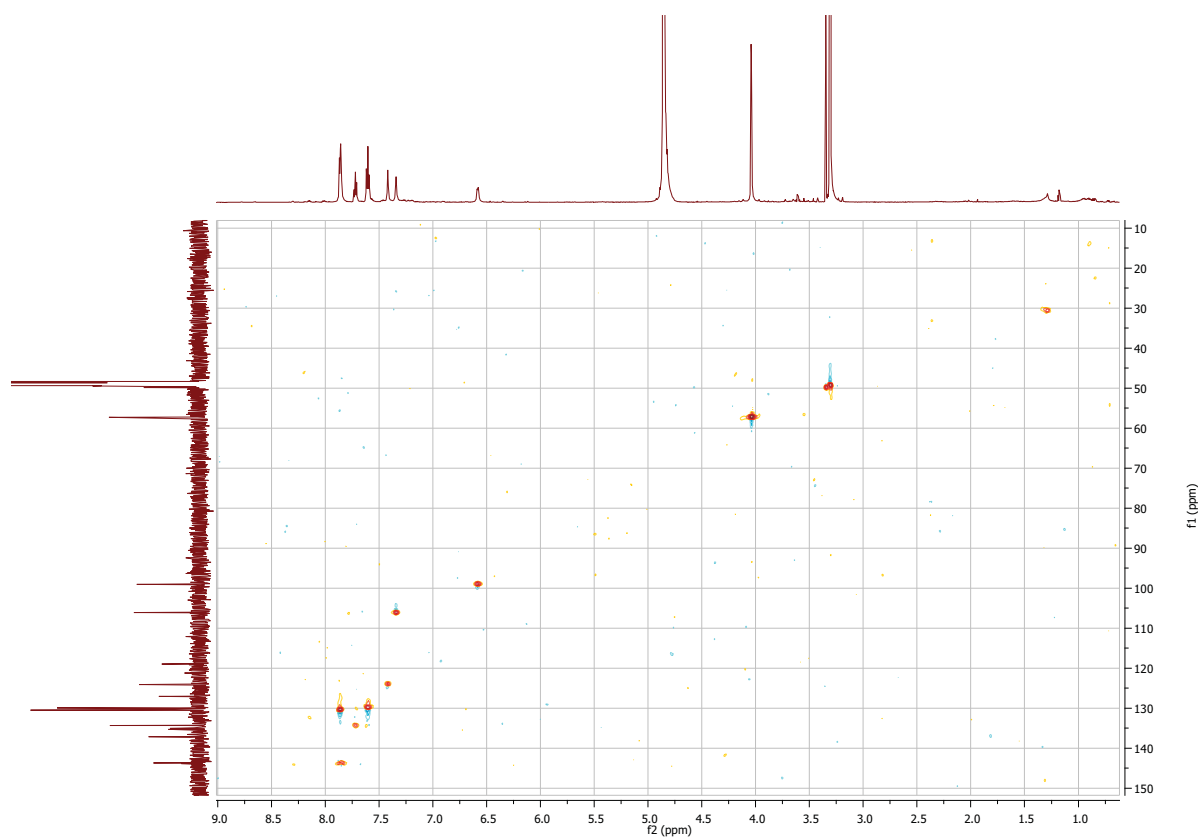


**Fig 3-4** HSQC spectrum of **3** in CD<sub>3</sub>OD

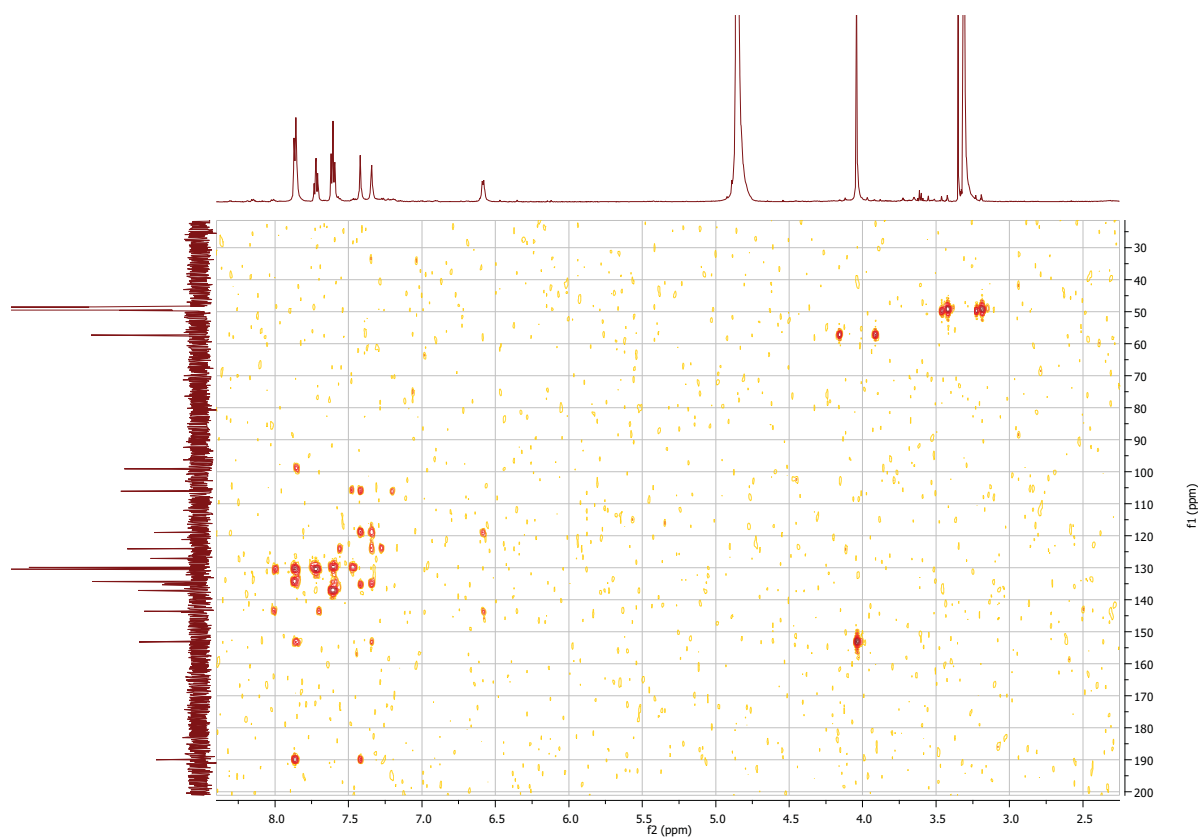
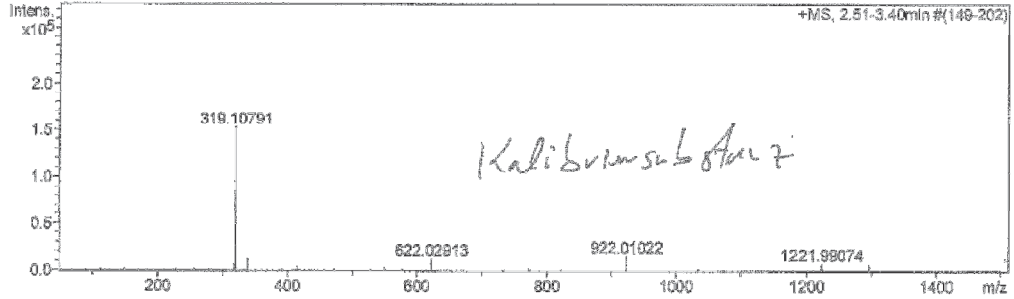


**Fig 3-5** HMBC spectrum of **3** in CD<sub>3</sub>OD

Mass Spectrum SmartFormula Report

<b>Analysis Info</b>		Acquisition Date	7/24/2012 2:39:22 PM
Analysis Name	D:\Data\HHU Service\Proksch000003.d	Operator	Peter Tommes
Method	tune_low.m	Instrument / Ser#	maXis 4G 20213
Sample Name	Cong-Dat Pharm TF33EH6S4.1SP2 in CH3OH		
Comment	0,5 ug/ml in ACN/H2O		

<b>Acquisition Parameter</b>					
Source Type	ESI	Ion Polarity	Positive	Set Nebulizer	0.3 Bar
Focus	Not active	Set Capillary	4000 V	Set Dry Heater	180 °C
Scan Begin	50 m/z	Set End Plate Offset	-500 V	Set Dry Gas	4.0 l/min
Scan End	1500 m/z	Set Collision Cell RF	600.0 Vpp	Set Divert Valve	Source



Meas. m/z	#	Formula	Score	m/z	err [mDa]	err [ppm]	mSigma	rdB	e <sup>-</sup> Conf	N-Rule
319.10791	1	C 19 H 15 N 2 O 3	100.00	319.10772	-0.19	-0.61	27.3	13.6	even	ok

Fig 3-6 HRESIMS spectrum of 3

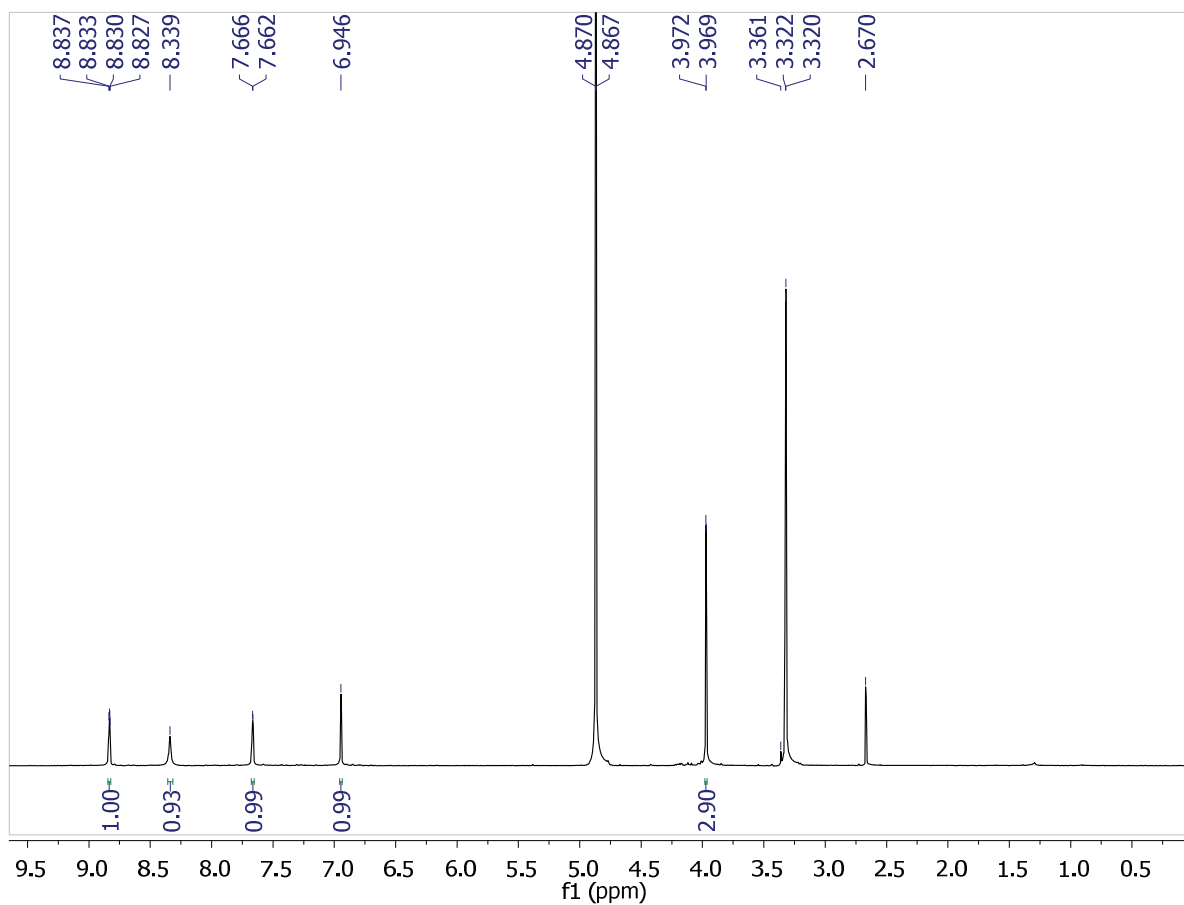


Fig 4-1  $^1\text{H}$  NMR spectrum of **4** in  $\text{CD}_3\text{OD}$

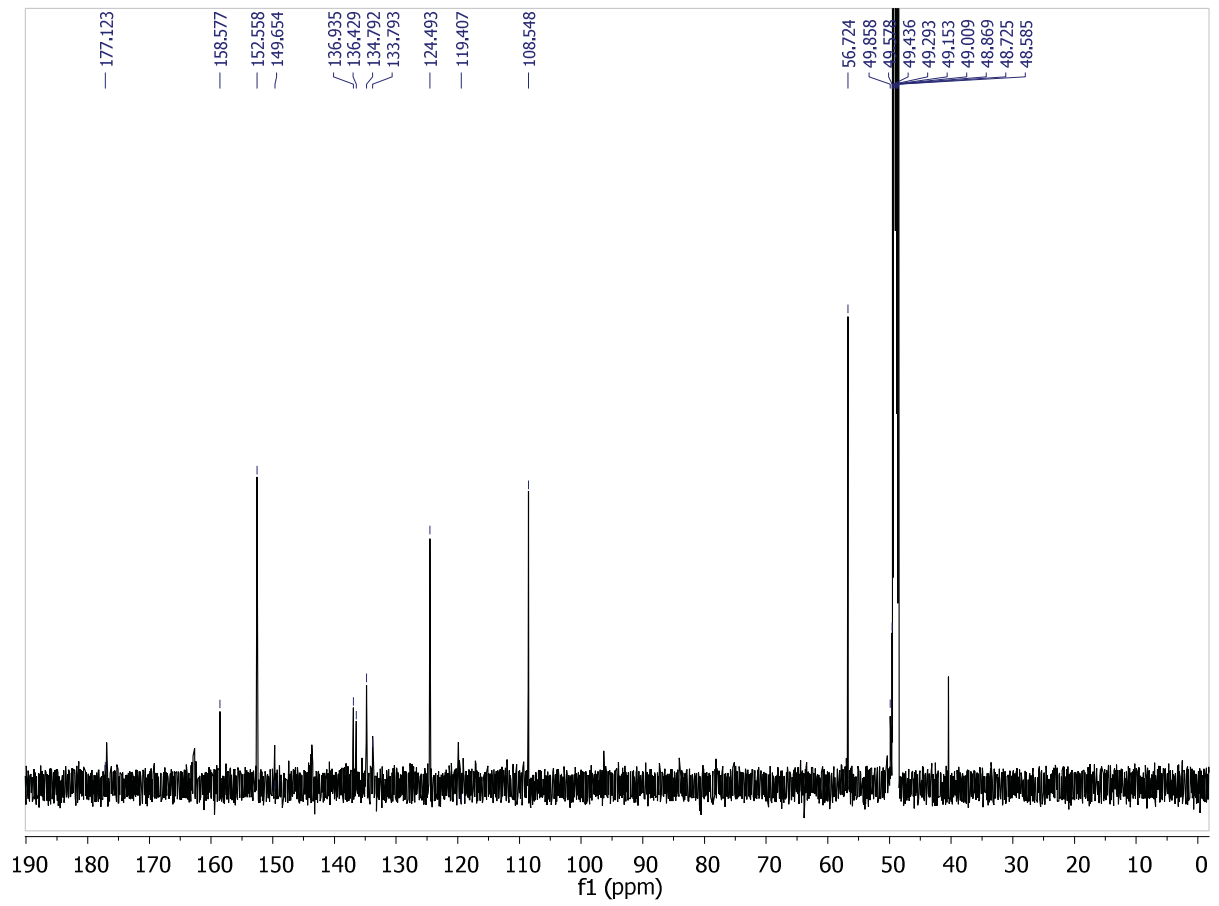


Fig 4-2  $^{13}\text{C}$  NMR spectrum of 4 in  $\text{CD}_3\text{OD}$

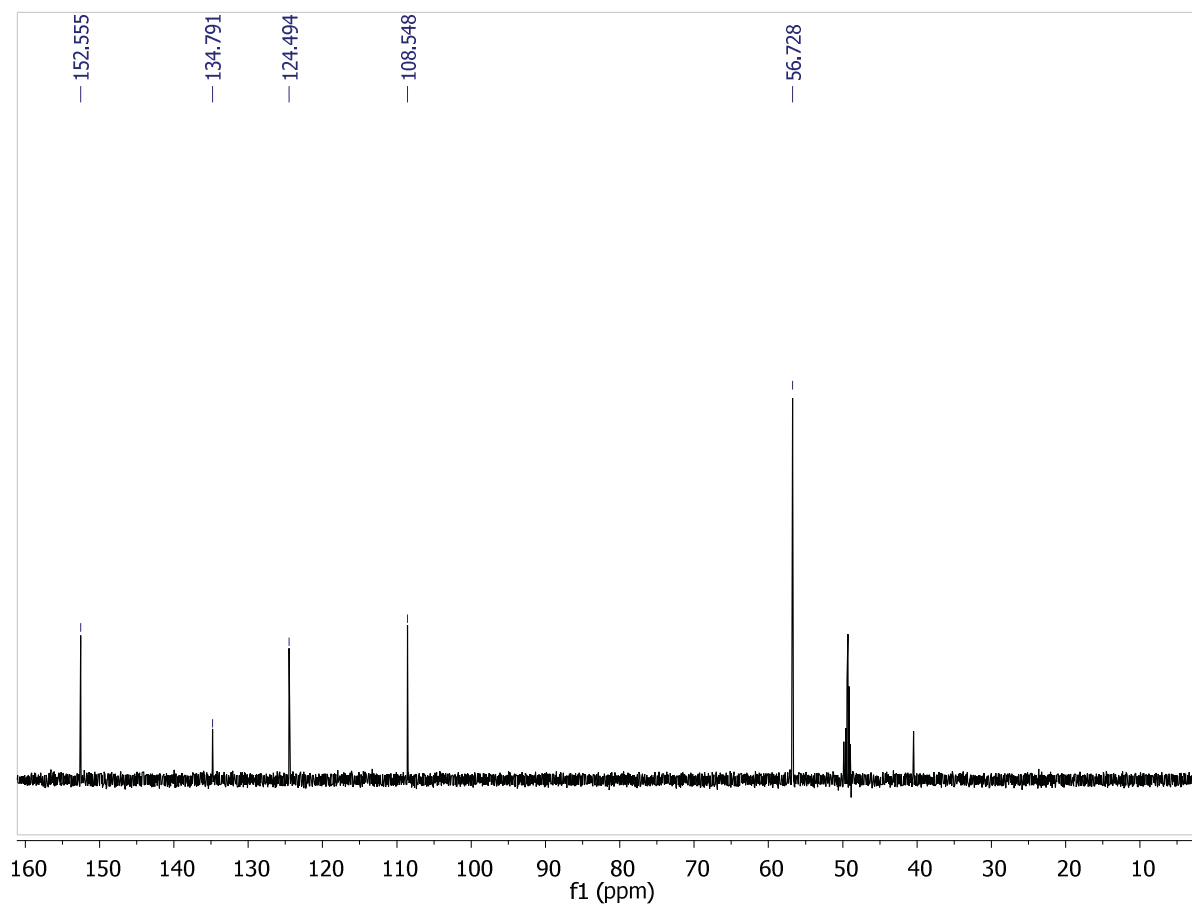


Fig 4-3 DEPT 135 spectrum of 4 in CD<sub>3</sub>OD

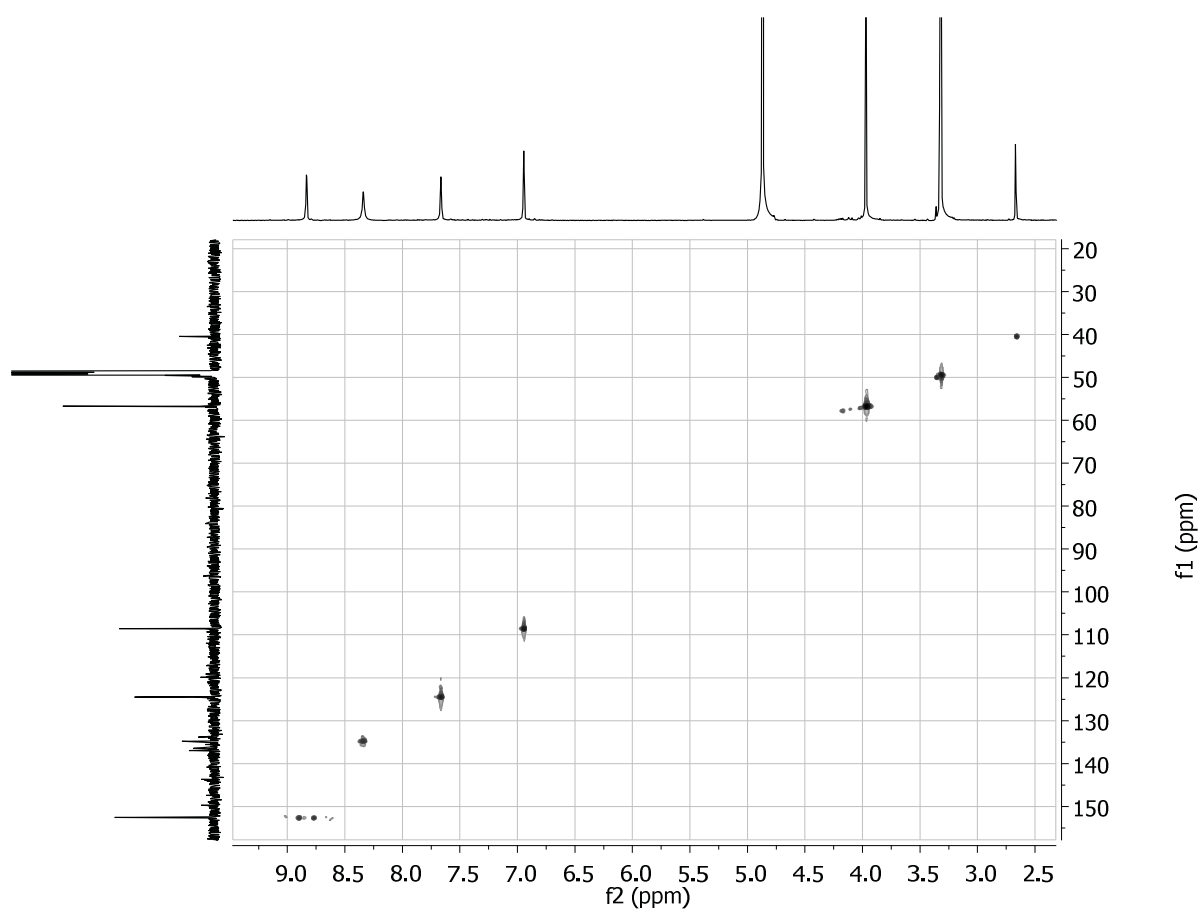


Fig 4-4 HSQC spectrum of 4 in CD<sub>3</sub>OD

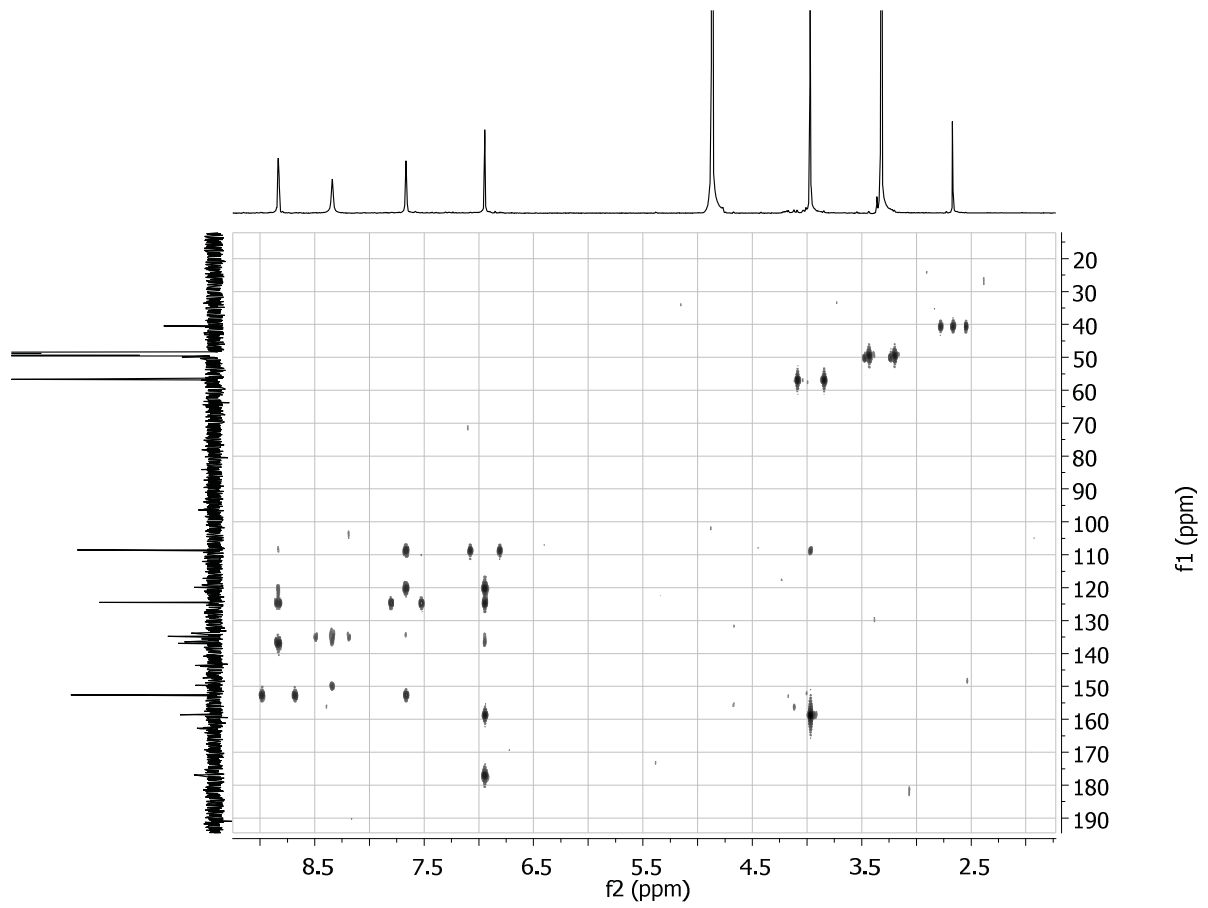


Fig 4-5 HMBC spectrum of 4 in CD<sub>3</sub>OD



C:\Xcalibur\data\N0124A

5/7/2012 11:36:25 AM

7085ot, CPBr13

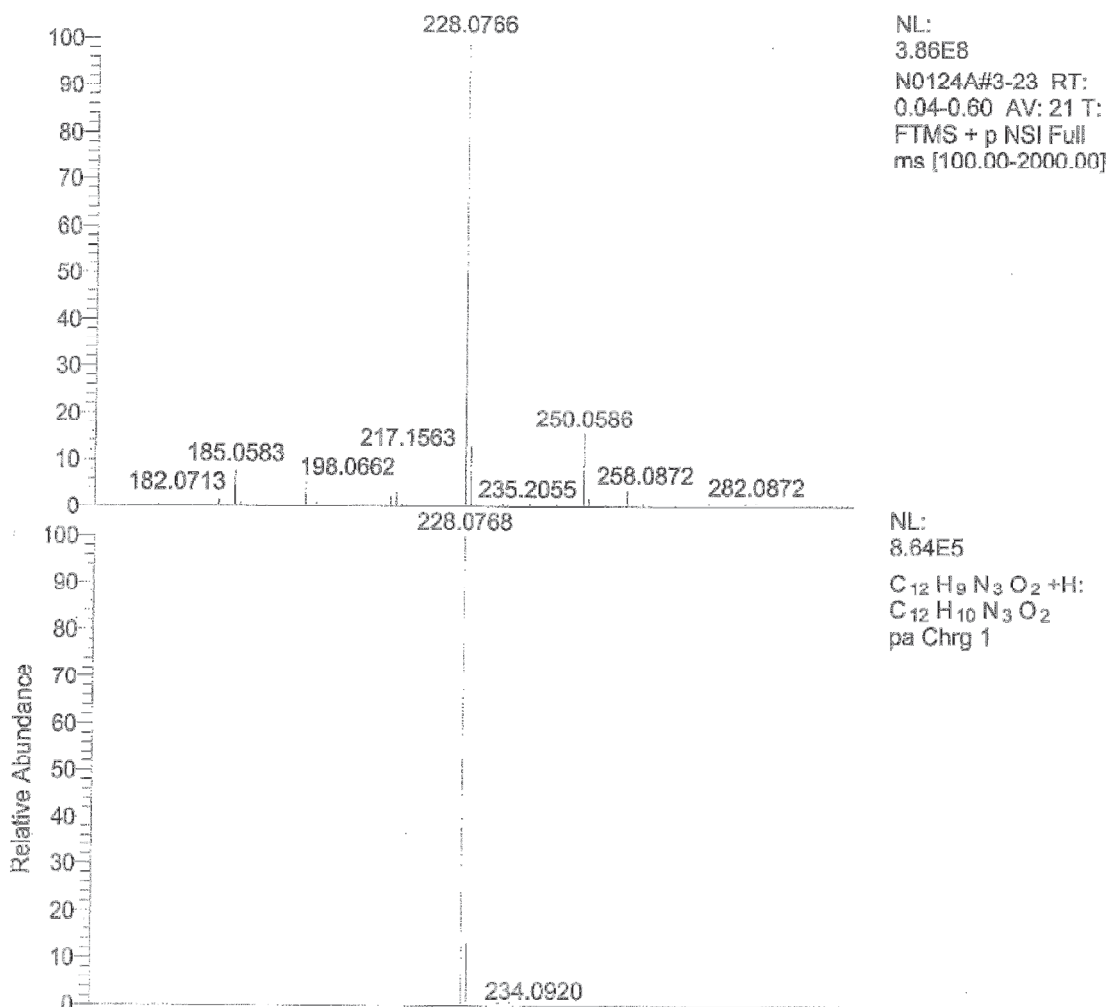


Fig 4-6 HRESIMS spectrum of 4

## 5. Publication 2: *Polycarpa aurata*

Published in: “Organic Letters”

Impact factor: 6.142

Contribution: 80%, first author, conducting most of the experiments (except those mentioned in “Declaration of academic honesty/Erklärung”), manuscript writing

Reprinted with permission from “Pham CD, Weber H, Hartmann R, Wray V, Lin WH, Lai DW, Proksch P. (2013) New Cytotoxic 1,2,4-Thiadiazole Alkaloids from the Ascidian *Polycarpa aurata*”. Org. Letters, 15: 2230-2233. Copyright 2013 American Chemical Society

# New Cytotoxic 1,2,4-Thiadiazole Alkaloids from the Ascidian *Polycarpa aurata*

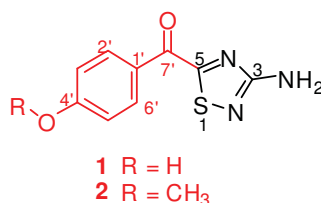
Cong-Dat Pham,<sup>†</sup> Horst Weber,<sup>‡</sup> Rudolf Hartmann,<sup>§</sup> Victor Wray,<sup>⊥</sup> Wenhan Lin,<sup>||</sup> Daowan Lai,<sup>\*,†</sup> and Peter Proksch<sup>\*,†</sup>

*Institute of Pharmaceutical Biology and Biotechnology, and Institute of Pharmaceutical and Medicinal Chemistry, Heinrich-Heine University, 40225 Düsseldorf, Germany, Institute of Complex Systems (ICS-6), Forschungszentrum Jülich GmbH, 52425 Jülich, Germany, Helmholtz Centre for Infection Research, D-38124 Braunschweig, Germany, and State Key Laboratory of Natural and Biomimetic Drugs, Peking University, Beijing 100191, PR China*

laidaowan123@gmail.com; proksch@uni-duesseldorf.de

Received March, 24 2013

## ABSTRACT



Two new alkaloids, polycarpathiamines A and B (1 and 2), were isolated from the ascidian *Polycarpa aurata*. Their structures were unambiguously determined by 1D, 2D NMR and HRESIMS measurements, and further confirmed by comparison with a closely related analogue, 3-dimethylamino-5-benzoyl-1,2,4-thiadiazole (4) that was prepared by chemical synthesis. Compounds 1 and 2 both feature an uncommon 1,2,4-thiadiazole ring whose biosynthetic origin is proposed. Compound 1 showed significant cytotoxic activity against L5178Y murine lymphoma cells (IC<sub>50</sub> 0.41 μM).

Marine invertebrates such as ascidians are prominent sources of a wide variety of natural products, many of them containing nitrogen atoms.<sup>1</sup> There is a high probability of discovering novel structures with unprecedented skeletons from these organisms as exemplified by ecteinascidin 743 (trabectedin), eudistomin C, dendrodoine and lissoclinotoxin A.<sup>2</sup> Ascidians of the genus *Polycarpa* are known for

producing various sulphur-containing alkaloids such as polycarpaurines A-C,<sup>3</sup> polycarpamines A-E,<sup>4</sup> the dimeric disulfide alkaloid polycarpine<sup>5</sup> and derivatives<sup>6</sup> thereof. These compounds exhibited diverse biological activities, such as antifungal activity,<sup>4</sup> cytotoxic<sup>3, 6a, 7</sup> and antitumor activities,<sup>7</sup> inhibition of inosine monophosphate dehydrogenase,<sup>5</sup> inhibition of inflammatory cytokine production in lipopolysaccharide-stimulated RAW 264.7

<sup>†</sup> Institute of Pharmaceutical Biology and Biotechnology

<sup>‡</sup> Institute of Pharmaceutical and Medicinal Chemistry

<sup>§</sup> Institute of Complex Systems (ICS-6)

<sup>⊥</sup> Helmholtz Centre for Infection Research

<sup>||</sup> Peking University

(<sup>1</sup>) Blunt, J. W.; Copp, B. R.; Keyzers, R. A.; Munro, M. H. G.; Prinsep, M. R. *Nat. Prod. Rep.* **2013**, *30*, 237.

(<sup>2</sup>) (a) Rinehart, K. L.; Holt, T. G.; Fregeau, N. L.; Keifer, P. A.; Wilson, G. R.; Perun, T. J.; Sakai, R.; Thompson, A. G.; Stroh, J. G.; Shield, L. S.; Seigler, D. S.; Li, L. H.; Martin, D. G.; Grimmelikhuijzen, C. J. P.; Gäde, G. *J. Nat. Prod.* **1990**, *53*, 771. (b) Rinehart, K. L.; Kobayashi, J.; Harbour, G. C.; Hughes, R. G.; Mizsak, S. A.; Scahill, T. A. *J. Am. Chem. Soc.* **1984**, *106*, 1524. (c) Heitz, S.; Durgeat, M.; Guyot, M.; Brassy, C.; Bachel, B. *Tetrahedron Lett.* **1980**, *21*, 1457. (d) Litaudon, M.; Guyot, M. *Tetrahedron Lett.* **1991**, *32*, 911.

(<sup>3</sup>) Wang, W.; Oda, T.; Fujita, A.; Mangindaan, R. E. P.; Nakazawa, T.; Ukai, K.; Kobayashi, H.; Namikoshi, M. *Tetrahedron* **2007**, *63*, 409.

(<sup>4</sup>) Lindquist, N.; Fenical, W. *Tetrahedron Lett.* **1990**, *31*, 2389.

(<sup>5</sup>) Abbas, S. A.; Hossain, M. B.; van der Helm, D.; Schmitz, F. J.; Laney, M.; Cabuslay, R.; Schatzman, R. C. *J. Org. Chem.* **1996**, *61*, 2709.

(<sup>6</sup>) (a) Kang, H.; Fenical, W. *Tetrahedron Lett.* **1996**, *37*, 2369. (b) Wessels, M.; König, G. M.; Wright, A. D. *J. Nat. Prod.* **2001**, *64*, 1556.

(<sup>7</sup>) Popov, A. M.; Novikov, V. L.; Radchenko, O. S.; Elyakov, G. B. *Dokl. Biochem. Biophys.* **2002**, *385*, 213.

cells,<sup>8</sup> and induction of apoptosis in JB6 cells through p53- and caspase 3-dependent pathways.<sup>9</sup> Thus, members of this genus are interesting sources of potentially new bioactive metabolites.

In our search for bioactive metabolites from marine organisms,<sup>10</sup> we observed that the ethanolic extract of the ascidian *Polycarpa aurata*, collected in Indonesia, completely inhibited the growth of the murine lymphoma cell line L5178Y at a concentration of 10 µg/mL. Chromatographic separation afforded two new alkaloids (**1-2**) (Figure 1), together with four known compounds, which were identified as polycarpaurine C (**3**),<sup>3</sup> *N,N*-didesmethylgrossularine-1,<sup>3</sup> 4-methoxybenzoic acid,<sup>6b</sup> and *N*-methyl-2-(4-methoxyphenyl)-2-oxoacetamide<sup>6b</sup> based on their spectral data and on comparison with the literature. Herein, we describe the structure elucidation of the new compounds **1** and **2** and cytotoxicity of the isolated compounds.

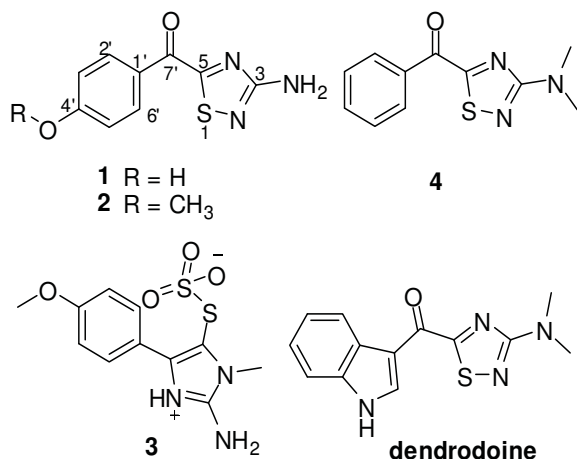


Figure 1. Structures of compounds 1-4 and dendrodoine.

Compound **1** was obtained as a dark yellow amorphous solid with a faint sulphur odour. The HRESIMS of **1** showed pseudo-molecular ion peaks at  $m/z$  222.0331 [M+H]<sup>+</sup>, 244.0148 [M+Na]<sup>+</sup>, and 465.0406 [2M+Na]<sup>+</sup> indicating a molecular formula C<sub>9</sub>H<sub>7</sub>N<sub>3</sub>O<sub>2</sub>S, bearing 8 double bond equivalents (8 DB). The <sup>1</sup>H NMR spectrum (DMSO-*d*<sub>6</sub>) exhibited signals at δ<sub>H</sub> 8.37 (2H, d, *J* = 8.8 Hz, H-2/6'), and 6.94 (2H, d, *J* = 8.8 Hz, H-3/5'), suggesting a typical AA'BB' spin system of a *para* substituted benzene ring, and further signals at δ<sub>H</sub> 10.77 (1H, br.s) for a hydroxy group and at δ<sub>H</sub> 7.05 (2H, s) for an NH<sub>2</sub> group. The <sup>13</sup>C NMR data for C-1'~C-7' (DMSO-*d*<sub>6</sub>, Table 1) together with the HMBC correlations from H-2/6' to C-4' (δ<sub>C</sub> 163.8), C-3/5' (δ<sub>C</sub> 115.6), C-6/2' (δ<sub>C</sub> 133.6), C-1' (δ<sub>C</sub> 125.1), and C-7' (δ<sub>C</sub>

180.6), and from H-3/5' to C-1', C-4', and C-5/3', revealed the presence of a 4-hydroxybenzoyl moiety, which is consistent with the observation of a base peak at  $m/z$  121 (C<sub>7</sub>H<sub>5</sub>O<sub>2</sub><sup>+</sup>) in EI-MS. Apart from this unit, two carbon atoms (δ<sub>C</sub> 185.7, 171.7), one NH<sub>2</sub> group (δ<sub>H</sub> 7.05), as well as one sulfur, and two nitrogen atoms remained to be assigned according to the molecular formula. Since the benzoyl group accounts for 5 DB, the remaining 3DB has to originate from the the -C<sub>2</sub>N<sub>2</sub>S-NH<sub>2</sub> moiety. This moiety (C<sub>2</sub>N<sub>2</sub>S) has to be cyclic, as otherwise a linear substructure with an alkyne group or cumulative double bonds must be formulated which is not supported by the carbon-13 chemical shifts. Theoretically, there are four possible heterocyclic ring structures for the -C<sub>2</sub>N<sub>2</sub>S- moiety of **1** (h-1~h-4, Figure 2). A thorough literature search for the possible ring structures was carried out, and the chemical shifts for the carbons in these heterocyclic rings were either extracted based on reported values, or assigned by NMR measurements for those compounds that were commercially available (see Table S1 in Supporting Information). The 1,2,4-thiadiazole substructure (h-3) was found to be the only possible heterocyclic ring in which one carbon resonates at around 170 ppm, and the second carbon at 180-189 ppm, which is very similar to the chemical shifts obtained for **1**. However, it was difficult to assign the positions of the NH<sub>2</sub> and benzoyl groups in this heterocyclic ring structure, since the sulfur bearing carbon (C<sub>5</sub>) generally resonates at 180-190 ppm regardless of the substitution (Table S1). Thus, two possible structures (i.e. **1a** and **1b**) remained (Figure 2). We strongly favored **1a**, a guanidine containing molecule, whose biogenetic origin could be easily explained since this substructure is also present in polycarpaurine C (**3**), and *N,N*-didesmethylgrossularine-1 that were likewise isolated from *P. aurata*. Moreover, an indole alkaloid, dendrodoine, featuring a similar 3-dimethylamino-1,2,4-thiadiazole moiety had previously been reported from the ascidian *Dendrodoa grossularia*.<sup>2c</sup> A comparison of the <sup>13</sup>C NMR data of **1** with those of dendrodoine<sup>2c, 11</sup> revealed close similarities in the 1,2,4-thiadiazole unit if one assumes that the original assignments for C-5 and carbonyl group of dendrodoine are wrong and should be interchanged.<sup>12</sup> A <sup>1</sup>H-<sup>15</sup>N HMBC measurement of **1** was performed to distinguish between the two possible structures **1a** and **1b** (Figure 2). The observed two three-bond correlations from the NH<sub>2</sub> group to two nitrogen atoms (δ<sub>N</sub> 171.3, 202.2) clearly indicate **1a** to be the correct structure for compound **1**.

In order to further confirm the existence of this unusual heterocyclic ring structure in **1**, we synthesised an analogous structure, 3-dimethylamino-5-benzoyl-1,2,4-thiadiazole (**4**), which closely resembles **1** and dendrodoine, following a method reported in the literature.<sup>11</sup> The analogue was synthesized according to a two-step reaction, 1) the formation of 5-dimethylamino-1,3,4-oxathiazol-2-one, which was used to produce *N,N*-dimethylaminonitrile sulfide in the following step via thermolysis; 2) a 1,3-dipolar

<sup>(8)</sup> Oda, T.; Lee, J.-S.; Sato, Y.; Kabe, Y.; Sakamoto, S.; Handa, H.; Mangindaan, R. E. P.; Namikoshi, M. *Mar. Drugs* **2009**, *7*, 589.

<sup>(9)</sup> Fedorov, S. N.; Bode, A. M.; Stonik, V. A.; Gorshkova, I. A.; Schmid, P. C.; Radchenko, O. S.; Berdyshev, E. V.; Dong, Z. *Pharm. Res.* **2004**, *21*, 2307.

<sup>(10)</sup> (a) Pham, C.-D.; Hartmann, R.; Müller, W. E. G.; de Voogd, N.; Lai, D.; Proksch, P. *J. Nat. Prod.* **2013**, *76*, 103. (b) Niemann, H.; Lin, W.; Müller, W. E. G.; Kubbutat, M.; Lai, D.; Proksch, P. *J. Nat. Prod.* **2013**, *76*, 121. (c) Lai, D.; Liu, D.; Deng, Z.; van Ofwegen, L.; Proksch, P.; Lin, W. *J. Nat. Prod.* **2012**, *75*, 1595.

<sup>(11)</sup> Hogan, I. T.; Sainsbury, M. *Tetrahedron* **1984**, *40*, 681.

<sup>(12)</sup> The original assignments (see ref 11) for C-5 at δ<sub>C</sub> 175.7, and the carbonyl conjugated with an indole group at δ<sub>C</sub> 187.8 were not consistent with the reported 1,2,4-thiadiazole derivatives (usually C-5 at 180-190 ppm, see Table S1), and the indole-3-carbonyl containing derivatives (eg. Rhopaladin D, δ<sub>C=O</sub> 177.4 (Sato, H.; Tsuda, M.; Watanabe, K.; Kobayashi, J. *Tetrahedron* **1998**, *54*, 8687), and such carbonyl usually resonates at lower than 180 ppm).

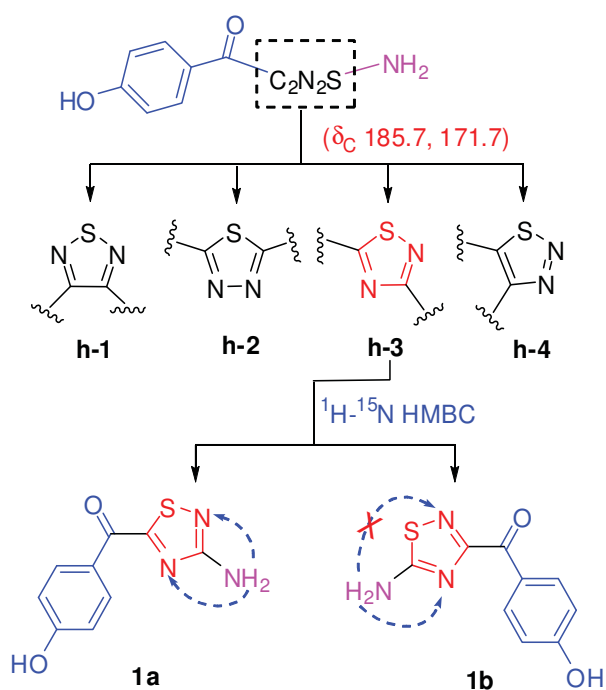


**Figure 2.** Assignment of the heterocyclic unit in **1** by analysis of the  $^{13}\text{C}$  NMR chemical shifts and  $^1\text{H}$ - $^{15}\text{N}$  HMBC correlations.

cycloaddition between the nitrile sulfide generated *in situ* and benzoylcyanide (Scheme 1). This synthetic analogue (**4**) has two *N*-methyl groups, which are helpful in assigning the chemical shifts of the thiadiazole unit. The HMBC correlations from both *N*-methyl groups to C-3 ( $\delta_{\text{C}}$  172.5), and from H-2'/6' to C-7' ( $\delta_{\text{C}}$  182.9) allow the unambiguous assignments for C-3 and C-7', thus the signal at  $\delta_{\text{C}}$  184.9 can only be assigned to C-5, which supports our assumption that the previously reported assignment for C-5 of dendrodoine was wrong. The strong similarity between the carbon chemical shifts of **1** and the synthetic analogue (**4**) in the thiadiazole unit independently supports the proposed structure for **1**. Therefore, compound **1** was determined as the new 3-amino-5-(4-hydroxybenzoyl)-1,2,4-thiadiazole, and named polycarpathiamine A.

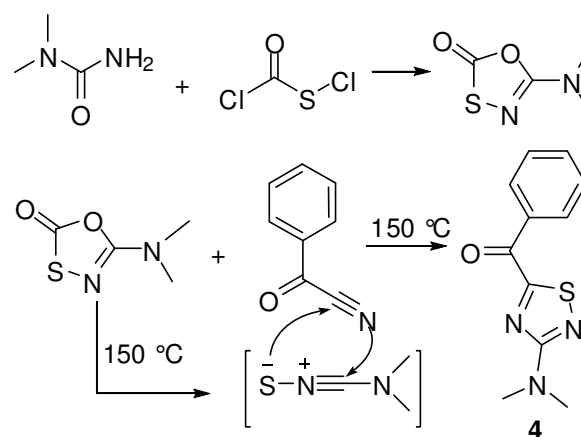
**Table 1.**  $^{13}\text{C}$  NMR data of **1-2**, and **4**

position	<b>1</b> <sup>a</sup>	<b>1</b> <sup>b</sup>	<b>2</b> <sup>c</sup>	<b>4</b> <sup>d</sup>
3	171.7 C	172.7 C	171.8 C	172.5 C
5	185.7 C	187.6 C	185.4 C	184.9 C
1'	125.1 C	127.2 C	126.6 C	134.0 C
2' /6'	133.6 CH	134.7 CH	133.3 CH	130.6 CH
3' /5'	115.6 CH	116.5 CH	114.3 CH	128.9 CH
4'	163.8 C	164.5 C	164.6 C	134.7 CH
7'	180.6 C	181.7 C	180.9 C	182.9 C
4'-OMe			55.8 CH <sub>3</sub>	
3-NMe <sub>2</sub>				38.6 CH <sub>3</sub>

<sup>a</sup> Recorded at 100 MHz in DMSO-*d*<sub>6</sub>; <sup>b</sup> Recorded at 150 MHz in acetone-*d*<sub>6</sub>; <sup>c</sup> Recorded at 75 MHz in DMSO-*d*<sub>6</sub>; <sup>d</sup> Recorded at 150 MHz in DMSO-*d*<sub>6</sub>.

Compound **2** was obtained as a dark yellow amorphous solid with a slight sulphur odour similar to compound **1**. HRESIMS of **2** showed signals at  $m/z$  236.0488 [M+H]<sup>+</sup> and 232.07 [M+Na]<sup>+</sup>, indicating the molecular formula C<sub>10</sub>H<sub>9</sub>N<sub>3</sub>O<sub>2</sub>S, which differs from that of **1** by a methyl substituent. The NMR data of **2** closely resemble those of

**Scheme 1.** Synthesis of 3-dimethylamino-5-benzoyl-1,2,4-thiadiazole (**4**)

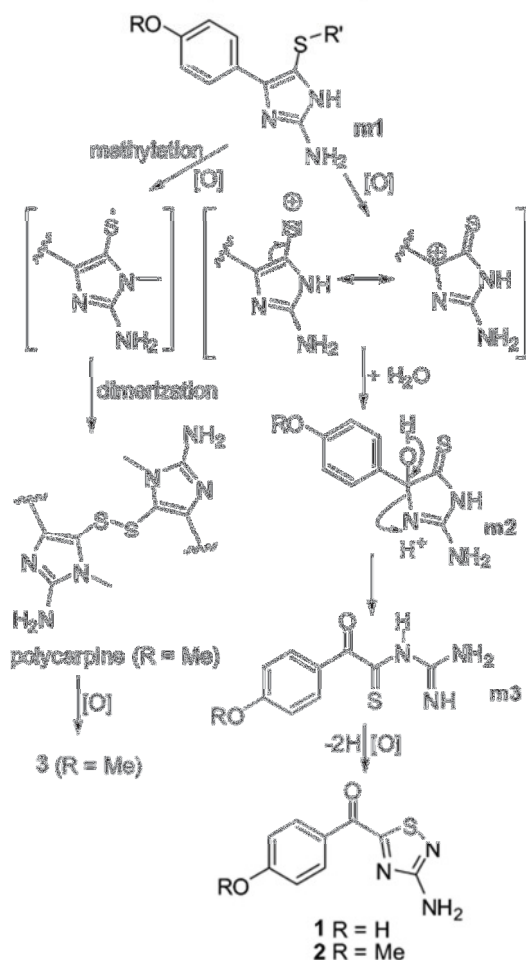


**1**, except for a methoxy group ( $\delta_{\text{H}}$  3.90,  $\delta_{\text{C}}$  55.8) in **2** instead of a hydroxyl substituent in **1**. The methoxy group is located at C-4', since it shows HMBC correlation to C-4'. Thus, compound **2** was identified as 3-amino-5-(4-methoxybenzoyl)-1,2,4-thiadiazole, and named polycarpathiamine B.

1,2,4-Thiadiazole alkaloids are rarely encountered in natural products. So far, only three natural products with this structural unit have been reported, including dendrodoine from the ascidian *Dendrodoa grossularia*,<sup>2c</sup> and a pair of enantiomers of an indole alkaloid from the root of *Isatis indigotica* in a recent paper.<sup>13</sup> The present study reports two new members of this class. It is worth mentioning that compounds **1** and **2** are the second and third example of 3-amino substituted 1,2,4-thiadiazole alkaloids from nature. Thus, their biosynthetic pathway should be different from the 1,2,4-thiadiazole alkaloid without a 3-amino substitution.<sup>13</sup> A plausible biosynthetic pathway for **1** and **2** is proposed (Scheme 2).

In light of the frequent occurrence of the dimeric disulfide alkaloid, polycarpine, in several ascidians from the genus *Polycarpa*,<sup>3,5,6a</sup> though not in the present study, we hypothesize a monomeric precursor (**m1**) being present in *P. aurata*, which would undergo methylation and oxidation to form a S-radical intermediate. A dimerization of this intermediate could afford polycarpine, in which the cleavage of the S-S or C-S bond accompanied by oxidation would give polycarpaurine B<sup>3</sup> or C (**3**), respectively. Further oxidation of **m1** and subsequent nucleophilic attack of water could produce an intermediate (**m2**), as similar derivatives with 2-carbonyl group were already reported from ascidians.<sup>5,6a</sup> A follow-up

(13) Chen, M.; Lin, S.; Li, L.; Zhu, C.; Wang, X.; Wang, Y.; Jiang, B.; Wang, S.; Li, Y.; Jiang, J.; Shi, J. *Org. Lett.* **2012**, *14*, 5668.

Scheme 2. Plausible Biosynthetic Pathway for **1** and **2**

reaction of m2 would give the guanidine amide of 2-aryl-2-oxothioacetic acid (m3). A similar compound N-methyl- (4-methoxyphenyl)-2-oxothioacetamide was isolated from an unrelated ascidian,<sup>2c</sup> it seems plausible that a similar biosynthetic pathway was also adopted here by using a precursor that features an indole group instead of benzene group in m1, as suggested by the occurrence of several indole analogues<sup>14</sup> that resemble those hypothetical intermediates shown in Scheme 2.

All isolated compounds were examined for their effects on the growth of L5178Y mouse lymphoma cells *in vitro* using the MTT assay<sup>10a, 15</sup>. Compound **1** and *N,N*-didesmethylgrossularine-1 inhibited the growth of L5178Y cells with IC<sub>50</sub> values (μM) of 0.41 and 1.86, respectively, while the other compounds were not active (IC<sub>50</sub> >10 μM). Compound **1** showed potent inhibitory activity in a sub-micromolar concentration, which is approximately 10-fold more active than the positive control kahalalide F (IC<sub>50</sub> 4.3 μM). Apparently, the hydroxyl functional group at C-4' of compound **1** should be unsubstituted in order to retain bioactivity since compound **2** was inactive. The unique

structure and notable cytotoxicity of **1** make it an interesting starting point for cytotoxic drug development. The further SAR and biological investigations are ongoing.

**Acknowledgements.** The financial support by grant of the BMBF to P.P. is gratefully acknowledged. We are indebted to Prof. W. E. G. Müller (Johannes Gutenberg University, Mainz, Germany) for cytotoxicity assays, and Dr. Nicole de Voogd (Naturalis Biodiversity Center, Leiden, The Netherlands) for identifying the ascidian. We want to thank Prof. Phillip Crews (University of California, Santa Cruz, United States) for helpful discussions.

**Supporting Information Available.** Experimental procedures, ascidian material, extraction and isolation, characterization data of **1-2**, synthetic procedures and spectral data of **4**, cytotoxic assay, and copies of 1D and 2D NMR and HRMS spectra of **1**, **2**, and **4**. This material is available free of charge via the Internet at <http://pubs.acs.org>.

(14) Mancini, I.; Guella, G.; Pietra, F.; Debitus, C.; Duhet, D. *Helv. Chim. Acta* **1994**, *77*, 1886.

(15) Ashour, M.; Edrada, R.; Ebel, R.; Wray, V.; Watjen, W.; Padmakumar, K.; Müller, W. E. G.; Lin, W. H.; Proksch, P. *J. Nat. Prod.* **2006**, *69*, 1547.

## Supporting Information

### New Cytotoxic 1,2,4-Thiadiazole Alkaloids from the Ascidian

#### *Polycarpa aurata*

Cong-Dat Pham,<sup>†</sup> Horst Weber,<sup>‡</sup> Rudolf Hartmann,<sup>§</sup> Victor Wray,<sup>⊥</sup> Wenhan Lin,<sup>||</sup> Daowan Lai,<sup>\*,†</sup> Peter Proksch<sup>\*,†</sup>

<sup>†</sup> Institute of Pharmaceutical Biology and Biotechnology, Heinrich-Heine University, 40225 Düsseldorf, Germany;

<sup>‡</sup> Institute of Pharmaceutical and Medicinal Chemistry, Heinrich-Heine University, Düsseldorf, Germany;

<sup>§</sup> Institute of Complex Systems (ICS-6), Forschungszentrum Jülich GmbH, 52425 Jülich, Germany;

<sup>⊥</sup> Helmholtz Centre for Infection Research, D-38124 Braunschweig, Germany;

<sup>||</sup> State Key Laboratory of Natural and Biomimetic Drugs, Peking University, Beijing 100191, PR China

*laidaowan123@gmail.com; proksch@uni-duesseldorf.de*



## Contents

<b>Experimental Section</b>	S62
<b>General experimental procedures</b> .....	S62
<b>Ascidian material</b> .....	S63
<b>Extraction and isolation</b> .....	S63
<b>Polycarpathiamine A (1)</b> .....	S63
<b>Polycarpathiamine B (2)</b> .....	S64
<b>Preparation of 5-dimethylamino-1,3,4-oxathiazol-2-one</b> .....	S64
<b>Preparation of 3-dimethylamino-5-benzoyl-1,2,4-thiadiazole (4)</b> .....	S64
<b>Bioassay</b> .....	S65
<b>Table S1</b> The $^{13}\text{C}$ NMR chemical shifts for the four possible ring structures	S66
<b>Figure S1</b> $^1\text{H}$ NMR spectrum of <b>1</b> (DMSO- $d_6$ )	S68
<b>Figure S2</b> $^{13}\text{C}$ NMR spectrum of <b>1</b> (DMSO- $d_6$ )	S68
<b>Figure S3</b> HMBC spectrum of <b>1</b> (DMSO- $d_6$ )	S69
<b>Figure S4</b> HRESIMS spectrum of <b>1</b>	S69
<b>Figure S5</b> $^1\text{H}$ - $^{15}\text{N}$ HMBC spectrum of <b>1</b> (DMSO- $d_6$ )	S70
<b>Figure S6</b> $^1\text{H}$ NMR spectrum of <b>2</b> (DMSO- $d_6$ )	S70
<b>Figure S7</b> $^{13}\text{C}$ NMR spectrum of <b>2</b> (DMSO- $d_6$ )	S71
<b>Figure S8</b> HMBC spectrum of <b>2</b> (DMSO- $d_6$ )	S71
<b>Figure S9</b> HRESIMS spectrum of <b>2</b>	S72
<b>Figure S10</b> $^1\text{H}$ NMR spectrum of <b>5-dimethylamino-1,3,4-oxathiazol-2-one</b> ( $\text{CDCl}_3$ )	S72
<b>Figure S11</b> $^{13}\text{C}$ NMR spectrum of <b>5-dimethylamino-1,3,4-oxathiazol-2-one</b> ( $\text{CDCl}_3$ )	S73
<b>Figure S12</b> $^1\text{H}$ NMR spectrum of <b>4</b> (DMSO- $d_6$ )	S73
<b>Figure S13</b> $^{13}\text{C}$ NMR spectrum of <b>4</b> (DMSO- $d_6$ )	S74
<b>Figure S14</b> HSQC spectrum of <b>4</b> (DMSO- $d_6$ )	S74
<b>Figure S15</b> HMBC spectrum of <b>4</b> (DMSO- $d_6$ )	S75
<b>Figure S16</b> HRESIMS spectrum of <b>4</b>	S76



## Experimental Section

### General experimental procedures

Melting points were measured on a Büchi B-540 melting point apparatus (not corrected). UV spectra were measured in a Perkin-Elmer Lambda 25 UV/vis spectrometer. IR spectra were measured directly in a Shimadzu IRAffinity-1 FT-IR spectrometer.  $^1\text{H}$ ,  $^{13}\text{C}$ , and 2D NMR spectra were recorded on Bruker ARX 300, 400 or Bruker AMX 600 NMR spectrometers, and the  $^1\text{H}$ - $^{15}\text{N}$  HMBC spectrum was recorded on a Agilent V800 NMR spectrometer at 25°C. The chemical shifts were referenced to the solvent residual peaks,  $\delta_{\text{H}}$  2.50 (DMSO- $d_6$ ), 2.05 (Acetone- $d_6$ ) and 7.24 ( $\text{CDCl}_3$ ) for  $^1\text{H}$  and  $\delta_{\text{C}}$  39.5 (DMSO- $d_6$ ), 29.92 (Acetone- $d_6$ ), and 77.23 ( $\text{CDCl}_3$ ) for  $^{13}\text{C}$ . Mass spectra (ESI) were recorded with a Finnigan LCQ Deca mass spectrometer, and HRMS (ESI) spectra were obtained with a FTHRMS-Orbitrap (Thermo-Finnigan) mass spectrometer. EI-MS measurements were carried out on a Finnigan Trace GC Ultra instrument equipped with Finnigan Trace DSQ mass spectrometer (Thermo Electron Corp.). Solvents were distilled prior to use, and spectral grade solvents were used for spectroscopic measurements. HPLC analysis was performed with a Dionex P580 system coupled to a photodiode array detector (UVD340S); routine detection was at 235, 254, 280, and 340 nm. The separation column (125 × 4 mm) was prefilled with Eurosphere-10 C<sub>18</sub> (Knauer, Germany), and the following gradient was used (MeOH, 0.1% HCOOH in H<sub>2</sub>O): 0-5 min (10% MeOH); 5-35 min (10-100% MeOH); 35-45 min (100% MeOH). Semi-preparative HPLC was performed using a Merck Hitachi HPLC System (UV detector L-7400; Pump L-7100; Eurosphere-100 C18, 300 × 8 mm, Knauer, Germany). Column chromatography included Diaion HP-20, LH-20 Sephadex and Merck MN Silica gel 60 M (0.04-0.063 mm) TLC plates with silica gel F254 (Merck, Darmstadt, Germany) were used to monitor fractions ( $\text{CH}_2\text{Cl}_2/\text{MeOH}$  mixtures as mobile phase); detection was under UV at 254 and 366 nm or by spraying the plates with anisaldehyde reagent.

**Ascidian material**

*Polycarpa aurata* – identified by Dr. Nicole de Voogd from the Naturalis Biodiversity Center in Leiden – was collected by SCUBA diving at Ambon, Indonesia, an October 1996 at a depth of 30 m. The colour of its exterior was beige to red with some dark blue stripes. The ascidian was preserved in a mixture of EtOH and H<sub>2</sub>O (70:30) and stored in a -20°C freezer. A voucher specimen (voucher number: RMNH UROCH. 01001) is stored at the Naturalis Biodiversity Center, Darwinweg 2, P.O. Box 9517, 2300 RA Leiden, The Netherlands.

**Extraction and isolation**

The frozen material was thawed and cut into small pieces. The wet weight was 500 g. It was extracted with EtOAc. We obtained a dry crude extract of 1.2 g which was subjected to chromatographic separation using Diaion HP-20 employing a step gradient of H<sub>2</sub>O/MeOH to yield eight fractions H1-H8. H5 was suspended in MeOH, then filtered, and compound **3** (6.5 mg) was obtained from the residue. H6 (750 mg) was submitted to LH-20 Sephadex size exclusion chromatography yielding twenty-two fractions S1-S22. From these fractions the other five compounds were obtained by semi-preparative HPLC. The yields were as follows: **1** (2.0 mg), **2** (4.0 mg), *N,N*-didesmethylgrossularine-1 (7.7 mg), 4-methoxybenzoic acid (15 mg), *N*-methyl-2-(4-methoxyphenyl)-2-oxoacetamide (2.5 mg).

**Polycarpathiamine A (1):**

Dark yellow amorphous solid; UV ( $\lambda_{\text{max}}$ , MeOH) (log  $\epsilon$ ) 204.5 (3.99), 226.8 (3.80), 325.8 (3.68) nm; IR (ATR) 3314, 3200, 1595, 1578, 1508, 1450, 1287, 1244, 1171, 1123 cm<sup>-1</sup>; <sup>1</sup>H NMR (DMSO-*d*<sub>6</sub>, 400MHz)  $\delta$  10.79 (1H, br.s, 4'-OH), 8.37 (2H, d, *J*= 8.8 Hz, H-2'/6'), 7.08 (2H, s, 3-NH<sub>2</sub>), 6.94 (2H, d, *J*= 8.8 Hz, H-3'/5'); and <sup>1</sup>H NMR (Acetone-*d*<sub>6</sub>, 600MHz)  $\delta$  9.58 (1H, br.s, 4'-OH), 8.48 (2H, d, *J*= 8.9 Hz, H-2'/6'), 7.01 (2H, d, *J*= 8.9 Hz, H-3'/5'), 6.44 (2H, s, 3-NH<sub>2</sub>); <sup>13</sup>C NMR data, see Table 1; EI-MS (rel., %) *m/z* 221 (49.5) [M<sup>+</sup>], 193 (6.9), 179 (8.2), 152 (10.6), 121 (100.0), 93 (16.0), 74 (15.3), 65(14.5); ESIMS *m/z* 221.8 [M + H]<sup>+</sup>, 244.1 [M + Na]<sup>+</sup>, 464.6 [2M+Na]<sup>+</sup>, and 220.2 [M-H]<sup>-</sup>; HRESIMS *m/z* 222.0331 [M+H]<sup>+</sup> (calcd for C<sub>9</sub>H<sub>8</sub>N<sub>3</sub>O<sub>2</sub>S 222.0332), 244.0148 [M+Na]<sup>+</sup> (calcd for C<sub>9</sub>H<sub>7</sub>N<sub>3</sub>O<sub>2</sub>SNa 244.0151), 465.0406 [2M+Na]<sup>+</sup> (calcd for C<sub>18</sub>H<sub>14</sub>N<sub>6</sub>O<sub>4</sub>S<sub>2</sub>Na 465.0410).

**Polycarpathiamine B (2):**

Dark yellow amorphous solid; UV ( $\lambda_{\max}$ , MeOH) (log  $\epsilon$ ) 204.3 (4.01), 227.2 (3.78), 326.8 (3.74) nm; IR (ATR) 3335, 3201, 2930 (w), 2850 (w), 1594, 1579, 1506 (sh), 1508, 1448, 1288  $\text{cm}^{-1}$ ;  $^1\text{H}$  NMR (DMSO- $d_6$ , 300MHz)  $\delta$  8.44 (2H, d,  $J=9.0$  Hz, H-2'/6'), 7.15 (2H, d,  $J=9.0$  Hz, H-3'/5'), 7.12 (2H, s, 3-NH<sub>2</sub>), 3.90 (3H, s, 4'-OMe);  $^{13}\text{C}$  NMR data, see Table 1; EI-MS (rel., %)  $m/z$  235 (50.4) [ $\text{M}^+$ ], 207 (4.6), 193 (6.6), 166 (14.6), 149 (22.6), 135 (100.0), 107 (9.1), 92 (11.3), 77 (14.5), 74 (9.0); ESIMS  $m/z$  236.0 [ $\text{M} + \text{H}$ ]<sup>+</sup>, 257.8 [ $\text{M} + \text{Na}$ ]<sup>+</sup>, 492.6 [ $2\text{M} + \text{Na}$ ]<sup>+</sup>; HRESIMS  $m/z$  236.0488 [ $\text{M} + \text{H}$ ]<sup>+</sup> (calcd for C<sub>10</sub>H<sub>10</sub>N<sub>3</sub>O<sub>2</sub>S 236.0488), 258.0307 [ $\text{M} + \text{Na}$ ]<sup>+</sup> (calcd for C<sub>10</sub>H<sub>9</sub>N<sub>3</sub>O<sub>2</sub>SNa 258.0308).

**Preparation of 5-dimethylamino-1,3,4-oxathiazol-2-one**

*N,N*-dimethylurea (3 g, 34.05 mmol) was suspended in 16 ml dry acetonitrile. Chlorocarbonylsulphenyl chloride (1.49 g, 11.35 mmol) was dissolved in 3 ml dry acetonitrile and added in portions to the suspension. After stirring for 1h at room temperature, the reaction mixture was filtrated. Excess of chlorocarbonylsulphenyl chloride was decomposed by adding 1 ml methanol to the filtrate. The reaction mixture was mingled with 8 g silica gel, evaporated under reduced pressure, loaded on top of a silica gel column and eluted with dichloromethane-hexane (3:1) to obtain 1.17 g (70%) of the title compound as a yellow oil.  $^1\text{H}$  NMR (CDCl<sub>3</sub>, 600MHz)  $\delta$  3.00 (6H, s, 2 $\times$  NCH<sub>3</sub>);  $^{13}\text{C}$  NMR (CDCl<sub>3</sub>, 150MHz)  $\delta$  174.6 (C-2), 153.3 (C-5), 37.5 (NCH<sub>3</sub>); EI-MS (rel.)  $m/z$  146 ( $\text{M}^+$ , 40%), 72 (100%).

**Preparation of 3-dimethylamino-5-benzoyl-1,2,4-thiadiazole (4)**

A solution of benzoyl cyanide (100 mg, 0.76 mmol) in 1 mL dry dimethylformamide was heated to 150°C on an oil bath. Then 5-dimethylamino-1,3,4-oxathiazol-2-one (336 mg, 2.30 mmol) was added drop by drop. After 10 min the reaction mixture was cooled down and put on top of a neutral aluminium oxide column. Elution was performed with mixtures of dichloromethane-hexane (1:1–2:1). The fractions of interest were purified by semi-preparative HPLC to afford 6 mg (3.4%) of the title compound as yellow crystals. m.p. 75–76°C; UV ( $\lambda_{\max}$ , MeOH) (log  $\epsilon$ ) 203.9 (4.09), 227.2 (3.84), 267.7 (3.80), 409.0 (2.97) nm; IR (ATR) 2924 (w), 2864 (w), 1636, 1595 (w), 1576 (w), 1549, 1501, 1454, 1414, 1283, 903, 849  $\text{cm}^{-1}$ ;  $^1\text{H}$  NMR (DMSO- $d_6$ , 600MHz)  $\delta$  8.40 (2H, dd,  $J=8.4, 1.2$  Hz, H-2'/6'),

7.63 (2H, dd,  $J= 8.4, 7.4$  Hz, H-3'/5'), 7.78 (1H, tt,  $J= 7.4, 1.2$  Hz), 3.19 (6H, s, 3-NMe<sub>2</sub>); <sup>13</sup>C NMR data, see Table 1; EI-MS (rel., %)  $m/z$  233 (100.0) [M<sup>+</sup>], 207 (5.2), 128 (16.4), 105 (63.1), 102 (76.1), 87 (22.5), 77 (43.8), 69 (7.2), 51 (14.9), 44 (31.3); ESIMS  $m/z$  234.1 [M+H]<sup>+</sup>; HRESIMS  $m/z$  234.06965 [M+H]<sup>+</sup> (calcd for C<sub>11</sub>H<sub>12</sub>N<sub>3</sub>OS 234.06956).

### Bioassay

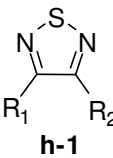
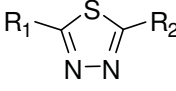
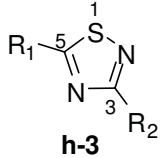
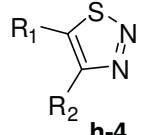
Cytotoxicity was tested against L5178Y mouse lymphoma cells using a microculture tetrazolium (MTT) assay and compared to that of untreated controls, as described previously<sup>16,17</sup>. Experiments were repeated three times and carried out in triplicate. As negative controls, media with 0.1% EGMME/ DMSO were included in the experiments. The depsipeptide kahalalide F, isolated from *Elysia grandifolia*<sup>2</sup> was used as a positive control.

---

(16) Pham, C.-D.; Hartmann, R.; Müller, W. E. G.; de Voogd, N.; Lai, D.; Proksch, P. *J. Nat. Prod.* **2013**, *76*, 103-106

(17) Ashour, M.; Edrada, R.; Ebel, R.; Wray, V.; Watjen, W.; Padmakumar, K.; Müller, W. E. G.; Lin, W. H.; Proksch, P. *J. Nat. Prod.* **2006**, *69*, 1547-1553

Table S1 The  $^{13}\text{C}$  NMR chemical shifts for the four possible ring structures

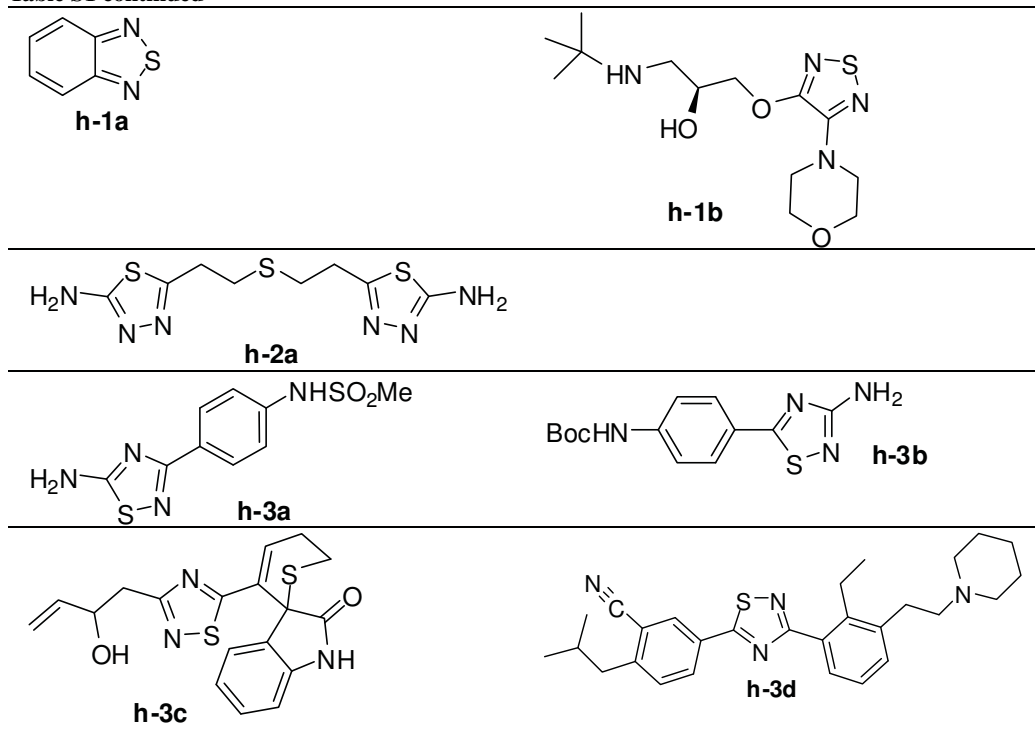
Ring systems	R <sub>1</sub>	R <sub>2</sub>	Chemical shifts / $\delta_{\text{C}}^a$	Ref.
 h-1	CN	CN	(CDCl <sub>3</sub> ) 136.8	1
	COCH <sub>3</sub>	COCH <sub>3</sub>	(CDCl <sub>3</sub> ) 159.5	1
	Ph	Ph	(DMSO- <i>d</i> <sub>6</sub> ) 159.6	2
	CH=CH <sub>2</sub>	OH	(CDCl <sub>3</sub> ) 162.8, 147.3	3
	CH <sub>2</sub> OH	OH	(CDCl <sub>3</sub> ) 161.6, 150.4	3
	CH <sub>2</sub> CH <sub>2</sub> SCH <sub>3</sub>	OH	(CDCl <sub>3</sub> ) 162.7, 150.8	3
	See h-1a See h-1b			(DMSO- <i>d</i> <sub>6</sub> ) 155.0 (CDCl <sub>3</sub> ) 153.7, 150.0
 h-2	Ph	Ph	(DMSO- <i>d</i> <sub>6</sub> ) 167.7 <sup>b</sup>	6
	Et	NH <sub>2</sub>	(DMSO- <i>d</i> <sub>6</sub> ) 168.1 (C <sub>2</sub> ), 159.7 (C <sub>5</sub> ) <sup>c</sup>	7
	See h-2a		(DMSO- <i>d</i> <sub>6</sub> ) 168.5, 156.4	7
 h-3	Me	Me	187.9 (C <sub>5</sub> ), 173.3 (C <sub>3</sub> )	8
	NHBoc	Ph	(CDCl <sub>3</sub> ) 178.4 (C <sub>5</sub> ), 167.6 (C <sub>3</sub> )	9
	NHBoc	CH=CH <sub>2</sub>	(DMSO- <i>d</i> <sub>6</sub> ) 177.0 (C <sub>5</sub> ), 167.2 (C <sub>3</sub> )	9
	Ph	NH <sub>2</sub>	(CDCl <sub>3</sub> ) 187.8 (C <sub>5</sub> ), 169.7 (C <sub>3</sub> )	9
	Ph	NH <sub>2</sub>	185.7 (C <sub>5</sub> ), 171.0 (C <sub>3</sub> )	10
	OMe	NH <sub>2</sub>	(DMSO- <i>d</i> <sub>6</sub> ) 189.6 (C <sub>5</sub> ), 165.3 (C <sub>3</sub> ) <sup>c</sup>	
	NH <sub>2</sub>	isopropyl	(DMSO- <i>d</i> <sub>6</sub> ) 183.2 (C <sub>5</sub> ), 177.6 (C <sub>3</sub> ) <sup>c</sup>	
	C <sub>6</sub> H <sub>5</sub> CO	Ph	187.0 (C <sub>5</sub> ), 174.3 (C <sub>3</sub> )	11
	C <sub>6</sub> H <sub>5</sub> CO	Me	186.7 (C <sub>5</sub> ), 174.6 (C <sub>3</sub> )	11
	2-Furoyl	Ph	185.7 (C <sub>5</sub> ), 174.3 (C <sub>3</sub> )	11
	Ac	Ph	185.9 (C <sub>5</sub> ), 174.4 (C <sub>3</sub> )	11
	CHCl <sub>2</sub>	Ph	185.9 (C <sub>5</sub> ), 173.6 (C <sub>3</sub> )	11
	See h-3a		(DMF- <i>d</i> <sub>7</sub> ) 184.3 (C <sub>5</sub> ), 168.8 (C <sub>3</sub> )	9
	See h-3b		(DMSO- <i>d</i> <sub>6</sub> ) 185.3 (C <sub>5</sub> ), 170.8 (C <sub>3</sub> )	9
	See h-3c		(DMSO- <i>d</i> <sub>6</sub> ) 185.7 (C <sub>5</sub> ), 172.9 (C <sub>3</sub> )	12
See h-3d		(DMSO- <i>d</i> <sub>6</sub> ) 184.9 (C <sub>5</sub> ), 174.1 (C <sub>3</sub> )	13	
 h-4	H	<i>t</i> -Bu	(CDCl <sub>3</sub> ) 129.3, 173.6	14
	H	Ph	(CDCl <sub>3</sub> ) 131.2, 163.3	14
	H	Me	(CDCl <sub>3</sub> ) 132.6, 160.0	14
	CH <sub>2</sub> OH	Me	(CDCl <sub>3</sub> ) 154.4, 152.9	15
	CHO	Me	(CDCl <sub>3</sub> ) 156.2, 154.2	15
	NH <sub>2</sub>	CSNH <sub>2</sub>	(DMSO- <i>d</i> <sub>6</sub> ) 168.4 (C <sub>5</sub> ), 136.7 (C <sub>4</sub> )	16
	NH <sub>2</sub>	COOEt	(DMSO- <i>d</i> <sub>6</sub> ) 162.5 (C <sub>5</sub> ), 132.5 (C <sub>4</sub> )	16

<sup>a</sup> Only the chemical shifts of the carbons in the heterocyclic ring are listed.

<sup>b</sup> The chemical shifts for the other symmetric analogues (with different substitutions in the aromatic rings) are in the range of 160.89-171.14 ppm (see ref. <sup>6</sup>)

<sup>c</sup> Commercially available substances purchased from Sigma, and the unambiguous assignments of the NMR data were finished by analysis of 1D, and 2D NMR (HSQC, HMBC) spectra.

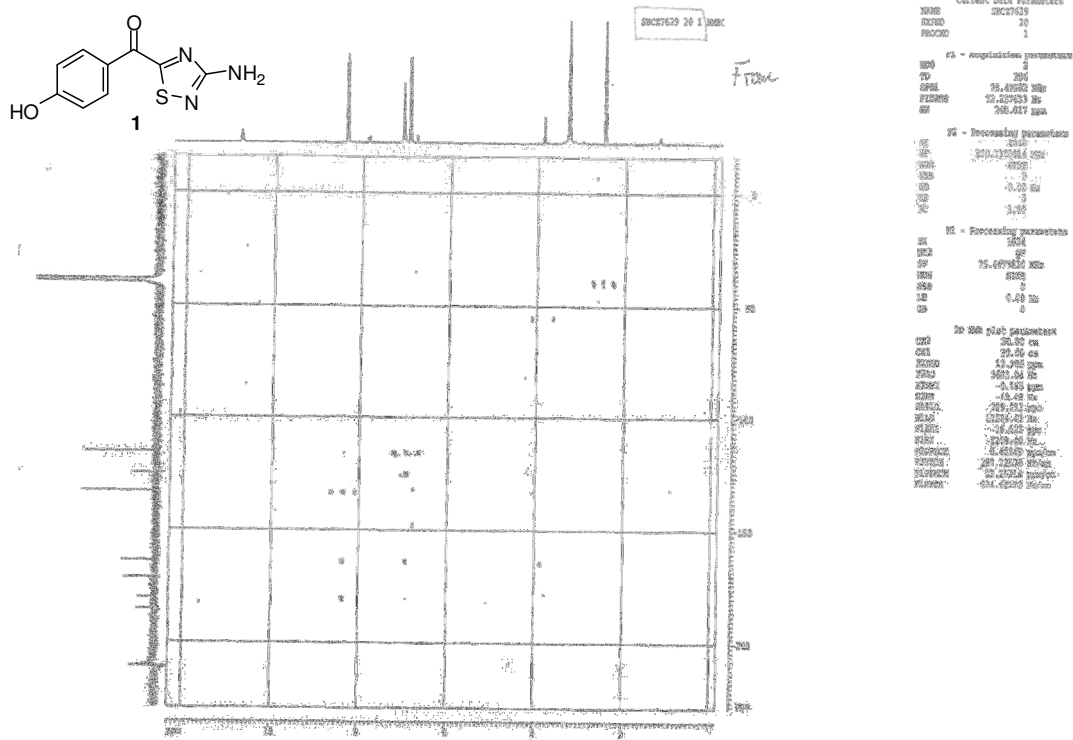
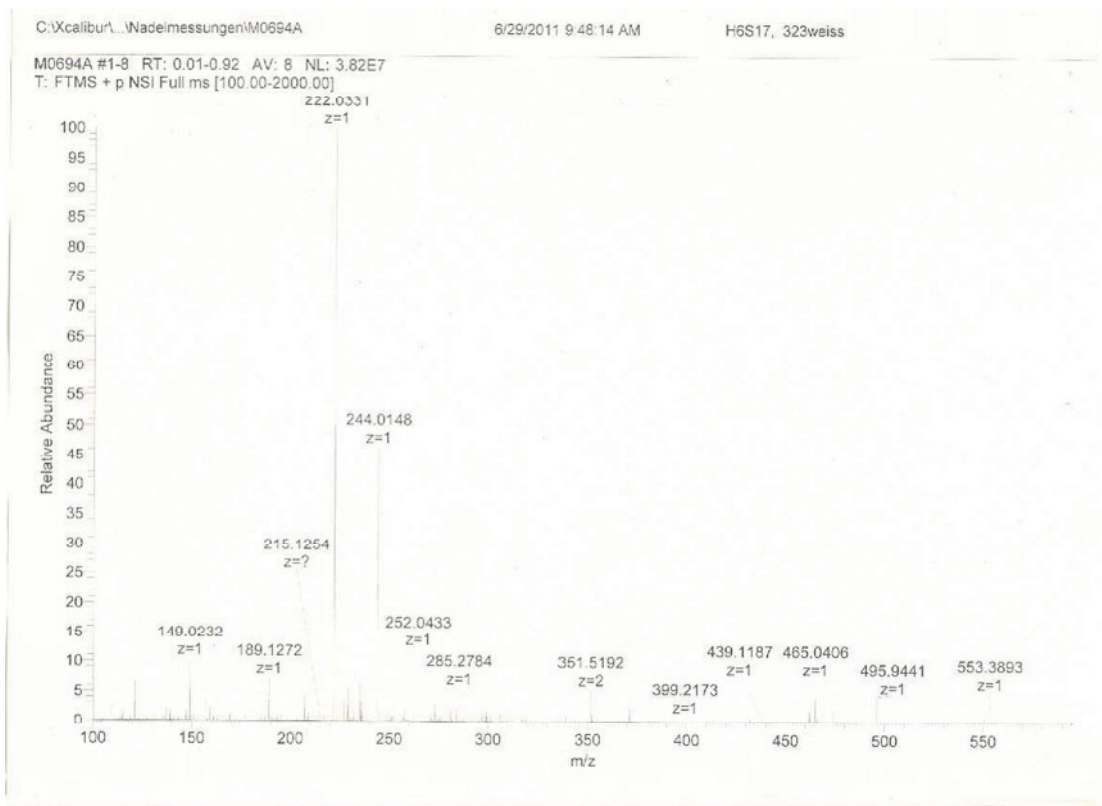
Table S1 continued



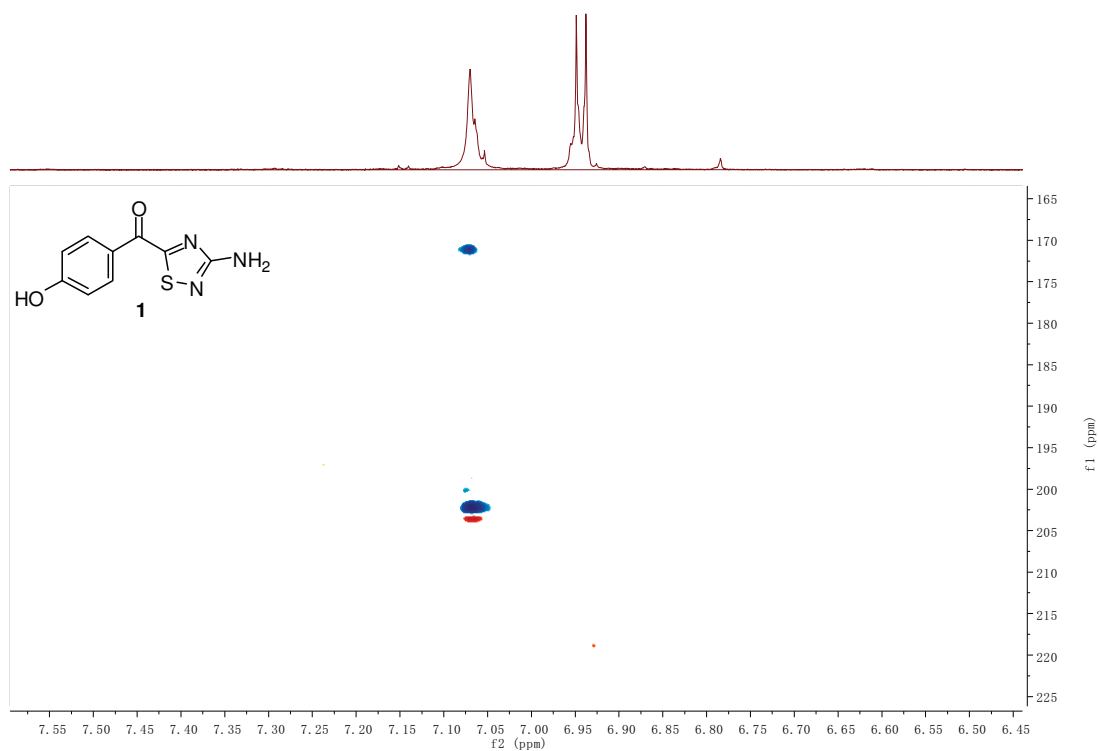
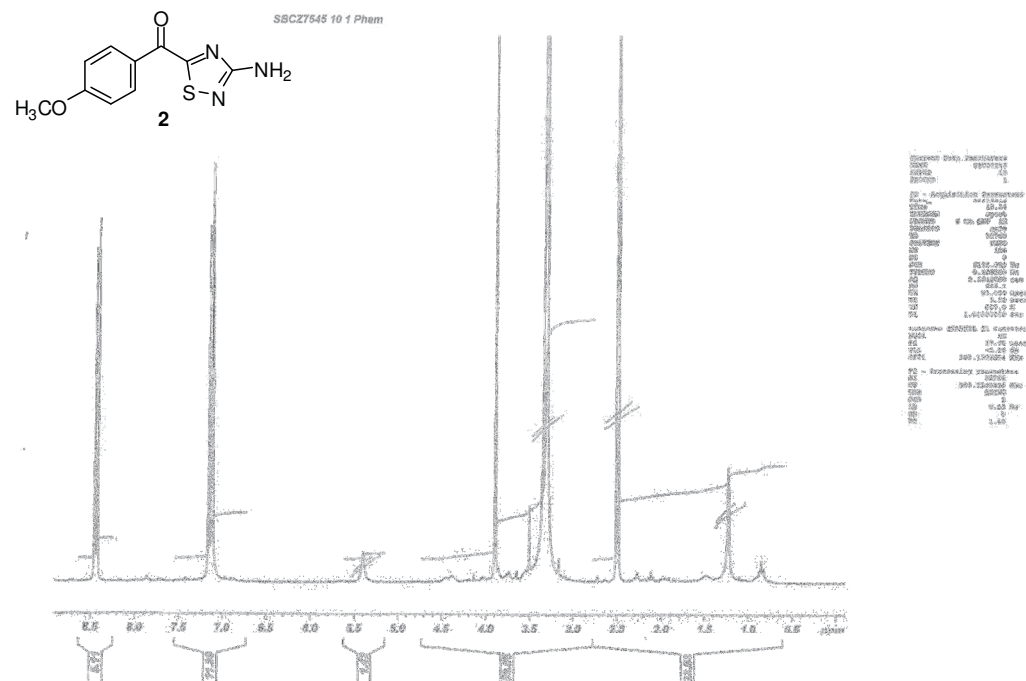
## References

- Dunn, P. J.; Rees, C. W. *J. Chem. Soc., Perkin Trans. 1* **1987**, 1579-1584.
- Kamiński, B.; Schilf, W.; Sitkowski, J.; Stefaniak, L.; Webb, G. A. *J. Crystallogr. Spectrosc. Res.* **1989**, *19*, 1003-1008.
- Philipp, D. M.; Müller, R.; Goddard, W. A.; Abboud, K. A.; Mullins, M. J.; Snelgrove, R. V.; Athey, P. S. *Tetrahedron Lett.* **2004**, *45*, 5441-5444.
- da Silva Miranda, F.; Signori, A. M.; Vicente, J.; de Souza, B.; Priebe, Jacks P.; Szpoganicz, B.; Gonçalves, N. S.; Neves, A. *Tetrahedron* **2008**, *64*, 5410-5415.
- Narina, S. V.; Sudalai, A. *Tetrahedron* **2007**, *63*, 3026-3030.
- Lebrini, M.; Bentiss, F.; Lagrenée, M. *J. Heterocycl. Chem.* **2005**, *42*, 991-994.
- Shukla, K.; Ferraris, D. V.; Thomas, A. G.; Stathis, M.; Duvall, B.; Delahanty, G.; Alt, J.; Rais, R.; Rojas, C.; Gao, P.; Xiang, Y.; Dang, C. V.; Slusher, B. S.; Tsukamoto, T. *J. Med. Chem.* **2012**, *55*, 10551-10563.
- Stanley Cameron, T.; Decken, A.; Fang, M.; Passmore, J.; Wood, D. J.; Parsons, S. *Chem. Commun.* **1999**, 1801-1802.
- Wehn, P. M.; Harrington, P. E.; Eksterowicz, J. E. *Org. Lett.* **2009**, *11*, 5666-5669 (the chemical shifts for other analogues are also available in this paper).
- Butler, R. N.; O'Donoghue, D. A.; O'Halloran, G. A. *J. Chem. Soc., Chem. Commun.* **1986**, 800-801.
- McKie, M. C.; Paton, R. M. *ARKIVOC* **2002**, 15-21.
- Chen, M.; Lin, S.; Li, L.; Zhu, C.; Wang, X.; Wang, Y.; Jiang, B.; Wang, S.; Li, Y.; Jiang, J.; Shi, J. *Org. Lett.* **2012**, *14*, 5668-5671.
- Ren, F.; Deng, G.; Wang, H.; Luan, L.; Meng, Q.; Xu, Q.; Xu, H.; Xu, X.; Zhang, H.; Zhao, B.; Li, C.; Guo, T. B.; Yang, J.; Zhang, W.; Zhao, Y.; Jia, Q.; Lu, H.; Xiang, J.-N.; Elliott, J. D.; Lin, X. *J. Med. Chem.* **2012**, *55*, 4286-4296 (The values for the other analogues are also similar and available in this paper).
- Sandrinelli, F.; Boudou, C.; Caupène, C.; Averbuch-Pouchot, M.T.; Perrio, S.; Metzner, P. *Synlett* **2006**, *2006*, 3289-3293.
- Porcal, W.; Hernández, P.; González, M.; Ferreira, A.; Olea-Azar, C.; Cerecetto, H.; Castro, A. *J. Med. Chem.* **2008**, *51*, 6150-6159.
- Bakulev, V. A.; Lebedev, A. T.; Dankova, E. F.; Mokrushin, V. S.; Petrosyan, V. S. *Tetrahedron* **1989**, *45*, 7329-7340.



Figure S3 HMBC spectrum of **1** (DMSO- $d_6$ )Figure S4 HRESIMS spectrum of **1**



Figure S5  $^1\text{H}$ - $^{15}\text{N}$  HMBC spectrum of **1** (DMSO- $d_6$ )Figure S6  $^1\text{H}$  NMR spectrum of **2** (DMSO- $d_6$ )



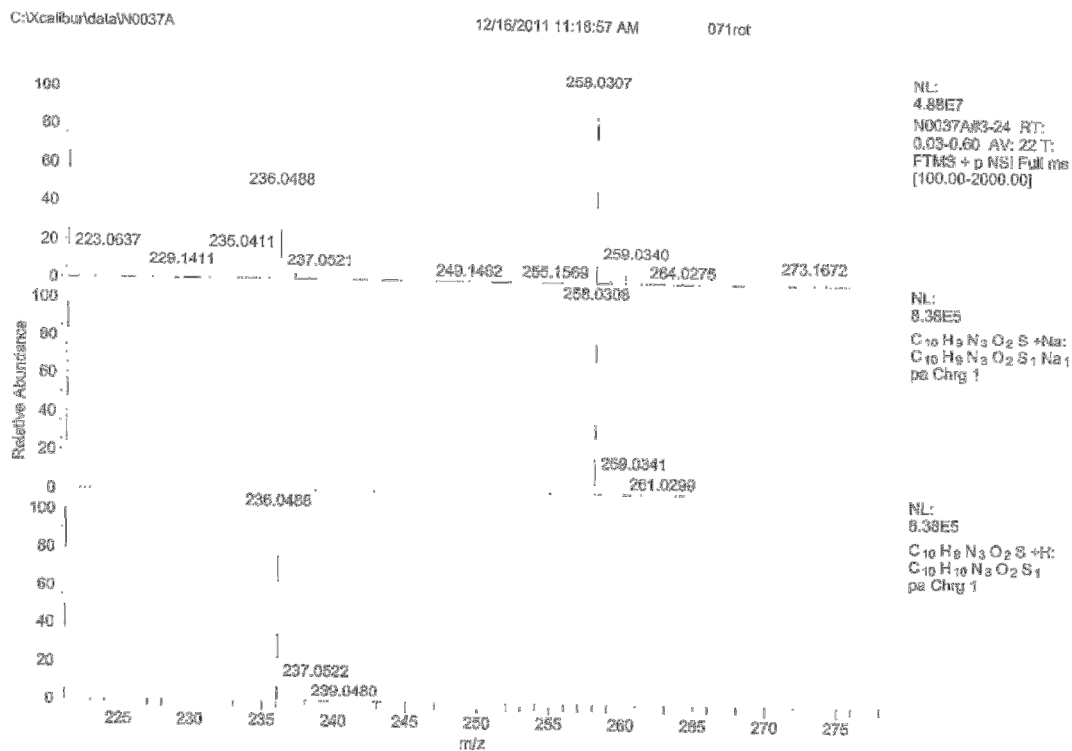


Figure S9 HRESIMS spectrum of 2

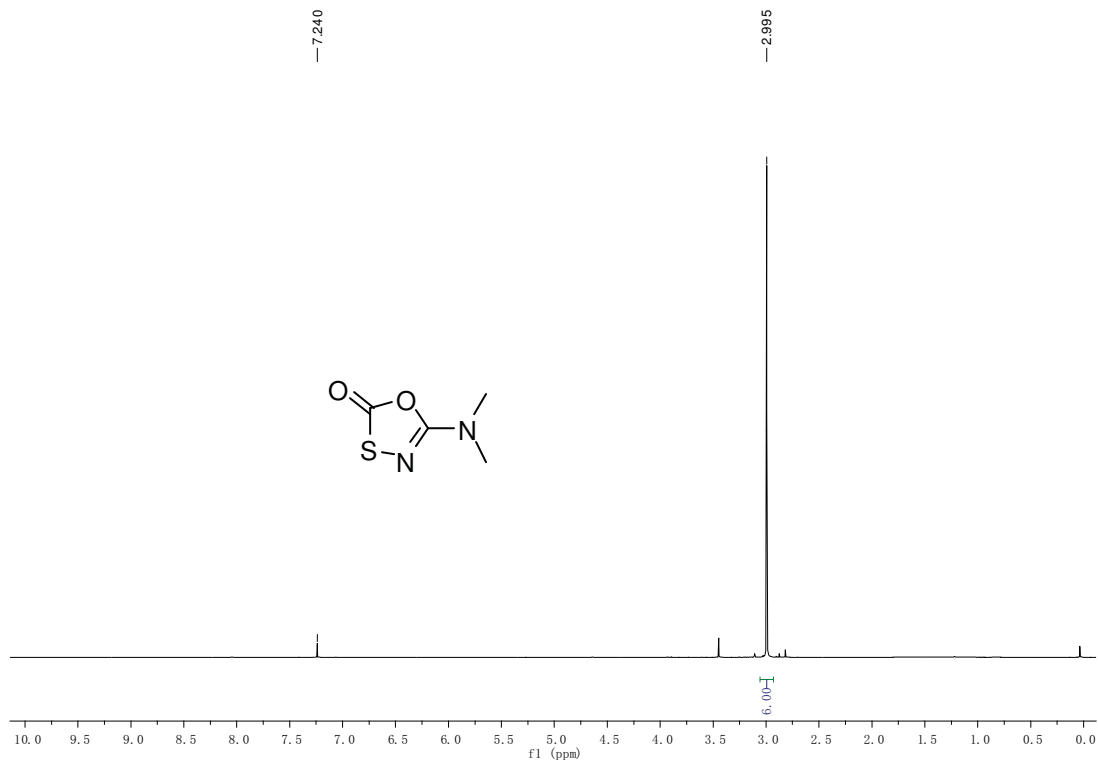
Figure S10 <sup>1</sup>H NMR spectrum of 5-dimethylamino-1,3,4-oxathiazol-2-one (CDCl<sub>3</sub>)



Figure S11  $^{13}\text{C}$  NMR spectrum of 5-dimethylamino-1,3,4-oxathiazol-2-one ( $\text{CDCl}_3$ )

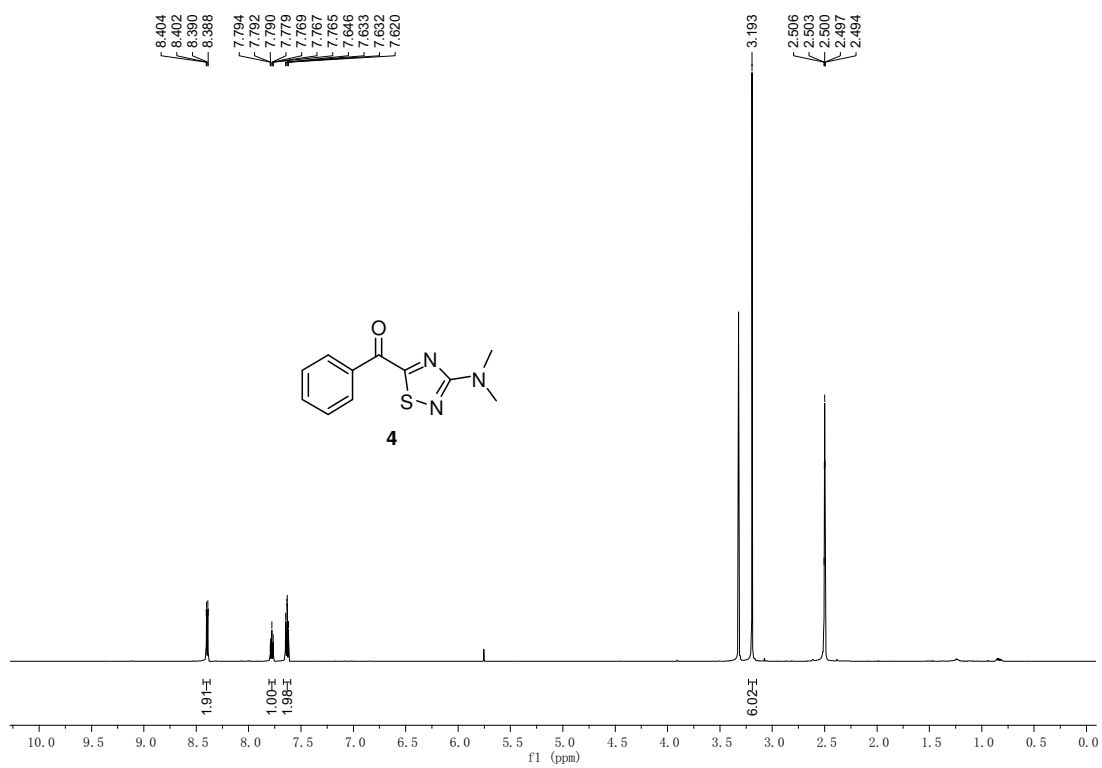


Figure S12  $^1\text{H}$  NMR spectrum of 4 ( $\text{DMSO}-d_6$ )

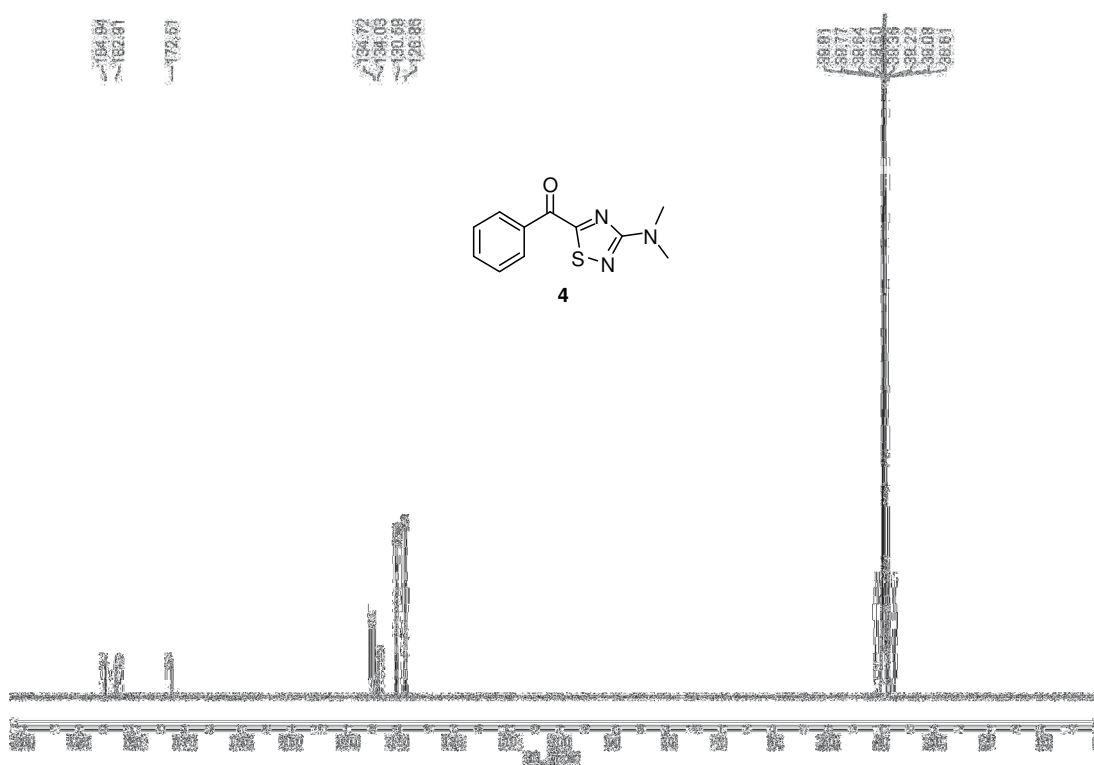


Figure S13  $^{13}\text{C}$  NMR spectrum of **4** ( $\text{DMSO-}d_6$ )

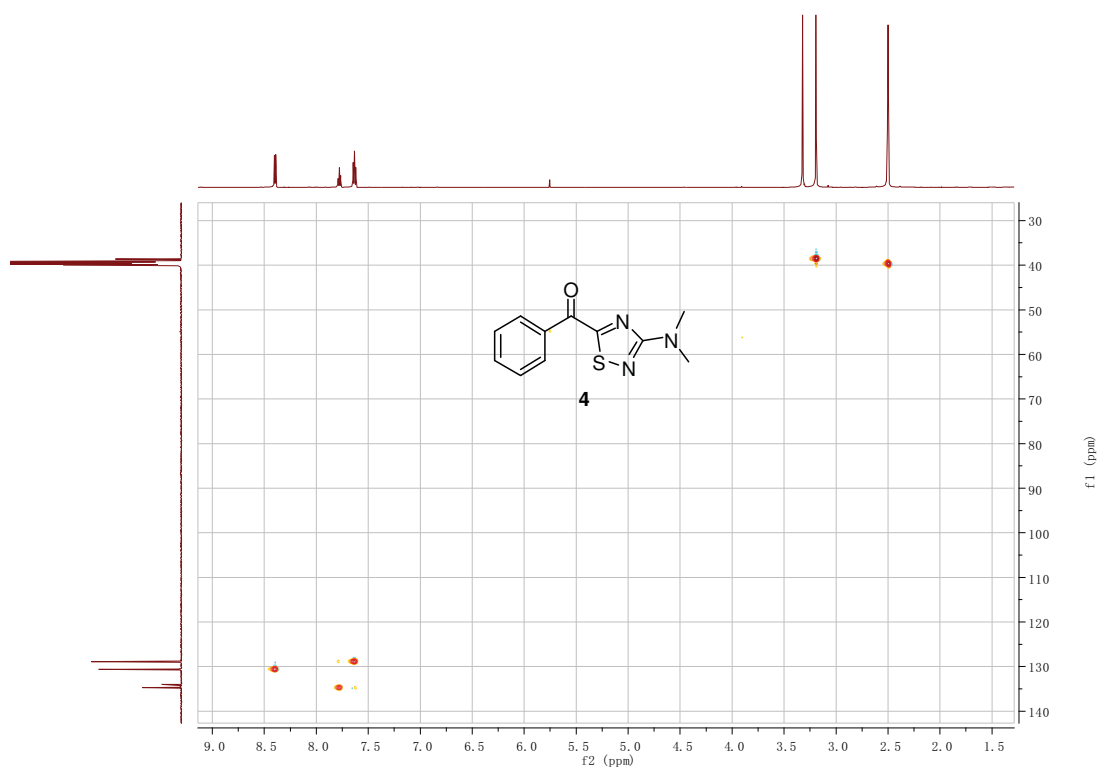


Figure S14 HSQC spectrum of **4** ( $\text{DMSO-}d_6$ )

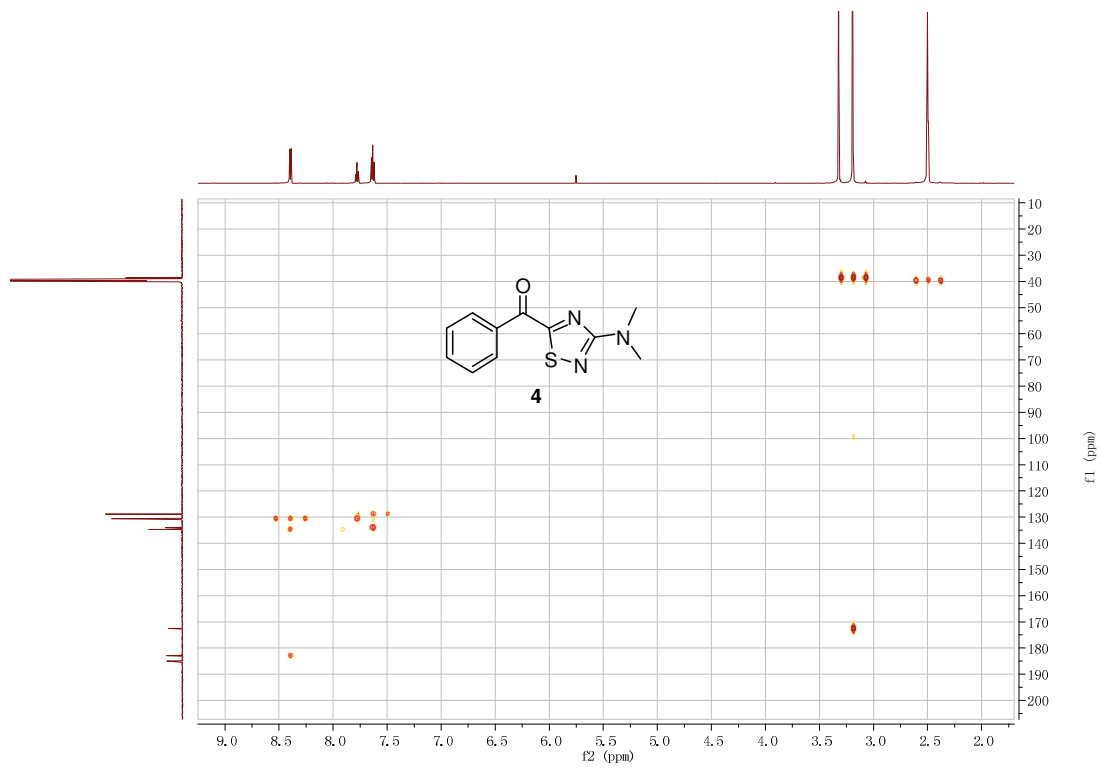
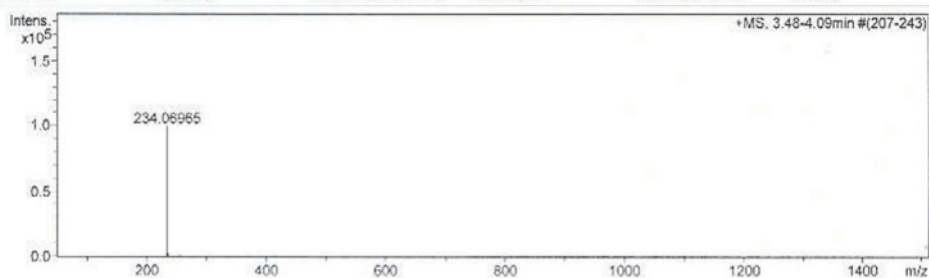


Figure S15 HMBC spectrum of **4** ( $\text{DMSO-}d_6$ )

## Mass Spectrum SmartFormula Report

**Analysis Info**  
Analyte Name: D:\Data\HHU\_Servic\Prokech13000015.d  
Method: tune\_low.m  
Sample Name: Cong-Dat Pham FB06 Syn2 EP in CH3OH (CH3CN/H2O)  
Comment:  
Acquisition Date: 3/4/2013 3:31:29 PM  
Operator: Peter Tommes  
Instrument / Ser#: maXis 4G 20213

**Acquisition Parameter**  
Source Type: ESI  
Focus: Not active  
Scan Begin: 50 m/z  
Scan End: 1500 m/z  
Ion Polarity: Positive  
Set Capillary: 4000 V  
Set End Plate Offset: -500 V  
Set Collision Cell RF: 800.0 Vpp  
Set Nebulizer: 0.3 Bar  
Set Dry Heater: 180 °C  
Set Dry Gas: 4.0 l/min  
Set Divert Valve: Source



Meas. m/z	#	Formula	Score	m/z	err [mDa]	err [ppm]	mSigma	rdB	e <sup>-</sup> Conf	N-Rule
234.06965	1	C 11 H 12 N 3 O S	100.00	234.06956	-0.10	-0.41	45.7	7.5	even	ok

Figure S16 HRESIMS spectrum of 4

**6. Publication 3: *Callyspongia* sp.**

Intended for submission to “Angewandte Chemie Int. Ed.”

Impact factor: 13.734

Contribution: 80%, first author, conducting most of the experiments (except those mentioned in “Declaration of academic honesty/Erklärung”), manuscript writing



## Callyspongiolide, an Unprecedented Cytotoxic Macrolide from the Marine Sponge *Callyspongia* sp.\*\*

Cong-Dat Pham, Rudolf Hartmann, Philip Böhler, Björn Stork, Sebastian Wesselborg, Wenhan Lin, Daowan Lai\*, and Peter Proksch\*

Macrolides have been reported from various marine macroorganisms<sup>[1]</sup> but are especially prominent for marine sponges as exemplified by the discovery of dictyostatin<sup>[2]</sup>, lasonolide A<sup>[3]</sup>, peloruside A<sup>[4]</sup>, salicylhalamides A and B<sup>[5]</sup>, candidaspongiolides<sup>[6]</sup>, and leiodermatolide<sup>[7]</sup>. Many macrolides display potent antiproliferative properties against cancer cells making them promising leads for the development of new chemotherapeutic agents<sup>[8]</sup>. Due to their unusual structures and pronounced bioactivity these compounds continue to be exciting targets for realizing a total synthesis<sup>[8c, 8d, 9]</sup>, which not only could confirm or solve the stereochemistry of the structure, but also contribute to further biochemical or clinical investigations that may be initially hampered by their low natural abundance.

Sponges belonging to the genus *Callyspongia* have proven to be rich sources of various cytotoxic substances, such as polyketides<sup>[10]</sup>, polyacetylenes<sup>[11]</sup>, alkaloids<sup>[12]</sup>, and cyclic peptides<sup>[13]</sup>. Macrolides, however, have not been reported from this genus prior to this study. In our search for bioactive metabolites from marine organisms<sup>[14]</sup>, we observed that a methanolic extract of the sponge *Callyspongia* sp., collected in Indonesia, completely inhibited the growth of the murine lymphoma cell line L5178Y at a concentration of 10 µg/mL. Chromatographic separation of the extract afforded a new bioactive

macrolide, named callyspongiolide (**1**) (4.6 mg, 0.00092 % wet weight). Herein, we report the structure elucidation, configurational analysis and cytotoxic activity of the first macrolide discovered from the genus *Callyspongia*. Callyspongiolide (**1**) was obtained as a light yellowish amorphous solid. The ESIMS spectrum of **1** showed pseudomolecular ion peaks ( $[M+Na]^+$ ) at  $m/z$  650.1 and 652.1 with approximately the same intensity, indicating the presence of one bromine atom in **1**. Its molecular formula was established as  $C_{33}H_{42}BrNO_6$  by HRESIMS measurement, as a prominent pseudomolecular ion peak was observed at  $m/z$  650.2085  $[M+Na]^+$ . The <sup>1</sup>H NMR spectrum showed signals attributable to three aromatic protons [ $\delta_H$  = 7.13 (t), 6.84 (dd), 6.83 ppm (dd)], eight olefinic protons [ $\delta_H$  = 6.36 (d), 6.13 (td), 6.06 (dd), 5.94 (dd), 5.93 (dd), 5.46 (dd), 5.22 (dd), 5.06 ppm (dd)], three oxygenated methine protons [ $\delta_H$  = 5.09 (dd), 4.89 (d), 4.47 ppm (br.dd)], and five methyl groups [ $\delta_H$  = 1.04 (s), 0.97 (d), 0.96 (s), 0.89 (d), 0.87 ppm (d)] (Table 1). In the <sup>13</sup>C NMR spectrum (Table 1), 33 resonances were clearly seen, which were assignable to one ester group ( $\delta_C$  = 164.2 ppm), one carbamate group ( $\delta_C$  = 156.7 ppm), one benzene ring ( $\delta_C$  = 153.3, 143.2, 126.9, 120.1, 114.3, 111.7 ppm), eight olefinic carbons ( $\delta_C$  = 151.6, 142.5, 139.6, 136.4, 132.0, 122.3, 113.4, 106.8 ppm), one alkyne group ( $\delta_C$  = 90.4, 86.3 ppm), and 15  $sp^3$  hybrid carbons. These functionalities account for 12 of the total 13 degrees of unsaturation as required by the molecular formula, thus implying that one additional ring is present in the structure of **1**.

[\*] C.-D. Pham, Dr. D. Lai, Prof. Dr. P. Proksch  
Institute of Pharmaceutical Biology and Biotechnology, Heinrich-Heine-University, 40225 Düsseldorf, Germany  
Fax: (+49) 211- 81 11923

E-mail: [laidaowan123@gmail.com](mailto:laidaowan123@gmail.com), [proksch@uni-duesseldorf.de](mailto:proksch@uni-duesseldorf.de)  
Homepage: [http://www.pharmazie.uni-duesseldorf.de/Institute/pharm\\_bio/arbeitskreise/ak\\_proksch](http://www.pharmazie.uni-duesseldorf.de/Institute/pharm_bio/arbeitskreise/ak_proksch)

Dr. R. Hartmann  
Institute of Complex Systems (ICS-6), Forschungszentrum Jülich GmbH, 52425 Jülich, Germany

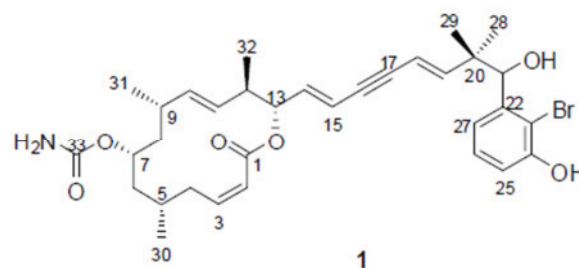
P. Böhler, Dr. B. Stork, Prof. Dr. S. Wesselborg  
Institute of Molecular Medicine, Heinrich-Heine-University, 40225 Düsseldorf, Germany

Prof. Dr. W. Lin  
State Key Laboratory of Natural and Biomimetic Drugs, Peking University, Beijing 100191, People's Republic of China

[\*\*] P.P. wants to thank BMBF for support. We wish to acknowledge the help and support of Dr. Elizabeth Ferdinandus (University of Ambon, Indonesia) during sponge collection and of Dr. Nicole de Voogd (Leiden, Naturalis Biodiversity Center, Leiden, The Netherlands) for identification of the sponge. We are indebted to Prof. W. E. G. Müller (Johannes Gutenberg University, Mainz, Germany) for cytotoxicity assays against L5178Y mouse lymphoma cells.



Supporting information for this article is available on the WWW under <http://dx.doi.org/10.1002/anie.201xxxxx>.



Detailed analysis of the phase sensitive COSY spectrum allowed the assignment of a long continuous spin system, which started from the olefinic proton, CH-2 [ $\delta_H$  = 5.93 ppm (dd)], and sequentially extended until the olefinic proton, CH-15 [ $\delta_H$  = 5.94 ppm (dd)] (Figure 1). In the <sup>1</sup>H NMR spectrum, resonances for three pairs of olefinic protons were discernable, which were assigned to three disubstituted double bonds that were placed at C-2/3, C-10/11, C-14/15, respectively. In addition, three methyl groups (Me-30/31/32) were enclosed in this unit, which were coupled to methine protons at C-5, C-9 and C-12, respectively, as evident by the COSY

spectrum. One oxymethine proton that resonated at 4.47 ppm was located at C-7, as it showed COSY correlations to CH<sub>2</sub>-6 and CH<sub>2</sub>-8. This conclusion was secured by analysis of the HMBC spectrum, since correlations from Me-30 [ $\delta_{\text{H}} = 0.97$  ppm (d)] to C-4 ( $\delta_{\text{C}} = 31.3$  ppm), C-5 ( $\delta_{\text{C}} = 26.9$  ppm), and C-6 ( $\delta_{\text{C}} = 41.1$  ppm); Me-31 [ $\delta_{\text{H}} = 0.87$  ppm (d)] to C-8 ( $\delta_{\text{C}} = 44.1$  ppm), C-9 ( $\delta_{\text{C}} = 33.2$  ppm), and C-10 ( $\delta_{\text{C}} = 136.4$  ppm); Me-32 [ $\delta_{\text{H}} = 0.89$  ppm (d)] to C-11 ( $\delta_{\text{C}} = 132.0$  ppm), C-12 ( $\delta_{\text{C}} = 41.8$  ppm), and C-13 ( $\delta_{\text{C}} = 75.7$  ppm); and from H-7 to C-5, C-6, C-8, and C-9 were discerned (Figure 1). The further HMBC correlation from H-7 to the carbamate group ( $\delta_{\text{C}} = 156.7$  ppm, C-33) suggested this group being located at C-7. The second oxymethine [ $\delta_{\text{H}} = 5.09$  ppm (dd);  $\delta_{\text{C}} = 75.7$  ppm] was assigned to CH-13 as indicated by analysis of the COSY and HMBC spectra (Figure 1). The key HMBC correlations from H-13 [ $\delta_{\text{H}} = 5.09$  ppm (dd)], H-2 [ $\delta_{\text{H}} = 5.93$  ppm (dd)], and H-3 [ $\delta_{\text{H}} = 6.13$  ppm (td)] to the ester carbonyl ( $\delta_{\text{C}} = 164.2$  ppm, C-1) allowed the establishment of a 14-membered macrocyclic ring in **1** with a C-14/15 double bond in the side chain.

The remaining resonances of two olefinic protons [ $\delta_{\text{H}} = 5.46$  (dd), 6.36 ppm (d)] were assigned to the fourth disubstituted double bond (C-18/19). An alkyne group was present in the side chain of **1**, which was consistent with the <sup>13</sup>C NMR chemical shifts ( $\delta_{\text{C}} = 86.3$ , 90.4 ppm). This group was enveloped by two disubstituted double bonds (i.e., <sup>14</sup> and <sup>18</sup>), as evident by the HMBC correlations observed from H-14 [ $\delta_{\text{H}} = 6.06$  ppm (dd)] to C-16 ( $\delta_{\text{C}} = 86.3$  ppm); H-15 [ $\delta_{\text{H}} = 5.94$  ppm (dd)] to C-17 ( $\delta_{\text{C}} = 90.4$  ppm); H-18 [ $\delta_{\text{H}} = 5.46$  ppm (dd)] to C-16, C-17; H-19 [ $\delta_{\text{H}} = 6.36$  ppm (d)] to C-17, which thus concluded a conjugated diene-ynic moiety. Notably, in this unsaturated system with sp-hybridized carbons, typical long-range correlations were observed through 4 or 5 bonds. For example, H-15 and H-18 were coupled to each other with coupling constant of 2.2 Hz (<sup>3</sup>J), while HMBC correlations were found from H-18 to C-14 ( $\delta_{\text{C}} = 139.6$  ppm), and C-15 ( $\delta_{\text{C}} = 113.4$  ppm), and from H-19 to C-16 (Figure 1).

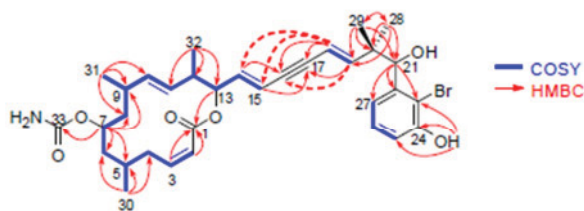


Figure 1. Key COSY and HMBC correlations of **1**.

The two remaining methyl groups, Me-28 [ $\delta_{\text{H}} = 1.04$  ppm (s)] and Me-29 [ $\delta_{\text{H}} = 0.96$  ppm (s)], were deduced to be connected to a quaternary carbon (C-20,  $\delta_{\text{C}} = 43.0$  ppm), since both of them appeared as a singlet in the <sup>1</sup>H NMR spectrum and showed HMBC correlations to C-20. A hydroxyl-bearing methine was assigned to C-21, as evident by its chemical shifts [ $\delta_{\text{H}} = 4.89$  ppm (d),  $\delta_{\text{C}} = 76.5$  ppm] and the COSY correlation between H-21 and OH-21 [ $\delta_{\text{H}} = 5.49$  ppm (d)]. The HMBC correlations from Me-28/29 to C-19 ( $\delta_{\text{C}} = 151.6$  ppm), and C-21 established the linkage between the diene-ynic group and C-21 through C-20. In addition, a 1,2,3-trisubstituted benzene ring was revealed by analysis of the coupling pattern of the aromatic protons [ $\delta_{\text{H}} = 6.83$  (dd,  $J = 7.9$ , 1.3 Hz), 7.13 (t,  $J = 7.9$  Hz), and 6.84 ppm (dd,  $J = 7.9$ , 1.3 Hz); an ABC spin system], in which one hydroxyl group was substituted at C-24 as supported by the HMBC correlations from OH-24 [ $\delta_{\text{H}} = 10.04$  ppm

Table 1. <sup>1</sup>H (600 MHz) and <sup>13</sup>C (100 MHz) NMR data of **1** (DMSO)

No.	$\delta_{\text{C}}$ [ppm], mult. <sup>[a]</sup>	$\delta_{\text{H}}$ [ppm], mult. ( $J$ in Hz) <sup>[b]</sup>
1	164.2, C	-
2	122.3, CH	5.93, dd (12.0, 2.6)
3	142.5, CH	6.13, td (12.0, 3.4)
4	31.3, CH <sub>2</sub>	3.41, ddd (14.8, 12.6, 4.8) 1.86, dq (14.8, 3.0)
5	26.9, CH	1.75, m
6	41.1, CH <sub>2</sub>	1.37, ddd (14.2, 11.4, 3.0) 1.01, overlapped
7	68.3, CH	4.47, br.dd (11.4, 10.1) 1.41, ddd (14.4, 10.1, 1.6)
8	44.1, CH <sub>2</sub>	1.03, overlapped
9	33.2, CH	2.00, m
10	136.4, CH	5.06, dd (15.0, 9.1)
11	132.0, CH	5.22, dd (15.0, 9.3)
12	41.8, CH	2.24, m
13	75.7, CH	5.09, dd (10.3, 7.7)
14	139.6, CH	6.06, dd (15.8, 7.7)
15	113.4, CH	5.94, dd (15.8, 2.2)
16	86.3, C	-
17	90.4, C	-
18	106.8, CH	5.46, dd (16.4, 2.2)
19	151.6, CH	6.36, d (16.4)
20	43.0, C	-
21	76.5, CH	4.89, d (4.4)
22	143.2, C	-
23	111.7, C	-
24	153.3, C	-
25	114.3, CH	6.83, dd (7.9, 1.6)
26	126.9, CH	7.13, t (7.9)
27	120.1, CH	6.84, dd (7.9, 1.6)
28 <sup>[c]</sup>	24.1, CH <sub>3</sub>	1.04, s
29 <sup>[c]</sup>	22.4, CH <sub>3</sub>	0.96, s
30	19.9, CH <sub>3</sub>	0.97, d (7.1)
31	22.0, CH <sub>3</sub>	0.87, d (6.8)
32	17.4, CH <sub>3</sub>	0.89, d (6.8)
33	156.7, C	-
OH-21	-	5.49, d (4.4)
OH-24	-	10.04, s

[a] Multiplicities were determined by DEPT-135, and HMQC experiments. [b] the methylene protons assigned in the upper line is referred to as proton "a", while the lower one as proton "b". [c] The assignments may be interchanged

(s)] to C-23 ( $\delta_{\text{C}} = 111.7$  ppm), C-24 ( $\delta_{\text{C}} = 153.3$  ppm), and C-25 ( $\delta_{\text{C}} = 114.3$  ppm), while CH-21 was attached to C-22, as H-21 showed HMBC correlations to C-22 ( $\delta_{\text{C}} = 143.2$  ppm), C-23, and C-27 ( $\delta_{\text{C}} = 120.1$  ppm) (Figure 1). Thus, the third substituent in the aromatic

ring had to be a bromine atom to complete the whole molecule of **1**. The geometry of the double bonds was deduced to be *2Z*, *10E*, *14E* and *18E* on the basis of the proton-proton coupling constants ( $J_{2,3}=12.0$  Hz,  $J_{10,11}=15.0$  Hz,  $J_{14,15}=15.8$  Hz,  $J_{18,19}=16.4$  Hz).

Callyspongiolide thus features a carbamate-substituted 14-membered macrocyclic lactone ring with a structurally unprecedented unsaturated side chain that incorporates a conjugated diene-yne and terminates at a brominated benzene ring. Callyspongiolide contains six stereogenic centers, including five in the macrocyclic ring and one in the side chain, which are spatially segregated.

The chemical shift differences of methylene protons and the presence of both large and small  $^1\text{H}$ - $^1\text{H}$  coupling constants at centers throughout the molecule that were not dependent on the NMR solvent used (DMSO- $d_6$ , MeOH- $d_4$ ), suggested the presence of a single predominant conformer<sup>[15]</sup>. Thus, the relative configuration of the stereocenters in the macrocyclic ring was deduced by combined analysis of the ROESY correlations and of the homonuclear ( $^3J_{\text{H,H}}$ ) and heteronuclear ( $^{2,3}J_{\text{C,H}}$ ) coupling constants<sup>[7, 16]</sup>.

The relative configuration of C-4 to C-9 is shown in Figure 2A. The small vicinal coupling constants of H-5/H-4a (4.8 Hz) and H-5/H-4b (3.0 Hz) suggested *gauche* relationships between these protons, while the large  $^3J_{\text{H-4a, C-30}}$  (8.6 Hz), and small  $^3J_{\text{H-4b, C-30}}$  (3.0 Hz) couplings indicated an *anti* relationship between H-4a and Me-30 and a *gauche* relationship between H-4b and Me-30. Small  $^3J_{\text{H-6a, H-5}}$  (3.0 Hz) and  $^3J_{\text{H-6a, C-30}}$  (2.3 Hz) couplings defined the *syn* relationships of H-6a/H-5, and H-6a/Me-30. Similarly, the *gauche* relationships of Me-30/H-6b and C-7/H-5 were consistent with the small coupling constants of  $^3J_{\text{H-6b, C-30}}$  (1.5 Hz) and  $^3J_{\text{H-5, C-7}}$  (~0 Hz). A large coupling constant of 11.4 Hz between H-6a and H-7 established the antiperiplanar relationship of both protons, while the small  $^3J_{\text{H-6b, C-8}}$  (1.0 Hz) coupling served to define the *syn* relationship between H-6b and C-8. An *anti* relationship between H-7 and H-8a was inferred from the large  $^3J_{\text{H-7, H-8a}}$  (10.1 Hz) coupling. The observation of a small coupling constant (1.0 Hz) between H-8b and C-6 established the *gauche* relationship between C9 and the carbamate group. A large coupling (7.3 Hz) between H-8a and C-10 suggested their *anti* relationship, while a small  $^3J_{\text{H-9, C-7}}$  (3.2 Hz) coupling indicated the *syn* relationship between H-9 and C-7, which was consistent with the  $^3J_{\text{H-8b, C-31}}$  (1.1 Hz) and  $^3J_{\text{H-8a, C-31}}$  (4.1 Hz) values. Taken together with the aforementioned conformational analysis, the relative stereochemical assignment of C-4 to C-9 was completed.

Similarly, the relative configuration of the remaining stereocenters (C-12 and C-13) within the macrocyclic ring was deduced by analysis of NOE and coupling constants. The large coupling (10.1 Hz) between H-12 and H-13 together with the ROESY correlations of Me-32/H-14, and H-12/H-14, established the relative configuration of C-12 and C-13 (Figure 2B). Moreover, the large coupling constants between H-9/H-10 (9.1 Hz), H-10/H-11 (15.0 Hz), H-11/H-12 (9.3 Hz), H-12/H-13 (10.3 Hz), H-13/H-14 (7.7 Hz), and H-14/H-15 (15.8 Hz), in association with the observed ROESY correlations between H-10, H-12 and H-14, and between H-9, H-11, H-13 and H-15 revealed the pseudo-planar nature of the C9-C13 backbone, in which vicinal protons were *anti* configured, as depicted in Figure 2B.

This preferred conformation was important for assigning the relative configuration of the stereocenters within C5-C9,

and C12-C13, as the C8 chain and O-C1 had to be co-facial in the pseudo-planar C9-C13 system to close the macrocyclic ring. As such, an *S*\* configuration of C-9 would lead to the interpretation of *12R*\*, and *13S*\* configuration. The relative configuration of stereocenters within the macrocyclic core was thus established. Further analysis of the ROESY spectrum corroborated the foregoing stereochemical assignment. Notably, transannular correlations were observed from H-7 to H-5, H-9, H-4a and H-11, from H-8b to H-10, and from H-10 to H-12, which suggested that H-4a, H-5, H-7, H-9 and H-11 were situated to a same face of the macrocyclic ring, while H-8b, H-10, and H-12 were directed to the opposite face (Figure 3).

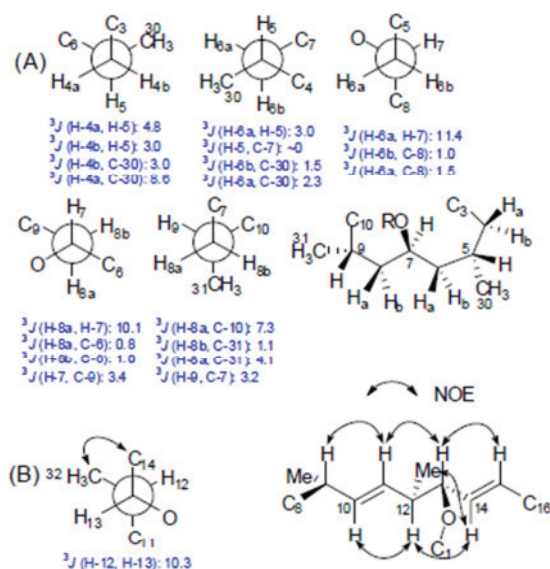


Figure 2. Conformational analyses for the macrocyclic region of **1**. (A) Rotamers determined for C4-C9 unit. (B) Rotamer determined for C12-C13 and key NOE correlations for C9-C13 backbone.

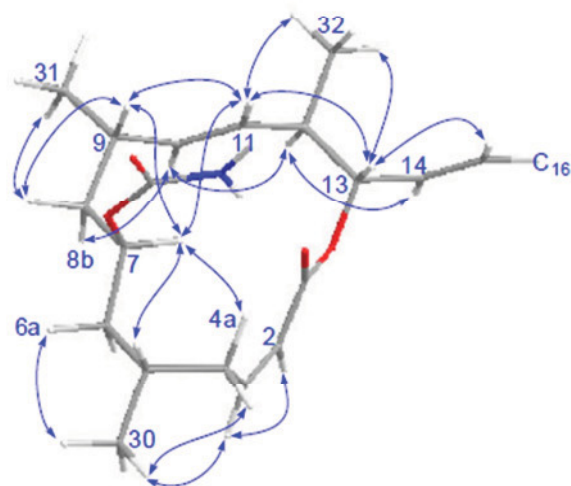


Figure 3. Selected key ROESY correlations for the macrocyclic ring of **1**.

No NOE enhancement was observed between H-15 and H-18 in the side chain, suggesting that C-14/C-15 and C18/C19 double bonds were *trans*-oriented with regard to the linear C-15-C-18 unit. The configuration of the sole stereocenter (C-21) in the side chain remained to be defined. We attempted to determine the absolute configuration of C-21 by using the modified Mosher's method<sup>[17]</sup>.



**Keywords:** cytotoxicity • marine macrolides • natural products • NMR spectroscopy • structure elucidation

For this purpose, **1** was treated with diazomethane to methylate the phenolic group prior to react with the (*R*)- or (*S*)-MTPACl. However, the latter reactions failed to give the corresponding MTPA esters, possibly due to the steric hindrance of C21. Hence, the absolute configuration of the stereocenters within this molecule was not assigned.

Callyspongiolide (**1**) was examined for its effects on the growth of L5178Y mouse lymphoma cells *in vitro* using the MTT assay<sup>[18]</sup>. It showed potent cytotoxicity in a sub-micromolar concentration with an IC<sub>50</sub> value of 320 nM, which is approximately 13-fold more active than the positive control kahalalide F (IC<sub>50</sub> 4.3 μM)<sup>[18]</sup>. More pronounced inhibitory activities were observed when tested against human Jurkat J16 T and Ramos B lymphocytes, which exhibited IC<sub>50</sub> values (nM) of 70 and 60, respectively, after 48 h treatment (Table 2, and Figure S12A in the Supporting information). This compound was further examined for its capacity to induce the generation of hypodiploid nuclei in Jurkat J16 T and Ramos B lymphocytes, and the results showed that it exhibited half maximal effective concentration (EC<sub>50</sub>) at 80 and 50 nM, respectively, after 48 h treatment (Figure S12B). Of note, the effect of callyspongiolide (**1**) on viability could not be blocked by the parallel treatment with QVD-OPh, a caspase-inhibitor (Figure S12C). This suggests that callyspongiolide (**1**) induces cell death in a caspase-independent fashion.

**Table 2.** cytotoxic and cell death-inducing effects of **1** (after 48 h treatment)

	Cytotoxic effect	cell death induction
	/ IC <sub>50</sub> (nM)	/ EC <sub>50</sub> (nM)
Jurkat J16 T lymphocytes	70	80
Ramos B lymphocytes	60	50

In summary, callyspongiolide (**1**) is a structurally unique polyketide-derived macrolide isolated from the marine sponge *Callyspongia* sp.. Notably, this macrolide features a conjugated diene-ynic side chain ending at a brominated benzene ring, which is unprecedented among all marine macrolides reported so far. It has been shown previously that highly potent antitumor polyketides such as swinholide A and onnamide A isolated from the marine sponge *Theonella swinhoei*, and psymberin isolated from *Psammocinia bulbosa* are in fact not of sponge origin but are rather biosynthesized by symbiotic bacteria that reside within the sponge<sup>[19]</sup>. Even though compound **1** was isolated from a *Callyspongia* and not from a *Theonella* or *Psammocinia* specimen, one may speculate that the true producer of callyspongiolide is likewise a bacterium. This hypothesis is supported by the observation that sponges of the genus *Callyspongia* produce very different sets of natural products depending on the location of sampling<sup>[10, 11b, 12-13]</sup>, which may reflect different bacteria that are either phagozytised or that reside within the sponge tissue. The potent activity of **1** makes it a potential lead for the development of anti-cancer drugs. Moreover, the unique structure of this compound would make it also an interesting target for realizing a total synthesis. Studies towards this aim will finally solve the stereochemical puzzles encountered in this report.

- [1] J. W. Blunt, B. R. Copp, R. A. Keyzers, M. H. G. Munro, M. R. Prinsep, *Nat. Prod. Rep.* **2013**, *30*, 237–323, and the previous reviews in this series.
- [2] G. R. Pettit, Z. A. Cichacz, F. Gao, M. R. Boyd, J. M. Schmidt, *J. Chem. Soc. Chem. Commun.* **1994**, 1111–1112.
- [3] P. A. Horton, F. E. Koehn, R. E. Longley, O. J. McConnell, *J. Am. Chem. Soc.* **1994**, *116*, 6015–6016.
- [4] L. M. West, P. T. Northcote, C. N. Battershill, *J. Org. Chem.* **1999**, *65*, 445–449.
- [5] K. L. Erickson, J. A. Beutler, J. H. Cardellina, M. R. Boyd, *J. Org. Chem.* **1997**, *62*, 8188–8192.
- [6] E. L. Whitson, K. M. Pluchino, M. D. Hall, J. B. McMahon, T. C. McKee, *Org. Lett.* **2011**, *13*, 3518–3521.
- [7] I. Paterson, S. M. Dalby, J. C. Roberts, G. J. Naylor, E. A. Guzmán, R., Isbrucker, T. P. Pitts, P. Linley, D. Divlianska, J. K. Reed, A. E. Wright, *Angew. Chem.* **2011**, *123*, 3277–3281; *Angew. Chem. Int. Ed.* **2011**, *50*, 3219–3223.
- [8] a) T. Higa, J. Tanaka, in *Studies in Natural Products Chemistry, Vol. 19* (Ed.: R. Atta ur), Elsevier, **1996**, pp. 549–626; b) J. G. Napolitano, A. H. Daranas, M. Norte, J. J. Fernandez, *Anti-Cancer Agents Med. Chem.* **2009**, *9*, 122–137; c) K.-S. Yeung, I. Paterson, *Chem. Rev.* **2005**, *105*, 4237–4313; d) A. Lorente, J. Lamariano-Merketegi, F. Albericio, M. Álvarez, *Chem. Rev.* **2013**, *113*, 4567–4610.
- [9] a) R. D. Norcross, I. Paterson, *Chem. Rev.* **1995**, *95*, 2041–2114; b) M. Shindo, in *Marine Natural Products, Vol. 5* (Ed.: H. Kiyota), Springer Berlin Heidelberg, **2006**, pp. 179–254.
- [10] M. Kobayashi, K. Higuchi, N. Murakami, H. Tajima, S. Aoki, *Tetrahedron Lett.* **1997**, *38*, 2859–2862.
- [11] D. T. A. Youssef, R. W. M. Van Soest, N. Fusetani, *J. Nat. Prod.* **2003**, *66*, 861–862; *J. Nat. Prod.* **2003**, *66*, 679–681.
- [12] M. S. Buchanan, A. R. Carroll, R. Addepalli, V. M. Avery, J. N. A. Hooper, R. J. Quinn, *J. Nat. Prod.* **2007**, *70*, 2040–2041.
- [13] S. R. M. Ibrahim, C. C. Min, F. Teuscher, R. Ebel, C. Kakoschke, W. Lin, V. Wray, R. Edrada-Ebel, P. Proksch, *Bioorg. Med. Chem.* **2010**, *18*, 4947–4956.
- [14] a) C.-D. Pham, H. Weber, R. Hartmann, V. Wray, W. Lin, D. Lai, P. Proksch, *Org. Lett.* **2013**, *15*, 2230–2233; b) C.-D. Pham, R. Hartmann, W. E. G. Müller, N. de Voogd, D. Lai, P. Proksch, *J. Nat. Prod.* **2013**, *76*, 103 106; c) H. Niemann, W. Lin, W. E. G. Müller, M. Kubbutat, D. Lai, P. Proksch, *J. Nat. Prod.* **2013**, *76*, 121–125.
- [15] K. Horst, *Angew. Chem.* **1982**, *94*, 509–520; *Angew. Chem. Int. Ed. Engl.* **1982**, *21*, 512–523.
- [16] a) J. S. Sandler, P. L. Colin, M. Kelly, W. Fenical, *J. Org. Chem.* **2006**, *71*, 7245–7251; b) N. Matsumori, D. Kaneno, M. Murata, H. Nakamura, K. Tachibana, *J. Org. Chem.* **1999**, *64*, 866–876.
- [17] I. Ohtani, T. Kusumi, Y. Kashman, H. Kakisawa, *J. Am. Chem. Soc.* **1991**, *113*, 4092–4096.
- [18] M. Ashour, R. Edrada, R. Ebel, V. Wray, W. Watjen, K. Padmakumar, W. E. G. Müller, W. H. Lin, P. Proksch, *J. Nat. Prod.* **2006**, *69*, 1547–1553.
- [19] a) C. A. Bewley, N. D. Holland, D. J. Faulkner, *Experientia* **1996**, *52*, 716–722; b) J. Piel, D. Hui, G. Wen, D. Butzke, M. Platzer, N. Fusetani, S. Matsunaga, *Proc. Natl. Acad. Sci. U. S. A.* **2004**, *101*, 16222–16227; c) K. M. Fisch, C. Gurgui, N. Heycke, S. A. van der Sar, S. A. Anderson, V. L. Webb, S. Taudien, M. Platzer, B. K. Rubio, S. J. Robinson, P. Crews, J. Piel, *Nat. Chem. Biol.* **2009**, *5*, 494–501; d) A. Uria, J. Piel, *Phytochem. Rev.* **2009**, *8*, 401–414; e) U. Hentschel, J. Piel, S. M. Degnan, M. W. Tavlör, *Nat. Rev. Microbiol.* **2012**, *10*, 641–654.

## Supporting Information

### **Callyspongiolide, an Unprecedented Cytotoxic Macrolide from the Marine Sponge *Callyspongia* sp.\*\***

*Cong-Dat Pham, Rudolf Hartmann, Philip Böhler, Björn Stork, Sebastian  
Wesselborg, Wenhan Lin, Daowan Lai\*, Peter Proksch\**

## Contents

<b>General experimental procedures</b>	S1
<b>Sponge material</b>	S2
<b>Extraction and isolation</b>	S2
<b>Callyspongiolide (1):</b>	S2
<b>Cell viability assay</b>	S3
<b>Analysis of hypodiploid nuclei</b>	S3
<b>References</b>	S3
<i>Table S1.</i> COSY, HMBC, and ROESY correlations of <b>1</b>	S4
<i>Table S2.</i> Selected ${}_{2,3}J_{\text{H,C}}$ heteronuclear coupling constants of <b>1</b>	S5
<i>Figure S1.1.</i> ${}^1\text{H}$ NMR spectrum of <b>1</b> (600MHz, DMSO- $d_6$ )	S6
<i>Figure S1.2.</i> ${}^1\text{H}$ NMR spectrum of <b>1</b> with assignments (Expansion 1)	S7
<i>Figure S1.3.</i> ${}^1\text{H}$ NMR spectrum of <b>1</b> with assignments (Expansion 2)	S8
<i>Figure S1.4.</i> Processed ${}^1\text{H}$ NMR spectrum of <b>1</b> using Gaussian multiplication	S9
<i>Figure S1.5.</i> Processed ${}^1\text{H}$ NMR spectrum of <b>1</b> using Gaussian multiplication (Expansion)	S10
<i>Figure S2.1.</i> ${}^{13}\text{C}$ NMR spectrum of <b>1</b> (100MHz, DMSO- $d_6$ )	S11
<i>Figure S2.2.</i> ${}^{13}\text{C}$ NMR spectrum of <b>1</b> with assignments (Expansion 1)	S12
<i>Figure S2.3.</i> ${}^{13}\text{C}$ NMR spectrum of <b>1</b> with assignments (Expansion 2)	S13
<i>Figure S3.1.</i> Phase sensitive COSY spectrum of <b>1</b> (DMSO- $d_6$ , 600MHz)	S14
<i>Figure S3.2.</i> Phase sensitive COSY spectrum of <b>1</b> (expansion 1)	S15
<i>Figure S3.3.</i> Phase sensitive COSY spectrum of <b>1</b> (expansion 2)	S16
<i>Figure S3.4.</i> Phase sensitive COSY spectrum of <b>1</b> (expansion 3)	S17
<i>Figure S4.1.</i> HMQC spectrum of <b>1</b> (DMSO- $d_6$ , 600MHz)	S18
<i>Figure S4.2.</i> HMQC spectrum of <b>1</b> (Expansion 1)	S19
<i>Figure S4.3.</i> HMQC spectrum of <b>1</b> (Expansion 2)	S20
<i>Figure S5.1.</i> HMBC spectrum of <b>1</b> (DMSO- $d_6$ , 600MHz)	S21
<i>Figure S5.2.</i> HMBC spectrum of <b>1</b> (Expansion 1)	S22
<i>Figure S5.3.</i> HMBC spectrum of <b>1</b> (Expansion 2)	S23
<i>Figure S5.4.</i> HMBC spectrum of <b>1</b> (Expansion 3)	S24
<i>Figure S6.1.</i> ROESY spectrum of <b>1</b> (DMSO- $d_6$ , 600MHz)	S25
<i>Figure S6.2.</i> ROESY spectrum of <b>1</b> (expansion 1)	S26
<i>Figure S6.3.</i> ROESY spectrum of <b>1</b> (expansion 2)	S27
<i>Figure S7.</i> HSQC-HECADE spectrum of <b>1</b> (DMSO- $d_6$ , 600MHz)	S28
<i>Figure S8.</i> UV spectrum of <b>1</b> (MeOH)	S29
<i>Figure S9.</i> IR spectrum of <b>1</b>	S30
<i>Figure S10.</i> LC/ESI-MS spectrum of <b>1</b>	S31
<i>Figure S11.</i> HRESI-MS spectrum of <b>1</b>	S32
<i>Figure S12.</i> Callyspongiolide ( <b>1</b> ) reduces cell viability and induces cell death in Jurkat J16 T-lymphocytes and Ramos B lymphocytes	S33

### General experimental procedures

UV spectra were measured in a Perkin-Elmer Lambda 25 UV/vis spectrometer. IR spectra were measured directly in a Shimadzu IRAffinity-1 FT-IR spectrometer.  $^1\text{H}$ ,  $^{13}\text{C}$ , and 2D NMR spectra were recorded on Bruker ARX 400 or Bruker AVANCE III HD 600 NMR spectrometers equipped with a HCNP-cryo-probe. The chemical shifts were referenced to the solvent residual peaks,  $\delta_{\text{H}}$  2.50 (DMSO- $d_6$ ) for  $^1\text{H}$  and  $\delta_{\text{C}}$  39.5 (DMSO- $d_6$ ) for  $^{13}\text{C}$ . Homonuclear coupling constants ( $^2J_{\text{HH}}$ ,  $^3J_{\text{HH}}$ ) were extracted from a  $^1\text{H}$  NMR spectrum that was processed by Gaussian multiplication to increase the resolution (LB = -2.5, GB = 0.3). Approximate heteronuclear coupling constants ( $^2J_{\text{CH}}$ ,  $^3J_{\text{CH}}$ ) were extracted from the HSQC-HECADE experiment. The HSQC-HECADE experiment was acquired in approximately 9 hours with a TOCSY mixing time of 60 ms and a  $J$  (scale) factor of 1. The acquisition parameters included 4K data points in F2 and 512 increments in echo-antiecho mode with 32 scans per increment in F1. The data was zero-filled to 8K in F2 and 1K in F1 for processing. The ROESY experiment was acquired in approximately 19 hours with 512 increments and 64 scans per increment in F1 and 2K data points in F2, a ROESY mixing time of 450 ms and a RF field strength of 5000 Hz. The irradiated ROESY spin-lock sequence was shifted relative to the spectral center alternated by +/- 5000 Hz to minimize Hartmann-Hahn transfer between scalar-coupled spins<sup>[1]</sup>. Mass spectra (ESI) were recorded with a Finnigan LCQ Deca mass spectrometer, and HRMS (ESI) spectra were obtained with a FTHRMS-Orbitrap (Thermo-Finnigan) mass spectrometer. EI-MS measurements were carried out on a Finnigan Trace GC Ultra instrument equipped with Finnigan Trace DSQ mass spectrometer (Thermo Electron Corp.). Solvents were distilled prior to use, and spectral grade solvents were used for spectroscopic measurements. HPLC analysis was performed with a Dionex P580 system coupled to a photodiode array detector (UVD340S); routine detection was at 235, 254, 280, and 340 nm. The separation column (125 × 4 mm) was prefilled with Eurosphere-10 C<sub>18</sub> (Knauer, Germany), and the following gradient was used (MeOH, 0.1% HCOOH in H<sub>2</sub>O): 0-5 min (10% MeOH); 5-35 min (10-100% MeOH); 35-45 min (100% MeOH). Semi-preparative HPLC was performed using a Merck Hitachi HPLC System (UV detector L-7400; Pump L-7100; Eurosphere-100 C18, 300×8 mm, Knauer, Germany). Column chromatography included Diaion HP-20, LH-20 Sephadex and Merck MN Silica gel 60 M (0.04-0.063 mm) TLC plates with silica gel F254 (Merck, Darmstadt, Germany) were used to monitor fractions (CH<sub>2</sub>Cl<sub>2</sub>/MeOH mixtures as mobile phase); detection was under UV at 254 and 366 nm or by spraying the plates with anisaldehyde reagent.

### Sponge material

*Callyspongia* sp. – identified by Dr. Nicole de Voogd from the Naturalis Biodiversity Center in Leiden – was collected by SCUBA diving at Ambon, Indonesia, an October 1996 at a depth of 10 m. The colour of its exterior was yellowish to reddish. Its body had small protrusions, cavities and branches. The sponge was preserved in a mixture of EtOH and H<sub>2</sub>O (70:30) and stored in a -20°C freezer. A voucher specimen (voucher number: RMNH POR 8059) is stored at the Naturalis Biodiversity Center, Darwinweg 2, P.O. Box 9517, 2300 RA Leiden, The Netherlands.

### Extraction and isolation

The frozen material was thawed and cut into small pieces. The wet weight was 500 g. It was extracted with MeOH. We obtained a dry crude extract of 40 g. The following liquid-liquid extraction with ethyl acetate yielded an extract of 1 g. This fraction was then subjected to column separation using Diaion HP-20 employing a step gradient of H<sub>2</sub>O/MeOH to yield eight fractions H1-H8. H6 (228.5 mg) was submitted to consecutive LH-20 Sephadex size exclusion chromatography. From one of these fractions 4.6 mg of callyspongiolide (**1**) was obtained by semi-preparative HPLC.

### Callyspongiolide (**1**):

light-yellow amorphous solid; UV ( $\lambda_{\max}$ , MeOH) (log  $\epsilon$ ) 204.1 (4.43), 270.8 (4.11), 285.7 (4.05);  $[\alpha]_{\text{D}}^{20} = -12.5$  (*c* 0.1, MeOH); IR (ATR) 3360, 2957, 2926, 1701, 1638, 1603, 1458, 1294, 1180, 1047, 1024, 968 cm<sup>-1</sup>; <sup>1</sup>H NMR data (DMSO-*d*<sub>6</sub>, 600MHz) see Table 1; <sup>13</sup>C NMR data (DMSO-*d*<sub>6</sub>, 100MHz), see Table 1; ESIMS *m/z* 650.1 [<sup>79</sup>Br-M+Na]<sup>+</sup> (100%), 652.1 [<sup>81</sup>Br-M+Na]<sup>+</sup> (92%), and 626.2 [<sup>79</sup>Br-M- H]<sup>-</sup> (100%), 628.2 [<sup>81</sup>Br-M-H]<sup>-</sup> (92%); HRESIMS *m/z* 650.2085 [M+Na]<sup>+</sup> (calcd. for C<sub>33</sub>H<sub>42</sub><sup>79</sup>BrNO<sub>6</sub>Na 650.2088).



### Cell viability assay

Cytotoxicity was tested against L5178Y mouse lymphoma cells using an MTT (=3-(4,5-dimethylthiazol-2-yl)-2,5-diphenyl-2*H*-tetrazolium bromide) assay and compared to that of untreated controls, as described previously.<sup>[2]</sup> Experiments were repeated three times and carried out in triplicate. As negative controls, media with 0.1% EGMME/ DMSO were included in the experiments. The depsipeptide kahalalide F, isolated from *Elysia grandifolia* was used as a positive control. For Jurkat J16 T lymphocytes and Ramos B lymphocytes, the MTT assay was carried out as previously described, except that incubation with DMSO at RT for 20 min was used to extract the formazan product from the cells<sup>[3]</sup>.

### Analysis of hypodiploid nuclei

Jurkat J16 T cells and Ramos B cells were cultivated in medium containing the indicated concentrations of callispongionolide (**1**) for 48 hrs and hypodiploid nuclei were measured. Nuclei were prepared by lysing cells in hypotonic lysis buffer [1% sodium citrate, 0.1% Triton X-100, 50 µg/mL propidium iodide] and subsequently analyzed by flow cytometry. Flow cytometric analyses were performed on LSRFortessa (BD Biosciences) using FACSDiva software.

### References

- [1] C. M. Thiele, K. Petzold, J. Schleucher, *Chem. Eur. J.* **2009**, *15*, 585–588.
- [2] M. Ashour, R. Edrada, R. Ebel, V. Wray, W. Watjen, K. Padmakumar, W. E. G. Müller, W. H. Lin, P. Proksch, *J. Nat. Prod.* **2006**, *69*, 1547–1553
- [3] H. Mueller, M. U. Kassack, M. Wiese, *J. Biomol. Screen.* **2004**, *9*, 506–515.

**Table S1.** COSY, HMBC, and ROESY correlations of **1**

No.	$\delta_C$	$\delta_H$	COSY	HMBC (H→C)	ROESY
1	164.2 s	-	-	-	-
2	122.3 d	5.93 dd (12.0, 2.6)	H-3, 4b (w)	C-4, 1	H-3
3	142.5 d	6.13 td (12.0, 3.4)	H-4a, 4b (w), 2	C-5, 1	H-2, 4b, 30
4a	31.3 t	3.41 ddd (14.8, 12.6, 4.8)	H-3, 4b	C-30, 5, 2, 3	H-7, 5
4b		1.86 dq (14.8, 3.0)	H-3, 4a, 2	-	H-30, 3
5	26.9 d	1.75 m	H-30, 4a (w), 6a (w), 6b	-	H-6a, 4a, 7 (w)
6a	41.1 t	1.37 ddd (14.2, 11.4, 3.0)	H-6b, 7		H-5, 30
6b		1.01 overlapped	H-5 (w), 6a		H-7
7	68.3 d	4.47 br.dd (11.4, 10.1)	H-8a, 8b (w), 6a, 6b (w)	C-5(w), 9, 6(w), 8(w), 33	H-6b, 8b, 11, 9, 4a, 5, 10(w)
8a	44.1 t	1.41 ddd (14.4, 10.1, 1.6)	H-8b, 7		H-9, 31
8b		1.03 overlapped	H-9, 8a		H-7, 10
9	33.2 d	2.00 m	H-31, 8b, 10	C-31, 11(w), 10(w)	H-8a, 7, 11
10	136.4 d	5.06 dd (15.0, 9.1)	H-9 (w), 11	C-31, 9, 12, 11	H-31, 12, 8b
11	132.0 d	5.22 dd (15.0, 9.3)	H-12 (w), 10	C-32, 9, 12, 10, 13	H-7, 9, 13, 32
12	41.8 d	2.24 m	H-32, 13, 11	C-32, 13, 11, 14, 10	H-10, 14, 15 (w)
13	75.7 d	5.09 dd (10.3, 7.7)	H-12, 14	C-12, 15, 14, 1, 11	H-32, 15
14	139.6 d	6.06 dd (15.8, 7.7)	H-13, 15	C-13, 16, 15, 12(w)	H-32, 12
15	113.4 d	5.94 dd (15.8, 2.2)	H-14, 18 (w)	C-13, 17, 14	H-13
16	86.3 s	-	-	-	-
17	90.4 s	-	-	-	-
18	106.8 d	5.46 dd (16.4, 2.2)	H-19, 15 (w)	C-20, 16, 15(w), 14(w), 19, 17(w)	H-28, 29
19	151.6 d	6.36 d (16.4)	H-18	C-20, 21, 17, 28, 29, 16(w), 18(w)	H-28, 29, 21, 27
20	43.0 s	-	-	-	-
21	76.5 d	4.89 d (4.4)	21-OH	C-29, 28, 20, 23, 27, 22, 19	H-19, 21-OH,
22	143.2 s	-	-	-	-
23	111.7 s	-	-	-	-
24	153.3 s	-	-	-	-
25	114.3 d	6.83 dd (7.9, 1.6)	H-26, 27	C-23, 27, 24	
26	126.9 d	7.13 t (7.9)	H-25, 27	C-23(w), 25(w), 27(w), 22, 24	
27	120.1 d	6.84 dd (7.9, 1.6)	H-26, 25	C-21, 23, 25	H-19, 28, 29
28	24.1 q	1.04 s	-	C-29, 20, 19, 21	
29	22.4 q	0.96 s	-	C-28, 20, 19, 21	
30	19.9 q	0.97 d (7.1)	H-5	C-5, 4, 6	H-3, 4b, 6a
31	22.0 q	0.87 d (6.8)	H-9	C-9, 10, 8	H-8a, 10
32	17.4 q	0.89 d (6.8)	H-12	C-12, 11, 13	H-13, 14, 15 (w), 11
33	156.7 s	-	-	-	-
OH-21	-	5.49 d (4.4)	H-21	C-20, 21, 22	
OH-24	-	10.04 s	-	C-23, 25, 24	

“w”: denotes weak correlation.

**Table S2.** Selected  $^{2,3}J_{\text{H,C}}$  heteronuclear coupling constants of **1** (extracted from HSQC-HECADE spectrum ( $\pm 0.2$  Hz))

C Atom	$^2J_{\text{H,C}}$ (Hz)	$^3J_{\text{H,C}}$ (Hz)
2	H-3 (-0)	H-4a (4.6), H-4b (5.7)
3	H-2 (~0), H-4a (5.4), H-4b (7.0)	
4	H-3 (1.0)	H-2 (8.5), H-30 (4.0)
5	H-4a (2.8), H-6a (2.6), H-30 (4.0)	H-7 (1.9)
6	H-7 (2.0), H-5 (2.1)	H-8a (0.8), H-8b (1.0), H-30 (4.8)
7	H-8a (8.1), H-6a (7.0), H-6b/8b (~0)	H-9 (3.2), H-5 (~0), H-30 (0.5, $^4J$ )
8	H-7 (1.7), H-9 (4.0)	H-10 (1.4), H-31 (5.2), H-6a (1.5), H-6b (1.0)
9	H-31 (4.2), H-8b (2.1), H-10 (3.1), H-8a (2.3)	H-11 (5.7), H-7 (3.4)
10	H-11 (0.7), H-9 (4.5)	H-12 (5.0), H-8a (7.3), H-31 (4.9)
11	H-12 (4.4)	H-9 (0.9)
12	H-11 (3.6), H-13 (2.8), H-32 (4.0)	H-14 (1.2), H-10 (5.9)
13	H-14 (3.0), H-12 (6.7)	H-15 (5.9), H-32 (5.9)
14	H-13 (2.8)	
15		H-18 ( $^4J$ , 1.3), H-13 (6.0)
30	H-5 (4.5)	H-6a (2.3), H-4a (8.6), H-4b (3.0), H-6b (1.5)
31	H-9 (3.5)	H-10 (3.1), H-8a (4.1), H-8b (1.1)
32	H-12 (4.2)	H-11 (2.6), H-13 (1.6)

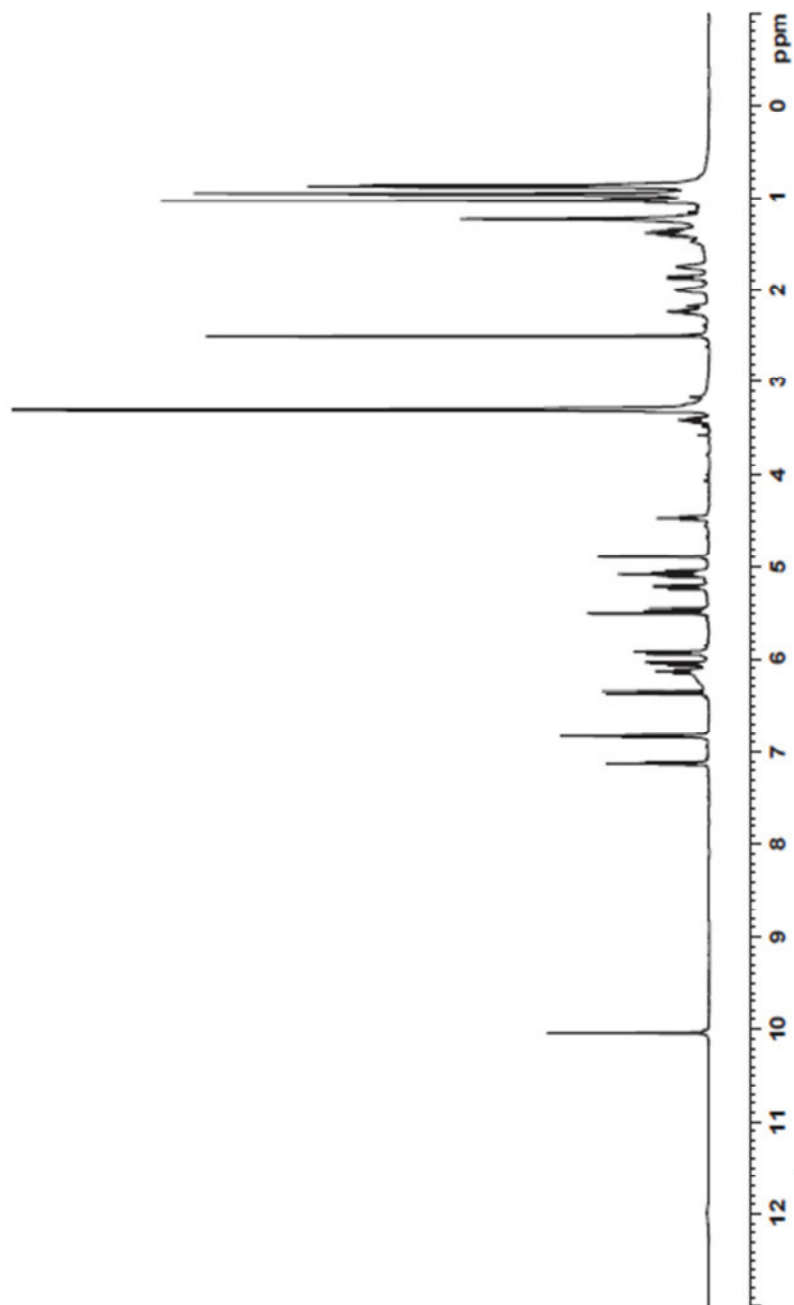


Figure S1.1.  $^1\text{H}$  NMR spectrum of **1** (600MHz,  $\text{DMSO-}d_6$ )

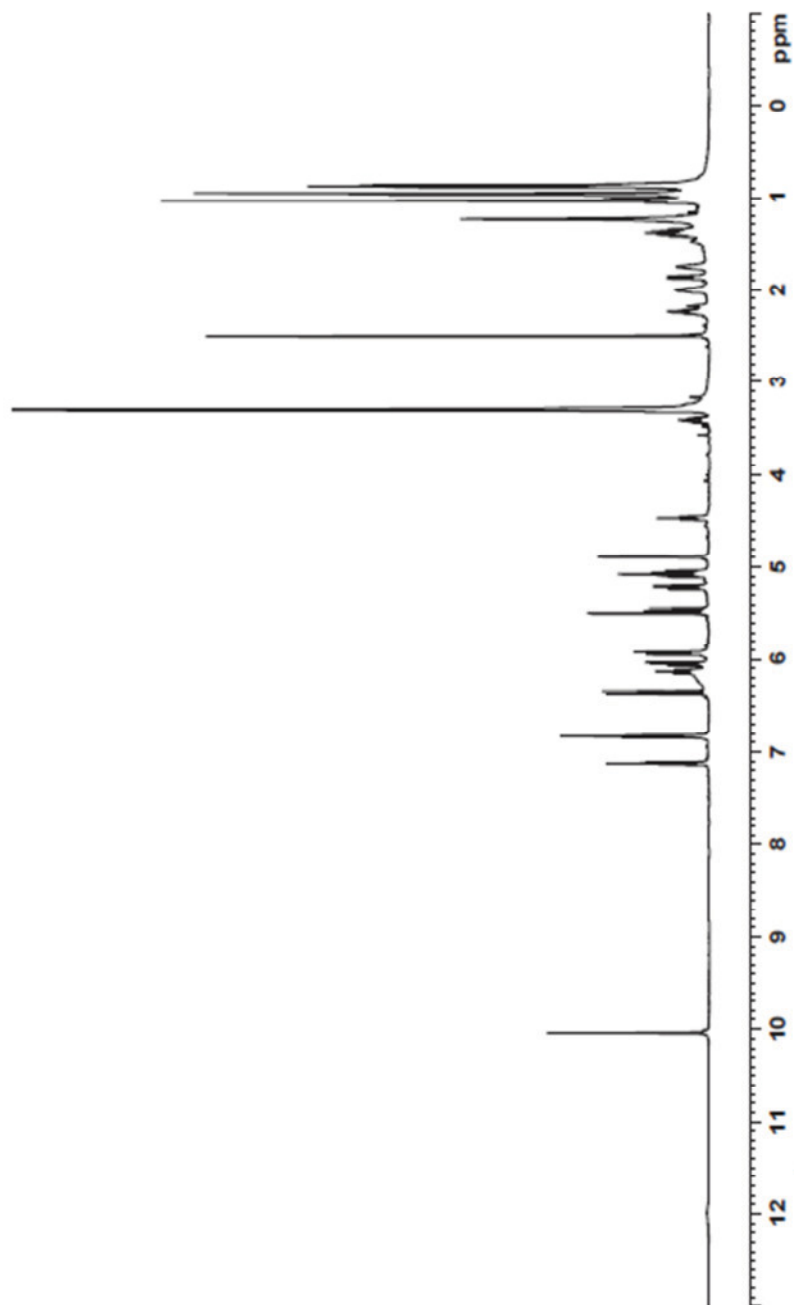


Figure S1.1.  $^1\text{H}$  NMR spectrum of **1** (600MHz,  $\text{DMSO-}d_6$ )

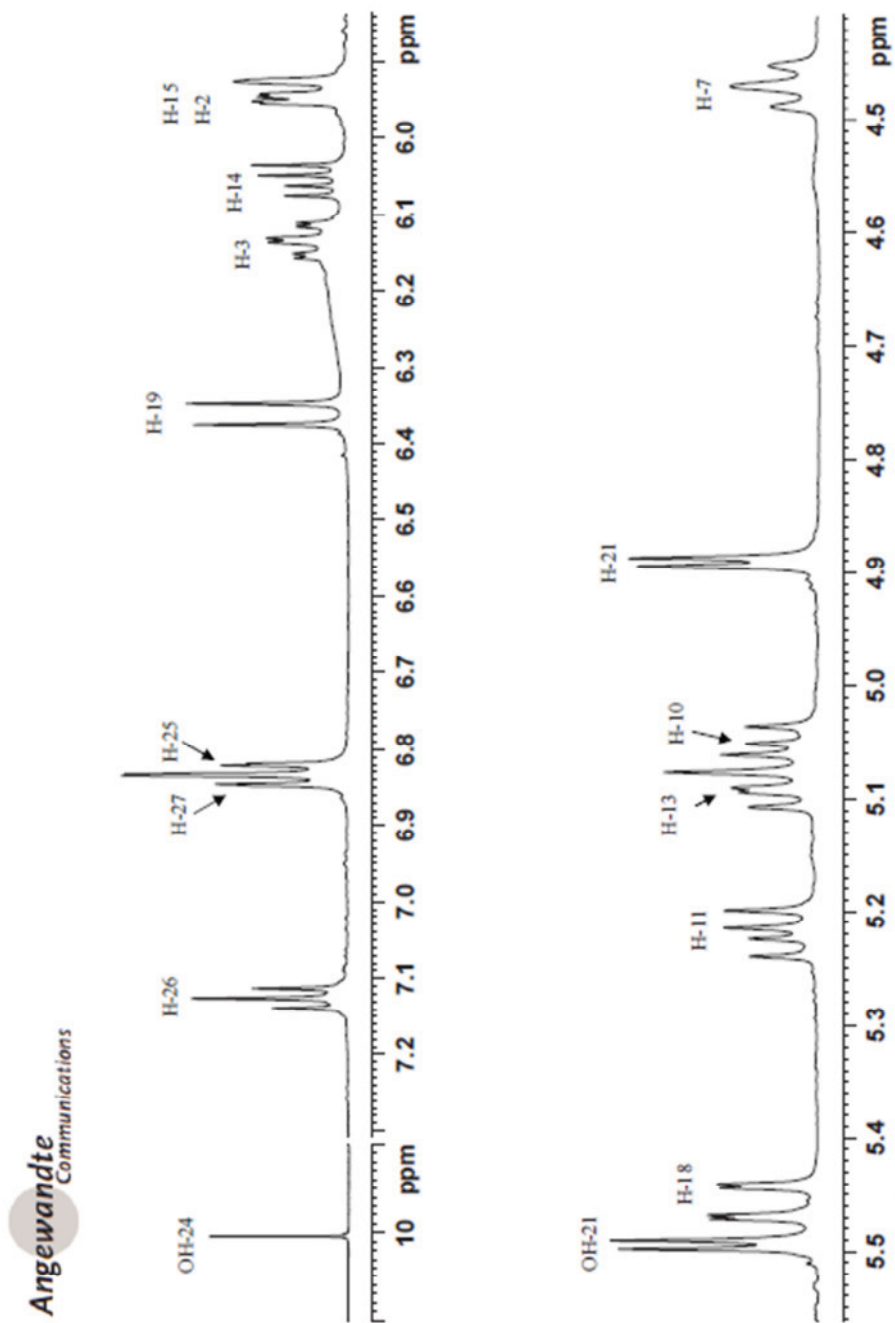


Figure S1.2.  $^1\text{H}$  NMR spectrum of **1** with assignments (Expansion 1)

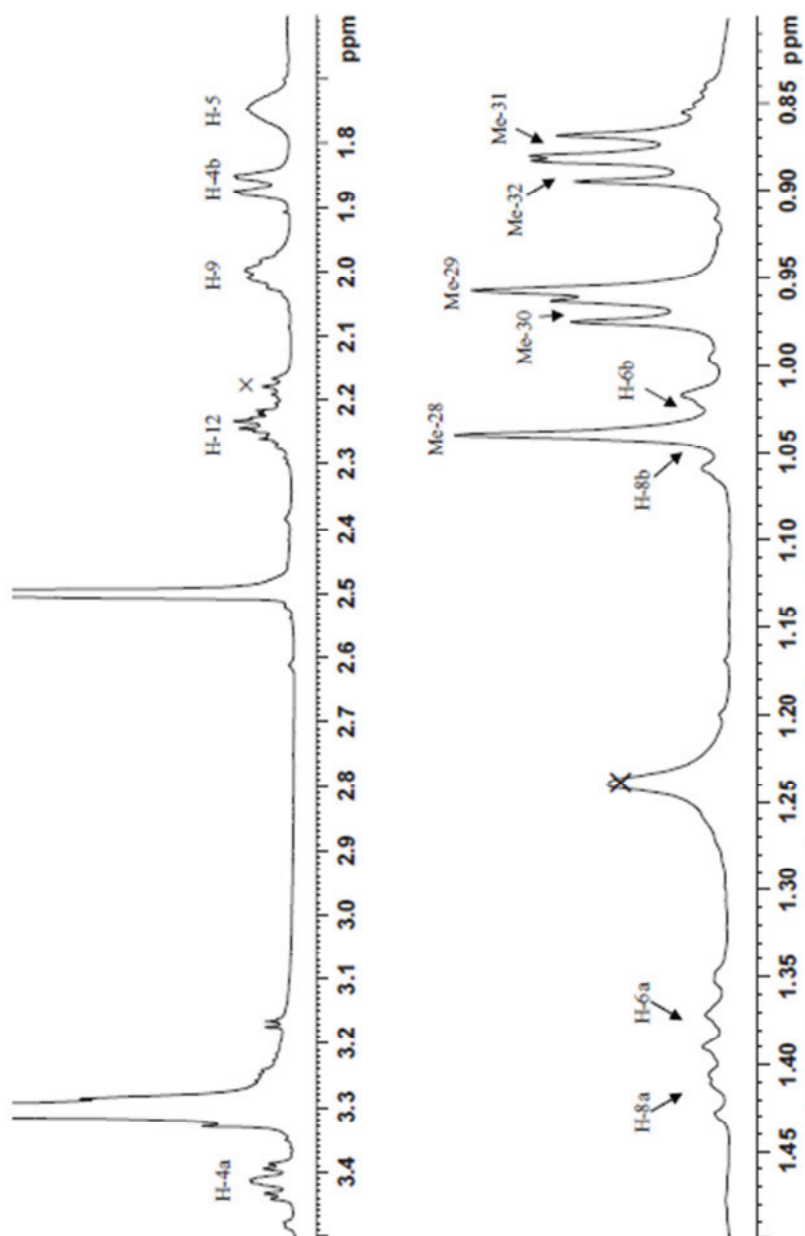


Figure S1.3.  $^1\text{H}$  NMR spectrum of **1** with assignments (Expansion 2)

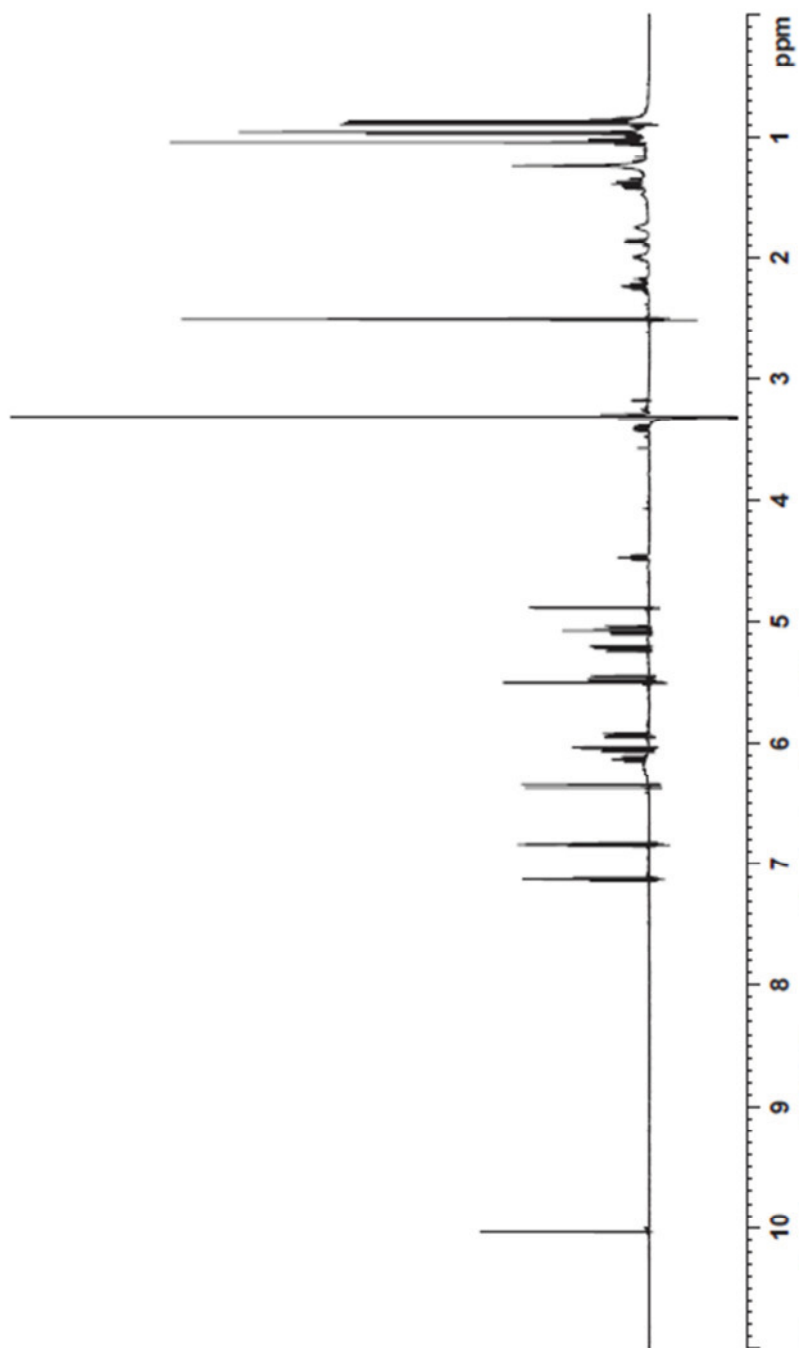


Figure SI.4. Processed  $^1\text{H}$  NMR spectrum of **1** using Gaussian multiplication



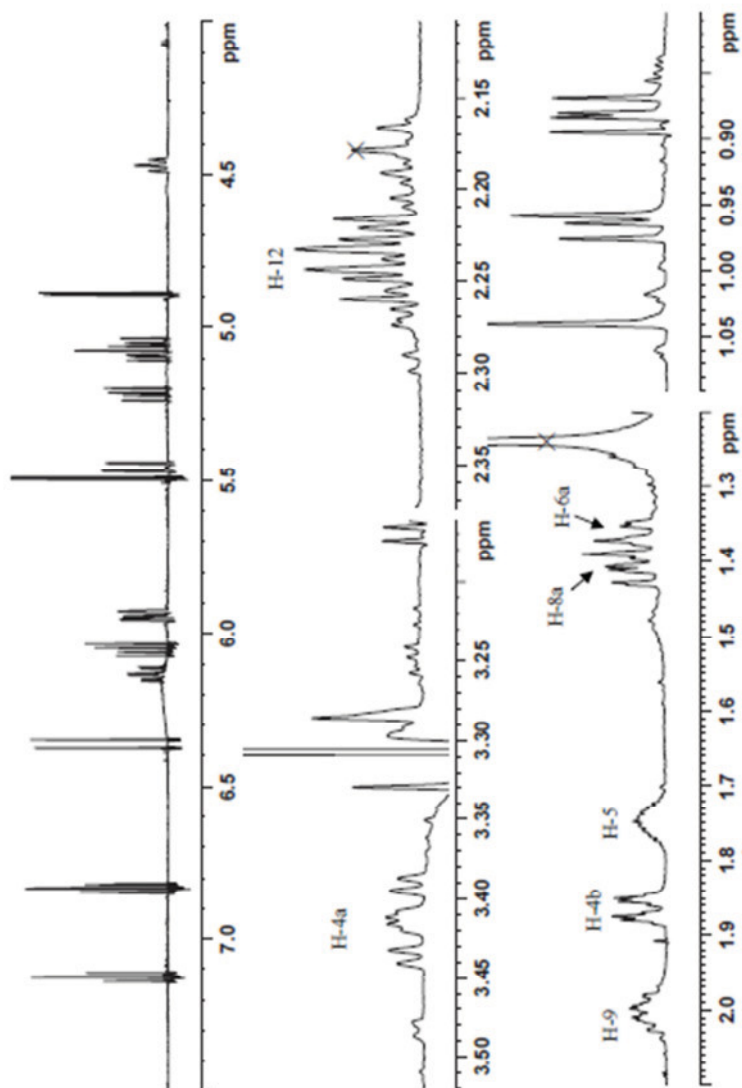


Figure S1.5. Processed  $^1\text{H}$  NMR spectrum of I using Gaussian multiplication (Expansion)

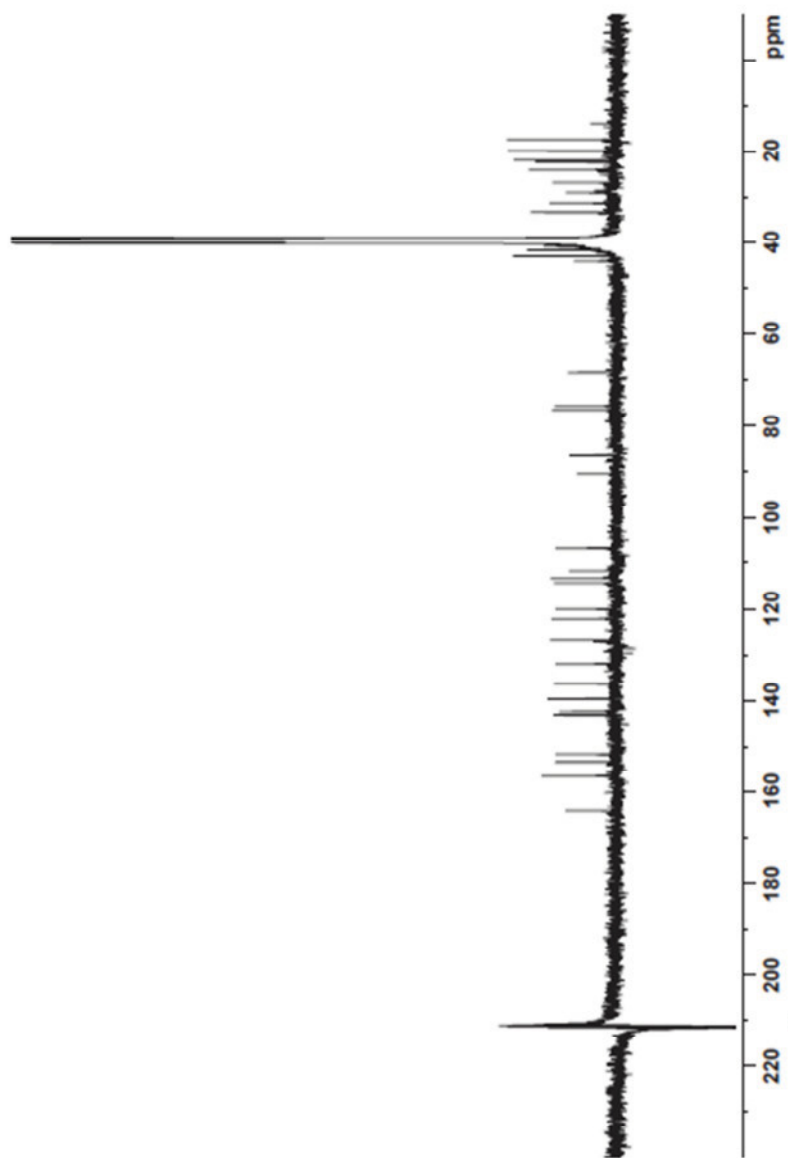
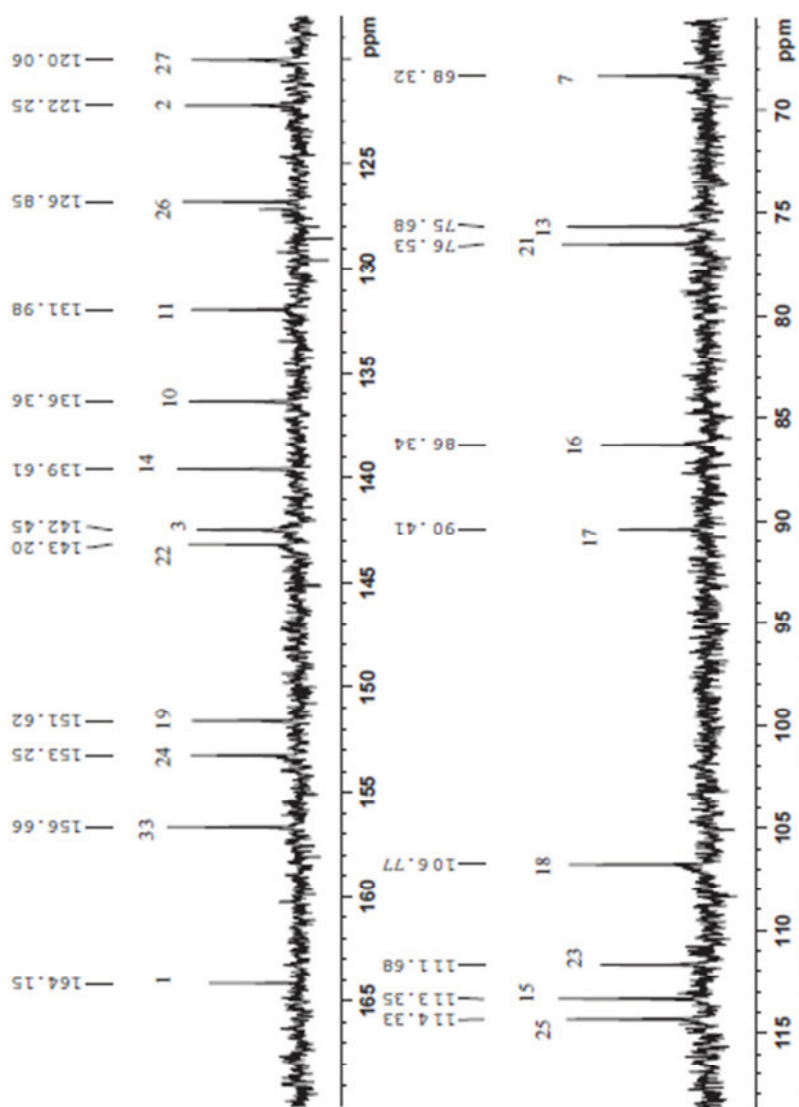


Figure S2.1.  $^{13}\text{C}$  NMR spectrum of **I** (100MHz,  $\text{DMSO-}d_6$ )

Figure S2.2.  $^{13}\text{C}$  NMR spectrum of **1** with assignments (Expansion 1)

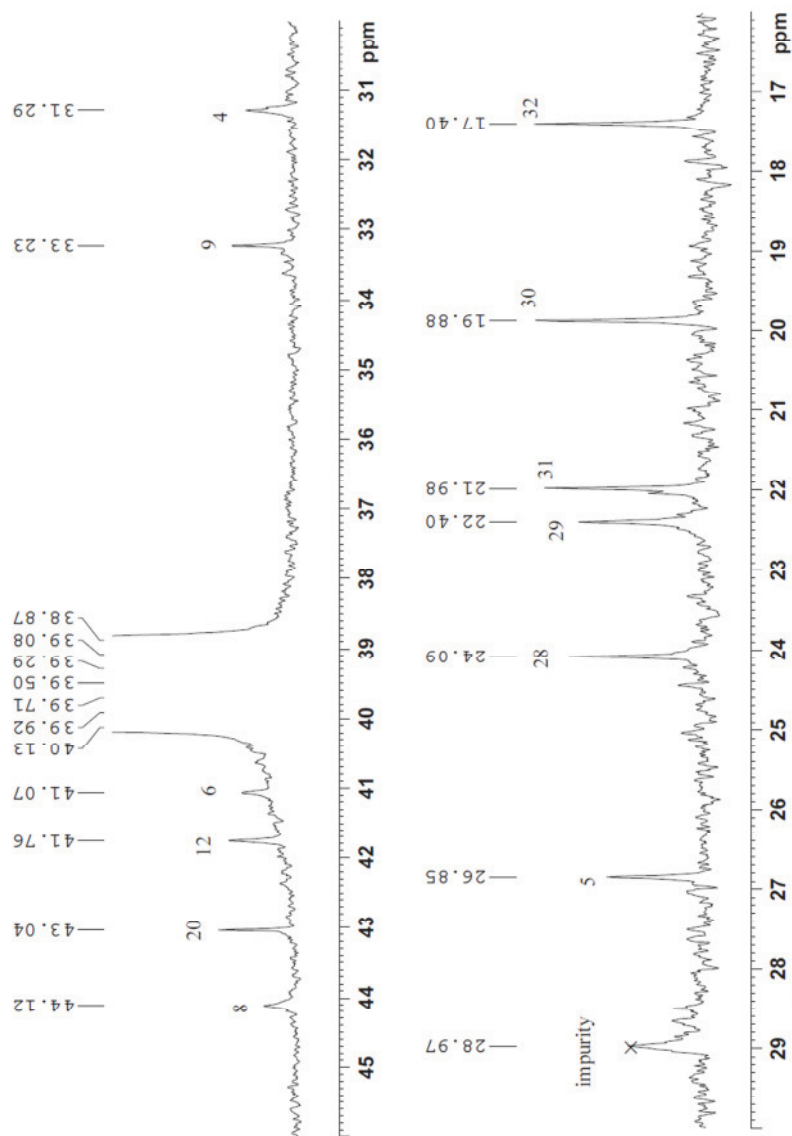


Figure S2.3.  $^{13}\text{C}$  NMR spectrum of 1 with assignments (Expansion 2)

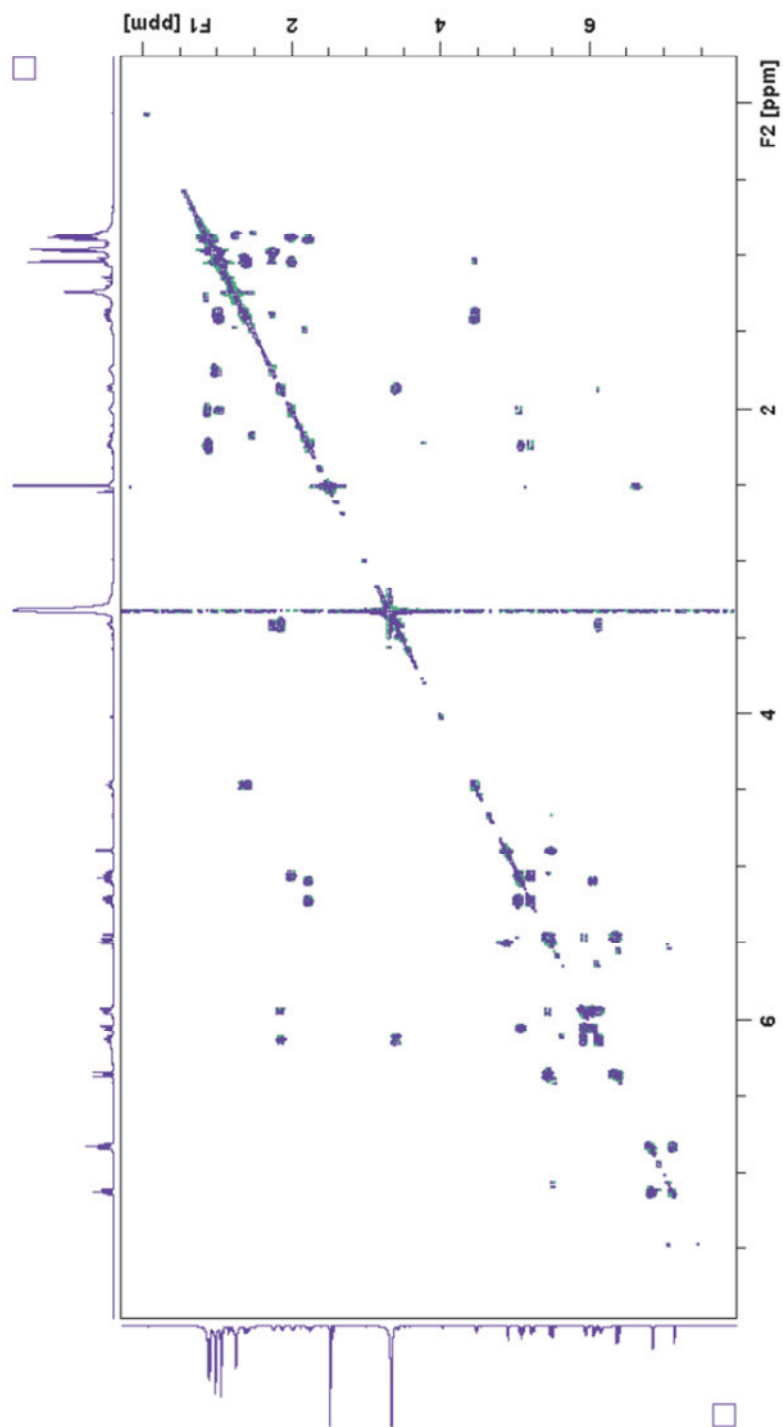


Figure S3.1. Phase sensitive COSY spectrum of **1** (DMSO- $d_6$ , 600MHz)

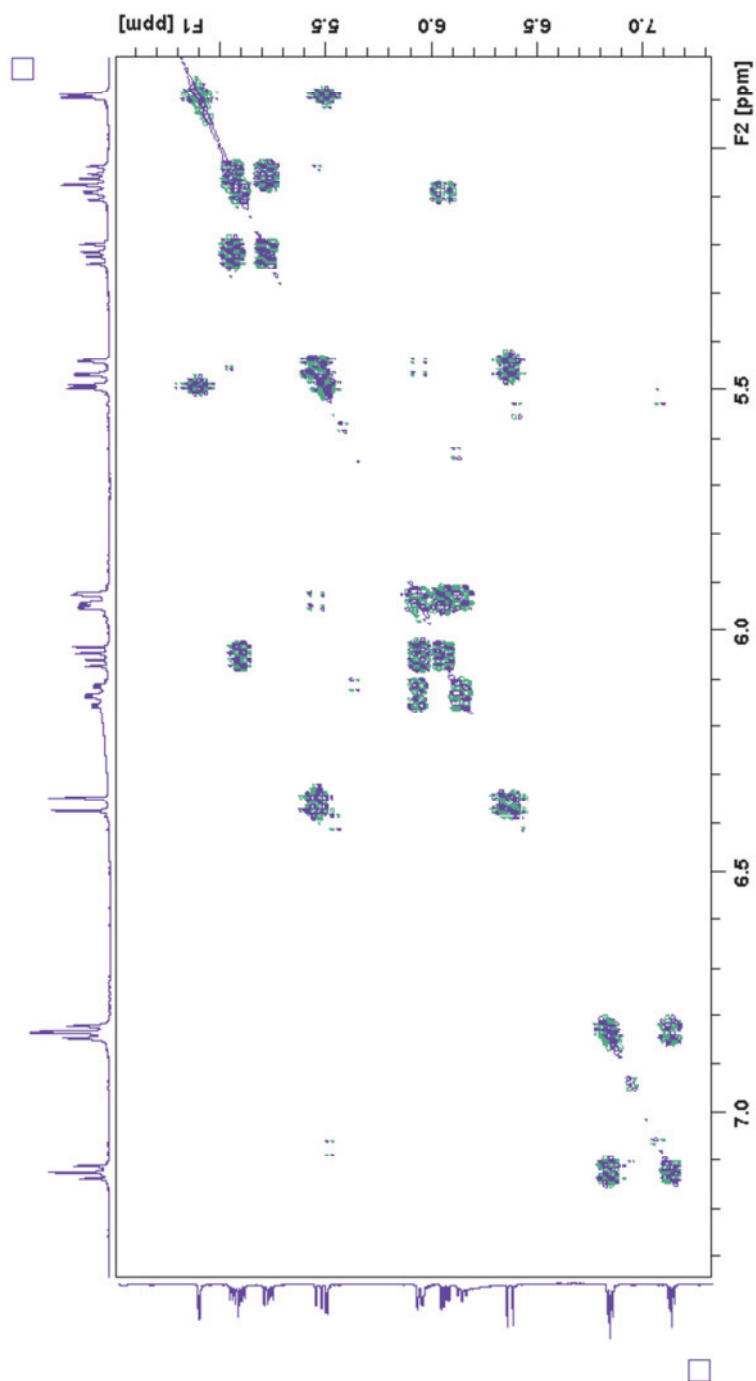


Figure S3.2. Phase sensitive COSY spectrum of **1** (expansion 1)

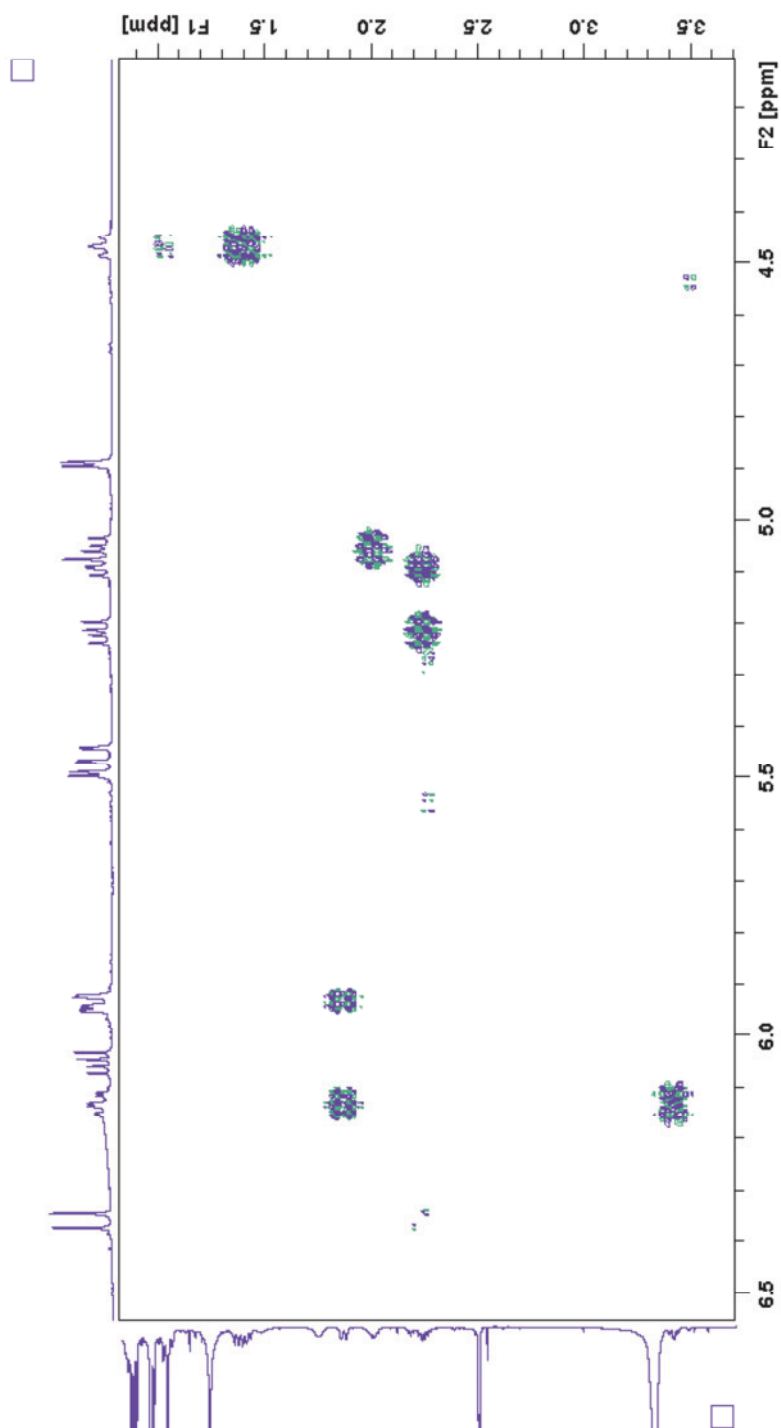


Figure S3.3. Phase sensitive COSY spectrum of **1** (expansion 2)

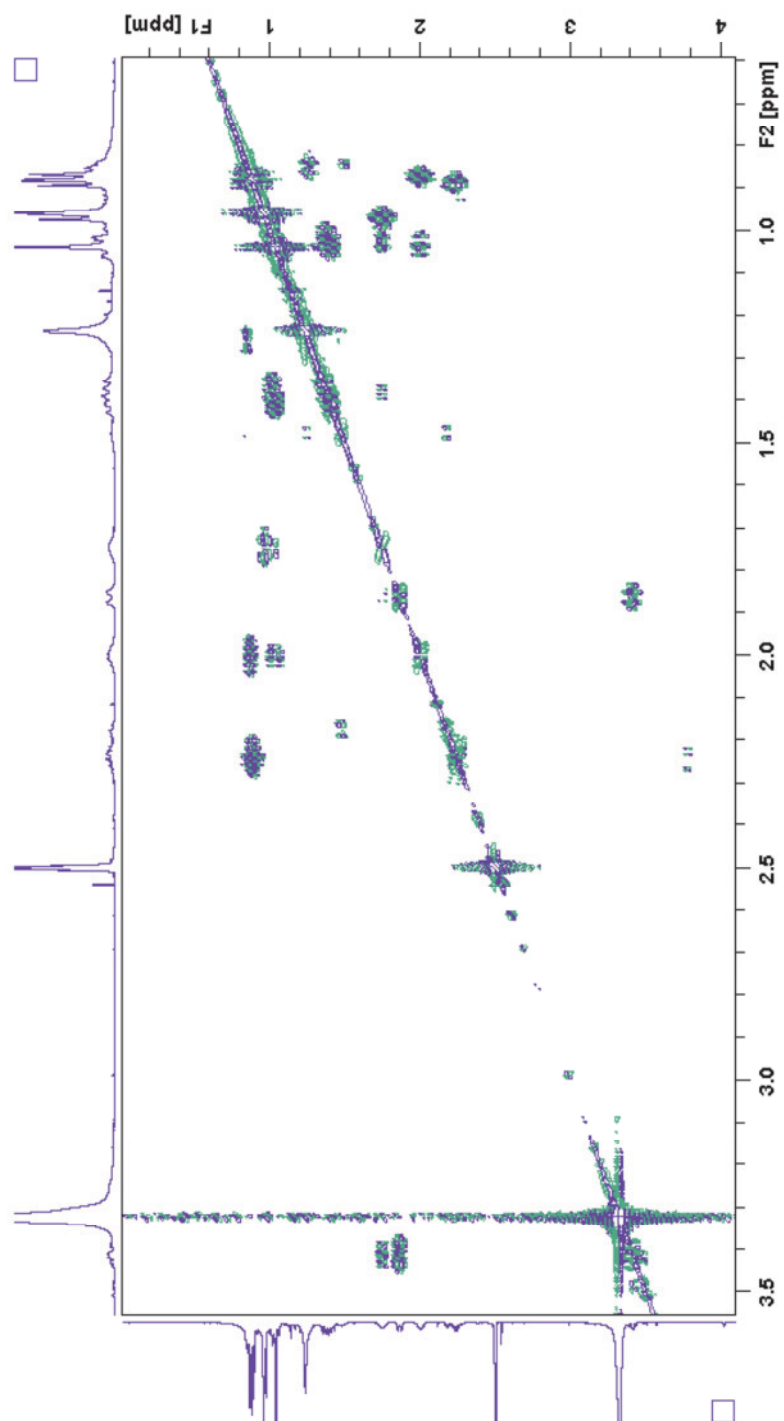


Figure S3.4. Phase sensitive COSY spectrum of **I** (expansion 3)



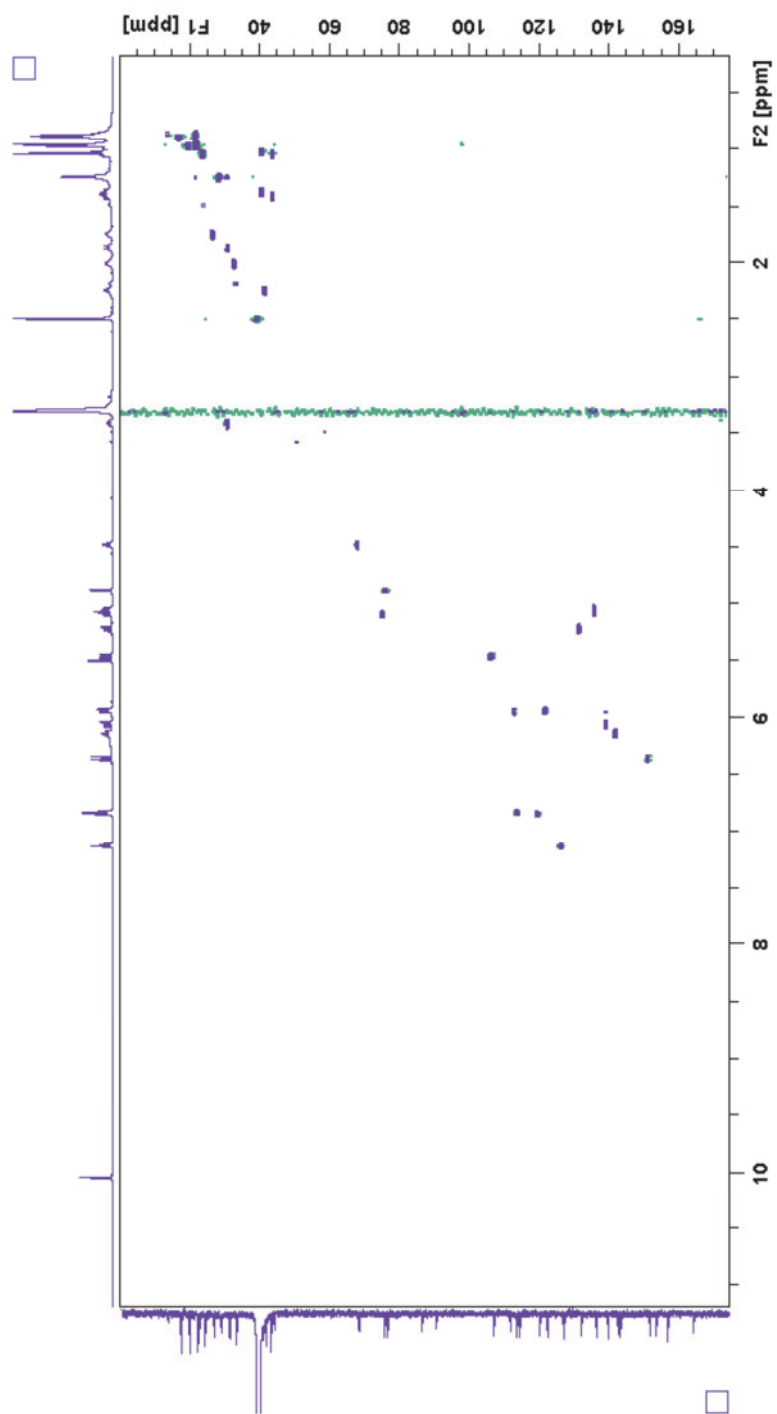


Figure S4.1. HMQC spectrum of **1** (DMSO-*d*<sub>6</sub>, 600MHz)

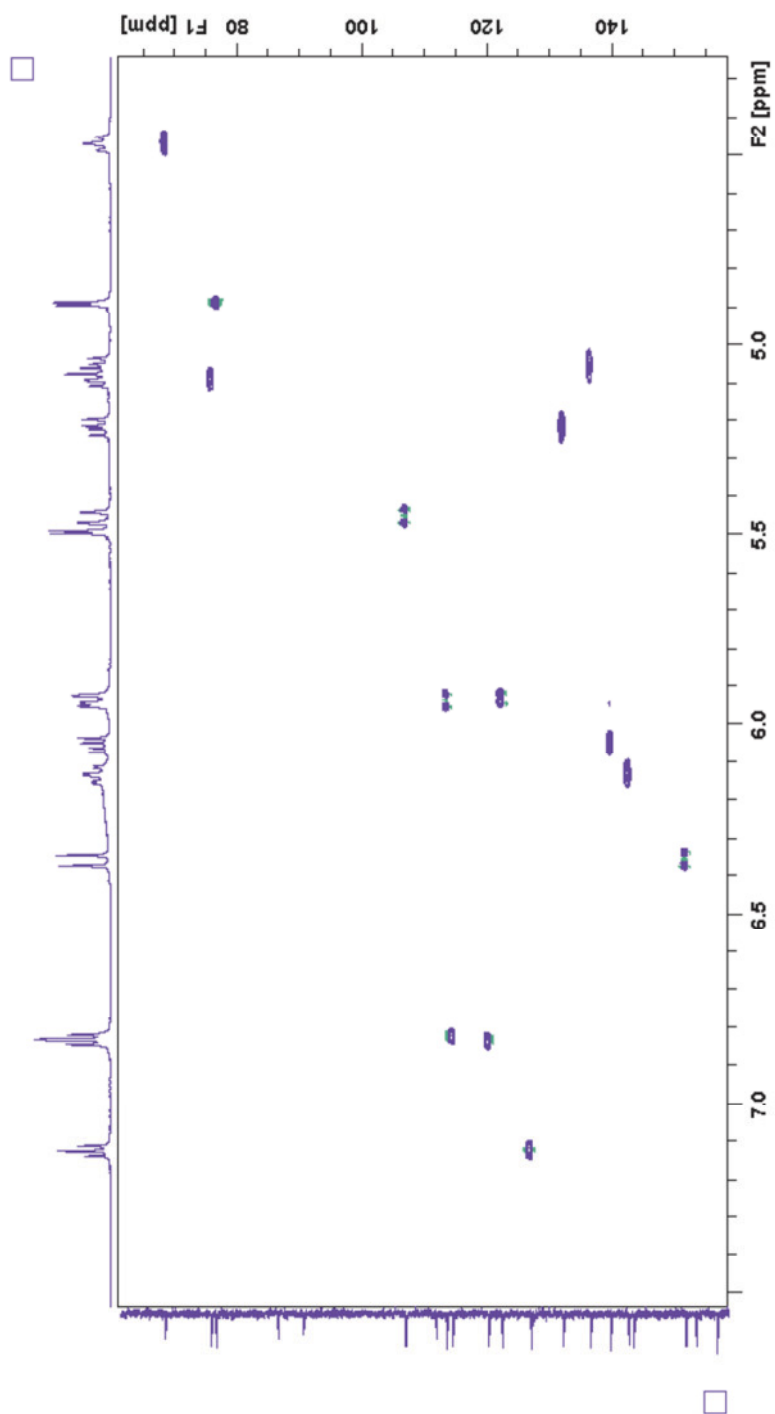
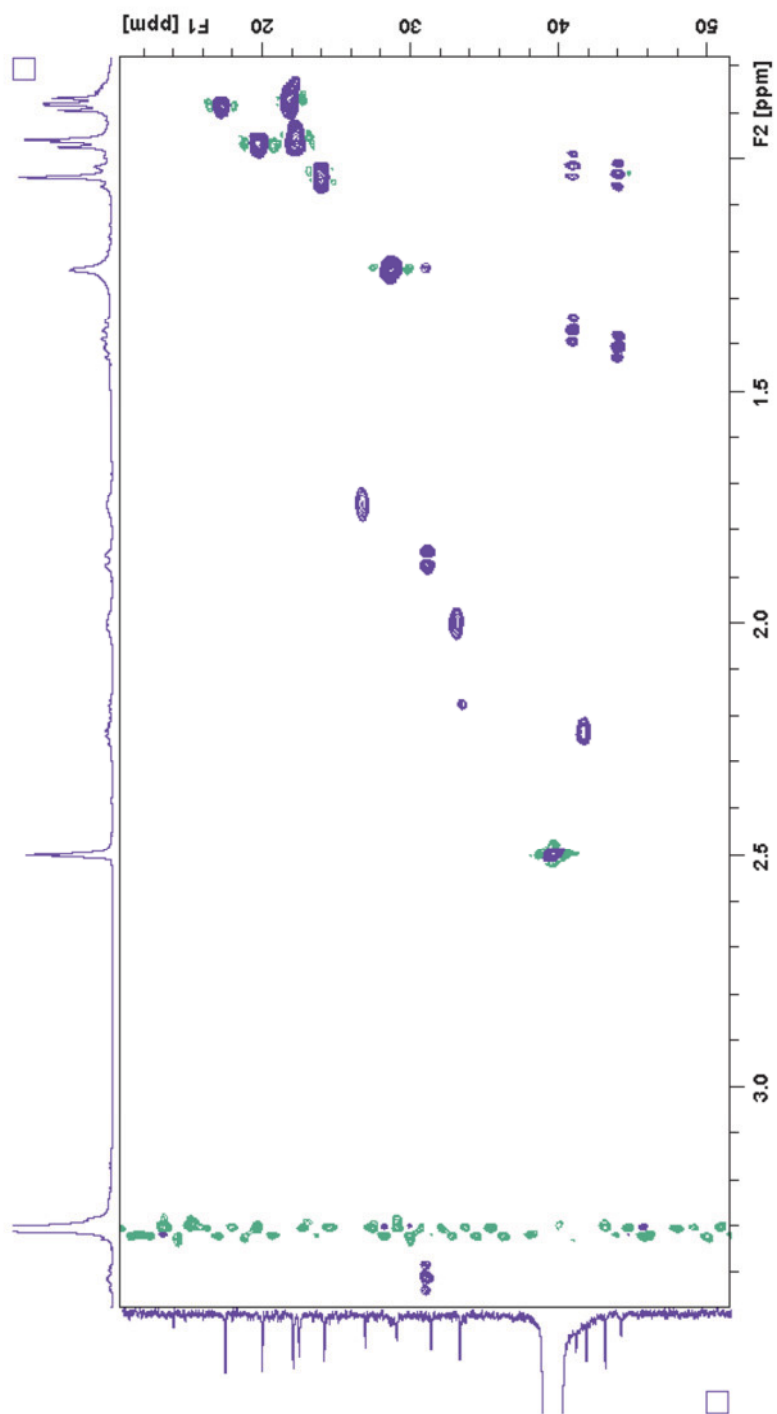
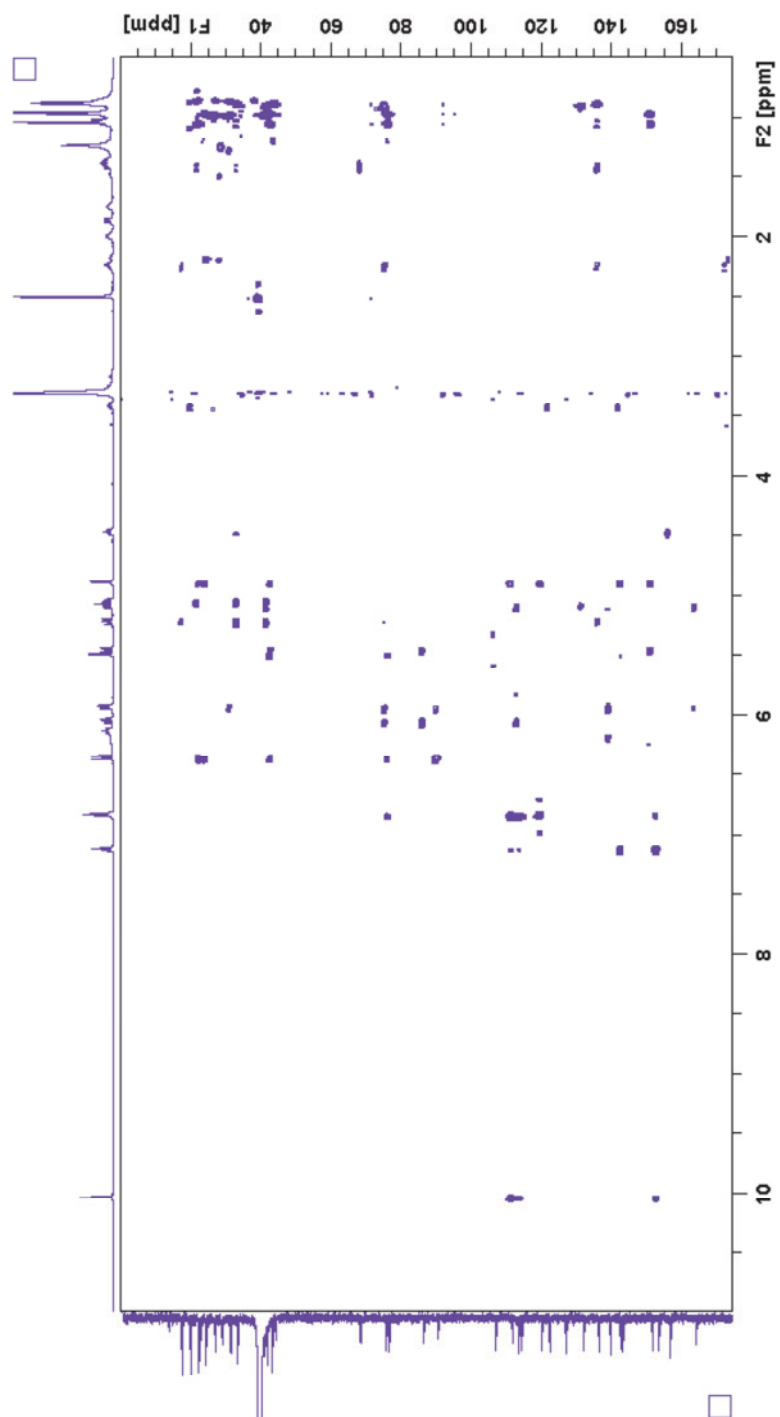
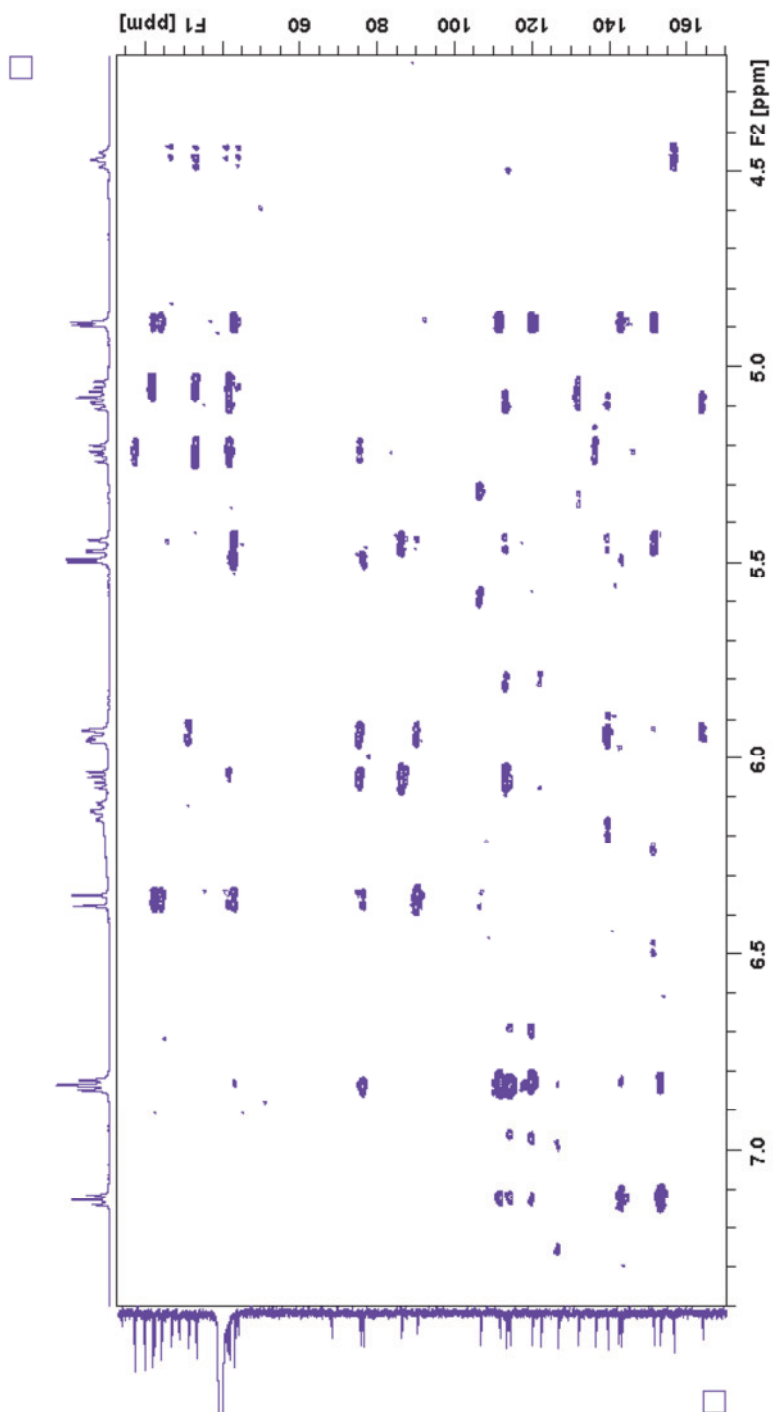
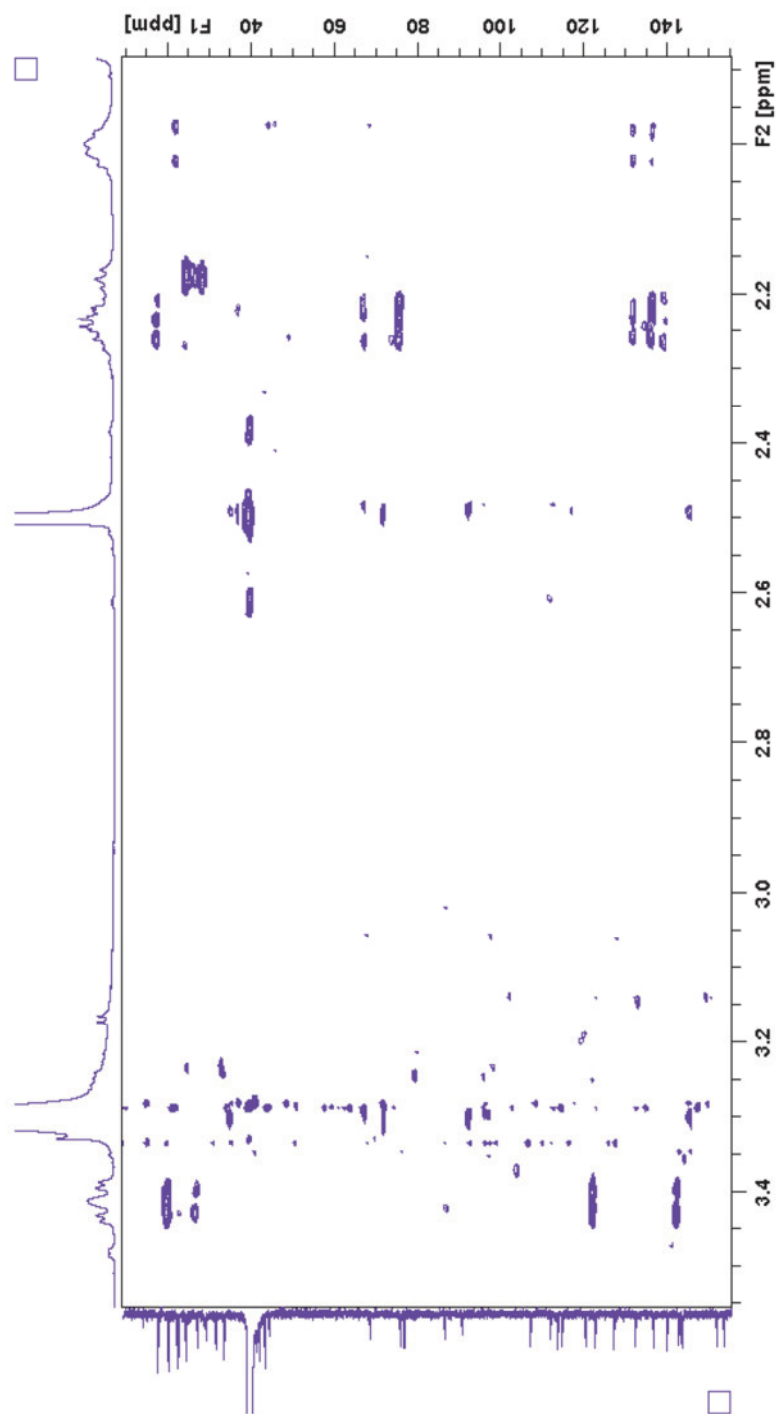


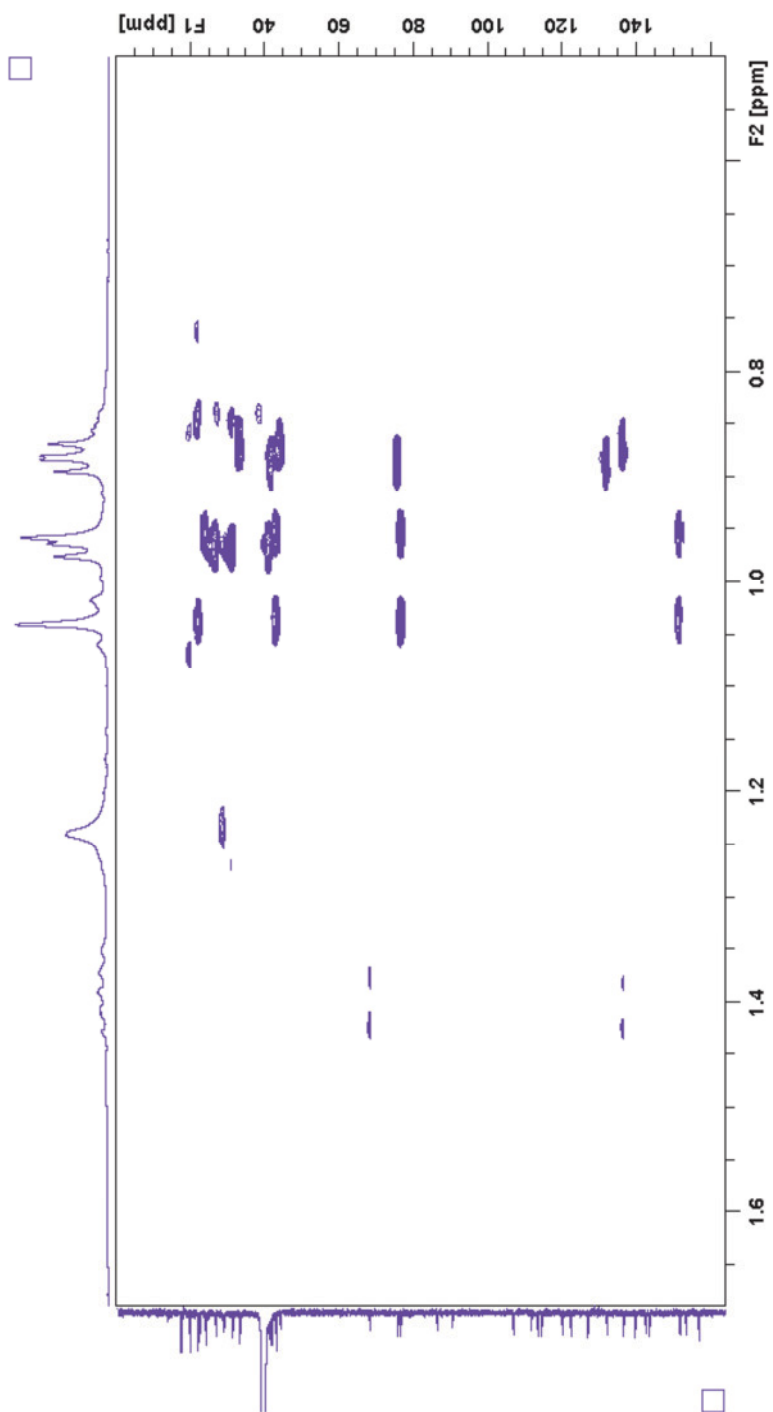
Figure S4.2. HMQC spectrum of **1** (Expansion 1)

Figure S4.3. HMQC spectrum of **1** (Expansion 2)

Figure S5.1. HMBC spectrum of **1** (DMSO-*d*<sub>6</sub>, 600MHz)

Figure S5.2. HMBC spectrum of **1** (Expansion 1)

Figure S5.3. HMBC spectrum of **1** (Expansion 2)

Figure S5.4. HMBC spectrum of **1** (Expansion 3)

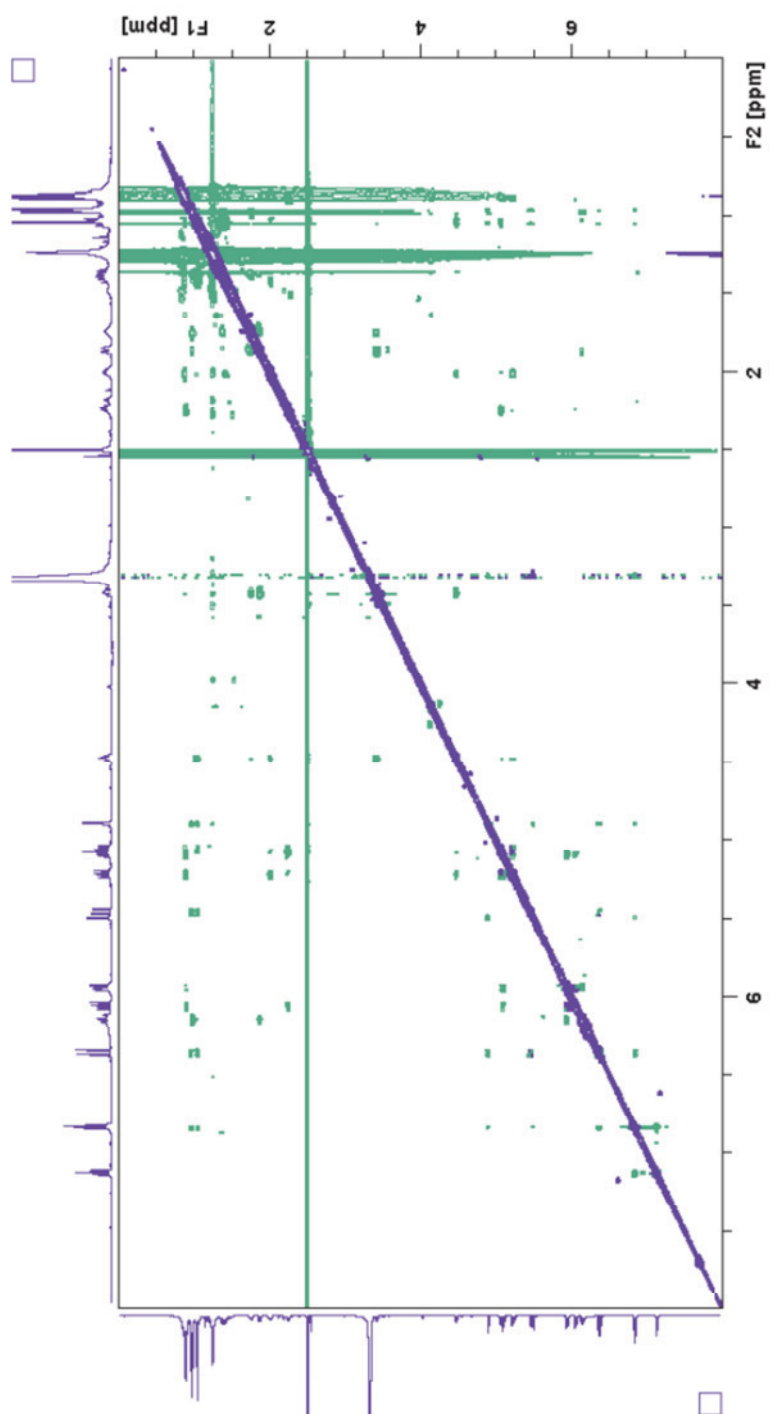
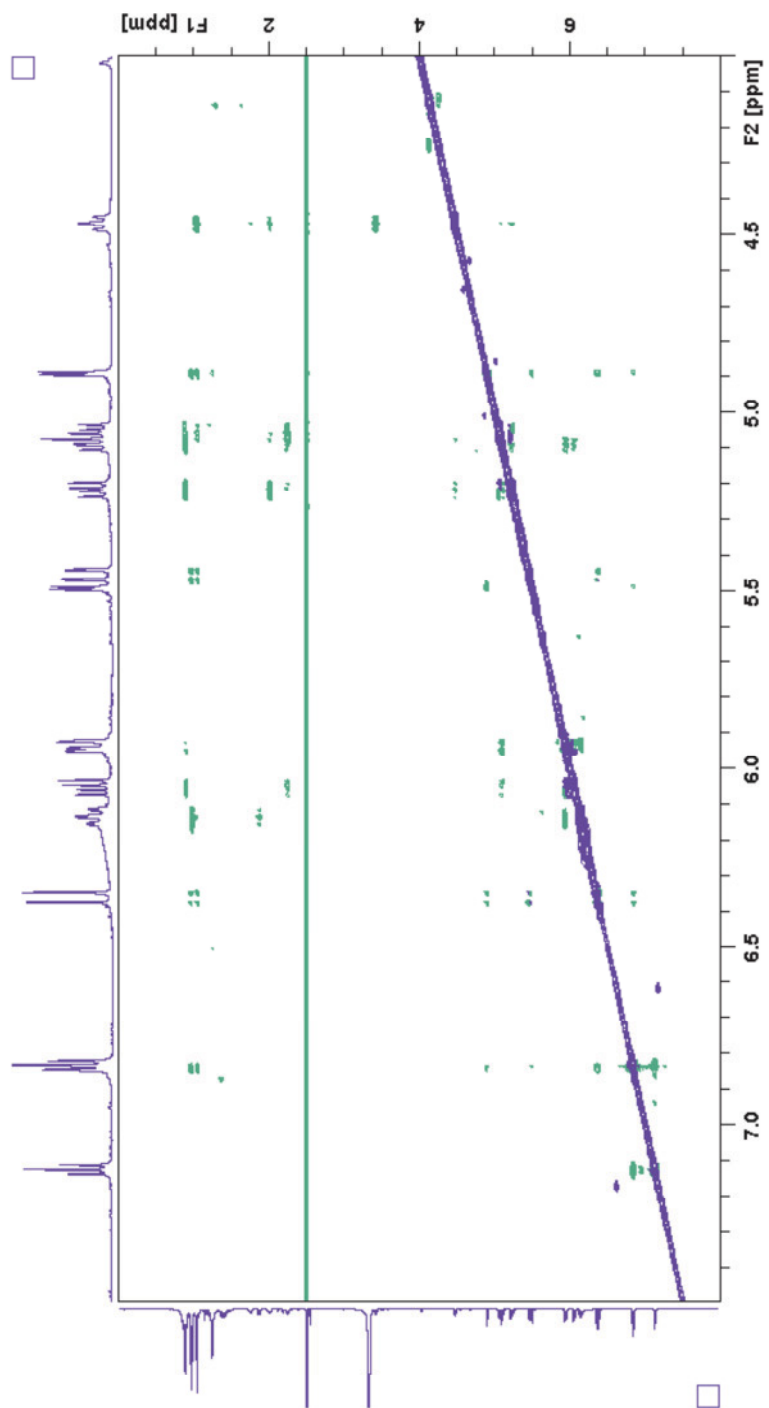
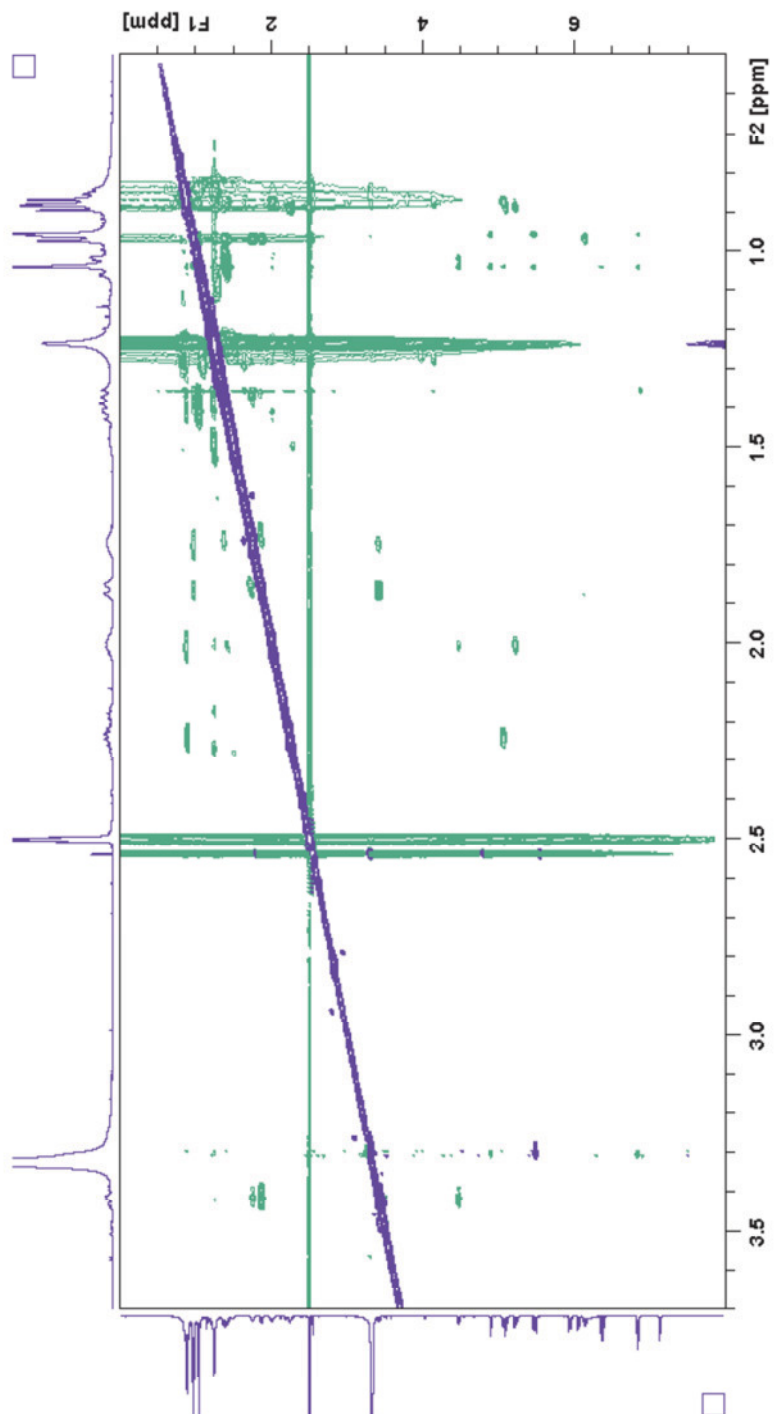


Figure S6.1. ROESY spectrum of **1** (DMSO- $d_6$ , 600MHz)



Figure S6.2. ROESY spectrum of **1** (expansion 1)

Figure S6.3. ROESY spectrum of **1** (expansion 2)

FB48-CF4, 600 MHz Magnex,  
13C-HECADE, 19.4.13 RH

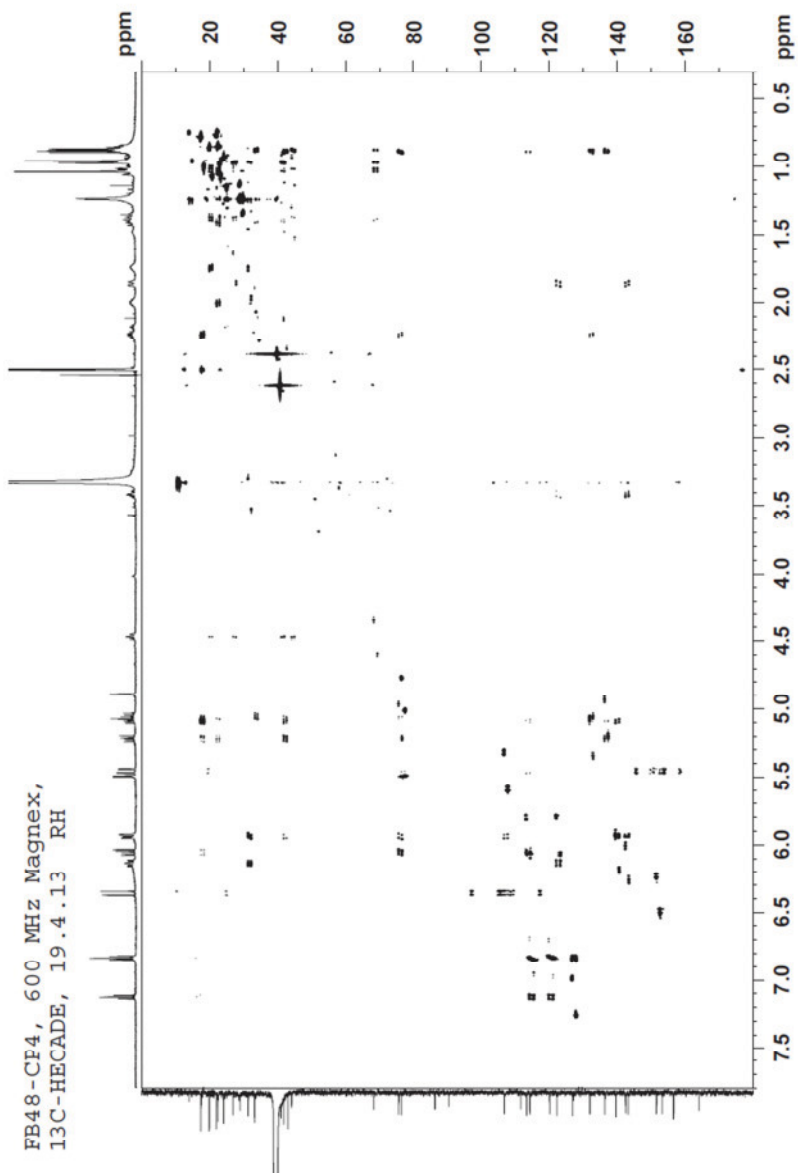


Figure S7. HSQC-HECADE spectrum of **1** (DMSO-*d*<sub>6</sub>, 600MHz)

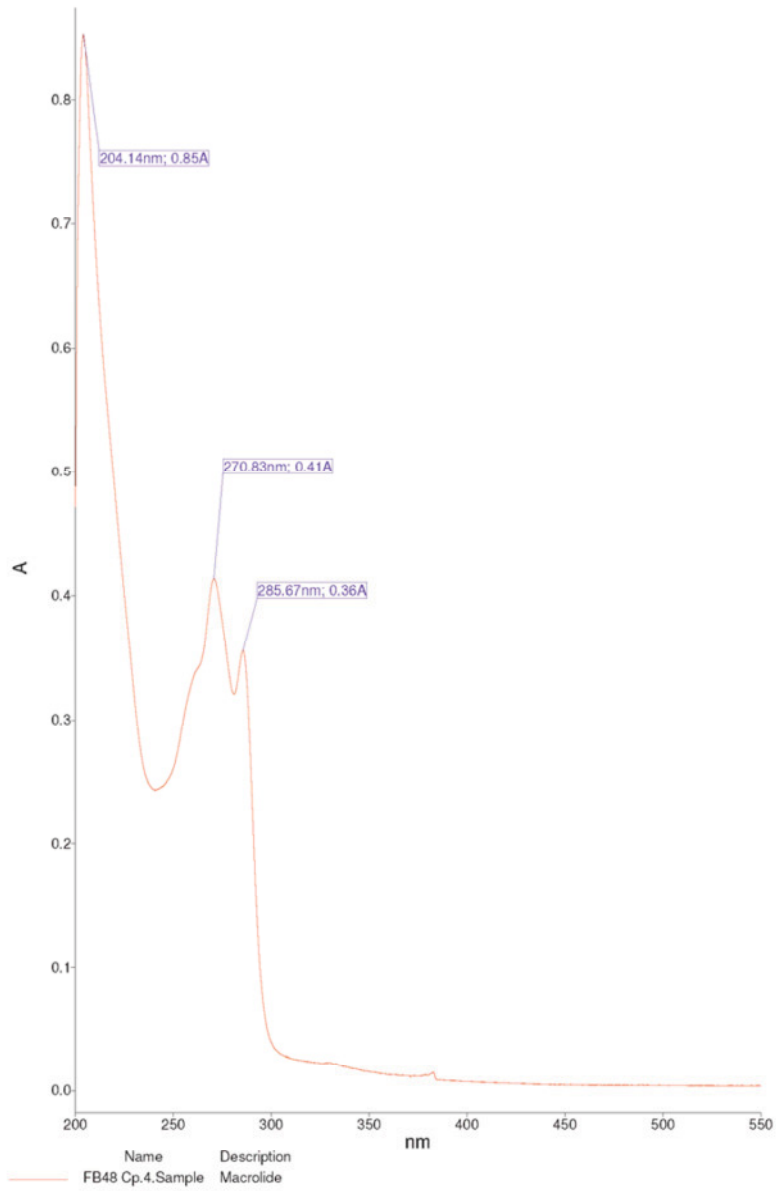


Figure S8. UV spectrum of **1** (MeOH)

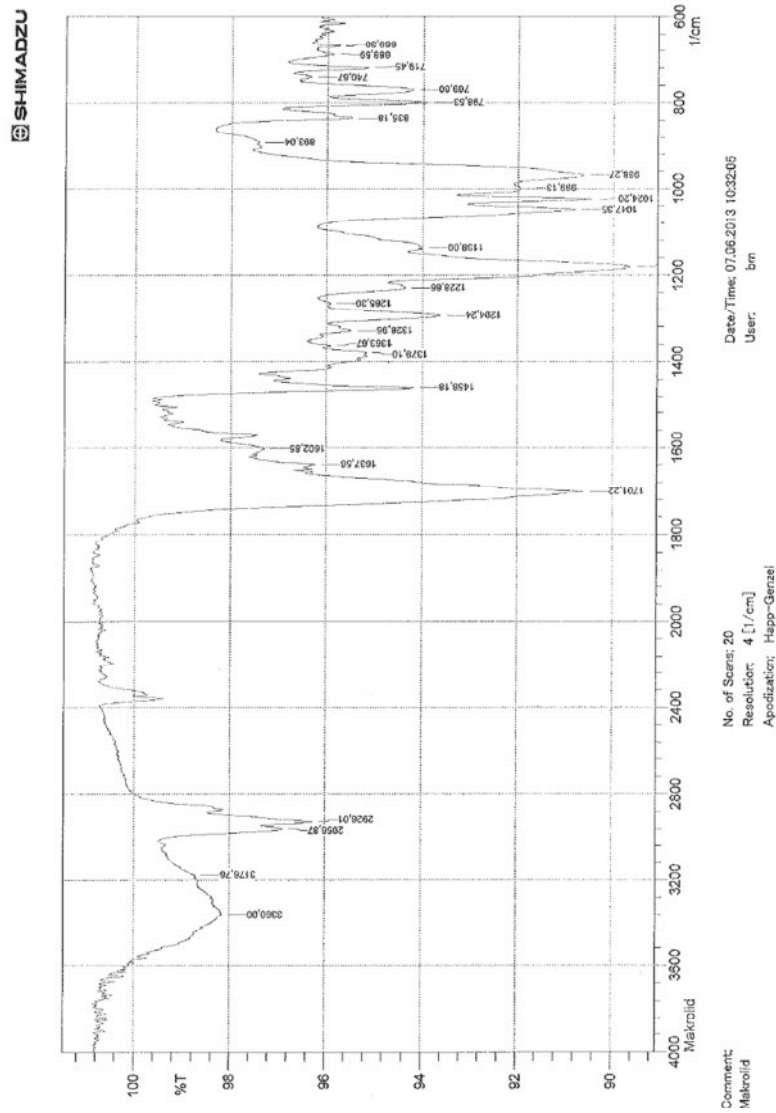


Figure S9. IR spectrum of 1

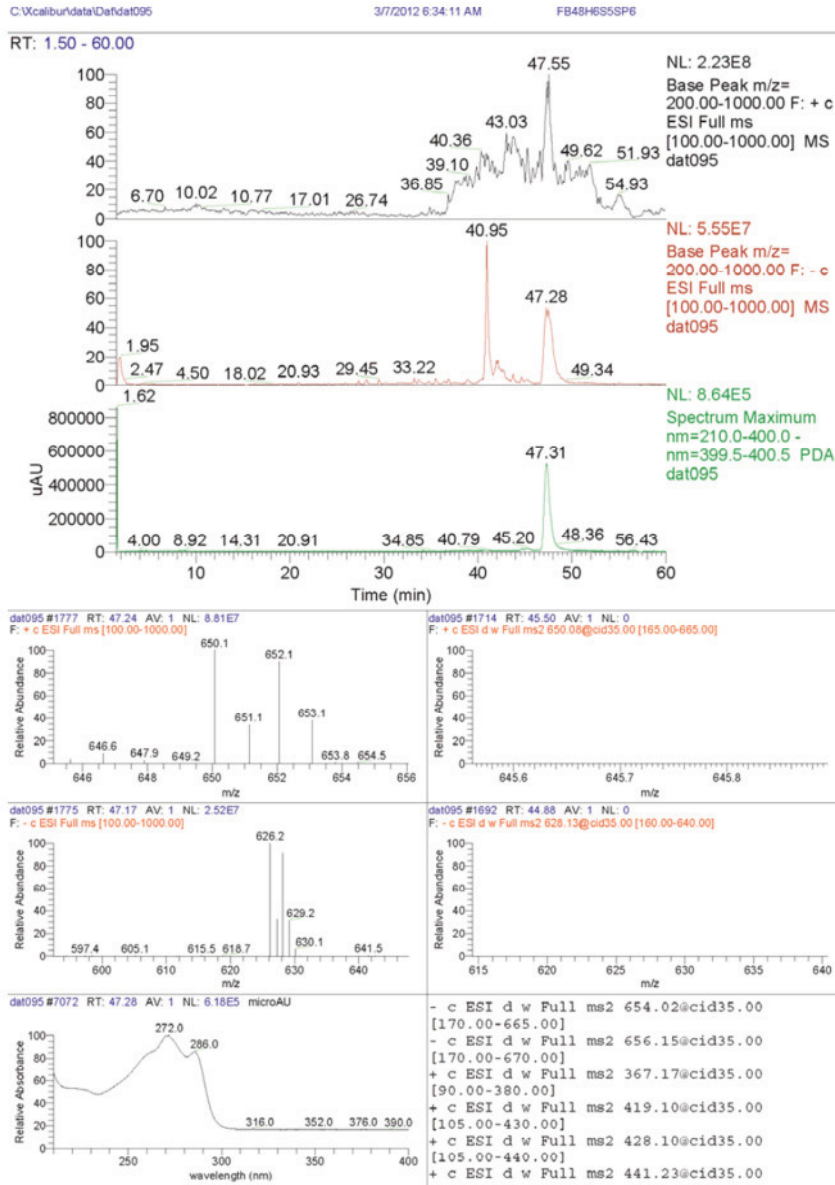


Figure S10. LC/ESI-MS spectrum of 1

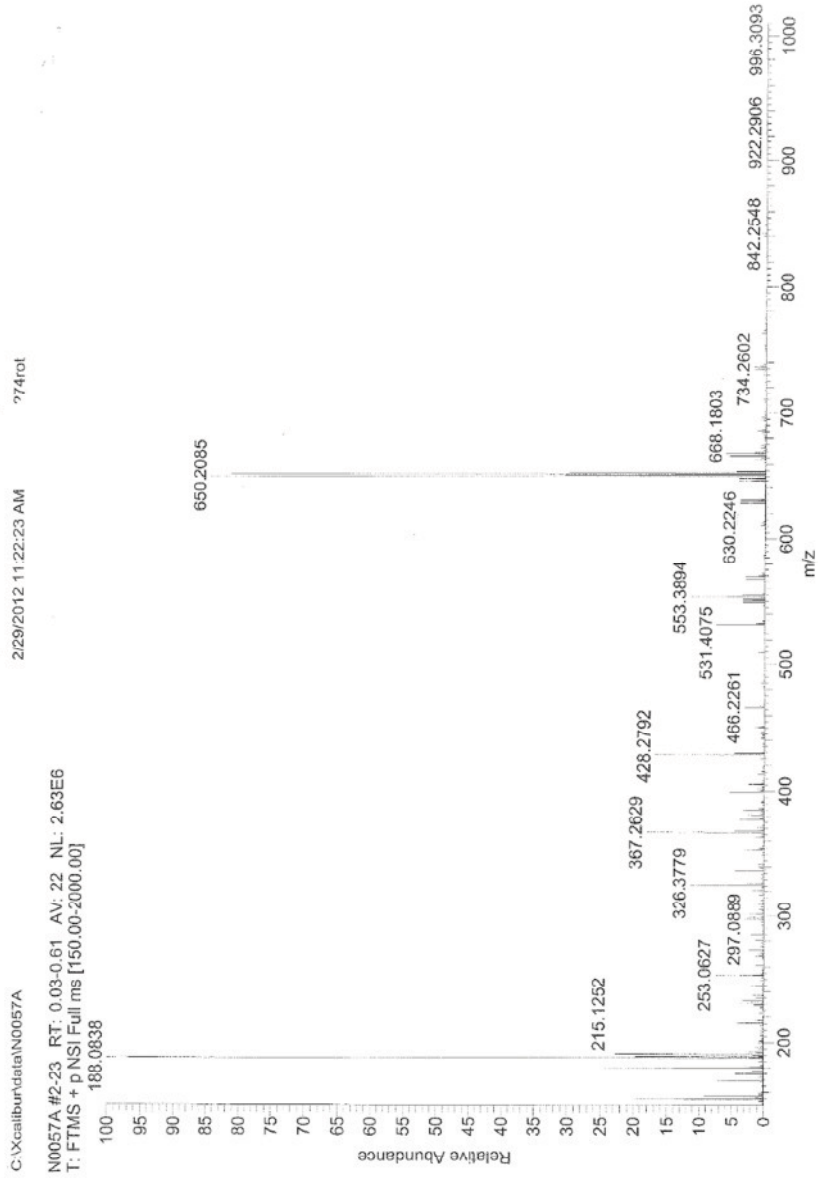
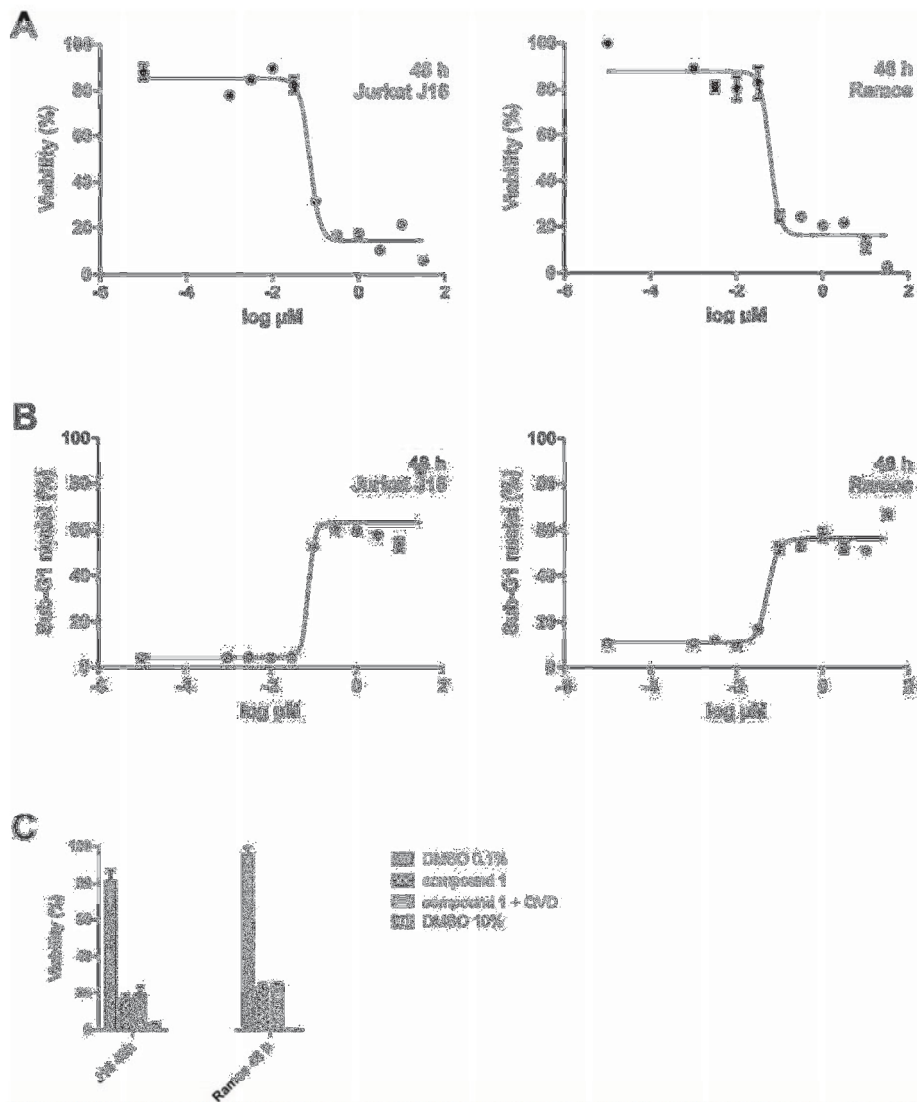


Figure S11. HRESI-MS spectrum of **1**



**Figure S12.** Callyspongiolide (**1**) reduces cell viability and induces cell death in Jurkat J16 T lymphocytes and Ramos B lymphocytes.

(A) Jurkat T cells and Ramos B cells were incubated with the indicated concentrations of compound **1** for 48 h and cell viability was assessed by MTT assay. (B) Jurkat T cells and Ramos B cells were treated as in (A). Subsequently, cell death was assessed by propidium iodide staining of hypodiploid nuclei and flow cytometry. (C) Jurkat T cells and Ramos B cells were incubated with 0.1 % DMSO, 10  $\mu\text{M}$  compound **1**, 10  $\mu\text{M}$  compound **1** in combination with 10  $\mu\text{M}$  QVD-Oph (caspase inhibitor), or 10 % DMSO for 48 h and cell viability was assessed by MTT assay. Analyses in (A-C) were performed in triplicates; error bars = SD.



## 7. Discussion

All compounds described in the following paragraphs are numbered according to their respective figures. All isolated compounds refer only to the organisms investigated within this study.

### 7.1 Isolated natural products from *Aaptos suberitoides*

#### 7.1.1 Benzo[de][1,6]-naphthyridine alkaloids

Aaptamine and its natural congeners, collectively known as ‘aaptamines’, are marine alkaloids, which feature a benzo[de][1,6]-naphthyridine framework. All known aaptamines have been isolated from Demospongiae, one of the four classes of the Porifera phylum. Although being named after *Aaptos aaptos* from where they have been first isolated, aaptamines occur across many unrelated sponges of even different taxonomic orders (Larghi, Kaufman et al. 2009) such as *Luffariella* sp. (Park, Kim et al. 1995) (order Dictyoceratida, family Thorectidae) and *Xestospongia* sp. (order Haplosclerida, family Petrosiidae)(Calcul, Longeon et al. 2003).

Considering the biosynthesis of the aaptamines, Larghi et al. proposed a pathway as shown in figure 2.1. They assumed that the formation of the aaptamine core could be explained by the condensation and cyclisation of L-DOPA (**1**) and  $\beta$ -alanine aldehyde (**2**), giving perhydroaaptamine (**3**). This reaction is followed by decarboxylation and dehydrogenation forming didesmethylaaptamine (**4**) and by further methylation and other reactions giving aaptamine and its congeners.

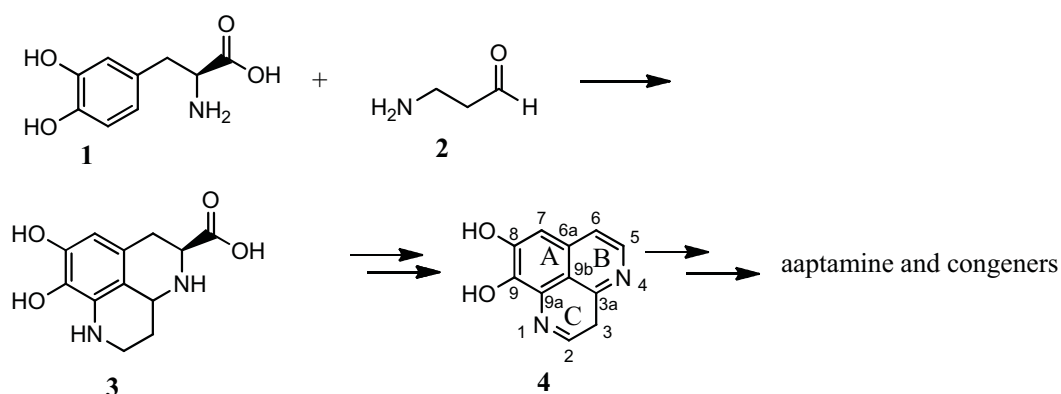


**Figure 2.1** proposed biosynthesis of aaptamine (Larghi et al., 2009)

The formation of the isolated compounds which are described in publication 1 can be explained as depicted in fig. 2.2: Starting from compounds (**4**), (**5**) and (**6**) could be easily formed by methylation through a phenolic 3-O-methyltransferase, for example. Further

oxidation of (6) at C-9 by a tyrosinase, for example, leads to the formation of (7), previously isolated from *Xestospongia* sp. (Calcul, Longeon et al. 2003). This molecule could further react to (10), an amino derivative, through a formal Michael addition of ammonia at C-3. In order to get (15) formally a benzoyl moiety (possibly in the form of benzoyl CoA) can be linked to C-3. The aptamine ketal (9) can be formed by an addition of two methanol molecules following an elimination of water. Formal additions of urea (possibly in the form of carbamoyl phosphate) and glycine to (7) lead to the hypothetical intermediates (7a-c). The subsequent water elimination, redox reactions (oxidoreductases) and methylation would create (8), (11) and (12) respectively.

Aptamine and its congeners are well known for their cytotoxic activity. The group of Hamann explained the cytotoxicity of aptamine by its ability to intercalate DNA, as assessed by a titration experiment monitored by UV-vis absorbance. The natural product binds with DNA in the same fashion as amsacrine does (Bowling, Pennaka et al. 2008). DNA intercalation seems plausible due to the planar structure of aptamine. The authors also suggested that antiviral activity shared this mechanism of action.

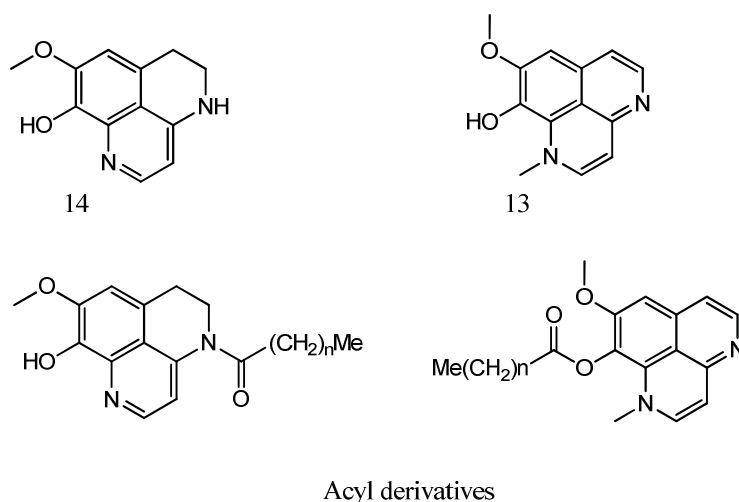


**Figure 2.2.** isoaptamine (13), dihydroaptamine (14) and acyl derivatives

The structure activity relationship between several aptamine derivatives is quite ambiguous. Though, it is clear that essential structural elements for bioactivity are a free hydroxyl group at C-9, an unsubstituted nitrogen at N-4 and complete aromaticity as pointed out in publication 1 in which (6) displayed a higher cytotoxicity than aptamine, whereas (9) could be considered inactive. A major structure activity study by (Shen, Lin et al. 1999) supported this finding. Therein, a series of acyl derivatives of isoaptamine (13) and dihydroaptamine (14) were prepared and their cytotoxic activity was tested against four tumor cell lines KB16 (epidermoid carcinoma of the nasopharynx), A549

(adenocarcinomic human alveolar basal epithelial cells), HT-29 (human colon adenocarcinoma), and P388 (murine leukemia) (Shen, Lin et al. 1999). Introduction of side chains at the crucial positions N-4 and C-9 led to a significant decrease of activity, as well as hydrogenation of the B ring as in (**14**) indicating that aromaticity is still important for activity. The decrease in activity of the acylated products against human tumor cells was explained by their low water solubility and low bioavailability. However, if the substituent contains 7, 8 and 10 methylene groups, bioactivity of these compounds ( $IC_{50} = 0.03-0.04 \mu\text{g/ml}$ ) neared that of isoaptamine ( $IC_{50} = 0.04 \mu\text{g/ml}$ ) again (Shen, Lin et al. 1999). Furthermore, oxidation of the hydroxyl group at C-9 into carbonyl group as in (**7**) led to an increased cytotoxicity ( $IC_{50} = 0.01 \mu\text{g/ml}$ ). However, this is not always the case, as it is shown in publication 1: substitution at C-3 as in (**10**) rather lowered the cytotoxic effect (growth inhibition 64.4%) against L5178Y cells instead of enhancing it. This ambiguity of the structure activity relationship of aptaminoids still remains unexplained and is the subject for future investigations.

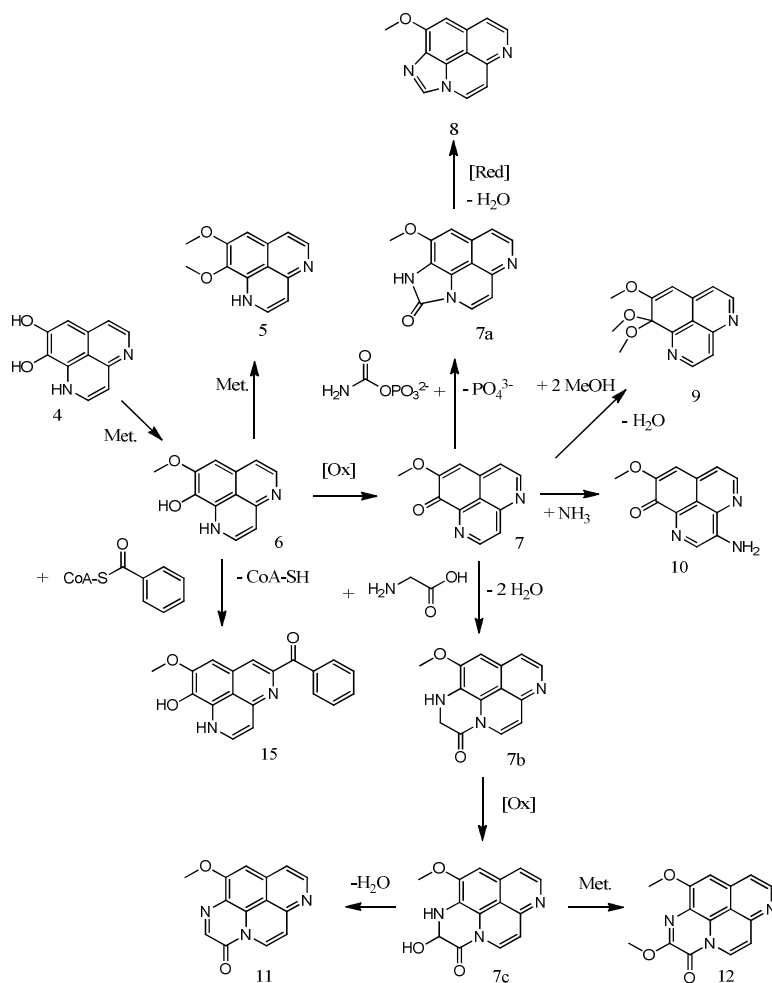


**Figure 2.3** proposed biosynthesis of isolates from *Aiptos suberitoides* based on Larghi et. al. (2009). Compounds **7a-c** are hypothetical intermediates

## 7.2 Isolated natural products from *Polycarpa aurata*

### 7.2.1 Sulfur containing guanidine alkaloids

Three sulfur containing alkaloids, polycarpathiamine A+B (**1-2**) and polycarpaurine C (**5**) were isolated from *Polycarpa aurata*. Each of them features a five membered guanidine containing heterocycle. Whereas the sulfur of the polycarpathiamines is endocyclic, polycarpaurine C possesses a thiosulfate group. Although sulfur containing marine natural products with diverse chemical structures are widespread across various marine invertebrates (Prinsep 2003), compounds which feature a 3-amino-1,2,4-thiadiazole substructure are extremely rare. The only natural product of this type prior to this study is dendrodoine which was isolated from *Dendrodoa grossularia* (Heitz, Durgeat et al. 1980). Biosynthetic considerations as mentioned in publication 2 were made in order to clarify the origin of the isolated compounds. It seems plausible that these substances are degradation products of polycarpine, a dimeric alkaloid which was isolated from the same ascidian in earlier investigations (Abas, Hossain et al. 1996; Wang, Oda et al. 2007). Figure 2.4 shows a complementary biosynthetic pathway to the one already described in publication 2.

4-Methoxy benzoic acid or p-anisic acid (**1**) which was isolated along with the alkaloids appears to be the major compound, since its yield was the highest (15 mg) and can be considered as the precursor of all occurring compounds within the organism except for the  $\alpha$ -carboline alkaloid N,N-didesmethylgrossularine-1. Through several addition and cyclisation reaction steps which might involve cysteine (sulfur donor) and arginine as putative reagents a hypothetic precursor (**1a**) of polycarpine is formed. Oxidation and addition of water would lead to the novel alkaloids (**6-7**) as described in publication 2. If (**1a**) is methylated into (**1c**), polycarpine (**4**) can be formed through radical oxidation (**1g**) and subsequent dimerization into (**4**). Further oxidation of the disulfide moiety yields the thiosulfate derivative polycarpaurine C (**5**). Analogous to (**1a**) (**1c**) can react to (**1d**) through oxidation and addition of water which yields the hypothetic intermediate (**1e**). In order to eliminate the guanidine function, an amidinotransferase could catalyze this reaction by transferring the guanidine of a donor compound onto an acceptor compound featuring an amino group (Walker 1973) leading to (**2**), another metabolite of polycarpine (Abas, Hossain et al. 1996). Amidinotransferases occur in prokaryotes as well as in eukaryotes and are involved in the synthesis of guanidino compounds, which play an important role in vertebrate energy metabolism and in secondary metabolite production by

higher plants and prokaryotes (Muenchhoff, Siddiqui et al. 2010). After the formation of (2) hydrolysis can take place and compound 4 is formed through elimination of H<sub>2</sub>S.

Polycarpathiamine A (6) was found to inhibit the growth of the murine lymphoma L5178Y cell line with an IC<sub>50</sub> = 0.41 μM. It appears that the heterocycle and a free aromatic hydroxyl group are essential for the bioactivity, as polycarpathiamine B which features an aromatic methoxy group was not active, so did (1) and (3) which do not have a heterocycle. Despite their rare occurrence there are a few investigations on 1,2,4-thiadiazoles including a mechanism of action study, though not necessarily directly related to cytotoxicity. In 2003 Leung-Toung et. al. synthesized a series of 1,2,4-thiadiazoles with enzyme inhibiting properties. Specifically, cathepsin B was targeted and the inhibition should take place via thiol trapping which could be easily explained by the oxidoreductive properties of the sulfur (Leung-Toung, Wodzinska et al. 2003). This thiol trapping property can also be suggested for dendrodoine and polycarpathiamine A, as the crucial element is sulfur. Another study on 1,2,4-thiadiazoles reports the isolation of an indole alkaloid containing such a heterocycle from the root of the herbaceous plant *Isatis indigotica* and its antiviral activity (Chen, Lin et al. 2012).

The biogenetic origin of the isolates is ambiguous, since (1) is actually one of the constituents of anisic oil from *Pimpinella anisum*, a terrestrial plant. As a phenolic acid derivative, (1) might stem from the shikimic acid pathway which is exclusively found in plants, bacteria and fungi (Morgan, Gibson et al. 1962; Barker and Frost 2001; Metzler 2003). This raises the question whether polycarpine and its derivatives are produced by the host organism, by the microbial symbionts or in participation of both. Further studies on bioactivities, mechanisms of action and biosynthesis have yet to be conducted.

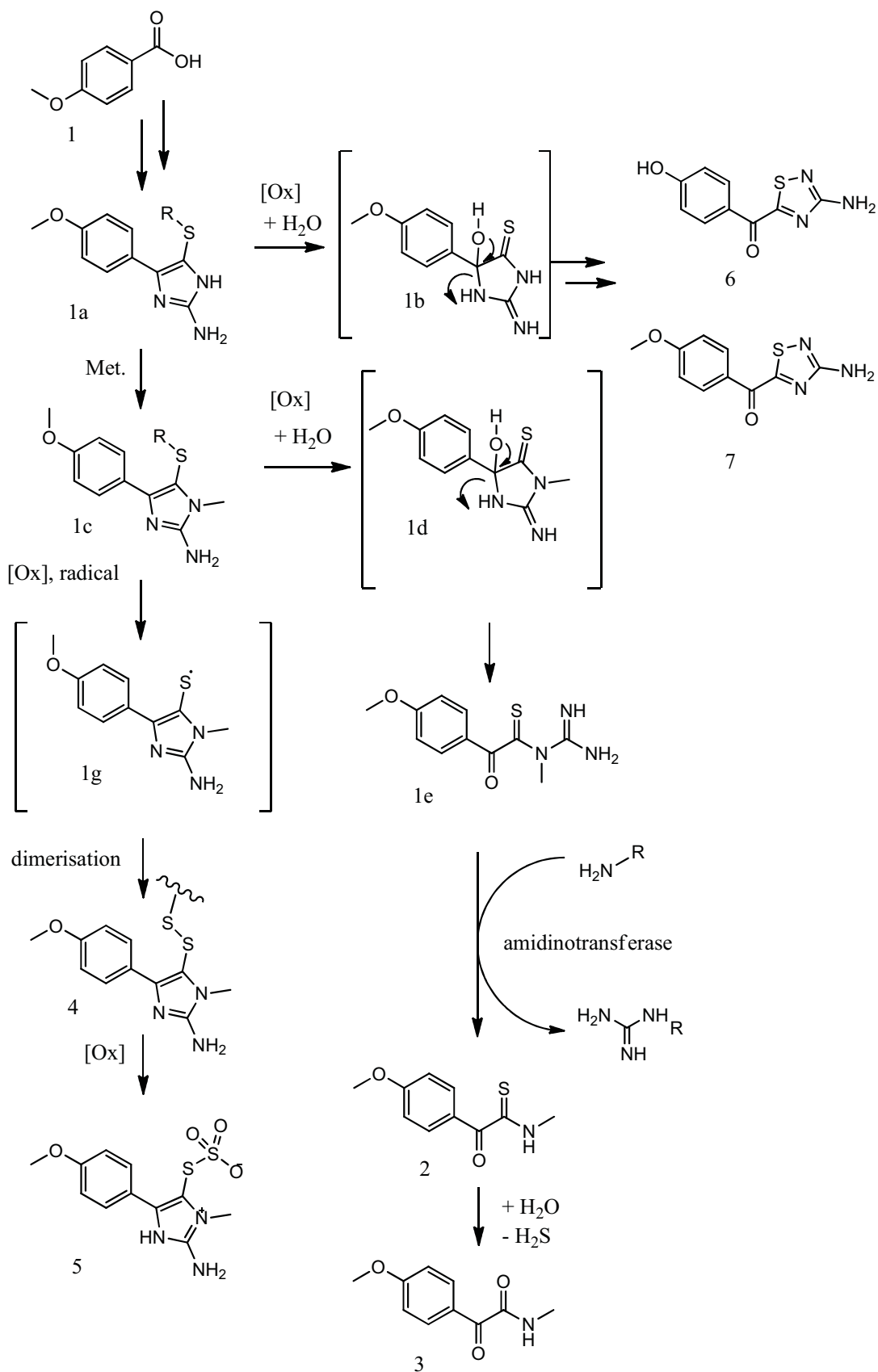


**Figure 2.4** proposed biosynthesis pathway of 4-methoxybenzoyl thioacetamide (2), 4-methoxybenzoyl acetamide (3), polycarpine (4), polycarpaurine C (5), polycarpathiamine A and B (6-7) (Walker 1973; Pham, Weber et al. 2013); 1a-f are hypothetical intermediates

### 7.2.2 $\alpha$ -Carboline alkaloids

N,N-didesmethylgrossularine-1, was isolated from *Polycarpa aurata* along with the before mentioned alkaloids. Whereas  $\beta$ -carbolines are common natural products, especially present in many plants, for example Passion flower or Syrian rue, the only naturally occurring  $\alpha$ -carboline alkaloids are grossularine-1 and 2 from *Dendrodoa grossularia* (Helbecque, Moquin et al. 1987) and N,N-didesmethylgrossularine 1 (DMG-1) from *Polycarpa aurata*. Grossularines-1 and -2, have exhibited cytotoxic activity on L1210 leukemia cells in culture (Helbecque, Moquin et al. 1987), however an anti-inflammatory activity has also been ascribed to DMG-1 (Oda, Lee et al. 2009). Grossularine-1 and -2 are DNA binding agents and their apparently planar structure would suggest an intercalative mode of action. However, this is only partly true, as Helbecque et al. reported an intercalative property of grossularine-2 and a non-intercalative mode of action for grossularine-1 due to a bulky indole moiety at the 2-position of the  $\alpha$ -carboline ring (Helbecque, Moquin et al. 1987). Accordingly, the mode of action of DGM-1 must be the same as that of grossularine-1 due to the almost identical chemical structure.

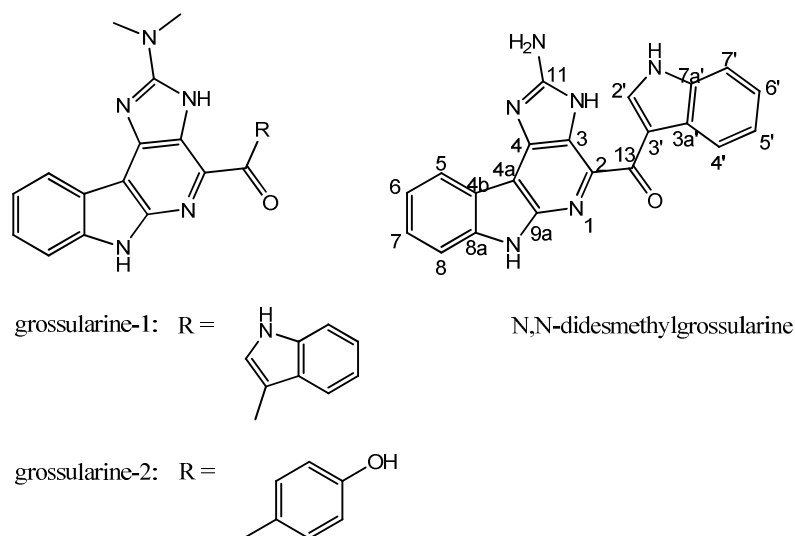


**Figure 2.5**  $\alpha$ -carboline alkaloids grossularine-1 and 2 and N,N-didesmethylgrossularine

### 7.3 Isolated natural products from *Callyspongia* sp.

#### 7.3.1 Polyketide macrolides

Polyketide macrolides are common natural products which are produced by terrestrial and marine microorganisms. Antibacterial, antifungal and cytotoxic activities are inherent properties of such substances. Notable examples are the therapeutically used antibiotic erythromycin and the antimycotic drug amphotericin B, either compounds are produced by *Streptomyces* bacteria. In the last three decades, more and more macrolides from marine sources have been discovered including leiodermatolide, bryostatin, mandelalides, candidaspongiolides etc. from sponges, bryozoans and sea squirts (Pettit, Herald et al. 1982; Meragelman, Willis et al. 2007; Paterson, Dalby et al. 2011; Sikorska, Hau et al. 2012). Notably, cytotoxicity is their most important biological property. Callyspongiolide (**3**) is the first polyketide macrolide isolated from a *Callyspongia* sponge. In the following, a plausible biosynthetic pathway for (**3**) is proposed which is consistent with that of Staunton and Weissman (Staunton and Weissman 2001). In general, polyketides are created through a sequential condensation of  $\beta$ -ketoesters under elimination of carbon dioxide. They themselves stem from the condensation of acetyl CoA and malonyl CoA. As depicted in figure 2.6, acetoacetyl CoA and malonyl CoA are the major components participating in the condensation reaction which is catalyzed by a polyketide synthase. The methyl group at C-12 might originate from methylmalonyl CoA (**1a**) formed by acetyl CoA and propionyl CoA (fig.3.1). A proposed short chain fatty acid (**1b**) containing a triple bond could be attached onto C-14. This substance could be formed from a fatty acid via desaturation by a desaturase and subsequently an acetylenase. Finally, the linkage of a brominated derivative of 3-hydroxybenzoic acid (**1d**) onto the tautomeric form (**1c**) of fatty acid moiety under water elimination at C-19 completes the structure of the callyspongiolide precursor (**2a**). In the following, the keto groups and the hydroxyl groups could be reduced with either NADH or FADH<sub>2</sub> as reducing equivalents leading to (**2b**). Then, elimination of water, cyclisation at C-13 and the addition of a carbamoyl function at C-7 finalize the formation of the 14 membered callyspongiolide (**3**).

Several studies on marine macrolides reported an antimitotic activity of such compounds. Like taxol, a cyclic diterpenoid anticancer agent from *Taxus brevifolia*, they cause hyperstabilization of microtubules thus inhibiting the cell cycle and ultimately leading to apoptosis. Such compounds include discodermolide, zampanolide and laulimalide (Buey, Barasoain et al. 2005; Field, Pera et al. 2012; Best, Matthews et al. 2013) (s.fig.2.7).



However, there are also antimetabolic agents that do not target tubulin: Spirastrellolide A methyl ester from the Caribbean marine sponge *Spirastrella coccinea* shows potent activity ( $IC_{50} = 100 \text{ ng/mL}$ ) in a cell-based assay that detects mitotic arrest, but it does not affect tubulin polymerization *in vitro*. It has the unusual biological property of being able to accelerate the entry of cells into mitosis from other cell-cycle stages, before it arrests them in mitosis. This unusual biological effect sets spirastrellolide A apart from the before mentioned antimetabolic agents (Williams, Roberge et al. 2003). Apart from antimetabolic activity there are also cytotoxic macrolides with other properties. For example, lanosolide A is a potent modulator of protein kinases C which are linked to carcinogenesis, since they can act as tumor promoters (Koivunen, Aaltonen et al. 2006). With regard to callispongolide, further bioassays including antimetabolic activity assays and mechanism of action studies should be the next steps.

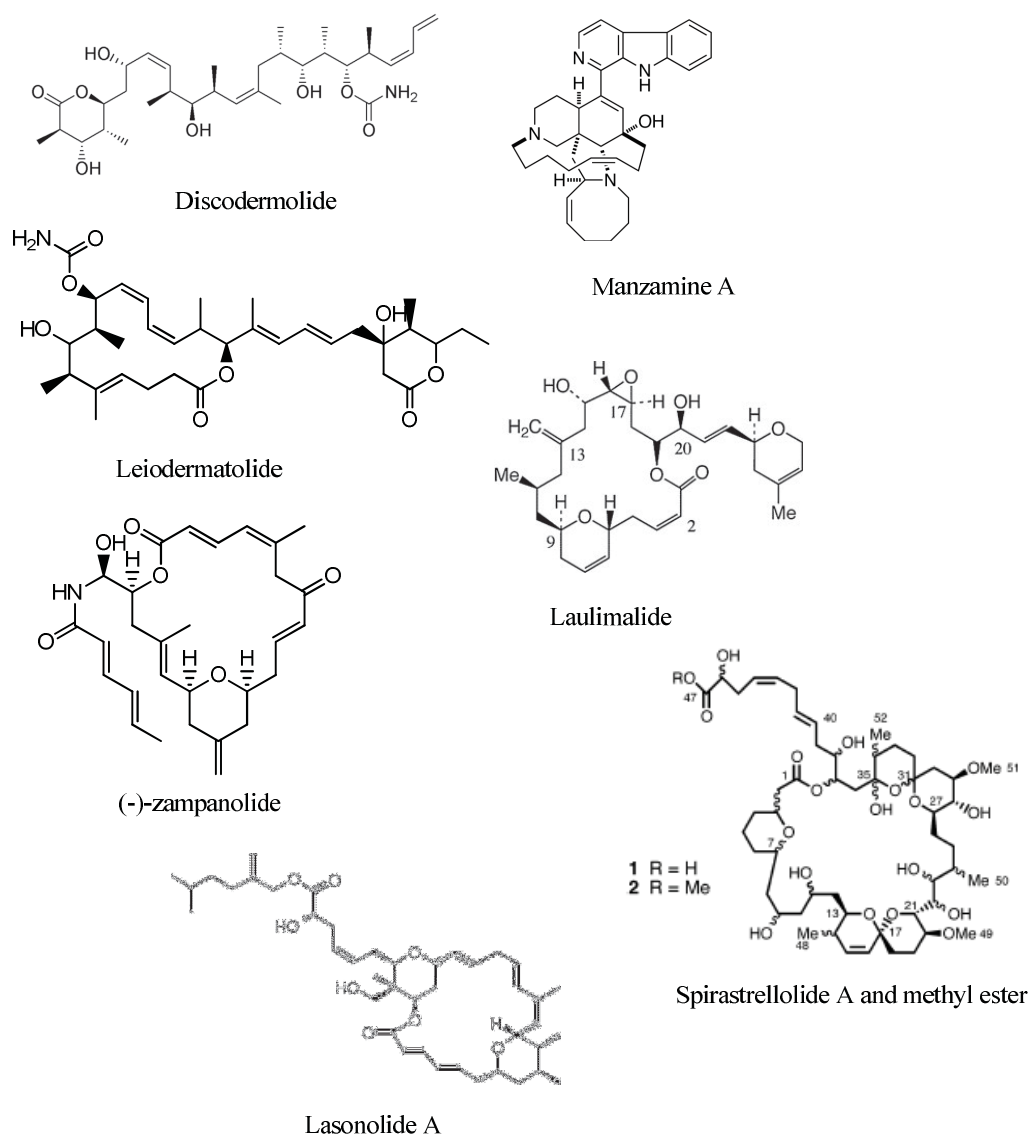


**Figure 2.6** marine (macrocyclic) polyketides

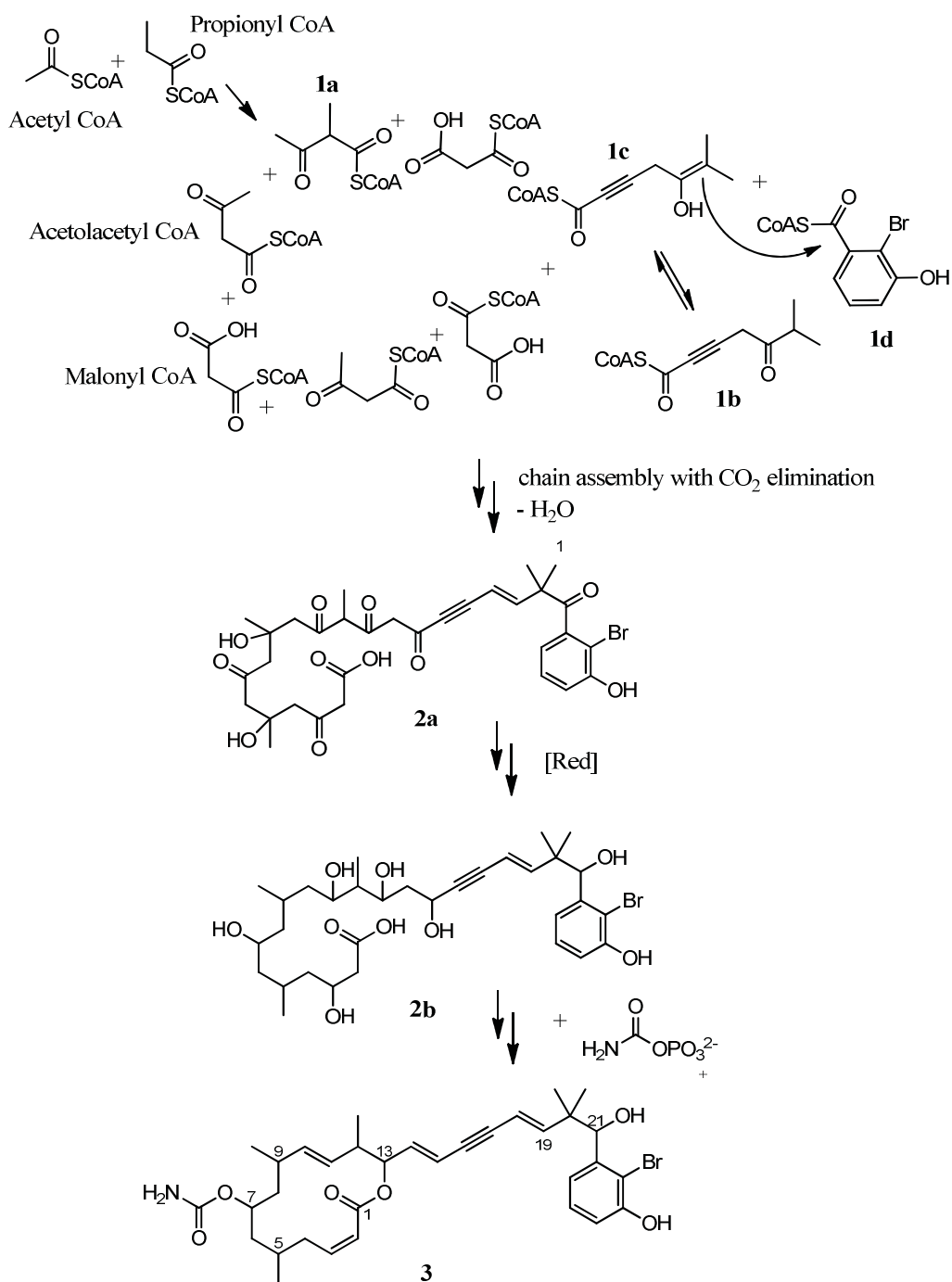


**Figure 2.7** proposed biosynthetic pathway for callispongolide (**3**) based on Staunton et. al. (2001); **1a-d** and **2a-b** are hypothetical intermediates

Although polyketide macrolides are present in many marine invertebrates, it is hypothesized that bacteria are the real producers of such substances. Although other microorganisms such as dinoflagellates (Kobayashi and Tsuda 2004) and fungi (Wang, Zhou et al. 2009) can also synthesize polyketide macrolides, the vast majority of macrolides are of bacterial origin. Especially marine sponges are also known as bacteriosponges because they host dense bacterial communities (Taylor, Radax et al. 2007). Apart from the works of Piel and Haygood which were mentioned earlier there are more recent investigations which give further insight into the microbiome of marine sponges: In a molecular biological study Trindade-Silva et al. have disclosed the microbiome of the marine sponge *Arenosclera brasiliensis* via cloning relevant genes (Trindade-Silva, Rua et al. 2013). They found a large diversity of type I modular polyketide synthase subtypes belonging to actinobacteria, cyanobacteria, alphaproteobacteria, and deltaproteobacteria (Burkholderia). Type I modular polyketide synthase (PKS) is a microbial enzyme involved in the macrolide biosynthesis. Specifically, it may be involved in the formation of the obvious macrocycloalkane/polyketide core of arenosclerin, an inherent alkaloid of *Arenosclera brasiliensis*. Another alkaloid with a macrocyclic system is manzamine A which is also believed to be synthesized by PKS. Additionally, manzamine A was found in several geographically and taxonomically unrelated haplosclerid sponges (Trindade-Silva, Rua et al. 2013). This observation provides further strong evidence of a symbiotic origin of manzamine A whose production is assigned to an Actinomycetales strain of the genus *Micromonospora* according to a patent (Hill, Peraud et al. 2005). Another study (Schirmer, Gadkari et al. 2005) reported a metagenomic analysis of the marine sponge *Discodermia dissolute*. This analysis revealed diverse polyketide synthase gene clusters in microorganisms associated with this sponge. Among these the genes of the endosymbiotic bacterium *Entotheonella* spp. were identified. The investigated gene clusters encode for a bacterial PKS which is responsible for the production of the inherent cytotoxic polyketide discodermolide. This study provides another strong evidence of the microbial nature of marine polyketide macrolides. Bearing all this in mind, it is only reasonable to suggest a bacterial origin of callyspongiolide, particularly in view of the fact that the aromatic subunit strongly resembles a 3-hydroxybenzoic acid, a clearly bacterial metabolite (Zhou, Huang et al. 2013).

## 8. Bibliography

Abas, S. A., M. B. Hossain, et al. (1996). "Alkaloids from the Tunicate *Polycarpa aurata* from Chuuk Atoll." J. Org. Chem. **61**: 2709-2712.

Aoki, S., Y. Watanabe, et al. (2006). "Cortistatins A, B, C, and D, anti-angiogenic steroidal alkaloids, from the marine sponge *Corticium simplex*." J. Am. Chem. Soc. **128**: 3148–3149.

Aoki, S., Y. Watanabe, et al. (2007). "Structure-activity relationship and biological property of cortistatins, anti-angiogenic spongean steroidal alkaloids." Bioorg. Med. Chem. **15**: 6758–6762.

Arrieta, J. M., S. Arnaud-Haond, et al. (2009). "What lies underneath: Conserving the oceans' genetic resources." PNAS Early Edition: 1-7.

Ausubel, J., D. T. Crist, et al. (2010). First Census of Marine Life 2010: Highlights of a decade of discovery. Washington DC: Census of Marine Life: 68 p.

Bai, R. L., K. D. Paull, et al. (1991). "Halichondrin B and homohalichondrin B, marine natural products binding in the vinca domain of tubulin. Discovery of tubulin-based mechanism of action by analysis of differential cytotoxicity data." J. Biol. Chem. **266**: 15882–15889.

Ballarin, L., A. Franchini, et al. (2001). "Morula cells as the major immunomodulatory hemocytes in ascidians: evidences from the colonial species *Botryllus schlosseri*." Biol Bull. **201**: 59-64.

Barker, J. L. and J. W. Frost (2001). "Microbial synthesis of p-hydroxybenzoic acid from glucose." Biotechnol. Bioeng. **76**: 376-390.

Barnes, R. D. (1982). Invertebrate Zoology. Philadelphia, Holt-Saunders International.

Bergmann, W. and R. J. Feeney (1951). "Contribution to the study of marine products. XXXII. The nucleotides of sponges I." J. Org. Chem. **16**: 981-987.

Best, H. A., J. H. Matthews, et al. (2013). "Laulimalide and peloruside A inhibit mitosis of *Saccharomyces cerevisiae* by preventing microtubule depolymerisation-dependent steps in chromosome separation and nuclear positioning." Mol. BioSyst. **9**: 2842-2852.

Bowling, J. J., H. K. Pennaka, et al. (2008). "Antiviral and anticancer optimization studies of the DNA-binding marine natural product aaptamine." Chem. Biol. Drug Des **71**: 205–215.

Brusca, R. C. and G. J. Brusca (1990). Invertebrates. . Sunderland, Massachusetts.

Buey, R. M., I. Barasoain, et al. (2005). "Microtubule interactions with chemically diverse stabilizing agents: Thermodynamics of binding to the paclitaxel site predicts cytotoxicity." Chem. Biol. **12**: 1269–1279.

Calcul, L., A. Longeon, et al. (2003). "Novel alkaloids of the aaptamine class from an Indonesian marine sponge of the genus *Xestospongia*." Tetrahedron **59**: 6539–6544.

Cee, V. J., D. Y. K. Chen, et al. (2009). "Cortistatin A is a high-affinity ligand of protein kinases ROCK, CDK8, and CDK11." Angew. Chem. Int. Ed. Engl. **48**: 8952–8957.

- Chen, M. H., S. Lin, et al. (2012). "Enantiomers of an indole alkaloid containing unusual dihydrothiopyran and 1,2,4 thiadiazole rings from the root of *Isatis indigotica*." Org. Lett.: 5668–5671.
- D'Incalci, M. and C. M. Galmarini (2010). "A Review of Trabectedin (ET-743): A Unique Mechanism of Action." Mol. Cancer Ther. **9**: 2157-2163.
- Davidson, S. K., S. W. Allen, et al. (2001). "Evidence for the Biosynthesis of Bryostatins by the Bacterial Symbiont "*Candidatus Endobugula sertula*" of the Bryozoan Bugula neritina." Applied and Environmental Microbiology **67**: 4531–4537.
- Dubois, E. A. and A. F. Cohen (2009). "New drug mechanisms." British Journal of Clinical Pharmacology **68**: 320–321.
- Field, J. J., B. Pera, et al. (2012). "Zampanolide, a potent new microtubule-stabilizing agent, covalently reacts with the taxane luminal site in tubulin  $\alpha,\beta$ -heterodimers and microtubules." Chem. Biol. **19**: 686-698.
- Hamel, E. and D. G. Covell (2002). "Antimitotic peptides and depsipeptides." Curr. Med. Chem. Anticancer Agents **2**: 19-53.
- Heitz, S., M. Durgeat, et al. (1980). "nouveau dérivé du indolique du thiadiazole-1,2,4, isolé d'un tunicier (*Dendrodoa grossularia*)." Tetrahedron Letters **21**: 1457 - 1458.
- Helbecque, N., C. Moquin, et al. (1987). "Grossularine-1 and grossularine-2, alpha carbolines from *Dendrodoa grossularia*, as possible intercalative agents." Cancer Biochem Biophys. **9**: 271-279.
- Hill, R. T., O. Peraud, et al. (2005). Manzamine-producing actinomycetes. USA. **20050244938A1**.
- Hirata, Y. U., D. (1986). "Halichondrins - antitumor polyether macrolides from a marine sponge." Pure Appl. Chem. **58**: 701–710.
- Hooper, J. N. A., R. W. M. Van Soest, et al. (2002). Systema Porifera: A guide to the classification of sponges. New York, Kluwer Academic/Plenum Publishers.
- Kobayashi, J. and M. Tsuda (2004). "Amphidinolides, bioactive macrolides from symbiotic marine dinoflagellates " Nat. Prod. Rep. **21**: 77–93.
- Koivunena, J., V. Aaltonena, et al. (2006). "Protein kinase C (PKC) family in cancer progression." Cancer Letters **235**: 1–10.
- Larghi, E. L., T. S. Kaufman, et al. (2009). "Aaptamine and related products. Their isolation, chemical syntheses, and biological activity." Tetrahedron **65**: 4257–4282.
- Leung-Toung, R., J. Wodzinska, et al. (2003). "1,2,4-Thiadiazole: A novel cathepsin B inhibitor." Bioorganic & Medicinal Chemistry **11**: 5529–5537.
- Mayer, A. M. S. (2013, 03/06/2013). "Marine pharmaceuticals: the clinical pipeline." Retrieved 09/27, 2013, from <http://marinepharmacology.midwestern.edu/clinPipeline.htm>.
- Mayer, A. M. S., A. D. Rodriguez, et al. (2013). "Marine Pharmacology in 2009–2011: Marine compounds with antibacterial, antidiabetic, antifungal, anti-inflammatory, antiprotozoal, antituberculosis, and antiviral activities; affecting the immune and nervous systems, and other miscellaneous mechanisms of action." Mar. Drugs **11**: 2510-2573.

- Meragelman, T. L., R. H. Willis, et al. (2007). "Candidaspongiolides, distinctive analogues of tedanolide from sponges of the genus *Candidaspongia*." J. Nat. Prod. **70**: 1133-1138.
- Metzler, D. E. (2003). Biochemistry. The chemical reactions of living cells., Elsevier Science.
- Michibata, H., T. Uyama, et al. (2002). ""Vanadocytes, cells hold the key to resolving the highly selective accumulation and reduction of vanadium in ascidians." Microscopy Research and Technique **56**: 421–434.
- Morgan, P. N., M. I. Gibson, et al. (1962). "Conversion of shikimic acid to aromatic compounds." Nature **194**: 1239-1241.
- Muenchhoff, J., K. S. Siddiqui, et al. (2010). "A novel prokaryotic L-arginine:glycine amidinotransferaseis involved in cylindrospermopsin biosynthesis." FEBS Journal **277**: 3844–3860.
- Núñez-Pons, L., M. Carbone, et al. (2012). "Natural products from antarctic colonial ascidians of the genera aplidium and synoicum: Variability and defensive role." Mar. Drugs **10**: 1741–1764.
- Oda, T., J. S. Lee , et al. (2009). "Inhibitory effect of N,N-didesmethylgrossularine-1 on inflammatory cytokine production in lipopolysaccharide-stimulated RAW 264.7 cells." Mar. Drugs **7**: 589-599.
- Park, S. K., S. S. Kim, et al. (1995). "A Study on the chemical constituents from marine sponge *Luffariella* sp." J. Korean Chem. Soc. **39**: 559–563.
- Paterson, I., S. M. Dalby, et al. (2011). "Leiodermatolide, a potent antimitotic macrolide from the marine sponge *Leiodermatium* sp." Angewandte Chemie **50**: 3219 –3223.
- Penn, J. S. (2008). Retinal and choroidal angiogenesis, Springer.
- Pettit, G. R., C. L. Herald, et al. (1982). "Isolation and structure of bryostatin 1." J. Am. Chem. Soc. **104**: 6846–6848.
- Pham, C. D., H. Weber, et al. (2013). "New cytotoxic 1,2,4-thiadiazole alkaloids from the ascidian *Polycarpa aurata*." Org. Lett. **15**: 2230-2233.
- Piel, J., D. Q. Hui, et al. (2004). "Antitumor polyketide biosynthesis by an uncultivated bacterial symbiont of the marine sponge *Theonella swinhoei*." Proc. Natl. Acad. Sci. USA **101**: 16222–16227.
- Prinsep, M. (2003). "Sulfur-containing natural products from marine invertebrates." Natural Products Chemistry **28**: 617-751.
- Ruppert, E. E., R. S. Fox, et al. (2004). Invertebrate Zoology 7th Edition, Brooks / Cole.
- Sato, S., A. Murata, et al. (2011). "Marine natural product aurilide activates the OPA1-mediated apoptosis by binding to prohibitin." Chem Biol. **18**: 131-139.
- Schirmer, A., R. Gadkari, et al. (2005). "Metagenomic analysis reveals diverse polyketide synthase gene clusters in microorganisms associated with the marine sponge *Discodermia dissoluta*." Appl. Environ. Microbiol. **71**: 4840–4849.

- Shen, Y.-C., T. S. Lin, et al. (1999). "Structures and cytotoxicity relationship of isoaptamine derivatives." J. Nat. Prod. **62**: 1264–1267.
- Sikorska, J., A. M. Hau, et al. (2012). "Mandelalides A–D, cytotoxic macrolides from a new *Lissoclinum* species of South African tunicate." J. Org. Chem. **77**: 6066–6075.
- Singh, N., R. Kumar, et al. (2008). "Antileishmanial activity in vitro and in vivo of constituents of sea cucumber *Actinopyga lecanora*." Parasitology research **103**: 351–354.
- Staunton, J. and K. J. Weissman (2001). "Polyketide biosynthesis: a millennium review." Nat. Prod. Rep. **18**: 380–416.
- Taylor, M. W., R. Radax, et al. (2007). "Sponge-associated microorganisms: evolution, ecology, and biotechnological potential." Mol. Biol. Rev. **71**: 295–347.
- Trindade-Silva, A. E., C. P. J. Rua, et al. (2013). "Polyketide synthase gene diversity within the microbiome of the sponge *Arenosclera brasiliensis*, endemic to the southern Atlantic Ocean." Applied and Environmental Microbiology **79**: 1598–1605.
- Walker, J. B. (1973). Amidinotransferases. New York, Academic Press.
- Wang, M., H. Zhou, et al. (2009). "A thioesterase from an iterative fungal polyketide synthase shows macrolization and cross-coupling activity, and may play a role in controlling iterative cycling through product off loading." Biochemistry **48**: 6288–6290.
- Wang, W. F., T. Oda, et al. (2007). "Three new sulfur-containing alkaloids, polycarpaurines A, B, and C, from an Indonesian ascidian *Polycarpa aurata*." Tetrahedron **63**: 409–412.
- Williams, D. E., M. Roberge, et al. (2003). "Spirastrellolide A, an antimetabolic macrolide isolated from the Caribbean marine sponge *Spirastrella coccinea*." J. Am. Chem. Soc. **125**: 5296–5297.
- Zheng, Y. L., X. L. Lu, et al. (2010). "Direct effects of fascaplysin on human umbilical vein endothelial cells attributing the anti-angiogenesis activity." Biomed. Pharmacother. **64**: 527–533.
- Zhou, L., T. W. Huang, et al. (2013). "The rice bacterial pathogen *Xanthomonas oryzae* pv. *oryzae* produces 3-hydroxybenzoic acid and 4-hydroxybenzoic acid via XanB2 for Use in xanthomonadin, ubiquinone, and exopolysaccharide biosynthesis." MPMI **26**: 1239–1248.

## 9. Abbreviations

List of used abbreviations

$[\alpha]^{20}_{\text{D}}$	Specific rotation at the sodium D-line
br	Broad signal
$^{13}\text{C}$	13 u carbon isotope
$\text{CDCl}_3$	Deuterated chloroform
$\text{CHCl}_3$	Chloroform
COSY	Correlation spectroscopy
d	Doublet
$\delta$	Chemical shift
DAD-HPLC	HPLC with diode array detector
dd	Doublet of doublet signal
DEPT	Distortionless enhancement by polarization transfer
DMSO	Dimethyl sulfoxide
$\text{DMSO-}d_6$	Deuterated dimethyl sulfoxide
$\epsilon$	Molar extinction coefficient
e.g.	<i>exempli gratia</i> (for the sake of example)
EI	Electron impact ionization
ESI	Electron spray ionization
<i>et al.</i>	<i>et alii</i> (and others)
EtOAc	Ethyl acetate
EtOH	Ethanol
eV	Electron Volt
FTHRMS	Fourier Transform High Resolution Mass Spectrometry
g	Gram
$^1\text{H}$	proton
HCOOH	Formic acid
HECADE	Heteronuclear Couplings from ASSCI-domain experiments with E.COSY-type crosspeaks
HMBC	Heteronuclear multiple bond connectivity
HMQC	Heteronuclear multiple quantum coherence
$\text{H}_2\text{O}$	Water
HPLC	High performance liquid chromatography
HR-MS	High resolution-mass spectrometry
Hz	Hertz
$\text{IC}_{50}$	Half maximal inhibitory concentration
J	Coupling constant
log	Decadic logarithm



---

L	Liter
LC	Liquid chromatography
LC-MS	Liquid chromatography-mass spectrometry
$\lambda_{\max}$	Wavelength maximum
m	Multiplet signal
MeOD	Deuterated methanol
MeOH	Methanol
mg	Milligram
MHz	Mega Hertz
min	Minute
mL	Milliliter
MS	Mass spectrometry
MTT	3-(4,5-Dimethylthiazol-2-yl)-2,5-diphenyltetrazolium bromide
$m/z$	Mass per charge
$\mu\text{g}$	Microgram
$\mu\text{L}$	Microliter
$\mu\text{M}$	Micromolar
MW	Molecular weight
ng	Nanogram
nm	Nanometer
<i>n</i> -BuOH	<i>n</i> -Butanol
$^{15}\text{N}$	15 u nitrogen isotope
NMR	Nuclear magnetic resonance
NOE	Nuclear Overhauser effect
NOESY	Nuclear Overhauser and exchange spectroscopy
ppm	Parts per million
q	Quartet signal
ROESY	Rotating frame Overhauser enhancement spectroscopy
RP-18	Reversed phase C 18
s	Singlet signal
SCUBA	self-contained underwater breathing apparatus
Si	Silica
t	Triplet signal
TFA	Trifluoroacetic acid
TLC	Thin layer chromatography
u	Atom mass
UV	Ultra-violet
VLC	Vacuum liquid chromatography

## 10. Research contributions

### Publications

Pham, C. D.; Hartmann, R.; Müller, W. E. G.; de Voogd, N.; Lai, D. W.; Proksch, P. (2013) Aaptamine derivatives from the Indonesian sponge *Aaptos suberitoides*. *J. Nat. Prod.* 76, 103–106.

Pham, C. D.; Weber, H.; Hartmann, R.; Wray, V.; Lin, W. H.; Lai, D. W.; Proksch, P. (2013) New cytotoxic 1,2,4-thiadiazole alkaloids from the ascidian *Polycarpa aurata*. *Org. Lett.* 15, 2230–2233.

Pham, C.D.; Hartmann, R.; Böhrer, P.; Stork, B.; Wesselborg, S.; Lai, D.W.; Proksch, P. (2013) Callyspongiolide, an unprecedented cytotoxic macrolide from the marine sponge *Callyspongia* sp. (submitted to *Angewandte Chemie Int. Ed.*)

## 11. Declaration of academic honesty/Erklärung

Die vorliegende Dissertation habe ich eigenständig und ohne unerlaubte Hilfe angefertigt. Die meisten der für die Anfertigung dieser Arbeit erforderlichen Methoden wurden vom Autor selbständig durchgeführt. Folgende Methoden wurden in anderen Institutionen durchgeführt:

**Elektronenstoßionisation-Massenspektrometrie (EI-MS):** Die Messungen wurden durch Herrn Dr. Peter Tommes und Herrn Ralf Bürgel am Institut für Anorganische Chemie der Heinrich-Heine-Universität Düsseldorf an einem Triple-Quadrupol-Massenspektrometer Finnigan TSQ 7000 durchgeführt.

**HR-ESI-Massenspektrometrie:** Die Messungen wurden durch Frau Andrea Berger am Institut für Biophysikalische Analytik am Helmholtz-Zentrum für Infektionsforschung GmbH in Braunschweig an einem Micromass Qtof2 Massenspektrometer durchgeführt. Einige Messungen wurden auch von Herrn Dr. Peter Tommes durchgeführt.

**IR-Spektroskopie:** Die Messungen wurden am Institut für Makromolekulare Chemie und Organische Chemie der Heinrich-Heine-Universität Düsseldorf durch Herrn Dr. Bernhard Mayer an einem Shimadzu IRAffinity-1 FT 1 FT -IR Spektrometer durchgeführt.

**NMR-Spektroskopie ( $^1\text{H}$ ,  $^{13}\text{C}$ , COSY, DEPT, HECADÉ-HMQC, HMQC, HMBC, ROESY):** Die Messungen wurden am Institut für Anorganische Chemie der Heinrich-Heine-Universität Düsseldorf (Bruker DRX-500) durch Herrn Peter Behm, am Institut für Organische Chemie und Makromolekulare Chemie (Bruker Avance III 600) durch Frau Maria Beuer, am Institut für Biophysikalische Analytik am Helmholtz-Zentrum für Infektionsforschung GmbH in Braunschweig (Bruker AM-300, ARX-400 und DMX-600) durch Frau Christel Kakoschke sowie am Institute of Complex Systems (ICS-6) im Forschungszentrum Jülich (Varian Inova 600 MHz Spektrometer, ausgestattet mit Z-axis pulse-field-gradient triple resonance cryoprobe) durch Herrn Dr. Rudolf Hartmann durchgeführt.

**Probenidentifikation:** Die taxonomische Identifikation der Schwamm- und Seescheidenproben wurden von Frau Dr. Nicole de Voogd vom Naturalis Biodiversity Center, Leiden, Niederlande durchgeführt.

**Zytotoxizität:** Die Untersuchungen auf zytotoxische Aktivität an Maus-Lymphom-Zellen (L5178Y) wurden durch Frau Renate Steffen am Institut für Physiologische Chemie der Johannes Gutenberg-Universität Mainz durchgeführt. Messungen zur Zytotoxizität an menschlichen Leukämie- und Lymphoblastom-Zelllinien (Ramos B-Lymphozyten, Jurkat T-Lymphozyten) wurden am Institut für Molekulare Medizin der Heinrich-Heine-Universität Düsseldorf durch Herrn Dr. Björn Stork und Herrn Philipp Böhler durchgeführt.

Die Genehmigungen zur Veröffentlichung der Publikationen im Rahmen dieser Dissertation wurden von den entsprechenden Verlagen eingeholt. Die Dissertation wurde in der vorgelegten oder in ähnlicher Form noch bei keiner anderen Institution eingereicht. Ich habe bisher keine erfolglosen Promotionsversuche unternommen.

Düsseldorf, den \_\_\_\_\_

(Cong-Dat Pham)

## 12. Acknowledgements

This study could not be successfully carried out without the support and acknowledgement of many colleagues, friends and my family. I would like to wholeheartedly express my gratitude to the following persons involved:

- Prof. Dr. Peter Proksch for providing me this valuable opportunity to pursue the doctoral research and for the excellent work facilities in the Institute of Pharmaceutical Biology and Biotechnology, Heinrich-Heine University, for his guidance, fruitful discussions and generous considerations during my stay in this institute.
- Prof. Dr. Matthias U. Kassack for estimating my PhD study as second referee.
- Prof. em. Dr. Horst Weber for his mentorship me during the synthesis work and for his fruitful advices in this matter.
- Dr. Daowan Lai for his mentorship during the last two years, as he always gave me valuable advices and generous help in NMR issues and structure elucidation and, especially, for his continuous efforts in pushing my publications forward so quickly. Without him I would not have come this far.
- Dr. Victor Wray, Prof. Dr. Bingui Wang (Laboratory of Experimental Marine Biology, Institute of Oceanology, Chinese Academy of Science), Prof. Wenhan Lin (National Research Laboratories of Natural and Biomimetic Drugs, Peking University, Health Science Center) for their fruitful discussions and constructive advices with regards to structure elucidation issues
- Prof. Dr. Claus Paßreiter for his support in organising the Bio II practical course and for his interesting conversations about work related as well as trivial matters.
- Mrs. Eva Müller for her continuous guidance and support in the Bio II practical course and especially for her patience. I also send special thanks to my colleagues Arta Kuci and Ingo Kolb for helping me out during the practical courses.
- Dr. Rudolf Hartmann for the crucial NMR measurements.
- Dr. Peter Tommes, Mr. Ralf Bürgel, Mrs. Renate Steffen, Mrs. Maria Beuer, Mr. Philipp Böhler, Dr. Björn Stork, Mrs. Christel Kakoschke, Dr. Bernhard Mayer for all the accurately performed NMR, EI/ESI-MS and cytotoxicity measurements including the fulfilling of “extra wishes”.
- Mrs. Claudia Eckelskemper for taking care of most of the administrative issues and for an always easy approachability.

- the technical staff team made up by Mrs. Waltraud Schlag, Mrs. Simone Miljanovic and Mrs. Katja Friedrich for supplying laboratory materials and logistics. I also give my thanks to Mr. Klaus Dieter Jansen and Mrs. Heike Goldbach-Gecke for their nice company.
- my buddy Robert “Roberto” Bara for showing me the ropes during my first weeks of graduate study and also for the great times outside the lab and for understanding the phonetic and linguistic differences of BE and AE.
- my lab mate Dr. David Rösberg for every overfriendly “Guten Morgen. Nah...” (falsetto) likewise. I always enjoyed his nice company, inside and outside the lab.
- my past and present fellows Dr. Bartosz Lipowicz, Dr. Yaming Zhou, Dr. Weeam Ibrahim, Dr. Amal Hassan, Dr. Sherif Sayed Ebada, Wera Döring (née Hauschild), Lena Hammerschmidt, Andreas Marmann, Imke Form, Catalina Frances Pérez Hemphill, Catherine Schumacher, Dhana Thomy, Kirsten Famulla, Dr. Peter Sass, Mariam Mousa, Meriem Bendouma, Amin Mokhlesi, Mi-Young Chung, Hendrik Niemann, Georgios Daletos, Mustapha ElAmrani, Fatima Zahra Kabbaj, Festus Okoye, Mousa. AlTarabeen, Mona ElNekity, Matthias Onyebuchi, Huiqin “Kitchen” Chen, Yang Liu, Yao Long Lew, Shuai Liu, Rini Muharini, Antonius Ola, Asep Supriadin, Chih-Hsuan Hsin, Dr. Shushan Gao, Dr. Jianping Wang, Dr. Zhiyong Guo and all the others for the nice multicultural time I spent with them, for their help and assistance whenever I needed it. Especially, I treasure my time with “Prof. Atomic Nuclear Paul Watt” (Dr. Paulwatt Nuclear) and thank him for the many funny moments. I also want to express my thanks to Dr. Mohamed Abdel-Aziz, Ahmed Shalabi and Ahmed Shokri for their hospitality during my stay in Egypt. I also remember the somewhat special and funny times with Ahmed Shokri at the end of my graduate study.
- the BMBF for the financial support for my research.
- my parents Van Hoa Pham and Kim Cuc Lien and my brother Cong-Toan Pham for always supporting me in good and bad times to finish this study. To all of you, thank you very very much.

